Journal of Healthcare Engineering

Internet of Medical Things for Healthcare Engineering

Lead Guest Editor: Xiwei Huang
Guest Editors: Hyungkook Jeon and Jiafeng Yao

Internet of Medical Things for Healthcare Engineering

Journal of Healthcare Engineering

Internet of Medical Things for Healthcare Engineering

Lead Guest Editor: Xiwei Huang
Guest Editors: Hyungkook Jeon and Jiafeng Yao

Contents

Hindawi
Journal of Healthcare Engineering
Volume 2020, Article ID 8864863, 10 pages
https://doi.org/10.1155/2020/8864863

Research Article

Detection of Snore from OSAHS Patients Based on Deep Learning

Fanlin Shen ,[1] Siyi Cheng,[1] Zhu Li,[1] Keqiang Yue ,[1] Wenjun Li ,[1] and Lili Dai[2]

[1]*Key Laboratory of RF Circuits and Systems, Ministry of Education, Hangzhou Dianzi University, Hangzhou, Zhejiang, China*
[2]*The Affiliated Hospital of Hangzhou Normal University, Hangzhou, Zhejiang, China*

Correspondence should be addressed to Wenjun Li; liwenjun@hdu.edu.cn

Received 17 August 2020; Revised 29 October 2020; Accepted 30 November 2020; Published 12 December 2020

Academic Editor: Jiafeng Yao

Obstructive sleep apnea-hypopnea syndrome (OSAHS) is extremely harmful to the human body and may cause neurological dysfunction and endocrine dysfunction, resulting in damage to multiple organs and multiple systems throughout the body and negatively affecting the cardiovascular, kidney, and mental systems. Clinically, doctors usually use standard PSG (Polysomnography) to assist diagnosis. PSG determines whether a person has apnea syndrome with multidimensional data such as brain waves, heart rate, and blood oxygen saturation. In this paper, we have presented a method of recognizing OSAHS, which is convenient for patients to monitor themselves in daily life to avoid delayed treatment. Firstly, we theoretically analyzed the difference between the snoring sounds of normal people and OSAHS patients in the time and frequency domains. Secondly, the snoring sounds related to apnea events and the nonapnea related snoring sounds were classified by deep learning, and then, the severity of OSAHS symptoms had been recognized. In the algorithm proposed in this paper, the snoring data features are extracted through the three feature extraction methods, which are MFCC, LPCC, and LPMFCC. Moreover, we adopted CNN and LSTM for classification. The experimental results show that the MFCC feature extraction method and the LSTM model have the highest accuracy rate which was 87% when it is adopted for binary-classification of snoring data. Moreover, the AHI value of the patient can be obtained by the algorithm system which can determine the severity degree of OSAHS.

1. Introduction

Obstructive apnea hypopnea syndrome (hereinafter called OSAHS) not only leads to poor sleep quality but also leads to chronic hypoxemia, hypercapnia, and even high-grade central nervous system dysfunction lesions, which brings great negative impact to people. Therefore, in order to analyze the reason and sum up the diagnosis method and response treatment policy of OSAHS, more and more researchers are devoted to the research of the disease [1–3]. In clinic practice, polysomnography (hereinafter called PSG) is used to assist doctors in diagnosing OSAHS. PSG obtains multidimensional data such as heart rate, brain waves, chest vibration, blood oxygen saturation, breathing, and snoring. AHI (Apnea Hypopnea Index) value of the patient can be obtained after these data are fused with a certain algorithm and weights by monitoring the patient's breathing throughout the night [4, 5], which means the number of apnea index per hour, hypopnea index and obstructive pause, central pause, and mixed pause. However, there are two practical problems with PSG: 1. PSG requires professional medical personnel to operate, and the users must lie in the hospital for monitoring; 2. PSG affects the quality of sleep because the user needs to plug in the corresponding equipment in many parts of the body during use. If there is a technology that does not rely on large medical equipment and is comfortable for patients in daily use, it can not only improve the experience of patients when they are monitored but also help doctors more accurately grasp the long-term clinical performance of patients.

In recent years, scholars have proposed a variety of OSAHS disease discrimination techniques based on various symptom characteristics. Among them, A. Garde used the visual midpoint (radius and angle) distribution characteristics of SpO_2 signals to distinguish OSAHS symptoms [6]; Kim used the patient's breathing sound signal to develop a classification of OSAHS severity model [7]; Volak made preliminary judgments on OSAHS through image recognition of children's dental features [8]; Castillo-Escario et al. develop an algorithm for detecting silence events and classifying them into apneas and hypopneas [9]. The current medical research reports show that the clinical apnea syndrome events manifestations of an adult are as follows [10, 11]. Snoring is loud and often be interrupted by an apnea event that lasts for about 10 s; then, a faint snoring sound appears during the incident. After the incident, the patient suffered from gasping, accompanied by loud snoring. The reason for the formation of OSAHS disease is the blockage of the internal cavity of the nose of patients initiated by the patient's oral and nasal diseases such as rhinitis or pharyngitis [12]. In general, snoring is the form of expression of OSAHS. In the study of snoring, the researchers first studied the technique of extracting snoring sounds from breathing sounds. For example, the nonlinear classification algorithm to identify snoring sounds was studied by Ankishan [13]; Lim proposed a snoring recognition method based on RNN [14, 15]. The study of OSAHS recognition based on snoring has also been proposed after the effective extraction of snoring signals: After extracting the time-domain features of snoring after apnea events, Temrat et al. judged the severity degree of OSAHS through distinguishing different types of snoring by the leave-one-out cross-validation technique [16]. However, the time domain features such as zero-crossing rate (ZCR), energy entropy (EE), and integrated electromyography (IEMG) extracting snoring from background noise in this paper have two problems: (1) The similar features of some audio data are not easy to be distinguished; (2) The feature dimension is too less. Therefore, in order to extract better features, researchers also introduced neural network classification methods into snoring recognition. The advantage of detecting snoring features based on deep learning is that the neural network can automatically extract features. For example, Takahiro Emoto classified snoring data related to OSAHS (SNR) based on ANN. Unfortunately, due to the limitation of the classification effect of ANN, its accuracy result can only reach 75% [17]. Moreover, the data used in this experiment is not obtained based on the test result data output in PSG which is currently the standard diagnostic procedure for obstructive sleep apnea (hereinafter called OSA) [18] but artificially annotated data by listening to the sound. Therefore, the reliability of the experiment could not be verified by the most reliable device: PSG. In addition, B. Daurai and P. Nayak detected apnea events by using three dimensions of the chest cavity, abdomen, and respiratory airflow. The equipment used for obtaining data is inconvenient to wear and may affect the quality of sleep of users [19]. In this paper, we presented a method for automatic recognition of OSAHS based on snoring sounds classification by a neural network model. Our method only used snoring sounds for recognition. Therefore data of patients could be easily collected by recording equipment. Firstly, the snoring sounds related to apnea events and nonapnea event-related snoring sounds (see Section 2.2) are identified. Secondly, the severity of the apnea event was judged by the result of snoring sound recognition. Each snoring data is converted from the time domain to the frequency domain. The MFCC features are calculated, and then the MFCC features are used as the input of a LSTM model for binary classification. The experiments result indicates that our method could realize a recognition with high accuracy.

2. Materials and Methods

2.1. Flow of the Proposed Method. The algorithm flow proposed in this paper is shown in Figure 1, which is divided into two steps: feature extraction and classification. After MFCC feature extraction, snoring audio data were inputted into the CNN/LSTM neural network for binary classification, and then the algorithm outputted the recognition result.

2.2. Feature Extraction. Figure 2 is the data derived from PSG. The results show the multidimensional data such as pulse and oxygen saturation during patient monitoring. As shown in the figure, an obstruction pause event occurs between 23 : 01 : 10–23 : 01 : 25. The blocking pause event is obtained by multidimensional data fusion. From the dimension data of snoring, the apnea event is accompanied by a very weak snoring sound, which is marked with purple in Figure 2. The snoring that appeared after the apnea event is marked with blue. Snoring sounds that occur during apnea events and after apnea events are recorded as snoring sounds related to apnea events, which are called abnormal snoring. The remaining snoring sounds related to nonapnea events are called normal snoring sounds. In order to identify the normal snoring and abnormal snoring, we firstly extracted features of snoring signals using three different feature extraction methods which are MFCC, LPCC, and LPMFCC. The flow of feature extraction is given in Figure 3.

2.2.1. MFCC. MFCC (Mel Frequency Cepstral Coefficient) is a feature inspired by the event that different human ears have different hearing sensitivity to sound waves which have different frequencies. MFCC is currently widely used in the field of audio recognition. Preemphasis, framing, and windowing pretreatment are performed in the time domain before feature extraction [20]. Preemphasis is to pass the speech signal through a high-pass filter in order to compensate for the loss of high-frequency components and improve the high-frequency components. Frame is to gather N sampling points into a set unit. The purpose is to make the parameters between one frame and another frame transition smoothly. Windowing is to multiply each frame by Hamming window, which is to reduce signal characteristics leak in the frequency domain. After pretreatment, the signal is converted to the frequency domain by Fourier transform and the power spectrum is calculated. Then, the Mel-scale triangular filter bank is used to smooth the frequency spectrum instead of avoiding the characteristic parameters that are affected by the pitch of the speech. Finally, we calculate the log energy and MFCC coefficient of each filter bank output [21]. As shown in Equation (1) and Equation (2), the log energy $s(m)$ output by each filter bank is obtained by Equation (1), where m represents the number of

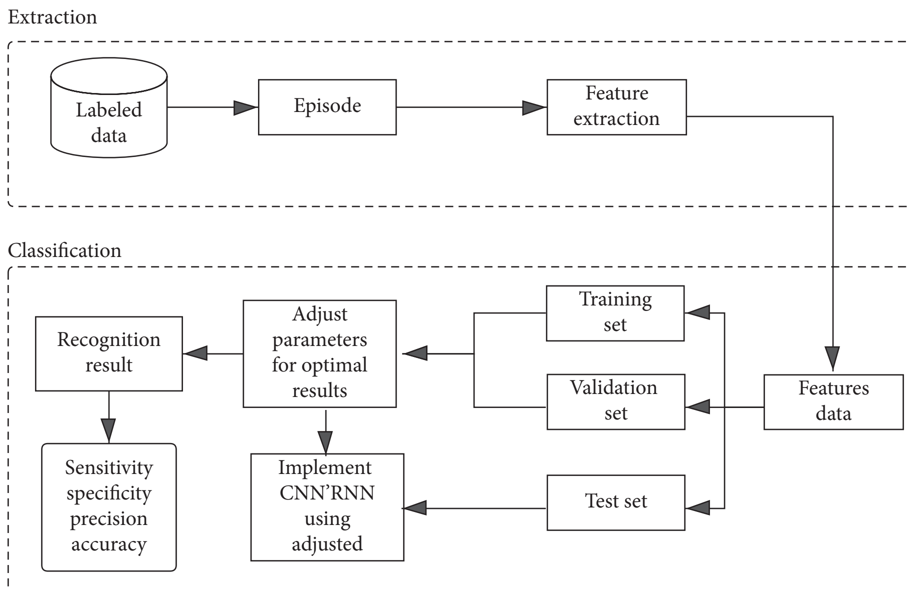

Figure 1: The flow of the proposed method.

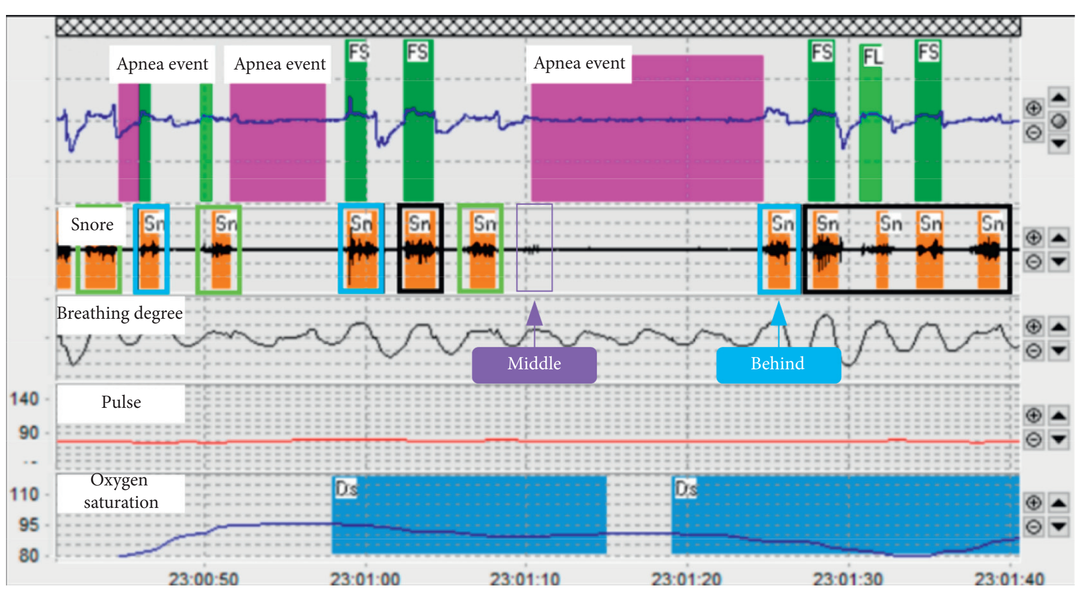

Figure 2: Data presented on PSG.

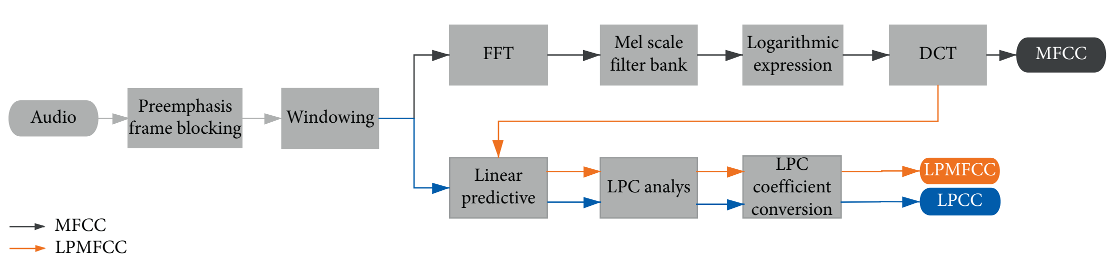

Figure 3: Three methods of feature extraction.

filters, k represents the number of Fourier transform points, n represents the order of MFCC coefficients, $Xa(k)$ represents the power of the speech signal spectrum obtained by performing fast Fourier transform of each frame signal and taking the modulus square; $H(k)$ represents the frequency response of the energy spectrum obtained by the triangular filter; the MFCC coefficient $C(n)$ is obtained based on DCT (discrete cosine transform) [21]:

$$s(m) = \ln\left(\sum_{k=0}^{N-1} |Xa(k)|^2 H(k)\right), \quad 0 \le m \le M, \tag{1}$$

$$C(n) = \sum_{m=0}^{N-1} s(m)\cos\left(\frac{\pi n(m-0.5)}{m}\right), \quad n = 1, 2, \ldots, L. \tag{2}$$

Each piece of snoring audio was divided into frames by 0.03 s length of frame and 0.01 s shift of frame, the extracted feature dimension of which is 298 ∗ 40.

2.2.2. LPCC. In order to obtain the basic parameters of speech signals, LPCC has become one of the main technologies to estimate the parameters of speech signals. The algorithm of LPCC is shown in Figure 1, except for the same pretreatment as shown in Section 2.2.1, the signal undergoes the current prediction model to calculate the LPC coefficients, and then is converted into LPCC coefficients in the form of the spectrum by cepstrum, $V(z)$ is the channel transfer function. G is the gain of the filter, a_k is the set of known linear regression coefficients (LPC) autoregressive coefficients, and p is the order of the all-pole filter. The LPC coefficients obtained by the autocorrelation method ensure the stability of the system so that the channel model transferred function corresponding to the following Equation (3) has a minimum phase [22]. Equation (4) can deduce the recursive relationship between the cepstral $c(n)$ of the speech signal and the LPC coefficient, where $c(1)$ is the DC component and reflects the spectral energy, and its value does not affect the spectral shape. The second formula is used when the number of LPCC coefficients is not greater than the number of LPC coefficients, and the third formula is used when the number of LPCC coefficients is greater than the number of LPC coefficients:

$$V(z) = \frac{G}{1 - \sum_{k=1}^{p} a_k + z^{-k}}, \tag{3}$$

$$\begin{cases} c(n) = a_1 \\ c(n) = a_n + \sum_{k=1}^{n-1}\left(1 - \frac{k}{n}\right) a_k c(n-k), & 1 < n < p \\ c(n) = \sum_{k=1}^{p}\left(1 - \frac{k}{n}\right) a_k c(n-k), & n > p \end{cases} \tag{4}$$

2.2.3. LPMFCC. The LPMFCC feature parameters are based on LPC. The process obtained by calculating the Mel Cepstrum of LPC is shown in formula (5). Firstly, the LPC coefficients are subjected to Fourier transform, and then the LPC coefficients are obtained through DFT Discrete spectrum$X_a(k)$. Secondly, the square of the spectrum amplitude is calculated to obtain the discrete energy spectrum $X_a(k)^2$. Among them, N represents the number of Fourier transform points. Thirdly, a set of Mel-scale triangular filters are used to filter the discrete energy spectrum, and then the output results are subjected to logarithm operation to obtain the log energy $Z_a(m)$, as shown in Equation (6), where $H_m(k)$ $(0 \le \mathrm{m} \le M)$ is several band-pass filters, and M is the number of filters. Finally, the above logarithmic energy is calculated by discrete cosine transform, and a new characteristic parameter LPMFCC is obtained:

$$X_a(k) = \sum_{n=0}^{N-1} x_a(n) e^{-(j2pnk/N)}, \quad 0 \le k \le N-1, \tag{5}$$

$$Z_a(m) = \ln\left(\sum_{k=0}^{N-1} \left|X_a(k)\right|^2 H_m(k)\right), \tag{6}$$

$$C_a(n) = \sum_{m=0}^{M-1} Z_a(m)\cos\left[\frac{pn(m+(1/2))}{M}\right], \quad 0 \le m \le M. \tag{7}$$

2.3. Model Recognition

2.3.1. CNN-Based Audio Recognition. Research on convolutional neural networks originated in the late 19th century. Since 2012, due to breakthroughs in hardware and algorithms, both image recognition and audio recognition have made leaps and bounds [23–25]. In the field of audio recognition, Google proposed the CNN model in 2017 to identify keywords [26]. The general convolutional neural network structure usually includes a convolutional layer, a fully connected layer, and a pooling layer. The CNN model used in this article consists of a three-layer CNN structure, and the extraction result of each CNN convolutional layer is activated and connected to the Relu activation function. The max-pooling layer is finally connected to the fully connected layer to map the distributed features to the sample label space (see Figure 4), and the model parameter settings are shown in Table 1. Considering that the input MFCC features are much less complex than the image data features in image recognition, it is not necessary to adopt very deep neural networks for recognition. If the structure of the recognition model is too deep, it will result in problems such as overfitting and excessive calculation. We will conduct a comparative experiment with 3-layer CNN and 5-layer CNN to verify this viewpoint in Section 3.4, and the construction of 3-layer CNN and 5-layer CNN are shown in Tables 1 and 2.

2.3.2. RNN-Based Audio Recognition. This paper also uses a recurrent neural network (RNN) model for comparing with CNN in classification performance. RNN is usually used to process a lot of sequence data $\{x_1, x_2, \ldots x_t\}$ and is widely used in natural language processing (NLP), speech recognition, translation, and so on. Unlike CNN, RNN has a memory function for time series, which can capture the connection and difference between the characteristics of this time point and the previous time point. RNN can be concluded as

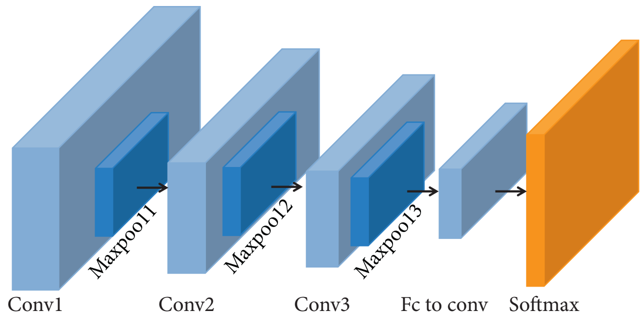

Figure 4: CNN architecture used in this paper.

Table 1: Parameters of our 3 layers CNN.

Block	Layer	Filter size	Filters (layer number)	Stride (step number)
Conv1 block	Conv1 maxPool1	20 ∗ 8 2 ∗ 2	64	2 2
Conv2 block	Conv2 maxPool2	10 ∗ 4 2 ∗ 2	64	2 2
Conv3 block	Conv3 maxPool3	5 ∗ 2 2 ∗ 2	64	1 2

Table 2: Parameters of our 5 layers CNN.

Block	Layer	Filter size	Filters (layer number)	Stride (step number)
Conv1 block	Conv1 maxPool1	20 ∗ 8 2 ∗ 2	64	2 2
Conv2 block	Conv2 maxPool2	10 ∗ 4 2 ∗ 2	64	2 2
Conv3 block	Conv3 maxPool3	5 ∗ 2 2 ∗ 2	64	1 2
Conv4 block	Conv4 maxPool4	2 ∗ 2 2 ∗ 2	64	1 2
Conv5 block	Conv5 maxPool5	2 ∗ 2 2 ∗ 2	64	1 2

ordinary RNN and special RNN. Special RNN refers to replacing ordinary short-term memory network unit (LSTM) or gated cycle unit (GRU) with ordinary RNN unit. In this paper, the LSTM unit is used for sequence identification. As shown in Figure 5(a), from left to right in a LSTM unit structure are the forget gate, the input gate, and the output gate. The output gate controls the output of information and filters the information to be output.

The expression at time t is shown in formulae (8) to (13). x_t represents the input information, h_{t-1} and h_t, respectively, represent the hidden coefficient output of the previous LSTM unit and the new LSTM unit. C_{t-1} and C_t represent the information output by the previous unit and the new information output by the unit, f_t represents the information that the unit selectively forgets, which is multiplied with the weight W_f and adds to the coefficient b_f. i_t and C_t' represent the memory information, and then are merged into C_t, which represents the final output state shown in formula (11). O_t represents the state of the three gates. Then h_t is obtained by the multiplication of O_t and $\tanh(c_t)$.

LSTM can make up for the shortcomings of ordinary RNN's short memory and uncontrollable storage content. The operation parameters of LSTM are less than the CNN parameters mentioned above, and the operation is faster, which helps avoid the gradient disappearance and explosion problems in typical RNN [27]. The RNN structure model is shown in Figure 5(b). According to the input audio spectrogram, the display dimension is $t * f = 298 * 40$ (where t represents time and f represents frequency). The input data x_t is input to the No.t RNN unit with the hidden unit h_{t-1} of the time frame output. Since one data input frame number is 298, the RNN model has 298 LSTM units, $x_0 \sim x_{297}$ represents the input feature, and y represents the output result (see Figure 5(b)):

$$f_t = \theta\left(W_f \cdot [h_{t-1}, x_t] + b_f\right), \tag{8}$$

$$i_t = \theta\left(W_i \cdot [h_{t-1}, x_t] + b_i\right), \tag{9}$$

$$C_t' = \tanh\left(W_c \cdot [h_{t-1}, x_t] + b_c\right), \tag{10}$$

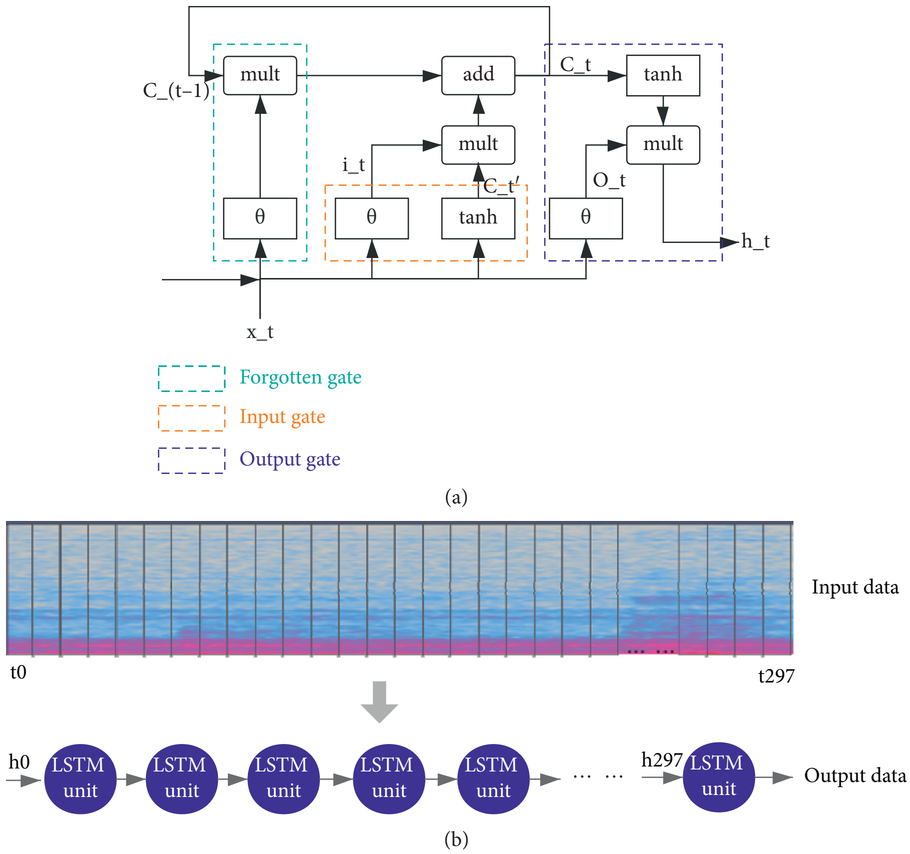

Figure 5: RNN-based audio recognition. (a) LSTM cell structure. (b) LSTM neural network model.

$$C_t = f_t * C_{t-1} + i_t * C_t', \tag{11}$$

$$O_t = \theta(W_o \cdot [h_{t-1}, x_t] + b_o), \tag{12}$$

$$h_t = O_t * tanh(c_t). \tag{13}$$

3. Results and Discussion

3.1. Database. In our experiments, sleep sounds are collected from 32 volunteers (including 16 normal people and 16 OSAHS patients) through a microphone for a whole night (8 h) at a sampling frequency of 16 KHz. The device can be used at home. Snoring sounds were extracted from breathing sounds and background noise through the endpoint detection technology [27], each case of which lasting 3 s. The training samples consisted of randomly selected 16 volunteers' snoring sounds (5 normal people and 11 OSAHS patients). We classified snoring data from OSAHS patients' sleeping sounds in the whole night according to the time period displayed by the PSG picture into four categories for ready: (1) Snoring data before each apnea event; (2) Snoring data in each apnea event; (3) Snoring data after each apnea event; (4) The other snoring data in OSAHS patients' snoring data in a whole sleeping night.

3.2. Experimental Evidence of Data Selection. In order to verify that the snoring data which during the apnea events and behind of the apnea events have obvious characteristics differences from normal snoring data extracted from 5 normal people while sleeping at night [20], we implemented four sets of comparative experiments (see Table 3): (1) Snoring data before, during, and after apnea events and normal snoring data extracted from normal people's sleeping sounds while at night as two-class sample sets; (2) Snoring data during and after apnea events and normal snoring data extracted from normal people's sleeping sounds in the whole night as two-class sample sets; (3) Snoring data before apnea events and normal snoring data extracted from normal people's sleeping sounds in the whole night as two-class sample sets; (4) All of the snoring data extracted from OSAHS patients and normal snoring data extracted from normal people's sleeping sounds in the whole night as two-class sample sets. Each set of data is about 10000 cases and the number ratio of the two categories is 1 : 1.

Conclusions can be drawn from this experiment: the data characteristics of snoring data during the apnea events and behind of the apnea events have the most obvious differences from normal snoring data extracted from normal people's whole sleeping night.

3.3. Experiment. Based on the above experimental evidence in Section 3.2, the positive sample (normal snoring) is the data from the 5 normal people's whole night snoring, and the negative sample (abnormal snoring) is the data from the

Table 3: Results of four groups of experiments.

Test group (number)	Sensitivity	Specificity	Precision	Accuracy
1	0.75	0.75	0.50	0.60
2	0.83	0.84	0.82	0.82
3	0.42	0.53	0.43	0.48
4	0.40	0.50	0.40	0.45

Table 4: Data distribution.

Subjects	16 people		16 people
Class	Training set	Validation set	Test set
Normal snoring(case)	5156	516	2065
Abnormal snoring (case)	5156	516	2065

OSAHS patients' whole night snoring, which were taken from the apnea event's middle and behind (see Figure 2). The snoring data of the remaining 16 volunteers were used to test the generalization performance of the model (see Table 4).

3.4. Environment. The experiment in this article is operated in the ubuntu 5.4.0 environment, rtx2048 graphics card. The model is built using TensorFlow 2.0 framework. The RNN and CNN network parameters are shown in Section 2.3.

3.5. Evaluation. The experimental results are evaluated by 5 methods which are accuracy, sensitivity, specificity, precision, and F1-score. The expressions of these methods are given by formulae (14) to (18). In these formulas, TP presents the number of positive samples that were actually identified as positive samples; FN presents the number of the positive samples that were identified as the negative samples falsely; TN presents the number of negative samples that were correctly identified as the negative sample; FP presents the number of the negative samples that were identified as the positive sample falsely:

$$\text{accuracy} = \frac{TP + TN}{TP + TN + FP + FN}, \tag{14}$$

$$\text{precision} = \frac{TP}{TP + FP}, \tag{15}$$

$$\text{sensitivity} = \text{recall} = \frac{TP}{TP + FN}, \tag{16}$$

$$\text{specificity} = \frac{TN}{TP + FP}, \tag{17}$$

$$F1 - \text{score} = \frac{2 * \text{precision} * \text{recall}}{\text{precision} + \text{recall}}, \tag{18}$$

3.6. Comparison of Three Feature Extraction Methods and Three Model Experiment Results. Table 5 shows the accuracy of the model test combined with the three feature extraction methods (MFCC, LPCC, LPMFCC) and the three models (3-layer CNN, 5-layer CNN, and LSTM). A horizontal comparison found that the classification effect of 5-layer CNN is the same as 3-layer CNN, and LSTM performs better than CNN in the connection and comparison of time series data features, and LSTM can make up for the shortcomings of ordinary RNNs with a short memory and uncontrollable storage content [27]. As shown in Table 5 and Figure 6, through longitudinal comparison, it is found that the feature extraction effect from the best to the worst are MFCC, LPMFCC, LPCC. This is because the LPCC algorithm has a linear prediction function for time series and can obtain more information from speech recognition [28], while MFCC maps the speech frequency to a nonlinear mel filter bank and converts it to the cepstrum domain [29]. The features extracted from the neighboring frames are almost independent and suitable for consonant recognition. The snoring sound produced by a person during sleep is caused by the blockage of the upper respiratory tract of the person due to some reason (rhinitis or pharyngitis or even cerebral nerves [30]), which causes the airflow to hit the soft tissue and generate large vibrations, like consonant. Therefore, the MFCC is more suitable for extracting a feature from snoring data in this paper.

3.7. Discussion of the Application. According to the snoring sounds data related to apnea events in 11 OSAHS patients and the whole night (about 8 hours) snoring sounds of 5 normal subjects as the test set, the LSTM model has a better classification effect than CNN, calculating the number of two types of snoring sounds from 16 volunteers' whole night after they were entered into the stored LSTM model for binary classification. Finally, calculating the AHI value according to the definition of AHI (number of sleep apnea per hour). As shown in formula (19), where AB represents the number of snoring sounds related to the apnea event (Abnormal snoring) recognized by the system, 2 represents 1 case of middle snoring sound and 1 case of posterior snore sound, and SH represents the length of sleep throughout the night. According to the AHI value, the severity of OSAHS patients can be obtained, which is divided into slight ($5 < \text{AHI} \leq 15$), moderate ($15 < \text{AHI} \leq 30$), and serious ($\text{AHI} > 30$) [31].

Table 5: Accuracy of three feature extraction methods and three models.

Feature extraction method	Evaluation	3 layers-CNN	5 layers-CNN	LSTM
MFCC	Sensitivity	0.83	0.82	0.84
	Specificity	0.84	0.81	0.91
	Precision	0.82	0.84	0.91
	Accuracy	0.82	0.85	0.87
	F1-score	0.82	0.83	0.87
LPMFCC	Sensitivity	0.58	0.6	0.67
	Specificity	0.64	0.67	0.72
	Precision	0.62	0.64	0.71
	Accuracy	0.61	0.63	0.69
	F1-score	0.6	0.62	0.69
LPCC	Sensitivity	0.54	0.56	0.56
	Specificity	0.6	0.6	0.62
	Precision	0.58	0.58	0.6
	Accuracy	0.57	0.58	0.59
	F1-score	0.56	0.57	0.58

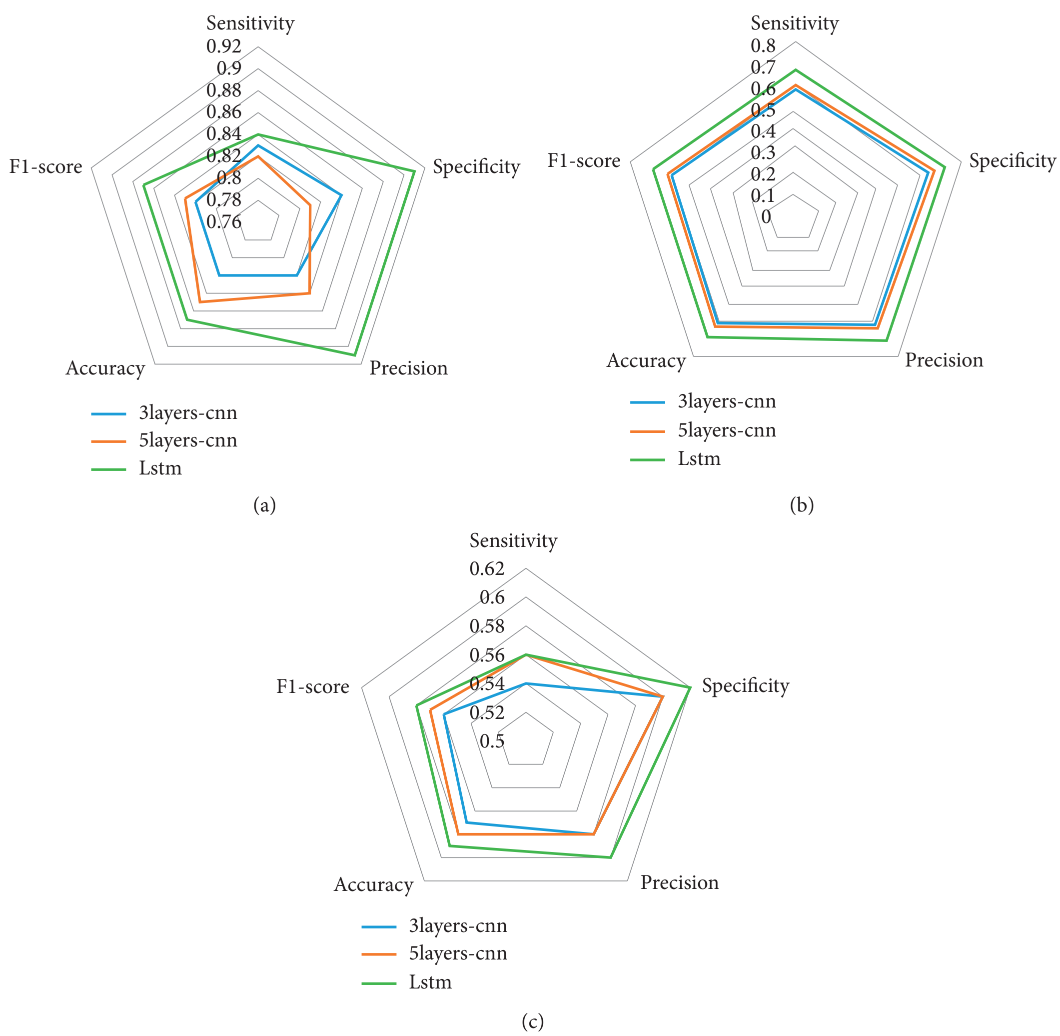

Figure 6: Accuracy of three feature extraction methods and three models. (a) Accuracy of MFCC method. (b) Accuracy of LPMFCC method. (c) Accuracy of LPCC method.

Table 6: Comparison of the OSAHS degree of the test result and the OSAHS degree data output in PSG.

Subject number	AHI (PSG)	AHI (test)	SQRT-AHI	Degree (PSG)	Degree (test)
01	5	2	0.75	0	0
02	4.7	0.37	1.08	0	0
03	1.7	6	1.07	0	1
04	2.8	1.7	0.28	0	0
05	1.5	1.7	0.05	0	0
06	41.9	50.3	2.1	3	3
07	25.3	28.1	0.7	2	2
08	7.2	8	0.2	1	1
09	31.7	31.4	0.075	3	3
10	8.6	41	8.1	1	3

As shown in Table 6(0 means no OSAHS, 1 means slight, 2 means moderate, and 3 means serious), 10 patients were tested, and the difference between the AHI which was calculated by test data and the AHI obtained by the patient through PSG actually is represented by squared different (SORT-AHI) shown in Table 6. It can be known from the table that the model has better recognition performance for the severity of OSAHS.

$$AHI = \frac{AB}{2}/SH. \tag{19}$$

4. Conclusions

In this study, the detection of OSAHS was quantified and evaluated using the feature extraction method and deep learning algorithm. We compared the differences in detection accuracy between three feature extraction methods and three neural networks. It is found that the MFCC performs best in feature extraction and the LSTM performs better than the CNN in classification, and the combination of MFCC and LSTM performed the best, in which the accuracy of classification reached 0.87. In addition, the model can not only judge whether someone else has OSAHS through snoring but also can detect the severity degree by AHI coefficient (see Table 5), and the model has solved the problem that PSG has. However, the accuracy of the system in this study is not very well. We are going to improve the performance of the system by producing a better neural network model in the feature.

Data Availability

Data are available upon request to the corresponding author.

Conflicts of Interest

The authors declare that they have no conflicts of interest.

Acknowledgments

The dataset was supported by the Affiliated Hospital of Hangzhou Normal University. This project was also supported by the grants from Zhejiang Key Research and Development Project (2019C03088) and Zhejiang Province Commonweal Projects (LGG18F010010).

References

[1] T. Mao, J. Zhang, Y. Qiao et al., "Uncovering synergistic mechanism of Chinese herbal medicine in the treatment of atrial fibrillation with obstructive sleep apnea hypopnea syndrome by network pharmacology," *Evidence-Based Complementary and Alternative Medicine*, vol. 2019, Article ID 8691608, 13 pages, 2019.

[2] L. Zhou, R. Ouyang, H. Luo et al., "Dysfunction of nrf2-ARE signaling pathway: potential pathogenesis in the development of neurocognitive impairment in patients with moderate to severe obstructive sleep apnea-hypopnea syndrome," *Oxidative Medicine and Cellular Longevity*, vol. 2018, Article ID 3529709, 15 pages, 2018.

[3] H.-W. Feng, T. Jiang, H.-P. Zhang et al., "Comparisons of thyroid hormone, intelligence, attention, and quality of life in children with obstructive sleep apnea hypopnea syndrome before and after endoscopic adenoidectomy," *BioMed Research International*, vol. 2015, Article ID 523716, 6 pages, 2015.

[4] E. Z. Osman, J. Osborne, P. D. Hill, and B. W. V. Lee, "Snoring assessment: do home studies and hospital studies give different results?" *Clinical Otolaryngology and Allied Sciences*, vol. 23, no. 6, pp. 524–527, 1998.

[5] L. Cai, J. Le, X. Ruan, and M. Du, "OSA patient monitoring system based on the Internet of Things framework," in *Proceedings of the 2019 4th International Conference on Smart and Sustainable Technologies (Splitech)*, pp. 12–15, Split, Croatia, August 2019.

[6] A. Garde, P. Dekhordi, C. L. Petersen et al., "Detecting obstructive sleep apnea in children by self-affine visualization of oximetry," in *Proceedings of the 2017 39th Annual International Conference of the IEEE Engineering in Medicine and Biology Society (EMBC)*, pp. 3757–3760, Seogwipo, Republic of Korea, July 2017.

[7] J. Kim, T. Kim, D. Lee, J.-W. Kim, and K. Lee, "Exploiting temporal and nonstationary features in breathing sound analysis for multiple obstructive sleep apnea severity classification," *BioMedical Engineering OnLine*, vol. 16, no. 1, 6 pages, 2017.

[8] J. Volák, D. Koniar, L. Hargaš, F. Jablončík, N. Sekelová, and P. Ďurdík, "RGB-D imaging used for OSAS diagnostics," in *Proceedings of the 2018 ELEKTRO*, pp. 1–5, Mikulov, Czech Republic, May 2018.

[9] Y. Castillo-Escario, I. Ferrer-Lluis, J. M. Montserrat, and R. Jane, "Entropy analysis of acoustic signals recorded with a smartphone for detecting apneas and hypopneas: a comparison with a commercial system for home sleep apnea diagnosis," *IEEE Access*, vol. 7, pp. 128224–128241, 2019.

[10] G. B. Salah, K. Abbes, C. Abdelmoula et al., "Obstructive sleep apnea OSA detection through esophageal pressure pes," in *Proceedings of the IEEE International Conference on Design & Test of Integrated Micro & Nano-Systems (DTS)*, pp. 1–4, Gammarth-Tunis, Tunisia, April 2019.

[11] A. Yilmaz, M. A. Mutlu, M. Günay et al., "Analysis of portable apnea devices: comparison with polysomnographic(psg) records," in *Proceedings of the 2019 27th Signal Processing and Communications Applications Conference (SIU)*, pp. 1–4, Sivas, Turkey, April 2019.

[12] K. Srividya, M. Hemamalini, K. Balaswathi et al., "Diagnosing the obstructive sleep APNEA from multi parameter values," in *Proceedings of the 2018 International Conference on Communication and Signal Processing (ICCSP)*, pp. 0616–0619, Chennai, India, April 2019.

[13] H. Ankishan and A. T. Tuncer, "A new portable device for the snore/non-snore classification," in *Proceedings of the International Conference on Engineering and Technology*, Kayseri, Turkey, February 2017.

[14] S. J. Lim, S. J. JangJ. Y. Lim et al., Classification of snoring sound based on a recurrent neural network," *Expert Systems with Applications*, vol. 123, pp. 237–2451, 2019.

[15] B. Arsenali et al., "Recurrent neural network for classification of snoring and non-snoring sound events," in *Proceedings of the 2018 40th Annual International Conference of the IEEE Engineering in Medicine and Biology Society (EMBC)*, pp. 328–331, Honolulu, HI, USA, July 2018.

[16] P. Temrat, Y. Jiraraksopakun, A. Bhatranand et al., "Suitable feature selection for OSA classification based on snoring sounds," in *Proceedings of the 2018 15th International Conference on Electrical Engineering/Electronics, Computer, Telecommunications and Information Technology (ECTI-CON)*, pp. 396–399, Chiang Rai, Thailand, July 2018.

[17] T. Emoto, U. R. Abeyratne, K. Kawano, T. Okada, O. Jinnouchi, and I. Kawata, "Detection of sleep breathing sound based on artificial neural network analysis," *Biomedical Signal Processing and Control*, vol. 41, pp. 81–89, 2018.

[18] L. Wen-Yen, C. Wen-Cheng, S. Tsu-Hui, S. Guang-Ming, L. Chin-Shan, and L. Ming-Yih, "Realization of a CORDIC-based plug-in accelerometer module for PSG system in head position monitoring for OSAS patients," *Journal of Healthcare Engineering*, vol. 2017, Article ID 4728187, 9 pages, 2017.

[19] B. Daurai, P. Nayak, and R. P. Mudhalwadkar, "Sleep physiological parameter measurement for breath, chest and abdomen effort to detect apnea hypopnea," in *Proceedings of the 2017 International Conference on Intelligent Computing and Control (I2C2)*, Coimbatore, India, June 2017.

[20] A. Winursito, R. Hidayat, and A. Bejo, "Improvement of MFCC feature extraction accuracy using PCA in Indonesian speech recognition," in *Proceedings of the 2018 International Conference on Information and Communications Technology (ICOIACT)*, pp. 379–383, Yogyakarta, Indonesia, March 2018.

[21] P. Peng, Z. He, and L. Wang, ".“Automatic classification of microseismic signals based on MFCC and GMM-HMM in underground mines," *Shock and Vibration*, vol. 2019, Article ID 5803184, 9 pages, 2019.

[22] K. Daqrouq and K. Y. Al Azzawi, "Average framing linear prediction coding with wavelet transform for text-independent speaker identification system," *Computers and Electrical Engineering*, vol. 38, no. 6, pp. 1467–1479, 2012.

[23] H. Yanagisawa, T. Yamashita, and H. Watanabe, "A study on object detection method from manga images using CNN," in *Proceedings of the 2018 International Workshop on Advanced Image Technology (IWAIT)*, pp. 1–4, Chiang Mai, Thailand, January 2018.

[24] X. Lin, J. Liu, and X. Kang, "Audio recapture detection with convolutional neural networks," *IEEE Transactions on Multimedia*, vol. 18, no. 8, pp. 1480–1487, 2016.

[25] C. Yang, W. Jiang, and Z. Guo, "Time series data classification based on dual path CNN-RNN cascade network," *IEEE Access*, vol. 7, pp. 155304–155312, 2019.

[26] O. A. Sercan and M. Kliegl, "Convolutional neural networks for small-footprint keyword spotting," Submitted on 15 Mar 2017 (v1), last revised 4 Jul 2017.

[27] D. Wu, Z. Tao, and Y. Wu, "Speech endpoint detection in noisy environment using Spectrogram Boundary Factor," in *Proceedings of the 2016 9th International Congress on Image and Signal Processing, BioMedical Engineering and Informatics (CISP-BMEI)*, pp. 964–968, Datong, China, October 2016.

[28] T. R. J. Kumari and H. S. Jayanna, "Comparison of LPCC and MFCC features and GMM and GMM-UBM modeling for limited data speaker verification," in *Proceedings of the 2014 IEEE International Conference on Computational Intelligence and Computing Research*, pp. 1–6, Coimbatore, India, December 2014.

[29] S. Misra, T. Das, P. Saha, U. Baruah, and R. H. Laskar, "Comparison of MFCC and LPCC for a fixed phrase speaker verification system, time complexity and failure analysis," in *Proceedings of the 2015 International Conference on Circuits, Power and Computing Technologies [ICCPCT-2015]*, pp. 1–4, Nagercoil, India, March 2015.

[30] V. Koka, S. Baron, D. Abedipour, V. Latournerie, and P. El Chater, "EK sign: a wrinkling of uvula and the base of uvula in obstructive sleep apnea-hypopnea syndrome," *Sleep Disorders*, vol. 2015, pp. 1–4, 2015.

[31] C. Zheng, H. Song, S. Wang et al., "Serum uric acid is independently associated with risk of obstructive sleep apnea-hypopnea syndrome in Chinese patients with type 2 diabetes," *Disease Markers*, vol. 2019, Article ID 4578327, 6 pages, 2019.

Hindawi
Journal of Healthcare Engineering
Volume 2020, Article ID 8829219, 8 pages
https://doi.org/10.1155/2020/8829219

Research Article

Clinical Named Entity Recognition from Chinese Electronic Medical Records Based on Deep Learning Pretraining

Lejun Gong,[1,2] **Zhifei Zhang**,[1] **and Shiqi Chen**[1]

[1]*Jiangsu Key Lab of Big Data Security & Intelligent Processing, School of Computer Science, Nanjing University of Posts and Telecommunications, Nanijing 210023, China*
[2]*Zhejiang Engineering Research Center of Intelligent Medicine, Wenzhou 325035, China*

Correspondence should be addressed to Lejun Gong; glj98226@163.com

Received 14 August 2020; Revised 26 October 2020; Accepted 2 November 2020; Published 24 November 2020

Academic Editor: Jiafeng Yao

Background. Clinical named entity recognition is the basic task of mining electronic medical records text, which are with some challenges containing the language features of Chinese electronic medical records text with many compound entities, serious missing sentence components, and unclear entity boundary. Moreover, the corpus of Chinese electronic medical records is difficult to obtain. *Methods*. Aiming at these characteristics of Chinese electronic medical records, this study proposed a Chinese clinical entity recognition model based on deep learning pretraining. The model used word embedding from domain corpus and fine-tuning of entity recognition model pretrained by relevant corpus. Then BiLSTM and Transformer are, respectively, used as feature extractors to identify four types of clinical entities including diseases, symptoms, drugs, and operations from the text of Chinese electronic medical records. *Results*. 75.06% Macro-*P*, 76.40% Macro-*R*, and 75.72% Macro-*F*1 aiming at test dataset could be achieved. These experiments show that the Chinese clinical entity recognition model based on deep learning pretraining can effectively improve the recognition effect. *Conclusions*. These experiments show that the proposed Chinese clinical entity recognition model based on deep learning pretraining can effectively improve the recognition performance.

1. Background

In recent years, medical informatization has produced a large number of electronic medical records. The electronic medical record not only completely preserves the detailed information of the patients' diagnosis and treatment process but also has the advantages of regular writing format, convenient retrieval, and storage, and it can better help telemedicine further. In addition, the rapid development of a large number of online consultation websites and cases discussion forums will also produce a large number of disease question and answer information. These medical texts are in the same form as electronic medical records. These data make up a very large amount of medical data resources.

Electronic medical records (EMR) record various symptoms and examination measures taken by patients from before admission to hospitalization and that medical personnel provides based on examination results such as disease diagnosis and treatment methods as medical resources constructed by professionals. As the core data of medical information system, how to make use of the large amount of potential medical information contained in electronic medical records has become one of the hot research directions. But electronic medical records are not fully structured data. Semistructured or unstructured free text data make up the majority. In order to convert these unstructured data into structured form that can be recognized by computer, it is necessary to use natural language processing technology to conduct text mining. As the basic task of text mining information extraction, the types of clinical entities to be recognized mainly include disease, symptoms, operations taken by medical personnel (including inspection operations and treatment operations), and drugs. Although the research on Chinese named entity recognition has been going on for some time, most of the researches focus on the open field. However, some studies have shown that the density of entity distribution in Chinese EMRs is much higher than that in open field texts. The proportion of entity characters in the corpus of Chinese EMRs is nearly twice that of the general Chinese corpus, which indicates that Chinese EMRs are a kind of knowledge-intensive text [1], and the data has considerable research value. But this density also creates more obstacles to the study of clinical named entity recognition from EMRs in Chinese. Since it is the entity recognition of Chinese electronic medical record, this paper keeps the entity in Chinese medical record as Chinese character format. This task has just started. In addition, it still has the following difficulties [2].

(1) Clinical entities have various types and a large number, and there are new entities with unregistered words, such as unregistered disease, drug, and inspection, which make it difficult to build a comprehensive clinical dictionary and obtain disease dictionary, drug dictionary, or inspection dictionary.
(2) Clinical entities are divided into simple entities and complex entities with relatively complex structure. The length of medical record entities in EMR is variable, and a large number of clinical entities are longer than common entities. There are a lot of nesting, alias, and acronym in clinical entities.
(3) In different parts of EMR, the extension of clinical entity is different, and there is fuzzy classification in category labeling. The boundary between different named entities is not clear, and the names of clinical manifestations often appear in the names of diseases. There are a lot of mutual inclusion and crossover phenomenon. For example, “上呼吸道感染” is generally considered to be the disease, but, in some cases, it also appears as a symptom.

The recognition of named entity in EMR has been studied in foreign countries. Because EMR involves more professional knowledge, the cost of corpus construction is higher. The informatics for Integrating Biology and the Bedside (I2B2) organized the multiple records related tasks and issued the relevant corpus and a number of shared tasks since 2006 [3]. The task of concept recognition and relation extraction evaluation of I2B2 2010 is the first to systematically classify English electronic medical record name entities. This classification refers to the semantic type defined by UMLS, which divides EMR entities into three categories, namely, medical problems (including diseases and symptoms), treatment, and examination.

Named entity recognition, as the key task of text data mining, has been the research foundation and hotspot of natural language processing. Named entity recognition in the general field mainly includes names, places, organizations, time expressions, and numerical expressions. In the field of biomedicine, most of the current research focuses on the identification of genes, proteins, cells, and other entities in the English medical literature. Although the specific objects identified are different, a large number of entity identification methods in the general field can still be applied to the biomedical field. These include early approaches based on the combination of dictionaries and rules and approaches based on machine learning.

The method based on the combination of dictionary and rule will match the dictionary and text firstly. Then it combines with the formulated rules for postprocessing and normalization. Its performance depends on the size of the dictionary and the quality of the rules [4]. Due to the variety of clinical entities and its strong professionalism, the construction of dictionaries and the formulation of rules need amount manpower, which is not only time-consuming, but also not portabl e. Therefore, dictionaries and rules are often used as auxiliary means in the task of named entity recognition.

In recent years, machine learning has been applied to named entity recognition [5, 6], such as maximum entropy (ME), conditional random field (CRF), support vector machine (SVM), and structural support vector machine (SSVM). Multiple deep learning methods are also applied to entity recognition tasks. For example, Recurrent Neural Networks (RNN) and Long Short-Term Memory Networks (LSTM). In addition, models combining deep learning with traditional machine learning have also been widely used.

Named entity recognition is often regarded as a sequential annotation task. Traditional machine learning methods, such as CRF [7], can achieve good performance in sequence annotation tasks but rely heavily on manually selected characteristics. By contrast, deep learning could automatically learn features, but a large amount of training data is needed to achieve excellent recognition effect [8, 9].

Related work of Chinese EMR is developing rapidly [10, 11]. Compared with English corpus, Chinese text has fuzzy word boundary and no obvious segmentation mark, so it is difficult to study the entity recognition [12]. The selection of features in traditional machine learning will directly affect the effect of entity recognition, so most studies focus on the construction and selection of different features. Lei et al. [13] compared the combination of CRF, SSVM, SVM, and ME with a variety of characteristics and recognized medical problems, examination, treatment, and drugs in the admission records and discharge records. Wang et al. [14] used the character position information and short clauses to reach the *F*1 value of 95.12% in the self-labeled Chinese medicine text corpus. Literature [15] studies the influence of multifeature combination such as linguistic symbol feature, part of speech feature, keyword feature, and dictionary feature on CRF sequence annotation.

There are also relevant studies on Chinese clinical entity recognition using the deep learning method [16–18], whose model is basically the sequence model RNN and its variants.

It is worth mentioning that Yang et al. [19] combined the characteristics of Chinese electronic language structure and, with the help of the guidance of professional medical personnel, combined EMR label specification in English and made a detailed EMR in Chinese named entity and entity relationship labeling regulations and completed the natural language processing research in the field of EMR in Chinese basic work. In addition, there are some identification methods that combine deep learning with supervised learning [20, 21]. However, as far as we know, BiLSTM and Transformer [22] combined methods have not been applied to clinical Chinese-named entity recognition.

In view of the above problems, this study proposes a named entity recognition method for Chinese EMR based on pretraining. The method is based on word embedding pretraining and fine-tuning of entity recognition model pretrained by relevant corpus. BiLSTM and Transformer are, respectively, used as feature extractors to effectively recognize clinical entities in Chinese EMR.

2. Methods

The problem of Chinese clinical entity recognition can be transformed into sequence labeling. Sequence annotation problem is to determine the output tag sequence $B = b_1, \ldots, b_n (b_i \in L, 1 \le i \le n)$ for input sequence $A = a_1, a_2, a_3, \ldots, a_n$ and tag set L. Its essence is to classify each element in the input sequence according to its context.

There were two specific practices for implementing the deep learning pretraining mode: firstly, the input is initialized by the same field corpus pretraining EMR embedding and, secondly, the entity recognition model pretrained by relevant corpus is fine-tuning. We studied the effect of this model on the recognition of clinical entities as shown in Figure 1.

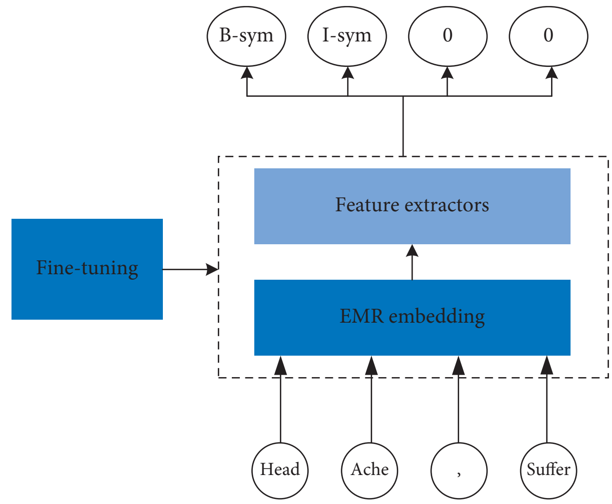

Figure 1: Pipeline of deep learning pretraining.

2.1. Datasets. Because of the protection policy of patient privacy in China, it is difficult to obtain electronic medical records in hospitals. Therefore, we got 1,064 respiratory records and 30,262 unrestricted records were crawled from the website (https://www.iiyi.com). 200 of the 1,064 respiratory department EMRs were manually annotated according to the annotation specification shown in Table 1 based on [19] and the semantic types of English I2B2 and UMLS, indicating four medical entities of disease, symptom, drug, and operation. Table 2 shows the distribution of training set and test set.

Skip-gram model of Word2vec was used to adopt the EMR word embedding from 30,262 sets of unmarked electronic medical records (115 MB), called the first dataset. In addition, in order to study the impact of word embedding language on downstream task, we also use the universal word embedding with 268G news corpus, called the second dataset.

For the sequential annotation task of entity recognition, the tag is composed of two parts: the entity category and the location in the entity. In this study, BIO representation is used to represent the entity category and the position of the entity and then character as the minimum annotation unit. In the BIO representation, B is at the beginning of the entity, I is inside the entity, and O is not an entity. Therefore, the labeled corpus contains 4 types of entities and 9 types of labels.

2.2. Pretraining. There is a pretraining with fine-tuning mode in addition to the character embedding of Chinese EMR. It is difficult to annotate the corpus of Chinese EMRs. In order to make full use of the resources of previous studies, it is used to fine-tune our recognition tasks based on a clinical entity recognition model (https://github.com/baiyyang/medical-entity-recognition) trained by medical data of CCKS2017 tasks. This model uses BiLSTM as feature extractor followed by CRF for sequence annotation. For the convenience of description, this paper calls it as BioModel.

Although the labeling target of BioModel is different from our task. However, Chinese EMR texts all have the same linguistic features, and the model's ability to learn this language feature can be well transferred to our task.

2.3. Bidirectional Long Short-Term Memory-Conditional Random Fields. In recent years, a variety of deep learning methods have been widely applied in named entity recognition tasks, usually using RNN model and its variants. RNN is theoretically capable of capturing remote context relationships, but, in practice, RNN cells often fail due to gradient disappearance or gradient explosion. Therefore, LSTM is usually used in practical applications.

LSTM uses a separate update gate Γ_u and a forget gate Γ_f, as well as an output gate Γ_o. The update gate selectively updates the state of the current moment, while the forget gate selectively forgets the state of the previous moment. And then the output gate controls the proportion of the output of the current state. Figure 2 depicts the internal structure of an LSTM cell [6]. The realization of LSTM is as follows:

$$\begin{aligned}
\widetilde{C}(t) &= \tanh\left(W_c[h(t-1), x(t)] + b_c\right), \\
\Gamma_u &= \text{sigmoid}\left(W_u[h(t-1), x(t)] + b_u\right), \\
\Gamma_f &= \text{sigmoid}\left(W_f[h(t-1), x(t)] + b_f\right), \\
\Gamma_o &= \text{sigmoid}\left(W_o[h(t-1), x(t)] + b_o\right), \\
C(t) &= \Gamma_u \widetilde{C}(t) + \Gamma_f C(t-1), \\
h(t) &= \Gamma_u * \tanh(C(t)).
\end{aligned} \tag{1}$$

In the named entity recognition task, simultaneous access to the context of the current moment can help predict

Table 1: Labeling rules.

Entity types	Definition	Medical entities
Disease	The diagnosis made by doctors to patients or entities ending with “病” or “症” are collectively referred to as diseases.	肺内隔离症
Symptoms	Symptoms of discomfort, abnormalities, normal or abnormal examination results, or an unhealthy state of the patient, as well as the patient’s self-reported history.	声音嘶哑、无结核病史
Drug	The specific drug name or class of drug given to the patient during treatment.	地塞米松、抗生素
Operation	This includes screening programs and treatments. A test item is given to a patient in order to discover, deny, confirm, and find out more about the disease. Treatment refers to the treatment procedures and interventions that are imposed on patients to solve the disease or relieve symptoms.	拍胸片、抗感染、胸腔穿刺术

Table 2: Distribution of entities among the training set and the test set.

Data	Disease	Symptoms	Drug	Operation	The total number of entities
Training set	701	2648	546	2138	6033
Test set	273	1043	208	918	2442

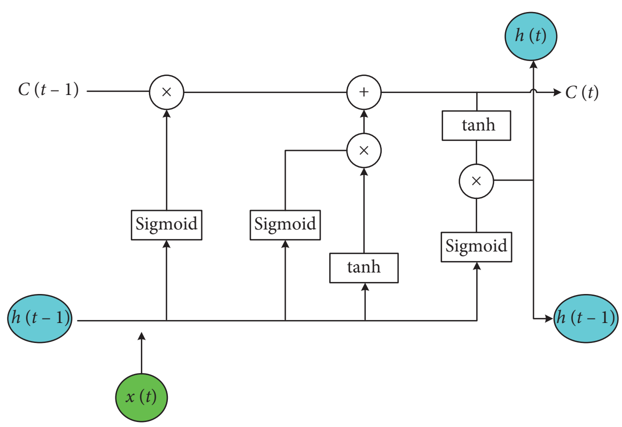

Figure 2: LSTM cell.

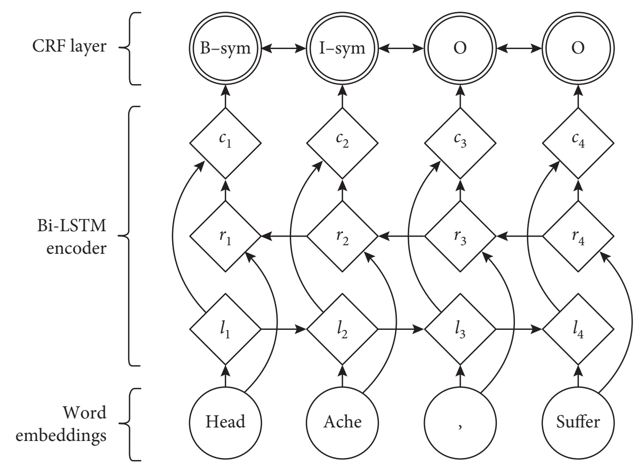

Figure 3: BiLSTM-CRF.

the current moment. However, LSTM’s hidden state $h(t)$ accepts only past information. Therefore, we use a bidirectional LSTM model to give the context of each state, using two independent hidden states from left to right and from right to left, while capturing past and future information.

BiLSTM converts the input sequence through the embedding layer into a vector sequence input into two LSTM networks and then contact the forward and reverse two hidden layer outputs into the Softmax layer for classification. However, LSTM can only learn the context relation of features but cannot directly learn the context relation of tags. Without the constraint of state transition, the model is likely to output a completely wrong tag sequence. Therefore, it is considered to replace Softmax layer with CRF layer. CRF is still responsible for sequence annotation, and BiLSTM is responsible for automatic feature selection. Figure 3 describes the BiLSTM-CRF model used in the clinical entity recognition.

2.4. Transformer-Conditional Random Fields. Although the structure of gate mechanism such as LSTM alleviates the problem of long-term dependence to some extent, LSTM is still unable to do anything for the special long-term dependence phenomenon. The calculation of LSTM is limited to sequence; that is, it can only be calculated in sequence from left to right or from right to left, and the loss of information in the process of sequential calculation is inevitable.

Transformer solves this problem by using the attention to reduce the distance between any two positions in the sequence to a constant. Therefore, Transformer, as a feature extractor, has a stronger learning ability than LSTM and has been widely used in the past two years.

As shown in Figure 4, Transformer is stacked with encoder and decoder, and, like all generation models, the output of the encoder is the input of the decoder [12]. All encoder blocks are structurally identical, but they do not share parameters. Each encoder block can be decomposed into two sublayers, composed of self-attention and Feed Forward Neural Network. After the data is passed through the self-attention module, the weighted feature vector Z is obtained and then sent to the next module of encoder block, namely, Feed Forward Neural Network, to obtain the output FFN (Z) of an encoder block.

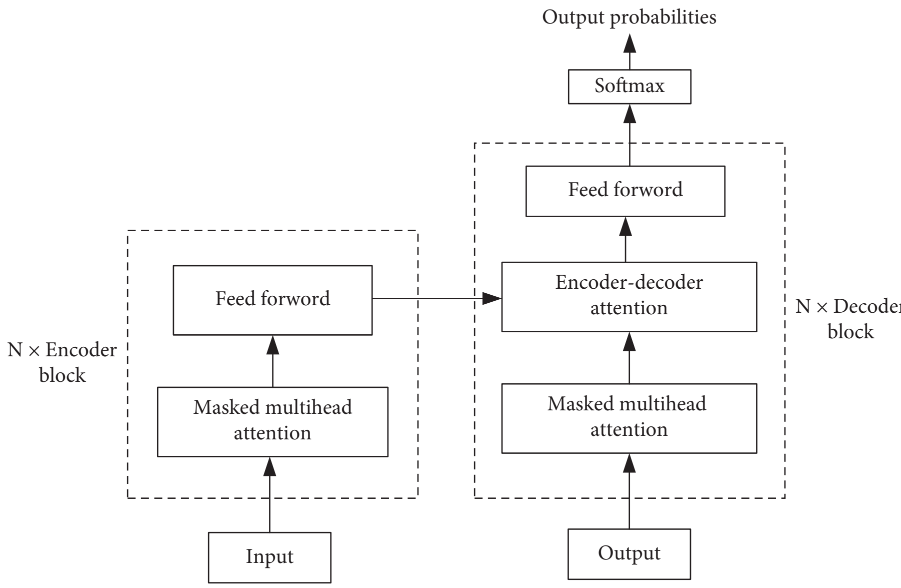

Figure 4: Transformer.

$$Z = \text{Attention}(Q, K, V) = \text{soft}\max\left(\frac{QK^T}{\sqrt{d_k}}\right)V, \qquad (2)$$

$$\text{FFN}(Z) = \max(0, ZW_1 + b_1)W_2 + b_2.$$

Among them, Q, K, and V are assumed to be composed of a series of <Q, K, V> data pairs. For any constituent element Q, the weight coefficient of each K corresponding to V can be obtained by calculating the similarity between the current element Q and other elements K, and then the weighted sum of V can be carried out to obtain the final attention value.

Decoder block has one more encoder-decoder attention than encoder. The two types of attention of decoder are used to calculate the weight of input and output, respectively. Self-attention is used to calculate the relationship between current output and preorder output. Encoder-decoder attention calculates the relationship between the current output and the encoder input eigenvector. In encoder-decoder attention, Q comes from the last output of decoder, and K and V come from the output of encoder.

Multihead self-attention represents the different ways of fusion of the target word and the semantic vector of other words in the text under various semantic scenes. Note that there are multiple sets of $Q/K/V$ weight matrices in the mechanism, each of which is randomly initialized, and after training, each set is used to embed the input word or the vector from the previous encoder/decoder into a different representation subspace.

3. Results and Discussion

In order to comprehensively consider the performance of the model on the whole dataset, macroaverage is adopted in this paper. Macroaverage refers to the arithmetic average of each kind of performance indicator, which can be divided into macroprecision (Macro-p), macrorecall (Macro-r), and Macro-$F1$ (Macro-$F1$).

$$\begin{aligned}
\text{Marco} - P &= \frac{\sum_{i=1}^{N_c} P_{\text{i}}}{N_c}, \\
\text{Marco} - R &= \frac{\sum_{i=1}^{N_c} R_{\text{i}}}{N_c}, \qquad (3) \\
\text{Marco} - F1 &= \frac{2 \times \text{Macro} - P \times \text{Macro} - R}{\text{Macro} - P + \text{Macro} - R},
\end{aligned}$$

N_{c} represents the total number of entity categories, P_{i} represents the precision of each category of entity, and R_{i} represents the recall of each category of entity.

In order to investigate the effect of BiLSTM-CRF embedding of different dimensions on the test set, we conducted this set of comparative experiments as shown in Table 3 using the first dataset as test dataset. From Table 3, if the dimension of word embedding is too small, the implied semantic information will be lost. If the dimension of word embedded is too large, it will bring noise. How to set the dimension of word embedding is related to the size and the language characteristics of the corpus.

In deep learning, the quality of word embedding has a great influence on the recognition results of deep neural network. In this study, the experiment effect of 150-dimension word embedding is the best. Therefore, two different word embeddings combined with BiLSTM-CRF and Transformer-CRF form the following four groups of experiments using the 150-dimension and the two types of dataset as shown in Table 4.

It can be seen from the results that EMR embedding has better common embedding than whatever model is used. Although the corpus size of EMR embedding is smaller than

Table 3: Comparison results of different dimensions.

Different dimensions	Marco-P (%)	Marco-R (%)	Marco-$F1$ (%)
Random embedding	69.52	69.70	69.38
50 embeddings	53.42	54.31	53.74
150 embeddings	**72.48**	**72.54**	**72.51**
300 embeddings	55.36	61.03	57.88

Table 4: Comparisons of different recognition models and different word embedding.

Models	Dataset	Marco-P (%)	Marco-R (%)	Marco-$F1$ (%)
BiLSTM-CRF + embedding	Second	68.37	70.84	69.58
BiLSTM-CRF + EMR embedding	**First**	**72.48**	**72.54**	**72.51**
Transformer-CRF + embedding	Second	52.70	69.50	59.90
Transformer-CRF + EMR embedding	First	52.70	72.10	60.70

that of common embedding, the strong relevance of EMR embedding to downstream tasks makes the effect of EMR embedding significantly better than that of embedding with universal corpus.

In addition, by comparing the experimental results of BiLSTM-CRF and Transformer-CRF, it can be found that although the feature extraction ability of Transformer is theoretically better than that of BiLSTM, the complex model structure of Transformer requires a large amount of training data for learning. With the case of fewer training samples, Transformer does not perform as well as BiLSTM.

To study the effectiveness of pretraining with the fine-tuning related entity recognition model, EMR embedding was adopted to BioModel fine-tuning aiming at the first dataset, and the medical entity recognition model was obtained, called BioModel-fine. As the basic network structure of BioModel is BiLSTM-CRF, the experimental control group has also used the BiLSTM-CRF network model embedding EMR. The performances of comparisons between pretraining and not pretraining is shown in Table 5.

BioModel has achieved 79% Macro-p, 80% Macro-r, and 80% Macro-$F1$ on its original test set in CCKS2017. However, the recognition target of its original corpus is different from ours. Using the first dataset as test data, BioModel could obtain 72.48% Macro-p, 72.54% Macro-r, and 72.51% Macro-$F1$. BioModel-fine model obtains 75.06% Macro-p, 76.40% Macro-r, and 75.72% Macro-$F1$. The more details of BioModel-fine model are as shown in Tables 5 and 6.

BioModel-fine is the model structure based on BioModel for pretraining. Compared with the above results without pretraining with fine tuning, fine-tuning can significantly improve the experimental results by utilizing the implied information learned by BioModel from its own training data. Further, $F1$ is used to measure the performances between pretraining and nonpretraining as shown in Figure 5.

From the above, we can see that the most different difference between the pretraining and nonpretraining modes is the disease. It is mainly because the BioModel also

Table 5: Comparisons between pretraining and not pretraining.

Models	Marco-P (%)	Marco-R (%)	Marco-$F1$ (%)
BioModel	72.48	72.54	72.51
BioModel-fine	**75.06**	**76.40**	**75.72**

Table 6: Performances of BioModel-fine.

Types	P (%)	R (%)	$F1$ (%)
Disease	77.07	75.09	76.07
Drug	70.81	71.15	70.98
Operation	79.28	80.56	79.91
Symptom	71.74	74.12	72.91
Average	**75.06**	**76.40**	**75.72**

recognized disease entity, and, for the disease entity, its word formation is similar, often ending with "病" and "症." Further, the positions appearing in the EMR are relatively stable, and these characteristics can be well learned based on the context. Relatively, the smallest difference between the pretraining and nonpretraining modes is the drug. This is because drug entities are mostly unfamiliar, and the word formation is quite different from the free text of other parts of the medical record. It is difficult to learn, and the drugs appearing in EMR from different departments tend to be quite different, and the recognition of drug is very difficult, in essence.

In addition, in Chinese electronic medical records, there are a large number of long entities and even super long entities with characters longer than 10, such as "双侧腋下扪及黄豆大小淋巴结" and "右肺中叶大片密度增高阴影." This paper also computes character length statistics for BioModel-fine entity recognition results with 4.63 average character. Though BiModel-fine model based on the deep neural network relies on the performance of adjacent words, the learned gate structure can retain more long-term effective information and has more advantages over the implied characteristics in long-term dependence. BioModel-fine has generally shown greater sensitivity to these medical entities with longer character lengths. Table 7 lists the five examples of identifying long entities by BiModel-fine model.

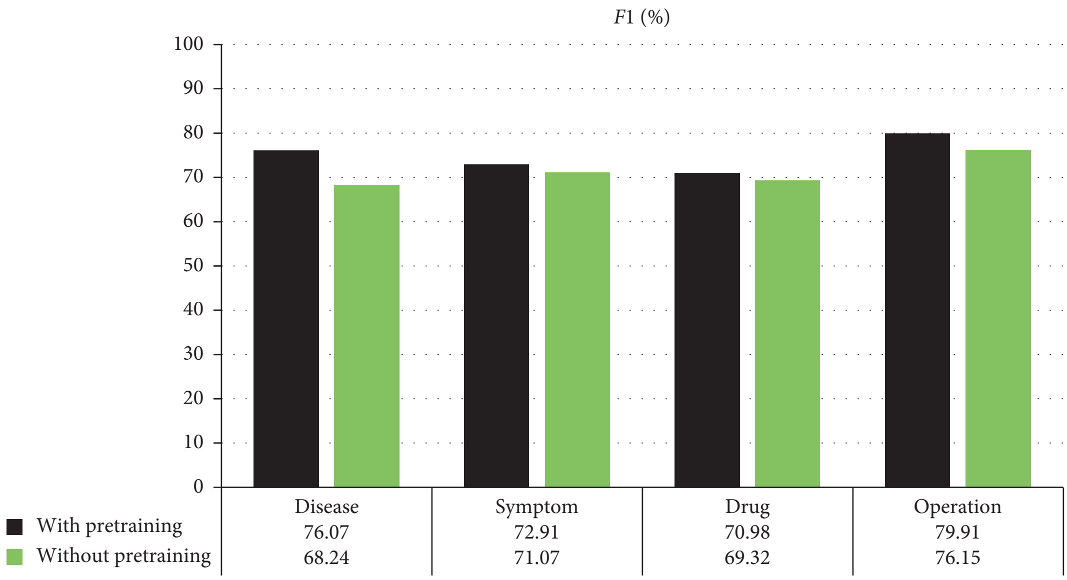

Figure 5: Two types of $F1$ comparison on entity.

Table 7: Identifying five examples of long entities by BiModle-fine model.

No	Identified medical entities
1	双侧腋下扪及黄豆大小淋巴结 (symptom)
2	右肺中叶大片密度增高阴影 (symptom)
3	两肺纹理间可见边界不清的粟粒样微小淡结节影 (symptom)
4	急性心肌梗塞 (disease)
5	结核 PCR 扩增实验 (operation)

4. Conclusions

In this study, a pretrained method for Chinese electronic medical record named entity recognition is proposed in view of the language features of Chinese EMR with many compound entities, serious missing sentence components, unclear entity boundary, and the difficulty in obtaining annotated corpus. Pretraining is divided into two steps. The first step is to adopt the same field of corpus pretraining word embedding and, respectively, use BiLSTM and Transformer as feature extractor to identify medical entities in Chinese electronic medical records. The second step is fine-tuning the named entity recognition model pretrained by other relevant corpus, so as to make full use of the existing annotated corpus and effectively improve the recognition effect of Chinese clinical entities when there are few annotated corpus. 75.06% Macro-P, 76.40% Macro-R, and 75.72% Macro-$F1$ could be achieved aiming at test dataset related to the Chinese electronic medical records. Experiment results show that the proposed Chinese clinical entity recognition model based on deep learning pretraining could effectively improve the recognition performance.

Data Availability

The data used to support the findings of this study are available from the corresponding author upon request.

Conflicts of Interest

The authors declare that they have no conflicts of interest.

Acknowledgments

This research was supported by the National Natural Science Foundation of China (Grant nos. 61502243, 61502247, and 61572263), Zhejiang Engineering Research Center of Intelligent Medicine under grant 2016E10011, China Postdoctoral Science Foundation (2018M632349), and Natural Science Foundation of the Higher Education Institutions of Jiangsu Province in China (no. 16KJD520003).

References

[1] L. B. Zhang, *Word Segmentation and Named Entity Mining Based on Semi Supervised Learning for Chinese EMR*, Dissertation, Harbin Institute of Technology, Harbin, China, 2014.

[2] W. Li, D. Zhao, L. Bo et al., "Combining CRF and rule based medical named entity recognition," *Application Research of Computers*, vol. 32, no. 4, pp. 1082–1086, 2015.

[3] O. Uzuner, B. R. South, S. Shen et al., "2010 i2b2/VA challenge on concepts, assertions, and relations in clinical text," *Journal of the American Medical Informatics Association*, vol. 18, no. 5, pp. 552–556, 2011.

[4] H. V. Cook and L. J. Jensen, "A guide to dictionary-based text mining," *Methods in Molecular Biology, Bioinformatics and Drug Discovery*, vol. 1939, pp. 73–89, 2019.

[5] X. Liu, S. Zhang, F. Wei, and M. Zhou, "Recognizing named entities in tweets," in *Proceedings of the 49th Annual Meeting of the Association for Computational Linguistics: Human Language Technologies*, Portland, USA, June 2011.

[6] Z. Huang, W. Xu, and K. Yu, "Bidirectional lstm-crf models for sequence tagging," 2015, http://arxiv.org/abs/1508.01991.

[7] Y. Zhang, X. W. Wang, Z. Hou et al., "Clinical named entity recognition from Chinese electronic health records via machine learning methods," *JMIR Medical Informatics*, vol. 6, no. 4, p. e50, 2018.

[8] S. Chowdhury, X. S. Dong, L. J. Qian et al., "A multitask bi-directional RNN model for named entity recognition on Chinese electronic medical records," *BMC Bioinformatics*, vol. 19, no. 17 Suppl, p. 499, 2018.
[9] Y. H. Wu, M. Jiang, J. B. Lei et al., "Named entity recognition in Chinese clinical text using deep neural networks," *Studies in Health Technology and Informatics*, vol. 216, pp. 624–628, 2015.
[10] Y. Wu, X. Yang, J. Bian, Y. Guo, H. Xu, and W. Hogan, "Combine factual medical knowledge and distributed word representation to improve clinical named entity recognition," *AMIA Annual Symposium Proceedings*, vol. 2018, pp. 1110–1117, 2018.
[11] Y. Xu, Y. Wang, T. Liu et al., "Joint segmentation and named entity recognition using dual decomposition in Chinese discharge summaries," *Journal of the American Medical Informatics Association*, vol. 21, no. e1, pp. e84–e92, 2014.
[12] H. Wang, W. Zhang, Q. Zeng, Z. Li, K. Feng, and L. Liu, "Extracting important information from Chinese operation notes with natural language processing methods," *Journal of Biomedical Informatics*, vol. 48, no. C, pp. 130–136, 2014.
[13] J. Lei, B. Tang, X. Lu, K. Gao, M. Jiang, and H. Xu, "A comprehensive study of named entity recognition in Chinese clinical text," *Journal of the American Medical Informatics Association*, vol. 21, no. 5, pp. 808–814, 2014.
[14] Y. Wang, Z. Yu, L. Chen et al., "Supervised methods for symptom name recognition in free-text clinical records of traditional Chinese medicine: an empirical study," *Journal of Biomedical Informatics*, vol. 47, no. 2, pp. 91–104, 2014.
[15] X. W. Zhang and Z. Li, "Chinese electronic medical record named entity recognition based on multi-feature fusion," *Software Guide*, vol. 16, no. 2, pp. 128–131, 2017.
[16] Y. B. Xia, J. L. Zhen, and Y. F. Zhao, "Electronic medical record named entity recognition based on deep learning," *Electronic Science and Technology*, vol. 31, no. 11, p. 31, 2018.
[17] F. Li, M. Zhang, B. Tian, B. Chen, G. Fu, and D. Ji, "Recognizing irregular entities in biomedical text via deep neural networks," *Pattern Recognition Letters*, vol. 105, pp. 105–113, 2018.
[18] Z. J. Liu, M. Yang, X. L. Wang et al., "Entity recognition from clinical texts via recurrent neural networks," *BMC Medical Informatics and Decision Making*, vol. 17, no. 2, p. 67, 2017.
[19] J. F. Yang, Y. Guan, B. He et al., "Chinese electronic medical record named entity and entity relationship corpus construction," *Journal of Software*, vol. 27, no. 11, pp. 2725–2746, 2016.
[20] Z. H. Huang, W. Xu, and k Yu, "Bidirectional LSTM-CRF models for sequence tagging," 2015, https://arxiv.org/abs/1508.01991.
[21] Q. K. Wei, T. Chen, R. F. Xu, Y. He, and L. Gui, "Disease named entity recognition by combining conditional random fields and bidirectional recurrent neural networks," *Database*, vol. 2016, 2016.
[22] A. Vaswani, N. Shazeer, N. Parmar et al., *Attention is all you need*, 2017, https://arxiv.org/abs/1706.03762.

Hindawi
Journal of Healthcare Engineering
Volume 2020, Article ID 8865264, 9 pages
https://doi.org/10.1155/2020/8865264

Research Article

Research on Standard Compliance Test Algorithm Based on Electronic Medical Records of Traditional Chinese Medicine Outpatients

Li He,[1] Zi Yi Zhou,[1] Fu Sheng Niu,[2] Yu Fan Yang,[2] Qiang Xu,[1] Chuan Biao Wen,[1] Tao Sun,[1] and Yue Luo [1]

[1]*School of Medical Information Engineering, Chengdu University of Traditional Chinese Medicine, Chengdu, Sichuan, China*
[2]*Chengdu University of Traditional Chinese Medicine, Institute of Digital Medicine, Chengdu, Sichuan, China*

Correspondence should be addressed to Yue Luo; luoyue@cdutcm.edu.cn

Received 25 June 2020; Revised 21 September 2020; Accepted 19 October 2020; Published 3 November 2020

Academic Editor: Xiwei Huang

Objectives. To effectively evaluate the compliance degree between the electronic medical records of Traditional Chinese Medicine (TCM) hospitals, as well as the information platform, and the related information standards of electronic medical records, a standard compliance testing scheme based on electronic medical records of TCM outpatients is proposed. *Methods*. This research selected the data of clinical outpatients accumulated in 10 years by the Digital Medicine Institute of Chengdu University of TCM and processed the data through security check and desensitization process. And then 28348 cases of processed electronic medical records of TCM outpatients were inputted into the standard compliance testing platform for assessment. The result was then outputted. *Results*. There are 924 cases among the 28348 that can be rated as five-star medical records, 84 cases four-star, 132 cases three-star, 12460 cases two-star, 13488 one-star, and 1260 cases zero-star through the integrity and standardization test. *Conclusion*. By the way of assessing the integrity and standardization of data, the standard compliance test algorithm scheme for electronic medical records of TCM outpatients introduced in this paper can solve the problems such as data unavailability caused by ununified codes and incomplete data in the data-sharing process and provides technical support for the construction of data standardization testing in electronic medical records of TCM outpatients.

1. Introduction

The Opinions of the CPC Central Committee and the State Council on Deepening the Reform of the Medical and Health System (hereinafter referred to as the Opinions) proposed to establish a practical and shared medical and health information system [1, 2] and employ artificial intelligence technology in promoting the construction of hospital informatization. In order to implement the Opinions, as well as to improve the quality of health services and management, it is urgently needed to establish and improve the health information standard system in our country, to unify information and code standards of various terms in the health field, and to enhance the corresponding exchange and technology standards. In addition, it is of crucial importance to cowork with related departments to strengthen the construction of information standardization and public information service platform [3].

With the deepening of medical and health system reform, the application of electronic medical record has become an inevitable trend of informatization construction in hospitals. In the new medical reform policy, the Ministry of Health and domestic medical institutions have shown certain understanding and attention in the standardization development of electronic medical records and revised successively about 150 health information standards such as the basic dataset of electronic medical record, specification for sharing document of electronic medical record, technical specification for hospital information platform based on electronic medical record [4], and so on. On the one hand, many hospitals have set up information system within hospitals with the development of national Jin Wei project, which laid a solid foundation for the study and application of electronic medical record in China; on the other hand, with the development of hospital HIS system in the direction of clinical information system (CIS), electronic medical record is getting more and more attention and a professional committee on it has been set up in China. At the same time, studies on standard compliance test methodology have appeared successively in scientific research filed. In light of the rapid development of computer network technology, it is of great value to transfer electronic medical records with the help of Internet technology. While at present, the development of electronic medical record in China has just started and the research related to compliance test for the electronic medical record digitization of TCM is yet to come. TCM is an important component of medical and healthcare, it is of great urgency to study the compliance test for electronic medical records of TCM digitization.

Therefore, this paper introduces the algorithm of standard compliance test into the health informatization construction of electronic medical records of TCM outpatients and tries to explore the specific medical and health informatization construction that fits China's national conditions. It has great guiding significance to the successful implementation of the standard compliance test for TCM electronic medical record. It can boost the application of information standards of TCM electronic medical records in our country, as well as promote the construction of efficient, unified, data-shared health informatization.

With the popularization of TCM electronic medical record system, the application of standards of TCM electronic medical records has become an important issue to be studied. And the research on standard compliance test for TCM electronic medical records information makes up the lack of health informatization construction and evaluates the application of information standards.

In addition to the characteristics of general electronic medical record, the electronic medical record of TCM outpatient has its own particularity, such as its unique contents, structure, and clinical information standardization [5]. TCM is different from Western medicine in dealing with clinical data from the aspects of disease classification, treatment, test, and so on. For example, TCM pays attention to holistic, dynamic, and personalized diagnosis and syndrome differentiation treatment, and clinical treatment combines four diagnoses, focusing more on the diagnosis and treatment of patients' overall function of their viscera, while Western medicine has a variety of biochemical and physical tests along with clear indicators of diagnostic results. Therefore, the electronic medical records of Western medicine are structured electronic medical records, while the electronic medical records of TCM are semistructured or unstructured. In light of these differences, the assessment for TCM electronic medical records' data as the test object can not only improve their integrity and standardization, but also the research on standard compliance test for TCM electronic medical records can test the application of the standard compliance testing platform, as well as verify whether the application of TCM electronic medical records' information standards is effective, normalized, and standardized.

2. Related Researches

This study retrieved related research from the database of China National Knowledge Infrastructure (CNKI) with "standard compliance testing platform" as the searching key words and without requirements for the publishing time. There are only 31 articles that are found related to "standard compliance testing platform," and these articles include "A Framework of SQL Conformance Test" by Li et al. [6] in 2003, "XML-Based Standards Compliance Testing Scheme" by Wu and Fan [7] in 2012, "Research and Development of Health Information Standard Conformance Test Case Library" by Xiao Youhua et al. [8] in 2015, and "Research on Conformance Testing of Data Standard" by Zhu et al. [9] in 2019. Among these studies, there are only 2 that are related to TCM electronic medical records, which is extremely rare. These two articles were published by Si Tong and Wang Wenjing, a master student in Hubei University of Chinese Medicine in 2014 as her graduation dissertation [10, 11]. Si Tong reviewed the current development of TCM electronic medical records in both home and abroad and then proposed and designed an outpatient electronic medical record software with Chinese traditional medicine characteristics [12], which presented a novel method for the development of TCM electronic medical records. While Wang's research was mainly related to the study of standard compliance of TCM electronic medical record information. Three articles are related to electronic health records, which mainly involve the study, proposition, and design of standard compliance test for electronic health records [13–15]. The searching result also shows that there are about 22 articles on standard compliance test, with contents covering from data element standards, platforms, e-commerce products, and e-government data exchange to ODBC standard testing framework [8, 16–28]. It indicates that the research on standard compliance testing platforms is in-depth in testing various types of standards, but short in the medical industry, such as TCM electronic medical records and electronic health records. In addition, from the overall trend of the research as shown in Figure 1, it can be seen that the development of research on the standard compliance testing platform is slow, or even stagnant.

In the era of rapid development of medical informatization, TCM hospitals have accumulated a large number of electronic medical records data. But the existing standard compliance testing and research platforms have their own specific standards, respectively, which leads to the fact that the tested data are not mutually relevant. Therefore, how to effectively utilize these data to improve medical and health service is of vital importance at present [29].

As shown in Figure 1, the selected literatures in this paper were mainly published in the year from 2003 to 2019 in CNKI, with an increase in the number of articles published since 2003. The number of researches on standard compliance testing platform reached a peak between 2012

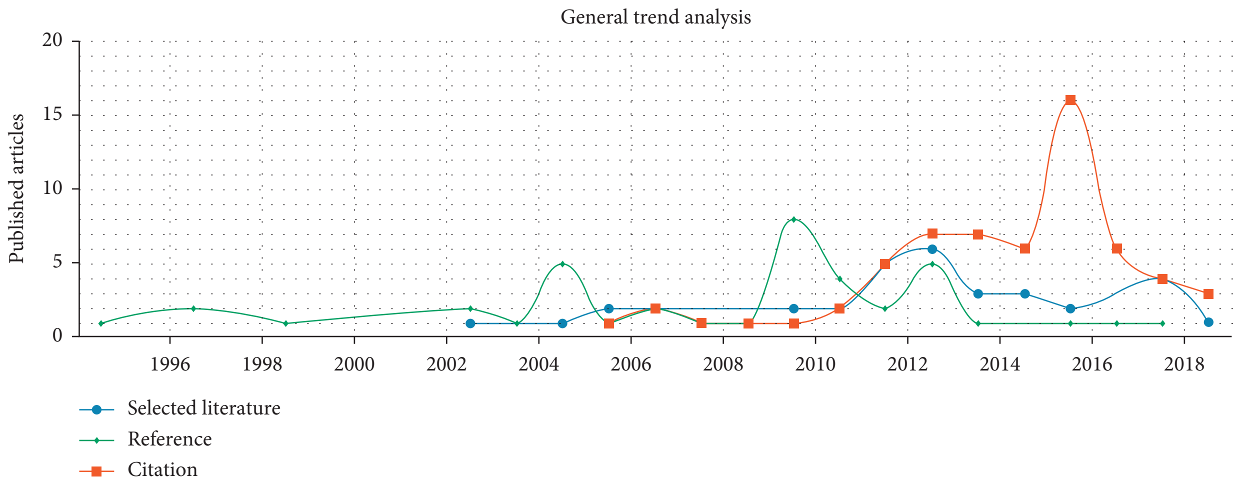

FIGURE 1: Overall research on standard compliance testing platform.

and 2013. The above figure also shows that the number of citations began to rise in 2005, reaching its peak in 2016 followed by a decline. The references of this paper were published as early as the 1990s or even earlier, which signifies that the topic of this paper appeared as early as back then, providing basic support and basis for current research, and that the research on standard compliance testing platforms has always been a hot issue which needs to be excavated deeply and widely.

This study starts from the literature review, which indicates that the research on the standard compliance test for TCM electronic medical records is rare and lacks available publicly labeled datasets [29]. In view of the fact that the research on entity standardization of electronic medical records being a hotspot driven by international public evaluation tasks[1], this paper then comes up with a research scheme for standard compliance test based on TCM electronic medical records. The electronic medical records data employed in this paper were randomly selected from the clinical outpatient data accumulated by the Institute of Digital Medicine of Chengdu University of TCM in the past 10 years. The basic four diagnosis and prescription information of TCM outpatients were first collected and processed through data security check and desensitization and then were inputted into the standard compliance testing platform, and the platform outputted the compliance test results subsequently. This research is believed to effectively promote the standardization of TCM outpatient electronic medical records and further bring positive impact on the medical cause.

3. Algorithm of Standard Compliance Test for Electronic Medical Records of TCM Outpatients

The two most representative evaluation tasks are ShARe/CLEF eHealth Shared Task 1b [30] in 2013 and SemEval Task 7 [31] in 2014, whose tasks are to find out the coding of entities in electronic medical records such as diseases and symptoms in Systematized Nomenclature of Medicine-Clinical Terms, abbreviated as SNOMED-CT [32].

The algorithm of standard compliance test based on electronic medical records of TCM outpatients includes score assessment algorithm and star-rating assessment algorithm.

3.1. *The Score Assessment Algorithm of the Standard Compliance Test.*

The score assessment algorithm is employed to check the integrity and coding standards of the electronic medical record data of TCM outpatients uploaded by medical institutions every single time and then evaluate its quality through certain rules. The score assessment algorithm consists of three parts, namely, integrity assessment, coding standard assessment, and total score assessment. Integrity test and coding standard test are targeted at the assessment of the integrity and coding standards of TCM outpatients' electronic medical records, while the total score is the sum of integrity assessment score and coding standard assessment score calculated according to their weight proportion.

The integrity assessment checks whether the mandatory items in TCM outpatients' electronic medical records are filled in. For example, the name and age of the patient must be put down, and if not, this standard will be scored zero. The mandatory items in TCM outpatients' electronic medical records determined in this study are shown in Table 1.

Coding standard assessment tests whether the codes of TCM symptoms, syndrome types, and treatments in TCM electronic medical records conform with related coding standards. The codes and their corresponding coding standards of TCM outpatients' electronic medical records determined in this study are shown in Table 2.

The integrity assessment algorithm, coding standard assessment algorithm, and total score assessment algorithm are, respectively, introduced as follows:

(1) Integrity assessment algorithm

Table 1: Mandatory items in TCM outpatient electronic medical records: number, item, and standard.

Number	Item	Standard
1	Location	Cannot be blank
2	Pathological nature	Cannot be blank
3	Four diagnosis	At least one
4	TCM symptom code	At least one
5	TCM symptom	At least one
6	TCM diagnosis	At least one
7	TCM syndrome type	At least one
8	TCM syndrome type code	At least one
9	TCM treatment	At least one
10	TCM treatment code	At least one
11	Name	Cannot be blank
12	ID number	Cannot be blank
13	Age	Cannot be blank
14	Gender code	Cannot be blank
15	Identification of dominant diseases in TCM	Cannot be blank
16	Code of dominant diseases in TCM	At least one

Table 2: Codes and standards of TCM outpatient electronic medical records.

Number	Item	Standard	Source of coding standard
	Ethnicity code	Within code range	People's Republic of China health industry standards WS 445.11-2014
	Code of medical insurance type	Within code range	People's Republic of China health industry standards WS 445.11-2014
	Level of disease severity	Within code range	People's Republic of China health industry standards WS 445.11-2014
	Biological gender code	Within code range	People's Republic of China health industry standards WS 445.11-2014
	Code of ID type	Within code range	People's Republic of China health industry Standards WS 445.11-2014
	Code of dominant diseases in TCM	Within code range	People's Republic of China health industry standards WS 445.11-2014
	Type of diagnosis	Within code range	People's Republic of China health industry standards WS 445.11-2014
	Code of payment method	Within code range	People's Republic of China health industry standards WS 445.11-2014
	Nationality code	Within code range	People's Republic of China health industry standards WS 445.11–2014
1	Clinic terminology of traditional Chinese medical diagnosis and treatment-Therapeutic methods	Within code range	National standard of the People's Republic of China [33]
2	Clinic terminology of traditional Chinese medical diagnosis and treatment-Syndromes	Within code range	National standard of the People's Republic of China [34]
3	Clinic terminology of traditional Chinese medical diagnosis and treatment-Diseases	Within code range	National standard of the People's Republic of China [35]
4	Classification and codes of diseases and Zheng of traditional Chinese medicine	Within code range	National standard of the People's Republic of China [36]

Provided that X_i is the number of missing items required in each medical record, n is the total number of medical records, k is the number of integrity items, and the integrity assessment score is S_i, the calculation of S_i is presented as

$$S_i = \left(1 - \sum_{1}^{n} \frac{X_i}{n * k}\right) * 100. \tag{1}$$

(2) Coding standard assessment algorithm

Table 3: Star-rating standards for each medical record.

Number	Determine field	Standard	Star-rating
1	Name	Cannot be blank	1-star
2	ID number	Cannot be blank	
3	Age	Cannot be blank	
4	Gender code	Cannot be blank. Within code range	
5	Identification of dominant diseases in TCM	Cannot be blank. Within code range	
6	TCM diagnosis	At least once	
7	TCM diagnosis code	At least one. Within code range	2-star
8	Syndrome type	At least one.	
9	Syndrome type code	At least one. Within code range	3-star
10	Four diagnosis	At least one.	
11	Symptom code	At least one. Within code range	4-star
12	Treatment	At least once	
13	Treatment code	At least once within code range	5-star
14	Prescription	At least once	

Provided that Y_j is the number of missing items, n is the total number of medical records, k is the number of coding items, and the coding standard assessment score is S_c, the calculation of S_c is shown as

$$S_c = \left(1 - \sum_{1}^{n} \frac{Y_j}{n * k}\right) * 100. \tag{2}$$

(3) Total score assessment algorithm

The total score of TCM electronic medical record is codetermined by the integrity assessment score and the coding standard assessment score. Provided that the total score is S_t, the calculation of S_t is stated as

$$S_t = S_i * 0.5 + S_c * 0.5. \tag{3}$$

3.2. The Star-Rating Assessment Algorithm

3.2.1. Star-Rating Assessment of Each Outpatient Electronic Medical Record. It is a process to star-rate every medical record uploaded by medical institutions via star-rating assessment algorithm. The star-rating process is conducted as

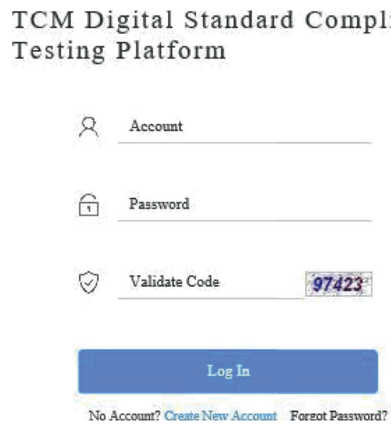

Figure 2: Login interface of digital standard compliance testing platform for TCM.

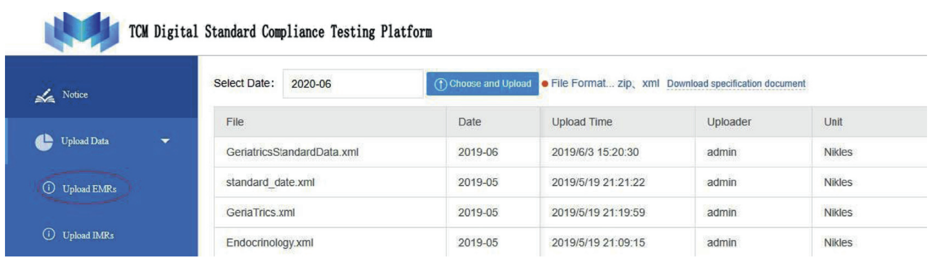

Figure 3: Interface of uploading outpatient medical record data by medical institutions.

per the standards described in Table 3, after the assessment of the integrity and coding standard of contents in medical records.

The following star-rating principles are indicated from Table 3:

(1) Medical records will be rated as one-star records if the above standards from no.1 to no.5 are met simultaneously.

(2) Medical records will be rated as two-star records if the above standards from no.1 to no.7 are met simultaneously.

(3) Medical records will be rated as three-star records if the above standards from no.1 to no.9 are met simultaneously.

(4) Medical records will be rated as four-star records if the above standards from no.1 to no.11 are met simultaneously.

(5) Medical records will be rated as five-star records if the above standards from no.1 to no.14 are met simultaneously.

3.2.2. Overall Star-Rating Assessment of Outpatient Medical Records Uploaded by Medical Institutions in a Single Time. The overall star-rating assessment of medical records uploaded by medical institutions every single time is composed of the star-ratings of the five-star, four-star, three-star, two-star, and one-star medical records as shown in Formula (4).

4. The Application of Standard Compliance Testing Platform for TCM Electronic Medical Records

Based on the above algorithm, the setting up of standard compliance testing platform for TCM electronic medical records is achieved via the applying of Visual Studio 2012 development tools, C# programming language, and SQL Server 2008 database management system.

After registering and logging in the standard compliance testing platform for TCM electronic medical records, as shown in Figure 2, medical institutions can upload outpatient electronic medical records by clicking the "Upload outpatient medical record" button under the menu of "Upload data," as shown in Figure 3.

The data of clinical outpatients accumulated in 10 years by the Digital Medicine Institute of Chengdu University of TCM were selected to be dealt with through security check and desensitization process. After processing, 28348 cases of electronic medical records of TCM outpatients were inputted into the standard compliance testing platform for assessment. The result was then outputted.

5. Result

The result of testing shows that in all the 28348 cases of TCM outpatient electronic medical records, there are 924 cases are rated as five-star, 84 cases four-star, 132 cases three-star, 12460 cases two-star, and 1260 cases zero-star, as shown in Table 4 and Figure 4.

Table 4: Test result of the application case.

Name of institution tested	Data content tested	Test result
Digital Medicine Institute of Chengdu University of TCM	Basic information of patients four diagnosis prescription	5-Star medical records: 924 4-Star medical records: 84 3-Star medical records: 132 2-Star medical records:12460 1-star medical records: 13488 0-Star medical records: 1260
Total		28348

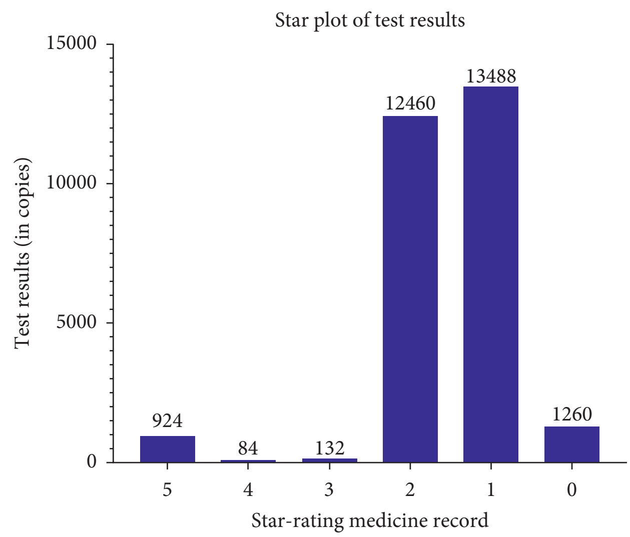

Figure 4: Star-rating of tested data.

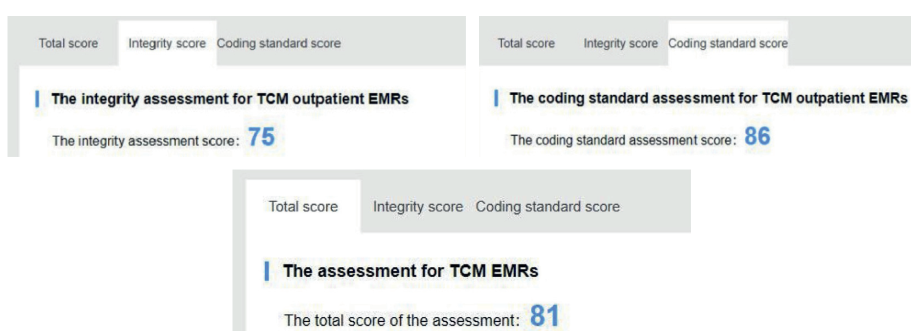

Figure 5: Scoring results of TCM outpatient electronic medical record case.

As a result of the integrity assessment and coding standards assessment, the integrity score and coding standard score of the TCM outpatient electronic medical records case data upload this time are 75 points and 86 points, respectively, and the total score is 81 points, as shown in Figure 5.

100 cases of TCM outpatient medical records were randomly selected manually and assessed by the above scoring and star-rating algorithm designed in this paper, and the result is consistent with the above result calculated by the standard compliance testing platform.

6. Conclusion

The algorithm of standard test for TCM outpatient electronic medical records put forward in this paper assesses outpatient electronic medical records from the aspects of integrity and coding standard while combining computer technology and traditional Chinese medicine. It presents a monitoring platform for the standard writing of TCM outpatient electric medical records, as well as a solution to problems such as data unavailability caused by disunified codes and incomplete data in the sharing process. Additionally, it gives feedbacks on the quality of data to hospitals which provide their electronic medical record data in order to correct the data timely and provides technical support for the construction of data standardization testing of TCM outpatient electronic medical records.

Data Availability

The basic data of our study come from the Institute of Digital Medicine of Chengdu University of Traditional Chinese Medicine. Through the cleaning, desensitization, and privacy security processing of the basic data, a total of 28348 data are obtained. And the basic data content can be obtained through the relevant platform of the Digital Medicine Research Institute of Chengdu University of Traditional Chinese Medicine.

Conflicts of Interest

The authors declare that they have no conflicts of interest regarding the publication of this paper.

Authors' Contributions

YL, CBW, and TS provided resources. LH and ZYZ performed formal analysis. YL and CBW supervised the study. YL was responsible for funding acquisition. FSN and YFY performed testing and verification. LH, QX, and YL wrote the original draft. LH, YL, CBW, and TS reviewed and edited the article. All authors read and approved the final manuscript.

Acknowledgments

The authors sincerely acknowledge the enormous contributions from authors and supports from many expert reviewers. This research was funded by the Scientific Research Project of Sichuan Health Information Society and the National Natural Science Foundation of China (no.81904324) and the National Key research and Development Program of China (2018YFC1707606).

References

[1] Q. Meng, "Focus on the implementation of efforts to create a new situation in health statistics and informatization," *Chinese Journal of Health Informatics and Management*, vol. 9, no. 2, pp. 2–7, 2019.

[2] Y. C. Wang, "Study on the development plan of health informatization during the 12th five-year plan period," *Chinese Journal of Health Informatics and Management*, vol. 9, no. 2, pp. 2–13, 2019.

[3] National Administration of Traditional Chinese Medicine and Ministry of Health, "Guidance on strengthening the construction of health informatization," 2012.

[4] Ministry of Health, "Technical solution for the construction of hospital information platform based on electronic medical records," 2011.

[5] B. Y. Liu, H. Zhang, and W. D. Ni, "TCM electronic medical record system and its particularity," *Medical Information*, vol. 17, no. 1, pp. 9–11, 2004.

[6] M. Li, Q. Lian, and X. K. Yang, "A framework of SQL conformance test," *Computer Engineering and Applications*, vol. 7, no. 20, pp. 173–175, 2003.

[7] J. M. Wu and G. M. Fan, "XML-based standards compliance testing scheme," *Journal of Computer Applications*, vol. 32, no. 2, pp. 551–553, 2012.

[8] Y. H. Xiao, Y. B. Ye, D. L. Feng, and P. He, "Research and development of health information standard conformance test case library," *Information Technology and Standardization*, vol. 10, no. 07, pp. 35–39, 2014.

[9] H. Zhu, A. Gao, and S. M. Wang, "Research on conformance testing of data standard," *Standard Science*, vol. 16, no. 07, pp. 53–57, 2019.

[10] S. Tong, "The current situation and innovational methods of TCM outpatient electronic medical records," *Journal of Medicine Informatics*, vol. 10, no. 09, pp. 37–39, 2008.

[11] W. J. Wang, "Traditional Chinese Medicine electronic medical records compliance information standard application research," Master thesis, Hubei University of Chinese Medicine, Wuhan, China, 2014.

[12] S. X. Tong, W. Y. Lin, N Yang et al., "Design and realization of the doctor's work station software for traditional Chinese Medicine Clinic," *Chinese Journal of Tissue Engineering Research*, vol. 43, pp. 183–185, 2006.

[13] J. P. Hu, X. J. Tang, J. M. Qu, Q. H. Huang, and F. J. Dong, "Research on methods of standard compliance test for electronic health records," *Chinese Digital Medicine*, vol. 15, no. 07, pp. 32–34, 2013.

[14] Q. Meng, J. P. Hu, X. J. Tang, J. F. Shen, and W. H. Zong, "Conformance testing of electronic health records," *Chinese Journal of Health Informatics and Management*, vol. 20, no. 01, pp. 31–34, 2013.

[15] L. N. Shen, J. P. Hu, X. J. Tang, L. X. Pu, and C. K. Wang, "Contents and design of conformance test for electronic health records in China," *Chinese Hospital Management*, vol. 5, no. 01, pp. 62–64, 2010.

[16] G. J. Liu, "Development and application of CNONIX standard compliance testing platform," *Information on Publication*, vol. 10, pp. 10–13, 2018.

[17] R. Duan, "Research on the validation method of relevant data elements based on CNONIX standard," Master thesis, North China University of Technology, Beijing, China, 2016.

[18] T. Pan, "The design and implementation of e-commerce products information standard conformance test," Master thesis, Beijing University of Technology, Beijing, China, 2015.

[19] X. Meng, L. Wei, J. P. Huang, and Y. Z. Zhang, "Research on standard conformance testing methodology of traffic signal controller communication protocol," *Information Technology and Standardization*, vol. 9, pp. 35–42, 2015.

[20] X. D. Guo, "Standard conformance test platform design and implementation based on oriented XML S1000D," Master thesis, University of Electronic Science and Technology of China, Sichuan, China, 2015.

[21] S. Z. Li, "Research and implement of the compliance testing of china online information exchange," Master thesis, North China University of Technology, Beijing, China, 2014.

[22] Q. Zhou, "Study of standard compliance test platform based on digital rights metadata," Master thesis, North China University of Technology, Beijing, China, 2013.

[23] J. J. Dong, B. Y. Wu, F. Shen, and Z. C. Wu, "Research on conformance test of sensor signal interface standard," *Computer Measurement and Control*, vol. 11, pp. 2867–2869, 2012.
[24] H. L. Wang and X. L. Shangguan, "Analysis on electronic signature conformance testing platform," *Information Technology and Standardization*, vol. 10, pp. 33–38, 2012.
[25] G. M. Fan, "Study and implementation of standard compliance test platform," Master thesis, North China University of Technology, Beijing, China., 2012.
[26] Y. W. Li, "Research and development of standard conformity test platform based on two-dimensional code of books," Master thesis, North China University of Technology, Beijing, China, 2011.
[27] X. D. Yang, "ODBC standard conformance test for database management system," Master thesis, University of Electronic Science and Technology of China, Sichuan, China, 2010.
[28] W. Qi, X. J. Ye, and J. M. Wang, "A framework for ODBC conformance test," *Computer Engineering*, vol. 20, pp. 101–103, 2005.
[29] Y. F. Zhao, J. L. Zheng, and X. L. Xu, "Deep learning based entity normalization of electronic medical records," *Software Guide.*vol. 18, no. 8, p. 12, 2009.
[30] H. Suominen and S. Velupillai, "Overview of the share/clef ehealth evaluation lab 2013," in *Proceedings of International Conference of the Cross-Language Evaluation Forum for European Language*, pp. 212–231, Springer, Heidelberg, Germany, September 2013.
[31] S. Pradhan, N. Elhadad, and W. Champman, "SemEval-2014 task 7: analysis of clinical text," in *Proceedings of the 8th International Workshop on Semantic Evaluation , (SemEval 2014)*, pp. 54–62, Dublin, Ireland, August 2014.
[32] T. S. De Silva, D. Macdonald, G. Paterson, K. C. Sikdar, and B. Cochrane, "Systematized nomenclature of medicine clinical terms , (SNOMED CT) to represent computed tomography procedures," *Computer Methods and Programs in Biomedicine*, vol. 101, no. 3, pp. 324–329, 2011.
[33] National Standard of the People's Republic of China-Clinic Terminology Traditional Chinese Medical Diagnosis and Treatment-Therapeutic Methods [GB]/T 16571.3-1997.
[34] National Standard of the People's Republic of China-Clinic Terminology Traditional Chinese Medical Diagnosis and Treatment-Syndromes [GB]/T 16751.2-1997.
[35] National Standard of the People's Republic of China-Clinic Terminology Traditional Chinese Medical Diagnosis and Treatment-Disease [GB]/T 16751.1-1997.
[36] National Standard of the People's Republic of China-Classification and Codes of Diseases and ZHENG of Traditional Chinese Medicine [GB]/T 15657-1995.

Hindawi
Journal of Healthcare Engineering
Volume 2020, Article ID 8840910, 8 pages
https://doi.org/10.1155/2020/8840910

Research Article

Influence of Optimization Design Based on Artificial Intelligence and Internet of Things on the Electrocardiogram Monitoring System

Ming Yin[1], **Ru Tang**[1], **Miao Liu**[1], **Ke Han**[1], **Xiao Lv**[2], **Maolin Huang**[2], **Ping Xu**[2], **Yongdeng Hu**[2], **Baobao Ma**[2], and **Yanrong Gai**[2]

[1]*The Second Medical Center and National Clinical Research Center for Geriatric Diseases, Chinese PLA General Hospital, Beijing 100853, China*
[2]*Lenovo Research, Lenovo Group, Beijing 100094, China*

Correspondence should be addressed to Ru Tang; 53100293@qq.com

Received 26 May 2020; Revised 19 September 2020; Accepted 15 October 2020; Published 27 October 2020

Academic Editor: Xiwei Huang

With the increasing emphasis on remote electrocardiogram (ECG) monitoring, a variety of wearable remote ECG monitoring systems have been developed. However, most of these systems need improvement in terms of efficiency, stability, and accuracy. In this study, the performance of an ECG monitoring system is optimized by improving various aspects of the system. These aspects include the following: the judgment, marking, and annotation of ECG reports using artificial intelligence (AI) technology; the use of Internet of Things (IoT) to connect all the devices of the system and transmit data and information; and the use of a cloud platform for the uploading, storage, calculation, and analysis of patient data. The use of AI improves the accuracy and efficiency of ECG reports and solves the problem of the shortage and uneven distribution of high-quality medical resources. IoT technology ensures the good performance of remote ECG monitoring systems in terms of instantaneity and rapidity and, thus, guarantees the maximum utilization efficiency of high-quality medical resources. Through the optimization of remote ECG monitoring systems with AI and IoT technology, the operating efficiency, accuracy of signal detection, and system stability have been greatly improved, thereby establishing an excellent health monitoring and auxiliary diagnostic platform for medical workers and patients.

1. Introduction

Estimations indicate that China has 290 million cardiovascular patients, including 13 million stroke, 11 million coronary heart disease, 5 million pulmonary heart disease, 4.5 million heart failure, 2.5 million rheumatic heart disease, 2 million congenital heart disease, and 245 million hypertension patients [1]. In the recent years, the death rate from cardiovascular diseases has been the highest—greater than that from tumor and other diseases. Two out of every five deaths have been linked to cardiovascular diseases, and the death rate in rural areas has been higher than that in urban areas. In rural areas, the death rate from cardiovascular diseases is 309.33/100000, including 151.18/100000 from heart diseases. In urban areas, the death rate from cardiovascular diseases is 265.11/100000, including 138.70/100000 from heart diseases. In rural areas, the deaths from cardiovascular diseases account for 45.50% of the total deaths, whereas in urban areas, they account for 43.16% of the total deaths. Because of the large number of patients, long duration of diseases, complex etiology, high cumulative cost of treatment, and frequent doctor-patient communication, not only is the medical system under great pressure but the medical cost is also very high. Hence, it is difficult for medical resources to be used for the benefit of all sections of society [2, 3].

Current well-established electrocardiogram (ECG) monitoring systems can be mainly divided into two types. In the first type of system, only the ECG signal acquisition from the patient side is considered. The signals are directly transmitted to the doctor via GPRS or 3G/4G remote communication or transmitted to the data relay node using Bluetooth, ZigBee, or Wi-Fi; the relay node, then, sends the ECG data to the doctor through the Internet. Research on this type of system has been happening for a relatively long period, and the technology is now well established. This type of system can be the foundation for the development of other systems with similar communication architectures in the future [4–6]. However, this type of system realizes only the remote real-time recording of ECG data [7], and a doctor is still needed to perform manual ECG diagnosis [8, 9]. In the second type of system, after collecting the ECG signal from the patient, the system transmits the ECG signal to a smartphone using Bluetooth, ZigBee, or Wi-Fi, allowing the mobile phone to display the ECG waveform in real time, perform ECG analysis and diagnosis, and then, transmit the relevant information to the doctor [10–12]. However, the hardware performance of smartphones is currently limited, and they are unable to support advanced ECG diagnostic algorithms. Therefore, the ECG analysis and diagnosis results do not meet the needs of patients [13, 14]. At present, these two types of ECG monitoring systems are subject to technical limitations [15, 16]. Because of the limitations of available facilities and technologies in terms of the electronic collection, storage, and analysis of ECG data (followed by automatic diagnosis), medical service centers cannot monitor the health status of the heart in a timely and effective manner [17, 18]. Consequently, valuable opportunities for diagnosis and treatment may be missed, and hence, the needs of patients cannot be satisfied.

2. Optimal Design of the ECG Monitoring System

In this study, artificial intelligence (AI) is used to automate the diagnosis, annotation, and detection of ECG reports, which are accurately and effectively judged and labeled. The user's ECG signal is uploaded to the cloud in real time through the Internet of Things (IoT) and shared with the corresponding medical staff, thereby reducing the burden on the medical staff, improving the accuracy of diagnosis, and reducing human interference and the influence of human factors on the ECG report [19, 20]. By using AI, users can be monitored remotely in a timely manner, more patients can access the system, more functions can be added to the system, and answers and treatment can be provided online to specific patients [21, 22]. For patients who are not likely to visit the hospital frequently, portable ECG monitoring equipment can provide many advantages and the quality of health monitoring can be guaranteed. Doctors can collect remote real-time data, conduct health evaluations, and undertake comprehensive monitoring of relevant physiological parameters, daily living habits, and mental states of family members. In this manner, patients can receive correct and efficient treatment without leaving the home and can save treatment cost. In particular, the system can track and manage the elderly and provide medical advice and self-help training. For general hospitals, heart disease experts at different research levels can be efficiently utilized, the heavy workload of doctors can be reduced, and the diagnosis and treatment of ECG diseases can be divided into several stages (prevention, treatment, or rehabilitation) to maximize the utilization of hospital resources.

2.1. Optimization of System Hardware. The self-adaption and optimized wireless sensor equipment (Figure 1) can be used by residents at home. The equipment is used to detect ECG data. The wireless sensor equipment has two innovative modes, which can meet the different needs of users.

According to the different needs of users, different detection accuracies are required, and accordingly, different lead methods can be selected. It is recommended that users use the simple low-lead method (Figure 2) during routine examinations or when they feel healthy. The complex multilead approach (Figure 3) can be applied if the user feels sick.

The materials used so far to attach various types of sensors to the body do not meet the skin-friendly nature required for long-term wear. Certain users such as patients with acute diseases are likely to experience an episode at any time, and hence, they need to be monitored without interruption. Therefore, there is a demand to improve the probe material such that it is skin friendly and does not cause damage to the body during long-term wear while simultaneously not affecting the data collection requirements.

2.2. Optimization of ECG Diagnostic Algorithm of the System. Typical ECG diagnostic algorithms include three essential steps [23]: signal data preprocessing, feature extraction from data, and feature classification. Signal preprocessing is related to the ability to process information content such that features can be extracted from the content, and feature classification is closely related to the ability of represent data features. Most ECG diagnostic algorithms still have not been able to eliminate the artificial feature extraction and classification steps. Some algorithms incorporate machine learning methods based on the abovementioned three steps, and the classification ability of the algorithms is improved through feature dimension reduction and feature selection [24]. The most important aspect to be noted is that the characteristics of data are chosen subjectively. Many algorithms have been proposed before, such as the probabilistic neural network analysis method based on feature dimension reduction, support vector machine method based on feature selection, and convolution neural network based on adaptive. These diagnostic algorithms were based on the traditional algorithm and proposed that the doctor should

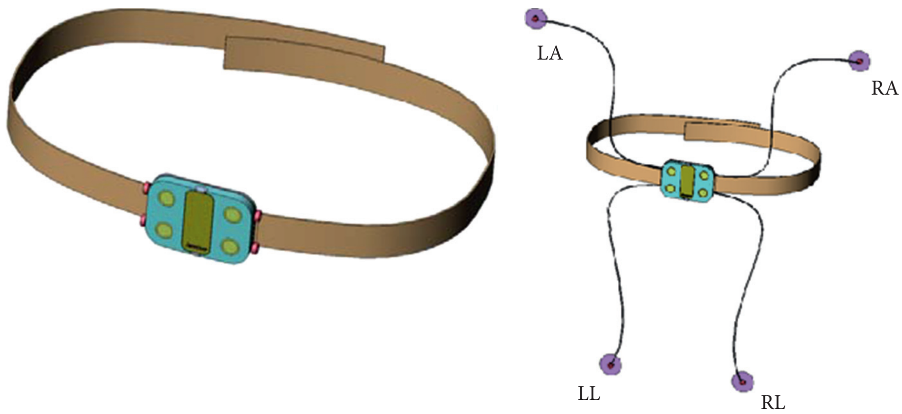

(a) (b)

Figure 1: Wireless sensor equipment. LA: left arm, LL: left leg, RA: right arm, and RL: right leg.

Figure 2: Simple low-lead method.

Figure 3: Complex multilead approach.

participate in the diagnosis to offset the problem of the robustness of the algorithm caused by feature selection subjectivity and patient specificity. First, a general algorithm is trained based on a general database, and then, the first 5 min of the ECG signal of the patient is collected. Next, the collected signal is provided to the algorithm as a new sample after the doctor's diagnosis to make the algorithm obtain the specificity of the patient. Accordingly, the most ambiguous part of the patient's ECG signal, which is the most difficult to determine, is extracted and handed to the doctor for diagnosis to reduce the burden on the doctor. Although this type of algorithm effectively solves the problem of the robustness of the algorithm, it still needs the doctor's participation and cannot perform automatic ECG analysis. ECG classification algorithms are usually based on artificial features of the ECG, such as the Fourier transform and morphology [25, 26], and the wavelet analysis indicators of ECG signals. However, doctors analyze ECG signals based on their personal experience about the features to be diagnosed. Therefore, the extraction of abstract features and deep mining of the information in the signal can effectively improve the accuracy and real-time performance of the system while preventing the decrease in robustness due to feature selection subjectivity and patient specificity [27].

However, these methods still include the step of artificial feature extraction. The disadvantage of this step is that when a new sample, that is, the electroanalytical analysis information of a new patient, is provided to a typical algorithm, the robustness of the algorithm is reduced and the accuracy of the algorithm cannot be guaranteed because of feature selection subjectivity and patient specificity. Thus, misjudgment may occur.

The data are uploaded to the cloud. The ECG report can be issued to the user, and the ECG data can be used for ECG trend prediction analysis. When the user's ECG signal is transmitted to the cloud, the correct signal is first identified, the filtered wave is selected, the R peak position is detected, the heartbeat is extracted by the R peak, and the heartbeat is classified by the Bidirectional Long- and Short-Term Memory network (Bilateral Long- and Short-Term Memory network, BiLSTM) method. Then, the algorithm detects ECG abnormalities, including Premature Ventricular Contraction (PVC), Premature Atrial Complex (PAC), and Atrial Fibrillation (AF). Finally, the labeled heartbeat data are used to train various classification algorithms such as neural networks, support vector machines, and logistic regression. The neural network with the best performance is selected as the ECG algorithm classifier, which completes the study of the ECG algorithm. According to the report, the corresponding doctor will be asked to treat the patient. The entire ECG algorithm process flow is shown in Figure 4.

After the automatic monitoring of the ECG signal is performed, the report is processed and distributed by the AI method, and the ECG report is dispatched, which increases the accuracy and timeliness of the report distribution while simultaneously reducing the burden of the operator, planner, and doctor. Furthermore, the AI workload will be gradually increased in the future to reduce manual operations. The 24 h ECG report grading delivery mechanism is shown in Figure 5. Finally, AI is expected to completely replace manual operations.

3. Automatic ECG Algorithm Test

In this paper, fast Convolutional Neural Networks (fast-CNNs) algorithm is used to process the one-dimensional ECG signal in two-dimensional graphics, so that the signal can be comprehensively grasped from a higher dimension. The algorithm uses a 32-layer convolution network structure to extract different levels of features from the input ECG graphic signals and can obtain useful features from the whole and subdivision levels. To evaluate the accuracy of the ECG algorithm and its various functional modules, two algorithm evaluation tests are performed. The first is based on standard ECG databases such as MIT-BIH (Table 1). By comparing the labeled information of each heartbeat, according to the YY 0885-2013 standard analysis algorithm, the sensitivity and true positive details are detected with respect to QRS, Ventricular Ectopic Beat (VEB), and Supraventricular Ectopic Beat (SVEB).

Next, data are collected from a real human body using a dynamic wearable ECG device and verified using the doctor's Lenovo-SEU-DB dataset, and the accuracies of different methods in each functional module are compared and evaluated. The details are shown in Table 2.

Although the classification accuracy of ECG algorithm in this paper may not be the best, it does not need to extract the complex signal features manually, and the algorithm itself can extract the ECG signal. Features are classified and recognized to achieve acceptable classification accuracy. Even if some cases are obviously disturbed by noise, the classification accuracy is acceptable.

Through the abovementioned two examples, we can see that the fast-CNN algorithm used in this paper can guarantee the high accuracy of the CNN for QRS wave detection and the real-time detection. This algorithm has the following advantages:

(1) After using this algorithm, it has higher detection sensitivity and accuracy for QRS detection and has better adaptability for worse Signal Noise Ratio (SNR) level: the algorithm adopts a 32-layer convolution network structure. In this way, compared with the traditional ECG detection algorithm, it has stronger robustness and adaptability to noise signals and higher detection accuracy.

(2) Although some existing algorithms, such as Regions with CNN features (R-CNN) and sppnet, make the deep neural network have some new technical breakthroughs in the field of target detection in ECG,

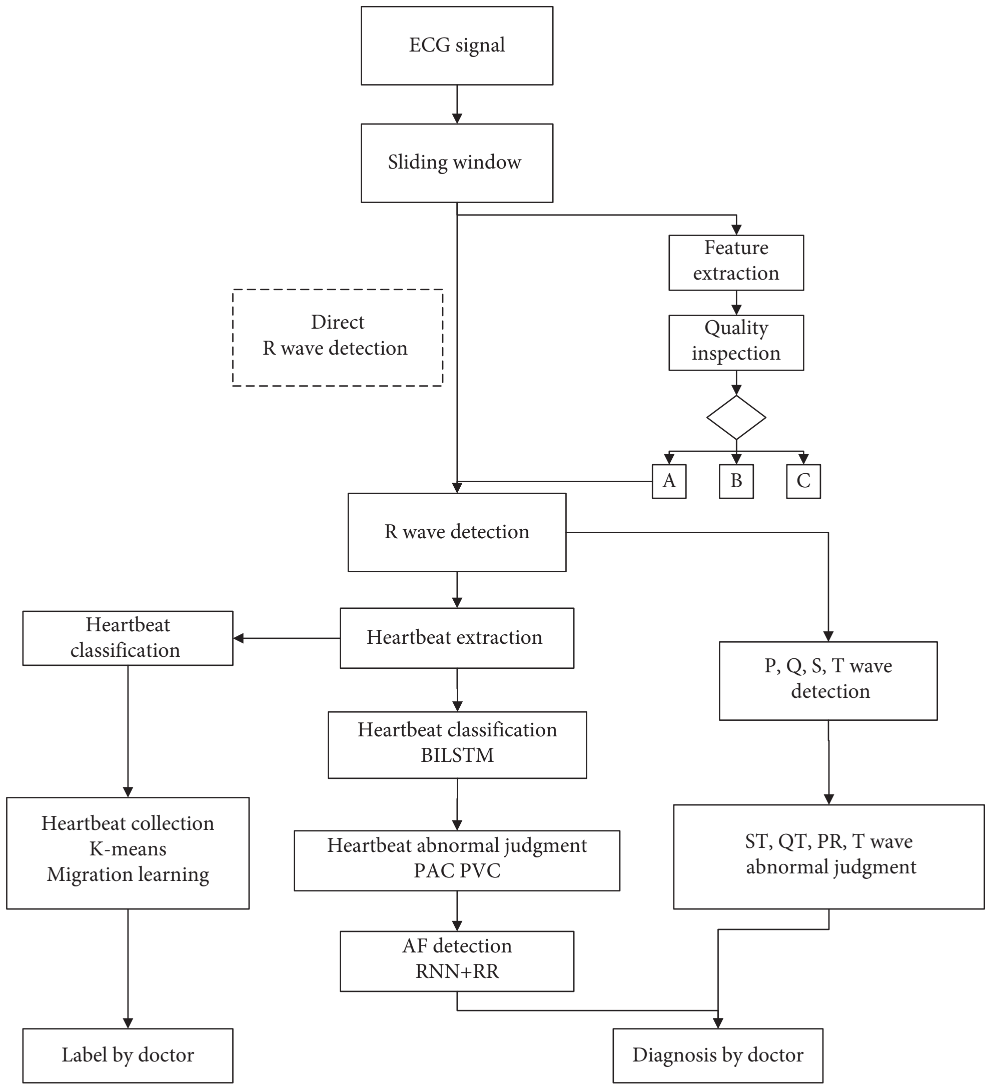

Figure 4: ECG algorithm process flow. Bilateral Long- and Short-Term Memory network, BiLSTM. Premature atrial complex, PAC. Premature ventricular contraction, PVC. Atrial fibrillation, AF. Recurrent neural network, RNN.

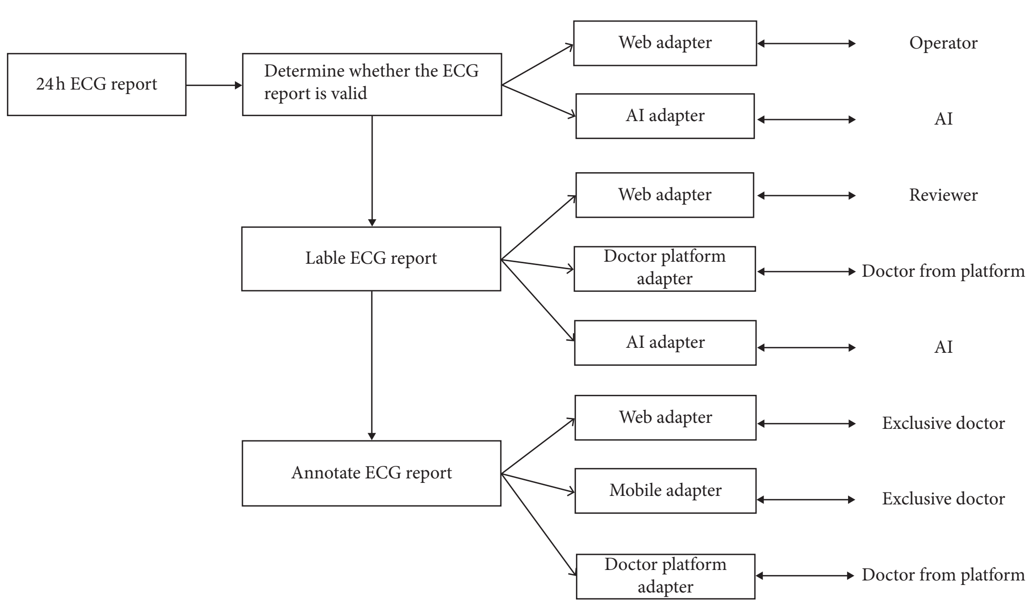

Figure 5: 24 h ECG report grading delivery mechanism.

Table 1: Algorithm test results based on MIT-BIH ECG databases

Database	Record	Total beats	QRS Se (%)	QRS P+ (%)
mitdb	100	2273	99.78	100.00
mitdb	101	1865	99.89	99.89
mitdb	102	2187	98.63	100.00
mitdb	103	2084	99.62	100.00
mitdb	104	2229	97.76	99.41
mitdb	105	2572	99.92	99.65
mitdb	106	2027	95.56	100.00
mitdb	107	2137	99.58	100.00
mitdb	108	1763	99.43	99.72
mitdb	109	2532	99.64	100.00
mitdb	111	2124	99.72	100.00
mitdb	112	2539	99.80	100.00
mitdb	113	1795	99.78	100.00
mitdb	114	1879	99.73	100.00
mitdb	115	1953	99.80	100.00
mitdb	116	2412	98.92	100.00
mitdb	117	1535	99.80	100.00
mitdb	118	2278	99.87	100.00
mitdb	119	1987	90.59	100.00
mitdb	121	1863	99.73	100.00
mitdb	122	2476	99.80	100.00
mitdb	123	1518	99.60	100.00
mitdb	124	1619	98.95	100.00
mitdb	200	2601	99.58	100.00
mitdb	201	1963	95.67	100.00
mitdb	202	2136	98.92	100.00
mitdb	203	2980	96.31	100.00
mitdb	205	2656	99.62	100.00
mitdb	207	2332	87.61	100.00
mitdb	208	2955	75.84	100.00
mitdb	209	3005	99.83	100.00
mitdb	210	2650	97.09	100.00
mitdb	212	2748	99.82	100.00
mitdb	213	3251	98.83	100.00
mitdb	214	2262	99.69	100.00
mitdb	215	3363	99.58	100.00
mitdb	217	2208	99.46	100.00
mitdb	219	2154	99.49	100.00
mitdb	220	2048	99.76	100.00
mitdb	221	2427	96.79	100.00
mitdb	222	2483	98.23	100.00
mitdb	223	2605	94.89	100.00
mitdb	228	2053	95.91	100.00
mitdb	230	2256	99.78	100.00
mitdb	231	1571	99.81	100.00
mitdb	232	1780	99.89	99.94
mitdb	233	3079	99.32	100.00
mitdb	234	2753	99.71	100.00
		Average	98.07	99.97

Table 2: Accuracy of different methods in each functional module.

Index	Fast-CNN				QRS based by P&T			
	Se	PPV	Acc	F1	Se	PPV	Acc	F1
1	0.9953	0.9908	0.9863	0.9931	0.9958	0.9922	0.9881	0.994
2	0.9716	0.9941	0.966	0.9845	0.9857	0.9834	0.9695	0.9827
3	0.9752	0.9857	0.9616	0.9804	0.9079	0.9128	0.8354	0.9103
4	0.9953	0.9995	0.9948	0.9974	0.9995	0.9991	0.9986	0.9993
5	0.986	0.9754	0.9621	0.9807	0.9808	0.9586	0.941	0.9696

Table 2: Continued.

Index	Fast-CNN				QRS based by P&T			
	Se	PPV	Acc	F1	Se	PPV	Acc	F1
6	0.9645	0.9828	0.9484	0.9735	0.9774	0.9738	0.9524	0.9756
7	0.9919	0.986	0.9781	0.9889	0.9953	0.979	0.9745	0.9871
8	0.9881	0.9851	0.9736	0.9866	0.9902	0.9868	0.9772	0.9885
9	0.9827	0.9596	0.9437	0.971	0.9637	0.9529	0.9199	0.9583
10	0.9592	0.9929	0.9526	0.9895	0.9865	0.9924	0.9791	0.9757
11	0.9939	0.9747	0.9688	0.9842	0.9898	0.9099	0.9015	0.9482
12	0.9978	0.9974	0.9952	0.9976	0.9958	0.9908	0.9866	0.9933
13	0.991	0.9959	0.9869	0.9934	0.9943	0.9762	0.9708	0.9852
14	0.983	0.9862	0.9697	0.9846	0.9898	0.9728	0.9631	0.9812
15	0.9796	0.9572	0.9384	0.9682	0.985	0.9806	0.9662	0.9828
16	0.9402	0.9461	0.8924	0.974	0.9749	0.9731	0.9493	0.9432
17	0.9844	0.9818	0.9668	0.9831	0.9757	0.9636	0.941	0.9696
18	0.9489	0.9644	0.9168	0.9566	0.9758	0.9634	0.9409	0.9696
19	0.9815	0.9923	0.974	0.9869	0.9834	0.9814	0.9654	0.9824
20	0.9811	0.9907	0.9721	0.9858	0.9814	0.9816	0.9637	0.9815
AVR	0.9796	0.9819	0.9624	0.9807	0.9814	0.971	0.9542	0.9762

Convolutional Neural Network, CNN. Sensitivity, Se. Positive predictive value, PPV. Accuracy, Acc. F1- measure, change the value of F function by adjusting alpha, F1 when alpha = 1.

it is far from the true real-time detection and end-to-end results. In this paper, fast-CNN is applied to the one-dimensional signal of ECG from the creative graph detection to ensure the real-time detection.

4. Conclusions

Through the requirements of remote ECG monitoring, a set of remote ECG monitoring schemes is put forward, and the requirements analysis and system design, the design of remote ECG monitoring system, and the design of ECG diagnosis algorithm are carried out. Finally, the remote ECG monitoring system is tested.

The main work of this paper is as follows:

(1) A three-layer structure of "acquisition end server end user end" of the remote ECG monitoring system is proposed, and a set of hardware platforms with signal acquisition and transmission function is built by using the existing hardware equipment to realize the acquisition and upload function of ECG signal

The collection end realizes the collection and upload function of the ECG signal, the server end realizes the storage management of data, the execution of diagnosis algorithm, and the response to the request of the user end, and the user end realizes the functions of user interface design, ECG drawing, and signal data acquisition. According to the principle of compatibility and expansibility, the software development platform of the system is built, which lays a solid foundation for the follow-up development and research.

(2) The ECG diagnosis algorithm and system of remote ECG monitoring system are tested. The performance of ECG diagnosis algorithm is tested and compared with the latest algorithm in feature engineering design and classification accuracy. The function of the system is tested, and the functions of the system are tested from the perspective of users. The test results show that each module of the remote monitoring system works normally and has a certain accuracy rate of arrhythmia diagnosis, which meets the expected requirements.

(3) Signal feature extraction needs further optimization. In the follow-up study, a variety of different network layers can be used for testing to achieve the best feature extraction effect.

Data Availability

The data used to support the findings of this study are available from the corresponding author upon request.

Conflicts of Interest

The authors have no conflicts of interest.

References

[1] L. Y. Ma, W. W. Chen, R. L. Gao et al., "China cardiovascular diseases report 2018: an updated summary," *Journal of Geriatric Cardiology: JGC*, vol. 17, no. 1, pp. 1–8, 2020.

[2] S. J. Curry, S. J. Curry, A. H. Krist et al., "Screening for cardiovascular disease risk with electrocardiography: US Preventive Services Task Force recommendation statement," *JAMA*, vol. 319, no. 22, pp. 2308–2314, 2018.

[3] A. L. Clark, G. C. Fonarow, and T. B. Horwich, "Waist circumference, body mass index, and survival in systolic heart failure: the obesity paradox revisited," *Journal of Cardiac Failure*, vol. 17, no. 5, pp. 374–380, 2011.

[4] N. Sriratanaviriyakul, C. Kangkagate, and R. Krittayaphong, "Prevalences and association of ECG findings and cardiovascular risk factor in Shinawatra employees," *Journal of the Medical Association of Thailand*, vol. 93, no. 1, pp. S1–S10, 2010.

[5] A. S. Desai and L. W. Stevenson, "Connecting the circle from home to heart-failure disease management," *New England Journal of Medicine*, vol. 363, no. 24, pp. 2364–2367, 2010.

[6] R. Wootton, "Twenty years of telemedicine in chronic disease management—an evidence synthesis," *Journal of Telemedicine and Telecare*, vol. 18, no. 4, pp. 211–220, 2012.

[7] S. Kitsiou, G. Paré, and M. Jaana, "Systematic reviews and meta-analyses of home telemonitoring interventions for patients with chronic diseases: a critical assessment of their methodological quality," *Journal of Medical Internet Research*, vol. 15, no. 7, p. e150, 2013.

[8] T. Inohara, S. Kohsaka, T. Okamura et al., "Cumulative impact of axial, structural, and repolarization ECG findings on long-term cardiovascular mortality among healthy individuals in Japan: national Integrated Project for Prospective Observation of Non-Communicable Disease and its Trends in the Aged, 1980 and 1990," *European Journal of Preventive Cardiology*, vol. 21, no. 12, pp. 1501–1508, 2014.

[9] V. Smith, D. Devane, C. M. Begley, and M. Clarke, "Methodology in conducting a systematic review of systematic reviews of healthcare interventions," *BMC Medical Research Methodology*, vol. 11, no. 1, p. 15, 2011.

[10] E. Lee, M. Dobbins, K. Decorby, L. McRae, D. Tirilis, and H Husson, "An optimal search filter for retrieving systematic reviews and meta-analyses," *BMC Medical Research Methodology*, vol. 12, p. 51, 2012.

[11] S. D. Anker, F. Koehler, and W. T. Abraham, "Telemedicine and remote management of patients with heart failure," *Lancet (London, England)*, vol. 378, no. 9792, pp. 731–739, 2011.

[12] B. J. Shea, J. M. Grimshaw, G. A. Wells et al., "Development of AMSTAR: a measurement tool to assess the methodological quality of systematic reviews," *BMC Medical Research Methodology*, vol. 7, no. 1, p. 10, 2007.

[13] N. Bashi, M. Karunanithi, F. Fatehi, H. Ding, and D. Walters, "Remote monitoring of patients with heart failure: an overview of systematic reviews," *Journal of Medical Internet Research*, vol. 19, no. 1, p. e18, 2017.

[14] M. K. Ong, P. S. Romano, S. Edgington et al., "Effectiveness of remote patient monitoring after discharge of hospitalized patients with heart failure," *JAMA Internal Medicine*, vol. 176, no. 3, pp. 310–318, 2016.

[15] A. Conway, S. C. Inglis, A. M. Chang, M. Horton-Breshears, J. G. Cleland, and R. A. Clark, "Not all systematic reviews are systematic: a meta-review of the quality of systematic reviews for non-invasive remote monitoring in heart failure," *Journal of Telemedicine and Telecare*, vol. 19, no. 6, pp. 326–337, 2013.

[16] A. Pandor, P. Thokala, T. Gomersall et al., "Home telemonitoring or structured telephone support programmes after recent discharge in patients with heart failure: systematic review and economic evaluation," *Health Technology Assess*, vol. 17, no. 32, pp. 1–207, 2013.

[17] S. Kitsiou, G. Paré, and M. Jaana, "Effects of home telemonitoring interventions on patients with chronic heart failure: an overview of systematic reviews," *Journal of Medical Internet Research*, vol. 17, no. 3, p. e63, 2015.

[18] V. Bhagyalakshmi, R. V. Pujeri, and G. D. Devanagavi, "GB-SVNN: genetic BAT assisted support vector neural network for arrhythmia classification using ECG signals," *Journal of King Saud University-Computer and Information Sciences*, 2018, In press.

[19] I. Saini, D. Singh, and A. Khosla, "QRS detection using K-nearest neighbor algorithm (KNN) and evaluation on standard ECG databases," *Journal of Advanced Research*, vol. 4, no. 4, pp. 331–344, 2013.

[20] M. M. A. Rahhal, Y. Bazi, H. AlHichri, N. Alajlan, F. Melgani, and R. R. Yager, "Deep learning approach for active classification of electrocardiogram signals," *Information Sciences*, vol. 345, pp. 340–354, 2016.

[21] J. Schläpfer and H. J. Wellens, "Computer-interpreted electrocardiograms," *Journal of the American College of Cardiology*, vol. 70, no. 9, pp. 1183–1192, 2017.

[22] H. Holst, M. Ohlsson, C. Peterson, and L. Edenbrandt, "A confident decision support system for interpreting electrocardiograms," *Clinical Physiology*, vol. 19, no. 5, pp. 410–418, 1999.

[23] S. M. Mathews, C. Kambhamettu, and K. E. Barner, "A novel application of deep learning for single-lead ECG classification," *Computers in Biology and Medicine*, vol. 99, pp. 53–62, 2018.

[24] R. Auer, D. C. Bauer, P. Marques-Vidal et al., "Association of major and minor ECG abnormalities with coronary heart disease events," *JAMA*, vol. 307, no. 14, pp. 1497–1505, 2012.

[25] Z. Golrizkhatami and A. Acan, "ECG classification using three-level fusion of different feature descriptors," *Expert Systems with Applications*, vol. 114, pp. 54–64, 2018.

[26] J. A. Laukkanen, E. Di Angelantonio, H. Khan, S. Kurl, K. Ronkainen, and P. Rautaharju, "T-wave inversion, QRS duration, and QRS/T angle as electrocardiographic predictors of the risk for sudden cardiac death," *The American Journal of Cardiology*, vol. 113, no. 7, pp. 1178–1183, 2014.

[27] M. Chen, G. J. Wang, P. W. Xie, Z. H. Sang, T. T. Lv et al., "Region aggregation network: improving convolutional neural network for ECG characteristic detection," in *Proceedings of the 2018 40th Annual International Conference of the IEEE Engineering in Medicine and Biology Society (EMBC)*, pp. 2559–2562, IEEE, Honolulu, HI, USA, 2018.

Hindawi
Journal of Healthcare Engineering
Volume 2020, Article ID 8840174, 9 pages
https://doi.org/10.1155/2020/8840174

Research Article

Hybrid Model Structure for Diabetic Retinopathy Classification

Hao Liu, Keqiang Yue, Siyi Cheng, Chengming Pan, Jie Sun, and Wenjun Li

Key Laboratory of RF Circuits and Systems, Ministry of Education, Hangzhou Dianzi University, Hangzhou, Zhejiang, China

Correspondence should be addressed to Keqiang Yue; kqyue@hdu.edu.cn

Received 13 August 2020; Revised 12 September 2020; Accepted 29 September 2020; Published 13 October 2020

Academic Editor: Xiwei Huang

Diabetic retinopathy (DR) is one of the most common complications of diabetes and the main cause of blindness. The progression of the disease can be prevented by early diagnosis of DR. Due to differences in the distribution of medical conditions and low labor efficiency, the best time for diagnosis and treatment was missed, which results in impaired vision. Using neural network models to classify and diagnose DR can improve efficiency and reduce costs. In this work, an improved loss function and three hybrid model structures Hybrid-a, Hybrid-f, and Hybrid-c were proposed to improve the performance of DR classification models. EfficientNetB4, EfficientNetB5, NASNetLarge, Xception, and InceptionResNetV2 CNNs were chosen as the basic models. These basic models were trained using enhance cross-entropy loss and cross-entropy loss, respectively. The output of the basic models was used to train the hybrid model structures. Experiments showed that enhance cross-entropy loss can effectively accelerate the training process of the basic models and improve the performance of the models under various evaluation metrics. The proposed hybrid model structures can also improve DR classification performance. Compared with the best-performing results in the basic models, the accuracy of DR classification was improved from 85.44% to 86.34%, the sensitivity was improved from 98.48% to 98.77%, the specificity was improved from 71.82% to 74.76%, the precision was improved from 90.27% to 91.37%, and the F1 score was improved from 93.62% to 93.9% by using hybrid model structures.

1. Introduction

Diabetic retinopathy (DR) is an ocular medical disease that damages the retina caused by diabetes. People with diabetes for a longer time are more likely to develop diabetic retinopathy. According to the severity, DR can be divided into the following five grades: no DR, mild, moderate, severe, and proliferative DR. Mild, moderate, and severe are classified as nonproliferative diabetic retinopathy (NPDR) stage. In the NPDR stage, the patients have no obvious symptoms. The way to detect NPDR is to examine the fundus by a trained ophthalmologist. As the condition worsens, DR will develop to Proliferative DR (PDR) stage. In the PDR stage, abnormal new blood vessels form at the back of the eye. These fragile blood vessels can burst and bleed, which blur vision and eventually lead to blindness. So far, the most effective treatment period for DR is in the NPDR stage. Therefore, regular screening of diabetic patients through fundus examination is the most effective method to detect early abnormal signs of DR. Early diagnosis and timely treatment are helpful to prevent DR in patients [1].

However, the screening of diabetic retinopathy needs professional clinical knowledge, experience, and diagnosis time of ophthalmologists. Ophthalmologists generally need to perform a direct examination of the patient's fundus and combine the fundus retinal images taken by special equipment to diagnose the severity of the patient's diabetic retinopathy. This process will take a lot of time. And the number of professional ophthalmologists is far from enough to meet the number of patients diagnosed. Therefore, the automatic classification algorithm of diabetic retinopathy severity plays an important role in improving the efficiency of DR diagnosis. Fundus images, the main images to study DR, are a current research hotspot [2,3]. Some research [4–7] uses machine learning and algorithms for DR detection and classification. However, as deep learning has done well in many competitions, more and more research uses deep learning methods for DR detection and classification. This research mainly focused on the end-to-end DR severity classification of fundus images by using CNNs. In a study, Li et al. [8] presented a novel cross-disease attention network (CANet) to jointly grade DR and DME. They proposed a disease-specific attention module and a disease-dependent attention module to extract useful features. Their network achieved AUC of 96.3% and accuracy of 92.6% for DR classification on the Messidor database. Shanthi and Sabeenian [9] proposed a modified AlexNet architecture [10] for classification of DR fundus images according to the severity of the disease with the application of suitable Pooling, Softmax, and Rectified Linear Activation Unit (ReLU) layers to obtain a high level of accuracy. And they validated the performance of the proposed algorithm using the Messidor database [11]. Finally, the proposed algorithm achieved a classification accuracy of 96.6% on the Messidor database. In a study, Hosseinzadeh et al. [12] presented a new feature extraction method using a modified Xception architecture for the diagnosis of DR disease. The proposed method is based on deep layer aggregation that combines multilevel features from different convolutional layers of Xception architecture. The modified Xception architecture that they proposed improved DR classification with a classification accuracy of 83.09% versus 79.59%, sensitivity of 88.24% versus 82.35%, and specificity of 87.00% versus 86.32% when compared with the original Xception architecture. Li et al. [13] extended a baseline network and created four convolutional networks with multiscale inputs. The proposed method obtained a new state-of-the-art kappa score in the task of diabetic retinopathy severity assessment task on EyePACS dataset. In the study [14], Hajabdollahi et al. modified original VGG16-Net [15] to reduce model's structural complexity for DR analysis by a hierarchical pruning method. The proposed method was evaluated using the Messidor database and 35% of the feature maps of VGG16-Net are pruned resulting in only 1.89% accuracy drop. Finally, Jain et al. [16] used 3 different CNN architectures including VGG16, VGG19, and InceptionV3 [17] and evaluated the CNN's performance for 2 classes and 5 classes of DR classification. They found out that the performance of the model was directly linked to the number of convolutional and pooling layers in the CNN. The best accuracy for 2 classes of DR classification was 80.40% achieved by VGG19.

The main contributions of this work are as follows: an improved loss function, enhance cross-entropy (E-CE) loss function, is to improve the performance of basic DR classification models and three proposed hybrid model structures are to fuse multiple basic models for the better performance of DR classification. In this work, preprocessing on the fundus images was firstly performed. During the training process of the basic models, data enhancement methods were used to expand the number of samples and the diversity samples for the DR fundus dataset. And different basic models were trained with E-CE loss and cross-entropy (CE) loss, respectively. Results (see Table 1) showed that our proposed E-CE loss can shorten the convergence time of loss. Under various evaluation metrics, the basic models trained with E-CE loss performed better than the models trained with CE loss. Then, the final output features of the better basic models in different ways were combined to train the hybrid model structures. Results showed that the performance of hybrid model structures is further improved compared to the basic models.

2. Materials and Methods

The proposed algorithm graph of this work is shown in Figure 1. The graph consists of three steps: fundus images preprocessing, basic CNN models prediction, hybrid model structures prediction, and DR grade output. First, the fundus images would be preprocessed. Then, each basic CNN model predicted the preprocessed fundus images. And the outputs of each basic CNN model were input into the hybrid model structures. Finally, the hybrid model structures output five predicted values, corresponding to the probability of the five DR grades, and the DR grade with the largest probability was taken as the result of the fundus image.

2.1. Dataset. The dataset for this work consists of three different datasets which come from the Kaggle diabetic retinopathy detection competition [18] provided by EyePACS, APTOS 2019 Blindness Detection organized by the 4th Asia Pacific Tele-Ophthalmology Society [19], and DeepDR Diabetic Retinopathy Image Dataset provided by the IEEE International Symposium on Biomedical Imaging (ISBI) 2020 [20]. EyePACS dataset contains 35,126 training fundus images and 53,576 test fundus images. APTOS dataset contains 3,662 training fundus images and 1,928 test fundus images. DeepDR dataset contains 1,200 training fundus images, 400 validation fundus images, and 400 test fundus images. All fundus images from the three datasets had been rated for the severity of diabetic retinopathy on a scale of 0 to 4: 0 is no DR, 1 is mild DR, 2 is moderate DR, 3 is severe DR, and 4 is proliferative DR. Examples of different severity of DR fundus images are shown in Figure 2. Each fundus image from the three datasets has a high resolution. The dataset for this work contains 39,988 fundus images which come from the training fundus images with rate of the three datasets because only the training fundus images from the three datasets are rated. As shown in Table 2, the class distribution of the dataset is highly imbalanced, and most of the fundus images are no DR grade.

2.2. Data Processing. There are two steps for data processing. One is preprocessing for the fundus images before training basic models; the other is the fundus images enhancement in the training process. The first step for data processing is mainly to remove the black border of the fundus images because the black border will bring useless information and weaken the ability to extract features of the basic models and resize the images to a suitable size for inputs of models. The details are as follows:

(1) Binary processing was performed on the fundus images to find the border between the black area and the fundus area and then cut the extra black border for each fundus image. The processes are shown in Figure 3.

Table 1: Classification results from the basic models and the hybrid model structures.

		Loss	Accuracy	Sensitivity	Specificity	Precision	F1 score
Basic models	EfficientNetB4	CE	0.8158	0.9442	0.7182	0.9027	0.9230
		E-CE	0.8544	0.9736	0.7061	0.9017	0.9362
	EfficientNetB5	CE	0.7932	0.9254	0.6782	0.8884	0.9065
		E-CE	0.8488	0.9809	0.6549	0.8872	0.9317
	NASNetLarge	CE	0.7828	0.9151	0.7031	0.8951	0.9050
		E-CE	0.8470	0.9845	0.6353	0.8820	0.9304
	InceptionResNetV2	CE	0.7888	0.9657	0.5177	0.8471	0.9025
		E-CE	0.8502	0.9739	0.6963	0.8987	0.9348
	Xception	CE	0.8100	0.9706	0.5742	0.8632	0.9138
		E-CE	0.8476	0.9848	0.6217	0.8781	0.9284
Hybrid model	Hybrid-model-a	CE	0.8584	**0.9877**	0.6481	0.8860	0.9341
	Hybrid-model-f	CE	0.8626	0.9652	**0.7476**	**0.9137**	0.9387
	Hybrid-model-c	CE	**0.8634**	0.9706	0.7325	0.9094	**0.9390**

CE indicates cross-entropy loss function; E-CE indicates enhance cross-entropy loss function; and the bold values indicate the best results.

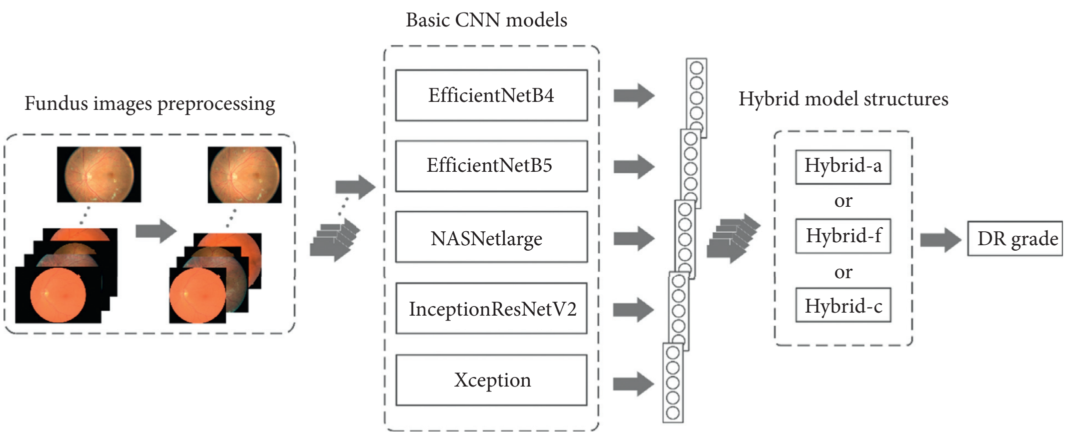

Figure 1: Graph of the proposed algorithm architecture.

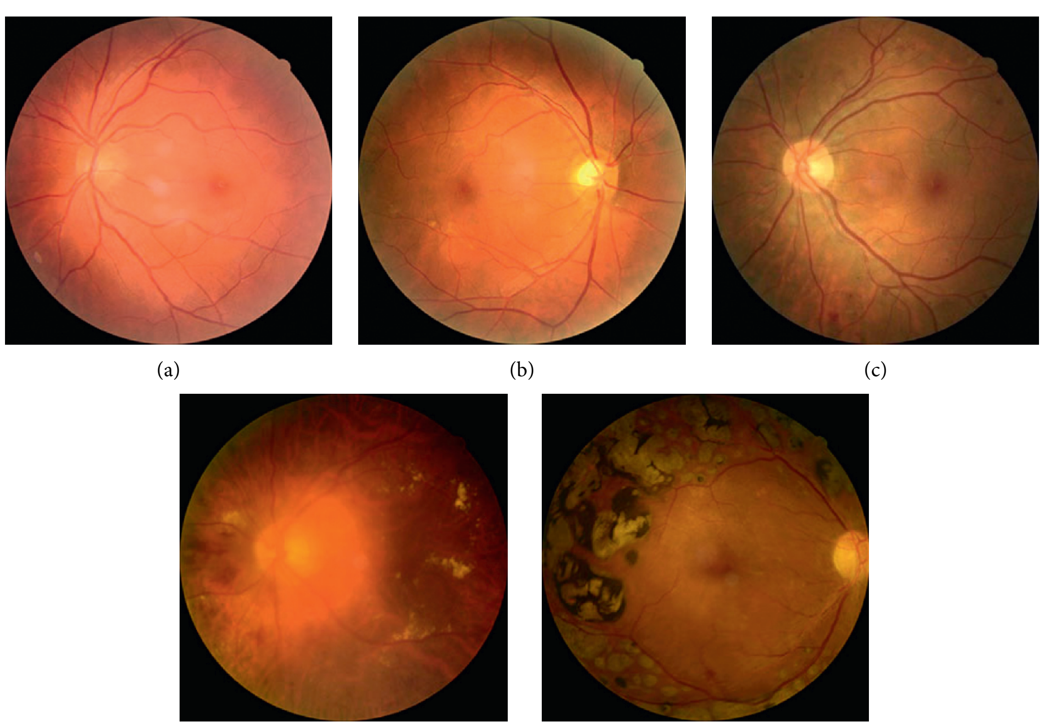

(a) (b) (c) (d) (e)

Figure 2: Examples of different severity of DR fundus images. (a) No DR. (b) Mild DR. (c) Moderate DR. (d) Severe DR. (e) Proliferative DR.

Table 2: The DR grade distribution of the dataset.

Datasets	DR grade					
	0	1	2	3	4	Total number
DeepDR	540	140	234	214	72	1200
APTOS	1805	370	999	193	295	3662
EyePACS	25810	2443	5292	873	708	35126
Total number	28155	2953	6525	1280	1075	39988
Percentage (%)	70.41	7.38	16.32	3.2	2.69	—

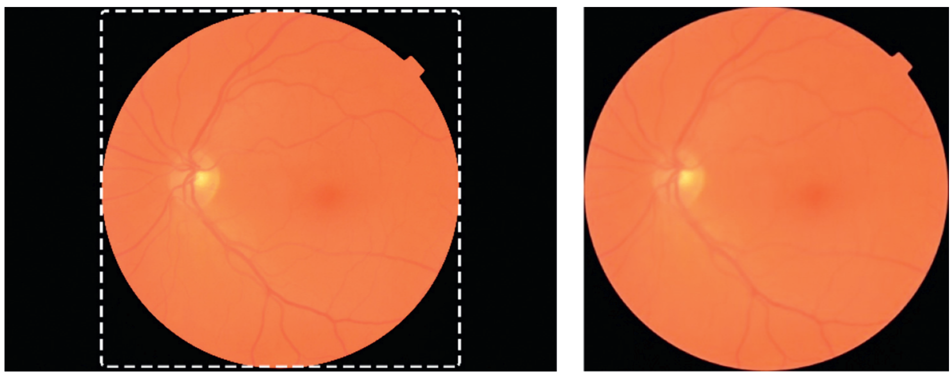

(a) (b)

Figure 3: The process of removing the black border of fundus images. (a) The unprocessed fundus image and (b) the processed fundus image.

(2) Because each fundus image has a higher resolution, which is not suitable for the input of the basic models, all images were resized to 380 × 380 pixels for EfficientNetB4, 380 × 380 pixels for EfficientNetB4, 331 × 331 pixels for NASNetLarge, and 299 × 299 pixels for EfficientNetB5, Xception, and Inception-ResNetV2.

In the training process, the following operations were performed on the fundus images: rotation, width shift, height shift, shear range, zoom, horizontal flip, and vertical flip. Then, RandAugment was used for the images. RandAugment [21] is an improved data augmentation method proposed by Cubuk et al. On the ImageNet dataset, Cubuk et al. achieved 85.0% accuracy, 0.6% increase over the previous state-of-the-art, and 1.0% increase over baseline augmentation by using RandAugment.

2.3. Basic Model Structures. In this work, hybrid model structures were proposed to improve the classification ability of the basic models. EfficientNetB4, EfficientNetB5, NASNetLarge, Xception, and InceptionResNetV2 CNNs were chosen as the basic models. And then three methods to implement the hybrid model structure were used. Finally, the experiments to verify the performance of the basic models and the basic models with the hybrid model structures were done. The results are shown in part 3. The structure of the basic models are as follows:

(1) EfficientNet: EfficientNet [22] is a family of models designed by Tan et al. They proposed a scaling method [23] that uniformly scales all dimensions of depth/width/resolution of CNNs using a simple yet highly effective compound coefficient. Then, they used a neural architecture search to design a new baseline network and used the scaling method to scale it up to obtain EfficientNet, which achieve much better accuracy and efficiency than previous ConvNets. In this work, EfficientNetB4 and EfficientNetB5 were chosen as basic models. The input size of EfficientNetB5 was changed to 299 × 299 pixels and EfficientNetB4 kept the original input resolution. Both of them were added a dropout layer with 0.4 drop rate and a fully-connected layer with 5 units and the activation function of the fully-connected layer was softmax function.

(2) NASNetLarge: the NASNet architecture, introduced by Zoph et al. [24], is the best architecture found on CIFAR-10 by the neural architecture search (NAS) framework [25]. Different versions of NASNets with different computational demands can be created by simply varying the number of the convolutional cells and the number of filters in the convolutional cells. The large NASNet-A which performed best on ImageNet image classification was chosen as our basic model. A dropout layer with 0.4 drop rate and a fully-connected layer with 5 units by using softmax function were used to replace the original model output.

(3) InceptionResNetV2: InceptionResNetV2 model [26] was proposed by Szegedy et al. InceptionResNetV2 is based on the inception network architecture [27] and

replaced the filter concatenation stage with residual connections [28] introduced by He et al. Training with residual connections accelerates the training of inception networks significantly. And residual inception networks outperform similarly expensive inception networks without residual connections by a thin margin. In this work, only the last fully-connected layer with 1000 units was replaced by a fully connected layer with 5 units by using softmax function.

(4) Xception: the Xception architecture, introduced by Chollet [29], is a convolutional neural network architecture based entirely on depthwise separable convolution layers inspired by Inception. The Xception architecture has 36 depthwise separable convolutional layers forming the feature extraction base of the network, which makes the architecture very easy to define and modify. The 36 convolutional layers are structured into 14 modules, all of which have linear residual connections around them, except for the first and last modules. In this work, the fully-connected layers and the logistic regression layer of the Xception architecture were replaced by a dropout layer and a fully-connected layer with 5 units by using softmax function.

2.4. Hybrid Model Structures. Three methods were proposed to implement the hybrid model structure, called Hybrid-a, Hybrid-f, and Hybrid-c. The details are as follows:

Hybrid-a: in Hybrid-a, the average value of each DR grade which the basic model outputs is calculated as the final output of the hybrid model structure. The formula is

$$Y_{\text{grade}} = \frac{1}{N}\sum_{n=1}^{N} y_n^{\text{grade}}, \quad (\text{grade} = 0, 1, 2, 3, 4), \tag{1}$$

where N denotes the number of the basic models. y_n^{grade} denotes the DR grade output of the nth model, and Y_{grade} denotes the DR grade of the final output of Hybrid-a.

Hybrid-f: Hybrid-f is a model mainly composed of fully-connected layers in short. The output of each basic model, which is a 5×1 column vector, is stacked vertically, and finally forms a 25×1 column vector as the input of the Hybrid-f model structure. Figure 4 shows the structure of Hybrid-f. Hybrid-f consists of 2 fully-connected layers. The hidden layer has 2048 units and the output layer has 5 units with softmax activation function.

Hybrid-c: Hybrid-c is mainly composed of 2D convolution layers. The 5×1 column vector output of each basic model is stacked horizontally and finally forms a 5×5 matrix as the input of the Hybrid-c model structure. The structure of Hybrid-c is shown in Figure 5, and the details of Hybrid-c are shown in Table 3. Three 2D convolution layers as the feature extraction layers make up the first half of the Hybrid-c structure, and then the Hybrid-f structure makes up the last part of Hybrid-c.

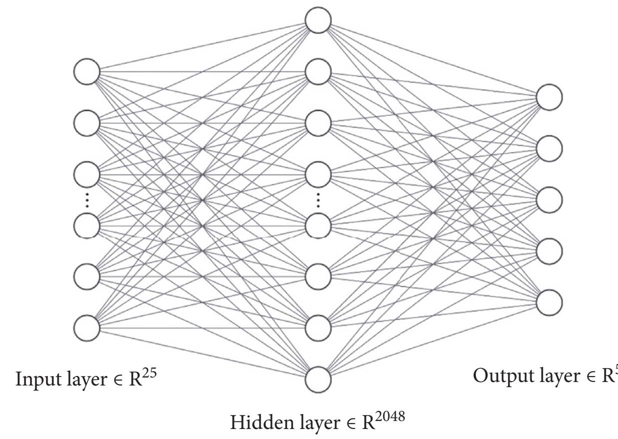

Figure 4: The structure of Hybrid-f.

2.5. Loss Function. Different loss functions have different effects on the training process and results of network models. In this work, an improved loss function, E-CE loss function, was proposed for the training process of the basic models. And comparison experiments with CE loss function were done. The formula of CE loss function is

$$L(\hat{y}, y) = -\frac{1}{N}\sum_{n=1}^{N}\left[y_n \log \hat{y}_n + (1-y_n)\log(1-\hat{y}_n)\right], \tag{2}$$

where y denotes the true value, $\hat{y}$ denotes the predicted value, and N denotes the total number of DR grade. The E-CE loss function is based on CE loss function and shown as follows:

$$L(\hat{y}, y) = -\frac{1}{N}\sum_{n=1}^{N}\left[y_n \log \hat{y}_n + (1-y_n)\log(1-\hat{y}_n) + \left|\frac{G_y - G_{\hat{y}}}{N-1}\right|\right], \tag{3}$$

where G_y denotes the DR grade of truth and $G_{\hat{y}}$ denotes the DR grade of prediction. DR grade is an integer in the range of 0 to 4. In the formula, a part of the loss is added to measure the impact of the misclassification of the basic models during the training process. The farther the output value of the model is from the true value during the model training process, the greater the excess loss will be. Experiments (see Part 3) showed that the E-CE loss function will accelerate the training of the basic models and improve the accuracy of the basic models.

3. Results and Discussion

3.1. Experiment Setup. Our experiment was carried out on a workstation with 4 NVIDIA GEFORCE RTX-2080Ti GPUs. The memory of each GPU is 11 GB. CPUs are Intel Xeon Silver 4110 processors, 2.1 GHz, a total of 4. The operating system for training models is Ubuntu 16.4. The deep learning framework used in training models is Keras. The backend of Keras used Tensorflow GPU 1.13.1. For each basic training model, the optimizer was RAdam [30] proposed by Liu et al. RAdam, Rectified Adam, is a novel variant of Adam by introducing a term to rectify the variance of the adaptive. And the initial learning rate for each model was set to 0.0008. During the models training, the learning rate could be

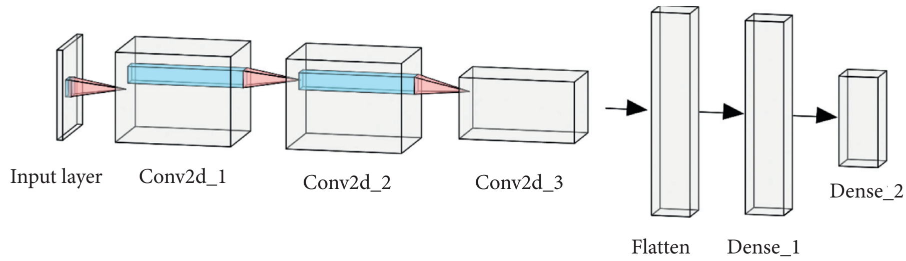

Figure 5: The structure of Hybrid-c.

Table 3: The details of the Hybrid-c structure.

Layer	Units	Filters	Kernel size	Padding	Output shape
Input	—	—	—	—	$5 \times 5 \times 1$
Conv2d_1	—	256	3	1	$5 \times 5 \times 256$
Conv2d_2	—	256	3	1	$5 \times 5 \times 256$
Conv2d_3	—	256	3	0	$3 \times 3 \times 256$
Flatten	—	—	—	—	2304
Dense_1	2048	—	—	—	2048
Dense_2	5	—	—	—	5

adjusted automatically. The batch size of EfficientNetB4, EfficientNetB5, NASNetLarge, Xception, and Inception-ResNetV2 are 32, 40, 64, 64, and 32, respectively. CE loss function and E-CE loss function were used to train each basic model for the control experiment. The epochs of for training each model were 50. Also, the pretraining weights on the ImageNet dataset were used to accelerate the training process of each basic model. For training Hybrid-f and Hybrid-c model structure, the optimizer was Adam. The initial learning rate was 0.001. And the loss function was cross-entropy loss function. Training epochs were 100.

3.2. Performance Evaluation. The performance of the basic models and the hybrid models are evaluated by 5 evaluation metrics which are accuracy, sensitivity, specificity, precision, and F1 score. The formulas are shown as follows, where TP denotes the number of positive samples actually identified as positive samples, TN denotes the number of negative samples correctly identified as the negative samples, FP denotes the number of negative samples falsely identified as the positive samples, and FN denotes the number of positive samples falsely identified as the negative samples:

$$\begin{aligned}\text{accuracy} &= \frac{\text{TP} + \text{TN}}{\text{TP} + \text{TN} + \text{FP} + \text{FN}},\\ \text{sensitivity} &= \frac{\text{TP}}{\text{TP} + \text{FN}},\\ \text{specificity} &= \frac{\text{TN}}{\text{TN} + \text{FP}},\\ \text{precision} &= \frac{\text{TP}}{\text{TP} + \text{FP}},\\ \text{F1score} &= 2 \cdot \frac{\text{precision} \cdot \text{sensitivity}}{\text{precision} + \text{sensitivity}}.\end{aligned} \tag{4}$$

3.3. Results and Discussion. The basic models were trained on 34,988 fundus images which were selected according to the DR grade ratio from the dataset consisting of EyePACS, APTOS, and DeepDR dataset. The remaining 5,000 images of the dataset were used as test images to evaluate the performance of the models.

In order to verify the performance of E-CE loss function, each basic model was trained with E-CE loss function and CE loss function, respectively. Figure 6 shows that the convergence speed of the basic models trained with E-CE loss function is faster than that trained with CE loss function. The accuracy of the basic models is also relatively improved faster.

The accuracy, sensitivity, specificity, precision, and F1 score of the obtained results are shown in Table 1. It can be seen from Table 1 that our proposed E-CE loss function improved the performance of the basic models under partial classification metrics, especially the performance in terms of accuracy and sensitivity. The model trained with E-CE loss function has an average performance improvement of about 5% on accuracy and 3.5% on sensitivity. This may be because an extra part of E-CE loss relative to CE loss increases the influence of the basic models on the misclassification of DR grade during the training process, which will optimize the basic models towards the correct classification faster.

The performance of our proposed hybrid model structures outperforms all the basic models in all classification metrics. Referring to Table 1, Hybrid-c has the highest accuracy which is 0.8634 and F1 score which is 0.939, Hybrid-a has the highest sensitivity which is 0.9877, and Hybrid-f has the highest specificity which is 0.7476 and precision which is 0.9137. As shown in Table 1, in terms of accuracy, Hybrid-c improves EfficientNetB4 by 0.9%, EfficientNetB5 by 1.46%, NASNetLarge by 1.64%, InceptionResNetV2 by 1.32%, and Xception by 1.58%. Results of the experiments prove that the hybrid model structures compared with the single basic model can

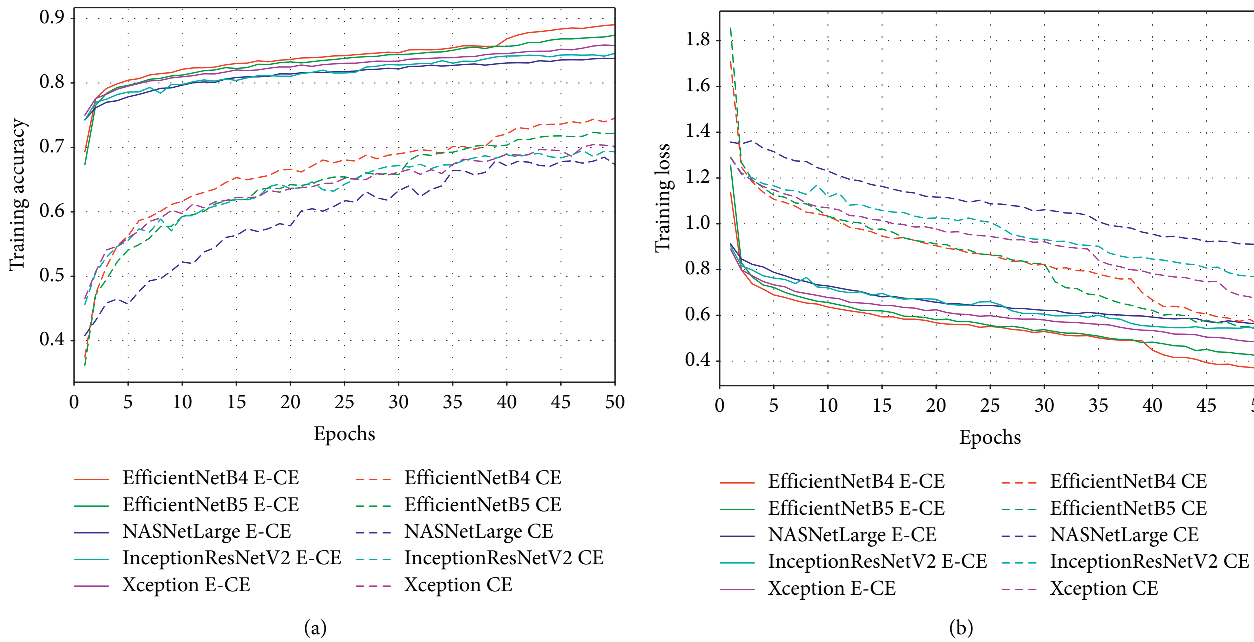

Figure 6: The epochs of training the basic models using E-CE loss and CE loss. (a) Training accuracy varies with epochs for basic models from EfficientNetB4 E-CE to Xception CE. (b) Training loss varies with epochs for basic models from EfficientNetB4 E-CE to Xception CE.

Table 4: The confusion matrix of Hybrid-c.

Predicted DR grade Actual DR grade	0	1	2	3	4
0	3565/97.06	36/0.98	68/1.85	1/0.03	3/0.08
1	204/58.96	87/25.14	54/15.61	0/0	1/0.29
2	140/18.62	47/6.25	540/71.81	15/1.99	10/1.33
3	7/5.69	0/0	55/44.72	54/43.9	7/5.69
4	4/3.78	1/0.94	18/16.98	12/11.32	71/66.98

The first item in each grid cell is the number of fundus images. The second item is the percentage of the images in the DR grade.

improve the classification performance in all aspects. The Hybrid-f and Hybrid-c with complex structures have better overall performance than Hybrid-a with simple structure. When the hybrid model structure is more complex, the difference between Hybrid-f and Hybrid-c is smaller. For the hybrid structure proposed in this work, although the higher complexity of the hybrid structure will not bring about a linear performance improvement, the hybrid structure will improve the performance of a single model performance in DR grade classification.

The confusion matrix of Hybrid-c on the testing fundus images is shown in Table 4. From Table 4, Hybrid-c performs the best in DR grade 0 classification, with an accuracy of 0.9706. The performance of Hybrid-c on DR grade 2 classification is better, which achieves 0.7181 score of accuracy. And Hybrid-c has good performance in the classification of DR grade 4, which achieves 0.6698 score of accuracy. For DR grade 1 images, Hybrid-c prefers to misclassify them to DR grade 0. For DR grade 3 images, Hybrid-c prefers to misclassify them to DR Grade 2. The reason for this situation may be as follows:

(1) The number of training fundus samples of DR grades 1 and 3 is relatively less compared to the number of DR grades 0 and 2, which causes the poor classification ability of the model for DR grades 1 and 3.

(2) The hidden features of fundus images in DR grades 1 and 3 are closer to those of DR grades 0 and 2. We found out the images of DR grades 1 and 3 which were misclassified to DR grades 0 and 2. From the observation of human eyes, the difference between DR grade 1 and DR grade 0 is small, the same as DR grades 3 and 2. For the model, some features extracted by the convolutional layers of DR grade 1 and DR grade 0 may be relatively similar, which may cause some images of DR grade 1 to be misclassified to DR grade 0. This can also explain that for DR grade 4. Although the number of samples in DR grade 4 is small, the features extracted by the model are quite different from those of other DR grades. So, the accuracy of DR grade 4 classification is better than that of DR grades 1 and 3.

(3) Experts rating the fundus images may be affected by their own subjective factors and DR grade judgment rules, which may cause some errors in rating DR grades 1 and 3 images. In addition, parts of some

fundus images, because of the camera, are dark, blurred, or highlights, which can also affect the judgment of experts.

In future work, we may improve the method of data enhancement to improve the impact of the imbalance of DR grade in the dataset and may extract the output of the intermediate layers of the basic convolution models as the input of the hybrid model structure to increase the richness of the input feature maps of the hybrid model.

4. Conclusions

In this work, we proposed an improved loss function, E-CE loss function, and proposed three hybrid model structures Hybrid-a, Hybrid-f, and Hybrid-c to improve the performance of a single model. The results show that the E-CE loss function can effectively accelerate the training process of a single basic model and can improve the performance of a single model compared with the CE loss function. The three different hybrid model structures can improve the performance of the basic models in all aspects. Although the increase in the complexity of the hybrid model does not bring a linear improvement in model performance, the more complex Hybrid-c and Hybrid-f perform better than the simple Hybrid-a in some evaluation metrics. Finally, the proposed algorithm achieved five classifications accuracy of 86.34%, sensitivity of 98.77%, specificity of 74.76%, precision of 91.37%, and F1 score of 93.9% in this work.

Data Availability

Data used were from the following: Kaggle Diabetic Retinopathy Detection Dataset, available at https://www.kaggle.com/c/diabetic-retinopathy-detection/data; APTOS 2019 Blindness Detection Dataset, available at https://www.kaggle.com/c/aptos2019-blindness-detection/data; DeepDR Diabetic Retinopathy Image Dataset, available at https://isbi.deepdr.org/download.html.

Conflicts of Interest

The authors declare that they have no conflicts of interest.

Acknowledgments

This project was supported by grants from Zhejiang Key Research and Development Project (2019C03088).

References

[1] L. Hill and L. E. Makaroff, "Early detection and timely treatment can prevent or delay diabetic retinopathy," *Diabetes Research and Clinical Practice*, vol. 120, pp. 241–243, 2016.

[2] Z. Yavuz and C. Köse, "Blood vessel extraction in color retinal fundus images with enhancement filtering and unsupervised classification," *Journal of Healthcare Engineering*, vol. 2017, Article ID 4897258, 12 pages, 2017.

[3] X. Feng, G. Cai, X. Gou, Z. Yun, W. Wang, and W. Yang, "Retinal mosaicking with vascular bifurcations detected on vessel mask by a convolutional network," *Journal of Healthcare Engineering*, vol. 2020, Article ID 7156408, 13 pages, 2020.

[4] H. Narasimha-Iyer, A. Can, B. Roysam et al., "Robust detection and classification of longitudinal changes in color retinal fundus images for monitoring diabetic retinopathy," *IEEE Transactions on Biomedical Engineering*, vol. 53, no. 6, pp. 1084–1098, 2006.

[5] B. Antal and A. Hajdu, "An ensemble-based system for microaneurysm detection and diabetic retinopathy grading," *IEEE Transactions on Biomedical Engineering*, vol. 59, no. 6, pp. 1720–1726, 2012.

[6] S. Roychowdhury, D. D. Koozekanani, and K. K. Parhi, "DREAM: diabetic retinopathy analysis using machine learning," *IEEE Journal of Biomedical and Health Informatics*, vol. 18, no. 5, pp. 1717–1728, 2014.

[7] K. M. Adal, P. G. van Etten, J. P. Martinez, K. W. Rouwen, K. A. Vermeer, and L. J. van Vliet, "An automated system for the detection and classification of retinal changes due to red lesions in longitudinal fundus images," *IEEE Transactions on Biomedical Engineering*, vol. 65, no. 6, pp. 1382–1390, 2018.

[8] X. Li, X. Hu, L. Yu, L. Zhu, C.-W. Fu, and P.-A. Heng, "CANet: cross-disease attention network for joint diabetic retinopathy and diabetic macular edema grading," *IEEE Transactions on Medical Imaging*, vol. 39, no. 5, pp. 1483–1493, 2019.

[9] T. Shanthi and R. S. Sabeenian, "Modified Alexnet architecture for classification of diabetic retinopathy images," *Computers & Electrical Engineering*, vol. 76, pp. 56–64, 2019.

[10] A. Krizhevsky, I. Sutskever, and E. H. Geoffrey, "ImageNet classification with deep convolutional neural networks," *Communications of the ACM*, vol. 60, no. 6, pp. 84–90, 2017.

[11] E. Decencière, X. Zhing, G. Cazuguel et al., "Feedback on a publicly distributed image database: the messidor database," *Image Analysis & Stereology*, vol. 33, no. 3, pp. 231–234, 2014.

[12] S. K. Hosseinzadeh, K. H. Peyman, R. Khazaeinezhad, J. W. Michal, A. S. Kevin, and D. Ralph, "Diabetic retinopathy classification using a modified xception architecture," in *Proceedings of the IEEE International Symposium on Signal Processing and Information Technology (ISSPIT)*, pp. 1–6, Ajman, UAE, December 2019.

[13] F. Li, D. Yuan, M. Zhang, C. Liang, X. zhou, and H. Zhang, "Multi-scale stepwise training strategy of convolutional neural networks for diabetic retinopathy severity assessment," in *Proceedings of the 2019 International Joint Conference on Neural Networks (IJCNN)*, pp. 1–5, Budapest, Hungary, July 2019.

[14] M. Hajabdollahi, R. Esfandiarpoor, K. Najarian, N. Karimi, S. Samavi, and S. M. R. Soroushmehr, "Hierarchical pruning for simplification of convolutional neural networks in diabetic retinopathy classification," in *Proceedings of the 2019 41st Annual International Conference of the IEEE Engineering in Medicine and Biology Society (EMBC)*, pp. 970–973, Berlin, Germany, July 2019.

[15] K. Simonyan and A. Zisserman, "Very deep convolutional networks for large-scale image recognition," *Computing Research Repository*, vol. 14091556 pages, 2014.

[16] A. Jain, A. Jalui, J. Jasani, Y. Lahoti, and R. Karani, "Deep learning for detection and severity classification of diabetic retinopathy," in *Proceedings of the 2019 1st International Conference on Innovations in Information and Communication Technology (ICIICT)*, pp. 1–6, Chennai, TN, India, March 2019.

[17] C. Szegedy, V. Vincent, L. Sergey, J. Shlens, and Z. Wojna, "Rethinking the inception architecture for computer vision,"

in *Proceedings of the 2016 IEEE Conference on Computer Vision and Pattern Recognition (CVPR)*, pp. 2818–2826, Las Vegas, NV, USA, July 2016.

[18] Kaggle, "Diabetic retinopathy detection," 2015, https://www.kaggle.com/c/diabetic-retinopathy-detection.

[19] Kaggle, APTOS 2019 Blindness Detection, https://www.kaggle.com/c/aptos2019-blindness-detection.

[20] DeepDR diabetic retinopathy image dataset, https://isbi.deepdr.org/index.html.

[21] E. D. Cubuk, B. Zoph, J. Shlens, and V. L. Quoc, "Randaugment: practical automated data augmentation with a reduced search space," in *Proceedings of the 2020 IEEE/CVF Conference on Computer Vision and Pattern Recognition Workshops (CVPRW)*, pp. 3008–3017, Seattle, WA, USA, June 2020.

[22] M. Tan and V. L. Quoc, "EfficientNet: Rethinking Model Scaling for Convolutional Neural Networks," 2019, https://arxiv.org/abs/1905.11946.

[23] M. Tan, Bo Chen, R. Pang, V. Vasudevan, and V. L. Quoc, "MnasNet: platform-aware neural architecture search for mobile," in *Proceedings of the 2019 IEEE/CVF Conference on Computer Vision and Pattern Recognition (CVPR)*, pp. 2815–2823, Seattle, WA, USA, June 2019.

[24] B. Zoph, V. Vasudevan, J. Shlens, and V. L. Quoc, "Learning Transferable Architectures for Scalable Image Recognition," in *Proceedings of the 2018 IEEE/CVF Conference on Computer Vision and Pattern Recognition*, pp. 8697–8710, Salt Lake, Utah, USA, June 2018.

[25] B. Zoph and V.L. Quoc, "Neural Architecture Search with Reinforcement Learning," 2017, https://arxiv.org/abs/1611.01578.

[26] C. Szegedy, S. Ioffe, V. Vincent, and A. Alemi, "Inception-v4, inception-ResNet and the impact of residual connections on learning," in *Association for the Advancement of Artificial Intelligence (AAAI)*, Palo Alto, CA, USA, February 2017.

[27] C. Szegedy, W. Liu, Y. Jia et al., "Going Deeper with convolutions," in *Proceedings of the 2015 IEEE Conference on Computer Vision and Pattern Recognition (CVPR)*, pp. 1–9, Boston, MA, USA, June 2015.

[28] K. He, X. Zhang, S. Ren, and J. Sun, "Deep Residual Learning for Image Recognition," in *Proceedings of the 2016 IEEE Conference on Computer Vision and Pattern Recognition (CVPR)*, pp. 770–778, Las Vegas, NV, USA, June 2016.

[29] F. Chollet, "Xception: deep learning with depthwise separable convolutions," in *Proceedings of the 2017 IEEE Conference on Computer Vision and Pattern Recognition (CVPR)*, pp. 1800–1807, Honolulu, HI, USA, July 2017.

[30] L. Liu, H. Jiang, P. He et al., "On the variance of the adaptive learning rate and beyond," 2020, https://arxiv.org/abs/1908.03265.

Hindawi
Journal of Healthcare Engineering
Volume 2020, Article ID 8822311, 16 pages
https://doi.org/10.1155/2020/8822311

Research Article

A Comparison of the Development of Medical Informatics in China and That in Western Countries from 2008 to 2018: A Bibliometric Analysis of Official Journal Publications

Jun Liang,[1] **Zhongan Zhang**,[2] **Lingye Fan**,[3] **Dongxia Shen**,[4] **Zhenying Chen**,[5] **Jie Xu**,[1] **Fangmin Ge**,[6] **Junyi Xin**,[7] **and Jianbo Lei**[8,9,10]

[1]*IT Center, Second Affiliated Hospital, School of Medicine, Zhejiang University, Hangzhou, Zhejiang Province, China*
[2]*Performance Management Department, Qingdao Central Hospital, Qingdao, Shandong Province, China*
[3]*Department of Obstetrics and Gynecology, Affiliated Hospital, Southwest Medical University, Luzhou, China*
[4]*Editorial Department of Journal of Practical Oncology, Second Affiliated Hospital, School of Medicine, Zhejiang University, Hangzhou, Zhejiang Province, China*
[5]*Library of Zhejiang University, Hangzhou, Zhejiang Province, China*
[6]*International Network Medical Center, Second Affiliated Hospital, School of Medicine, Zhejiang University, Hangzhou, Zhejiang Province, China*
[7]*Hangzhou Medical College, Hangzhou, Zhejiang Province 310000, China*
[8]*Institute of Medical Technology, Health Science Center, Peking University, Beijing, China*
[9]*Center for Medical Informatics, Peking University, Beijing, China*
[10]*School of Medical Informatics and Engineering, Southwest Medical University, Luzhou, Sichuan Province, China*

Correspondence should be addressed to Jianbo Lei; jblei@hsc.pku.edu.cn

Received 20 July 2020; Revised 28 August 2020; Accepted 29 September 2020; Published 12 October 2020

Academic Editor: Xiwei Huang

Objective. We focused on medical informatics journal publications rather than on conference proceedings by comparing and analyzing the data from journals and conferences from a broader perspective. The aim is to summarize the unique contributions of China to medical digitization and foster more multilevel international cooperation. *Method*. In February 2019, publications from 2008 to 2018 in three major English-language medical informatics journals were retrieved through Scopus, including the journals, namely, International Journal of Medical Informatics (IJMI, international community), JAMIA (United States), and Methods of Information in Medicine (MIM, Europe). Three major Chinese-language journals, namely, China Digital Medicine (CDM), Chinese Journal of Health Informatics and Management (CJHIM), and Chinese Journal of Medical Library and Information Science (CJMLIS), were searched within the major three Chinese literature databases. The datasets were preprocessed using the NLP package on Python, and a smart local moving algorithm was used as a clustering method for identifying the aforementioned journals. *Result*. Between 2008 and 2018, the total number of published papers and H-index of the three English-language journals was 1371 and 67 (IJMI), 1752 and 86 (JAMIA), and 637 and 35 (MIM), respectively. In the same period, the total number of published papers and H-index in the three Chinese-language journals was 6668 and 23 (CDM), 1668 and 22 (CJHIM), and 2557 and 25 (CJMLIS), respectively. IJMI, JAMIA, and MIM received submissions from 82, 59, and 62 countries/regions, respectively. By contrast, the three Chinese journals only received submissions from seven foreign countries. The proportions of authors from institutional affiliations were similar between the three English-language journals (IJMI, JAMIA, and MIM) and CJMLIS because the majority of the authors were from universities (81%, 74%, 73%, and 65.2%), followed by medical institutions (12%, 10%, 9%, and 23.4%) or research institutes (2%, 4%, 10%, and 4.3%). Furthermore, the proportions of the authors from enterprises were low (2%, 6%, 4%, and 0.3%) for all journals. However, the authors in CDM and CJHIM were mainly from medical institutions (50% and 40%), followed by universities (33% and 32%) and research institutes (3% and 4%). In addition, the proportions of enterprises were only 3% and 2%, respectively. Among the top five authors in three English-language journals (ranked in terms of the number of published papers), 100% had doctoral or master's degrees, compared with only 60% in the Chinese journals. Additionally, 28204 different keywords were extracted from the aforementioned papers, covering 275 specific high-frequency key terms. Based on these key terms, four clusters were found in the English literature—"Health and Clinical Information Systems," "Internet and Telemedicine," "Medical Data Statistical Analysis," and "EHRs and Information Management"—and three clusters were found in the Chinese literature: "Hospital Information Systems and EMR," "Library Science and Bibliometrics Analysis," and "Medical Reform Policy and Health Digitization." Only two clusters are similar, and Chinese-language journals focus more on health information in technology and industrial applications than in medical informatics basic research. *Conclusion*. This study provides important insights into the development of medical informatics (MI) in China and Western countries showing that the medical informatics journals of China, the United States, and Europe have distinct characteristics. Specifically, first, compared with the Western journals, the number of papers published in the journals of professional associations in the field of MI in China is large and the application value is high, but the academic influence and academic value are relatively low; second, most of the authors of the Chinese papers are from hospitals, and most of the counterparts in the Western countries are from universities. The proportion of master's or doctoral degrees in the former is also lower than that of the latter; furthermore, regarding paper themes, on the one hand, China MI has no theoretical and basic research on medical data statistics and consumer health based on the Internet and telemedicine; on the other hand, after nearly 10 years of hospital digital development, China has fully used the latecomer and application advantages in hospitals and, through extensive international cooperation, has made significant advancements in and contributions to the development of medical information.

1. Introduction

Medical informatics (MI) can be defined as the acquiring, storing, retrieving, and using of healthcare information to foster better collaboration among a patient's various healthcare providers [1], which originated in 1959 when Ledley et al. published "Reasoning Foundations of Medical Diagnosis; Symbolic Logic, Probability and Value Theory Aid Our Understanding of How Physicians Reason" in Science [2]. Increasing MI is a fundamental requirement for building effective and efficient health information systems at the local, national, and global levels [3]. With the increasingly extensive application of computer science and information technology in medical fields, MI has gradually become an interdisciplinary field theoretically based on computer technology and science that integrates medicine and information science and management to achieve digitized medical management at the global level [3].

The establishment and development of a discipline rely on the foundation and support of a system, including relevant institutions and associations, mainstream auxiliary journals, and publications [4], for which there is no exception for MI. Most developed nations have all established corresponding disciplinary systems, including institutes, conferences, and journals, and have actively developed talent, culture, and scientific research. IMIA was founded in 1978, is the acknowledged leader of international MI, and comprises over 45 state-level organization institutes and four regional conferences. IMIA holds one MI academic conference, MedInfo, biannually. IMIA has four official journals, which are all included in the Science Citation Index (SCI), namely, the International Journal of Medical Informatics (IJMI), Applied Clinical Informatics, Informatics for Health and Social Care, and Methods of Information in Medicine (MIM). Of these four journals, IJMI is the most influential. The European Federation for Medical Informatics (EFMI), established in 1976, is one of four regional conferences of the IMIA, comprises 30 state-level institutes, and is mainly devoted to exchanges among European countries. It holds its MI academic conference (MIE) annually. EFMI has four official journals, of which two are included in the SCI, namely, MIM (founded in 1962) and IJMI. AMIA is the official representative institution of the United States in IMIA and was jointly founded from three organizations in 1990. Its members are not limited to the United States and are from interdisciplinary organizations across 65 countries, including those of doctors, nurses, engineers, medical librarians, institute researchers, and educators. AMIA holds annual conferences, and its official journal, *Journal of the American Association* (JAMIA), is also included in the SCI.

Different from MI in Western countries that developed from computer applications to medicine, MI in China evolved from medical library information science in the early 1980s. Along with the development of hospital digitization in China, this discipline did not become independent until 2010. To date, only a few educational institutions in China have established an MI institute or graduate courses (27 programs for a master's degree, five programs for a doctorate), and the majority of participants are undergraduates [5]. Furthermore, China currently has four state-level medical information associations, of which three have journals: China Digital Medicine (CDM) from the China Hospital Information Management Association (CHIMA), Chinese Journal of Medical Library and Information Science (CJMLIS) from the Chinese Society of Medical Information (CSMI) (founded by Chinese Medical Association), and Chinese Journal of Health Informatics and Management (CJHIM) from the Chinese Health Information Association (CHIA) (formerly known as the Chinese Health Statistics Association).

To efficiently, accurately, and timely understand the research hot spots and developing trends of medical informatics, researchers have adopted bibliometrics to study the frontiers of MI from three aspects: academies, conferences, and journals. As for academies, V. Maojo et al. in 2012 reviewed the members attending three mainstream academies of MI, including Medical Informatics Europe (MIE) 2005–2008, MedInfo 2004, 2007, and 2010, and AMIA 2005–2009, and thought that the influence of these academies outside this discipline was very low [6]. As for conferences, Liang et al. compared the characteristics between Chinese and international mainstream MI conferences from the aspects of conference history, scales, and themes [7]. Jia et al. comprehensively analyzed the authors, academic values, and themes between Chinese and international mainstream MI conference publications [8]. Moreover, as for journals, by using online bibliographic search filters, Van Kasteren. et al. analyzed the abstracts, titles, and keywords among JMIR, MIM, JAMIA, and IJMI in 2001–2015 and analyzed and summarized the changing trends of themes in these English-language MI journals [9]. With UCINET, NetDraw, and SPSS, Deng et al. analyzed 1340 papers published by Chinese academics in 18 journals listed in the 2016 JCR under the MI category, plotted keyword cluster trees and cooccurrence network diagrams, and found that the research hot spots of Chinese-language journals were MI systems, mobile healthcare, and telecare [5]. Kim and Delen analyzed the themes of 26407 English-language papers published in 23 journals listed in the 2012 JCR under the MI category during 2002–2013 by using keyword clustering and found that the research hotspots and mainstreams in MI were HIT, Internet-enabled research, and EMR/EHRs [10]. Gukesen and Haux analyzed the theme trends of English-language papers published in 23 journals listed in the 2016 JCR under the MI category during 2013–2017 using VOSviewer, and they recognized 5 theme clusters, including biomedical data analysis and clinical informatics [11]. However, the existing studies are quantitative analyses of medical informatics research hotspots performed internationally or in China, but there is rare comprehensive comparison of the two, and the existing comparisons are limited by the nonunification of time dimensions. Our study is based on the overall research framework of our previous studies, or, namely, the principle that this discipline cannot be developed without the support from professional academies, mainstream conferences, and journals. We have expanded and added the comprehensive analysis of MI academic journals in China, the United States, and Europe and from the international MI community (IMIA) to find gaps in Chinese MI. We then summarized the shared experiences with other countries to promote international exchange and help improve and develop Chinese MI. Our research filled the gap in comprehensive comparative analysis and had unique contributions.

2. Materials and Methods

2.1. Journal Sources and Selection Criteria. Under the framework of Preferred Reporting Items for Systematic Reviews and Meta-Analysis (PRISMA) [12], We selected three representative English-language MI association journals—International Journal of Medical Informatics (IJMI: IMIA, global), Journal of the American Medical Informatics Association (JAMIA: AMIA, United States), and MIM (EFMI, Europe)—that represent different research groups and regions. For the Chinese-language MI journals, we selected three representative journals and the largest-scale professional journal from state-level MI associations: the official journal of CHIMA: CDM (CHIMA, China); CJHIM (CHIA, China) from CHIA; and the CJMLIS (CSMI, China) from the Medical Information Subassociation.

2.2. Data Collection and Preprocessing. First, the English-language papers were searched on Scopus, which provided comprehensive preprocessed data from academic publications and has been accepted as one of the best databases for literature analysis [13]. The search period was limited to 2008–2018, and the literature types searched for were articles and reviews. Second, the Chinese-language papers were searched through three major Chinese literature databases: Chinese Science and Technology Journal Database (CQVIP) [14], Chinese National Knowledge Infrastructure (CNKI) [15], and WanFang Data [16]. EndNote X7 was used for a preliminary analysis of the general information assembled since it is able to not only merge and filter bibliographic records in different formats but also exclude some articles such as book reviews, conference notifications, and those which are not related to MI. The searching period was from 2008 to 2018, and to ensure data consistency, all searches were conducted on February 7, 2019.

Because all the databases had standard functions for data analysis and abstraction, we selected and imported the following information:

(1) Metadata of journals, including the names of journals, organization of the sponsors, organization of the publication, time of publication, period of publication, place of publication, and database of inclusion

(2) Metadata and contents of periodical papers, including the title; keywords; abstract; year of publication; citations of papers; and authors' names and education level, affiliations, and country

Next, to maximize the effectiveness and accuracy of co-word analysis and data visualization, we preprocessed the target datasets. First, the titles and keywords of the included articles were standardized into lowercase, and the morphology and abbreviations were reproduced in Python 2.7 + NLTK NLP [17]. Second, because all the Chinese-language MI periodical papers were written in Chinese, we used the self-developed Chinese Latin tool to convert the Chinese names into Pinyin. Pinyin (phonetic alphabet) is a system of romanization of Chinese characters and represents the pronunciation of Chinese characters. Pinyin was approved in 1958 by the government of the People's Republic of China and officially adopted in 1979. Pinyin is not used officially in Taiwan [18]. Furthermore, using the Youdao AICloud translation package [19], we translated the titles and keywords into English and manually emended and examined them. Finally, these preprocessed datasets of periodical papers were collected and imported into Microsoft Excel 2011 and EndNote X2 for further qualitative and quantitative analyses.

2.3. Bibliometric Analysis. The basic characteristics of the papers were analyzed with the built-in functions of Scopus, CQVIP, CNKI, and WanFang Data. The author affiliations were clustered using self-developed tool based on Python 2.7. The tool clusters the authors' affiliations into six categories: medical institutions, universities, manufacturers, research institutions, and others. The H-index was designed as a measure of scientific research impact [20], which indicates that a scholar or country has published H papers, and each of which has been cited in other publications at least H times. Therefore, the H-index reflects both the number of publications and the number of citations per publication [21]. Co-word analysis was proposed by Michel and Jean-Pierre from the France National Centre for Scientific Research [22]. In this case, on the one hand, we adopted a smart local moving algorithm [23] as the word clustering method; on the other hand, the results of clustering were visualized on VOSviewer (Centre for Science and Technology Studies, Leiden, Netherlands) [24]. The process is illustrated in Figure 1.

3. Results

3.1. Overall Trends of Journal Papers. Papers published in MI journals between 2008 and 2018, including the three Chinese MI journals (CDM, CJHIM, and CJMLIS) and the three English MI journals (IJMI, MIM, and JAMIA), were analyzed both quantitatively and qualitatively. The basic information of each journal is listed in Supplementary Materials Table S1. Since CDM was founded in 2007, we selected papers published after 2008, which facilitated a comparison between different MI journals.

From the three mainstream Chinese-language databases, 6668, 1668, and 2557 articles between 2008 and 2018 were identified from CDM, CJHIM, and CJMLIS, respectively, with a total of 10893 and an annual rate of 990 articles. Using Scopus, 1371, 637, and 1752 articles were identified from IJMI, MIM, and JAMIA, respectively, with a total of 3760 and an annual rate of 341 articles. The number of Chinese-language papers was 2.89 times that of English-language papers, and the number of papers in CDM was 1.77 times that of the total number of English-language papers (Figure 2). The proceedings from Chinese mainstream MI association conferences, including the China Conference (CMIAAS), China Hospital Information Network Conference (CHINC), Chinese Health Information Technology Exchange Conference (CHITEC), and Chinese Medical Association National Medical Information Conference (CPMI), had no unified search database and were not continuous or complete [8, 25]. However, the papers published in CDM, CJHIM, and CJMLIS could be completely and timely retrieved from the three mainstream Chinese-language databases. These phenomena all suggest Chinese MI journals as the main disciplinary systems that support the establishment and development of the MI discipline in China.

3.2. Academic Influence of Professional Journals. The academic influence of the professional MI journals is significantly different. JAMIA and IJMI are top-ranked journals, followed by MIM; however, the Chinese MI journals (CDM, CJHIM, CJMLIS) are ranked much lower. JAMIA published 1752 papers between 2008 and 2018, which were cited 44051 times, with an average of 25.1 times per paper and an H-index of 86 (Figure 3). IJMI published 1371 papers in this period, which were cited 26900 times, with an average of 19.6 times per paper and an H-index of 67. MIM published 637 papers in this period, which were cited 6827 times, with an average of 10.7 times per paper and an H-index of 35. The aforementioned three journals can all be retrieved on SCI, and the 2017 impact factors of JAMIA, IJMI, and MIM were 4.27, 2.975, and 1.531, respectively.

We compared similar statistics from the three Chinese MI journals, and the results suggest that the total citations of the three Chinese MI journals are slightly lower than that of IJMI (23184 vs. 26900) but far lower than that of JAMIA (44051), even though the total number of papers published by the three Chinese journals was 16.9 and 13.2 times those in IJMI and JAMIA, respectively.

3.3. Author Analysis of MI Journals

3.3.1. Author Distributions of Journal Papers. Similar to the country distribution of authors in the MI conference proceedings, the regional MI journals, including JAMIA (AMIA, United States) and MIM (EFMI, Europe), and Chinese MI journals (CDM, CJHIM, and CJMLIS) were dominated by local authors, whereas the international journals such as IJMI (IMIA, global) represented authors from various regions. Between 2008 and 2018, JAMIA published submissions from authors of 58 countries or regions, and the number of countries or regions with >10 manuscripts was 15; however, the majority of authors were from the United States (approximately 69%), followed by Europe (~10%). By contrast, the proportion of the authors from China (including mainland China, Taiwan, Hong Kong, Macao) was only 4%. MIM published submissions of the authors from 62 countries or regions, and the number of countries or regions with >10 manuscripts were 21. However, most authors were from Europe (approximately 63%), followed by the United States (about 16%), and the proportion of authors from China (including mainland China, Taiwan, Hong Kong, Macao) was only 2.4%. IJMI published submissions from the authors of 81 countries or regions; the number of countries or regions with >10 manuscripts was 28; and approximately 27%, 40%, and 6% of authors were from the United States, Europe, and China (including mainland China, Taiwan, Hong Kong, Macao), respectively. The Chinese MI journals (CDM, CJHIM, CJMLIS) were less internationalized because publications by foreign authors were only from Japan, Canada, the United States, South Korea, the United Kingdom, Netherlands, and Germany. Figure 4 shows the countries with more than 1% of the authors.

3.3.2. Author Characteristics of Journal Papers. The affiliations and academic backgrounds of the authors were largely different among journals. The proportions of

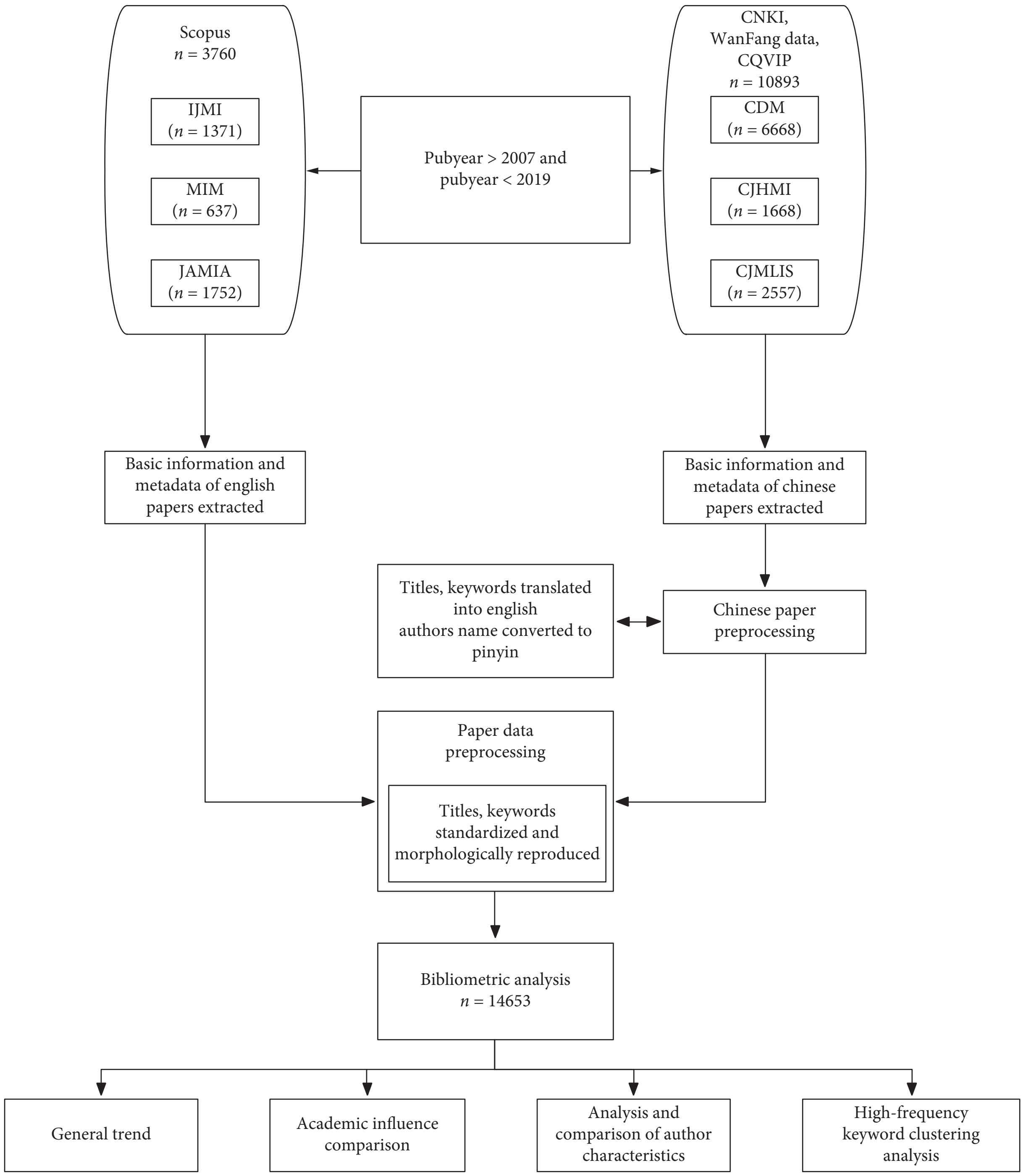

Figure 1: Workflow of the target article search and major manipulations.

different affiliations were similar between the English-language journals (IJMI, JAMIA, MIM) and the Chinese journal CJMLIS because the majority (>50%) of authors were from universities (81%, 74%, 73%, and 65.2%, respectively), followed by medical institutions (12%, 10%, 9%, and 23.4%, respectively) or research institutes (2%, 4%, 10%, and 4.3%, respectively). Furthermore, the proportions of enterprises were low (only 2%, 6%, 4%, and 0.3%, respectively) across all journals. However, the authors in CDM and CJHIM were mainly from medical institutions (50% and 40%, respectively), followed by universities (33% and 32%, respectively) and research institutes (3% and 4%, respectively), and the proportions of enterprises were only 3% and 2%, respectively (Figure 5). These data are very similar to the affiliation distributions in the international MI conference proceedings; however, they differ from those in the Chinese MI conference proceedings because the latter is dominated by medical institutions (54%), followed by universities (17%), institutes (10%), and enterprises (7%) [25].

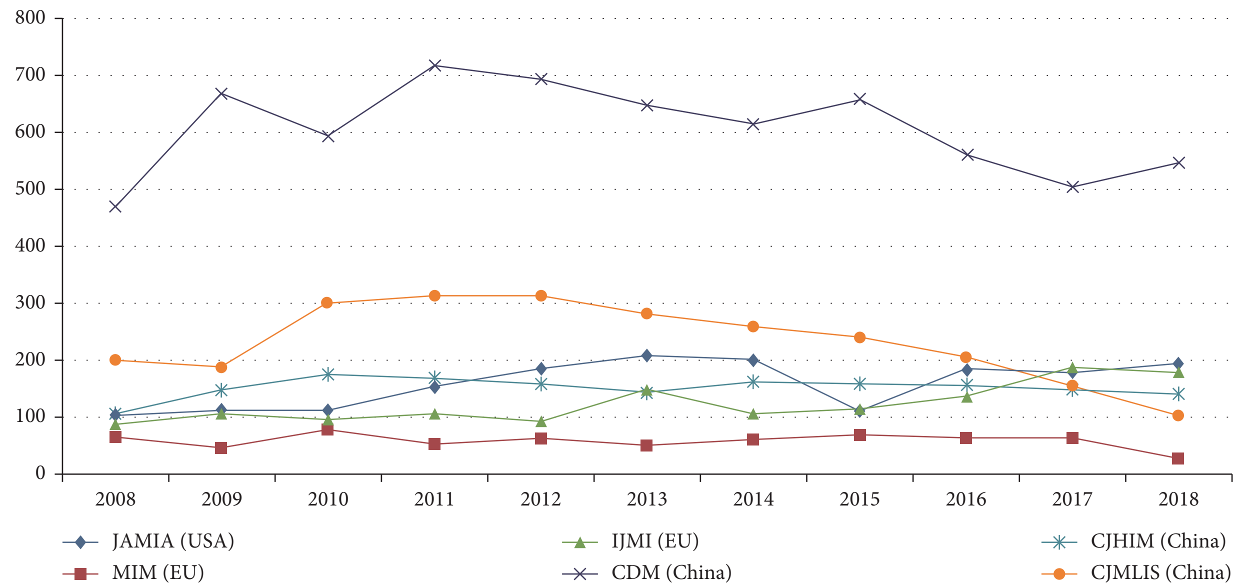

FIGURE 2: Journal articles of the IJMI, JAMIA, MIM, CDM, CJHIM, and CJMLIS from 2008 to 2018.

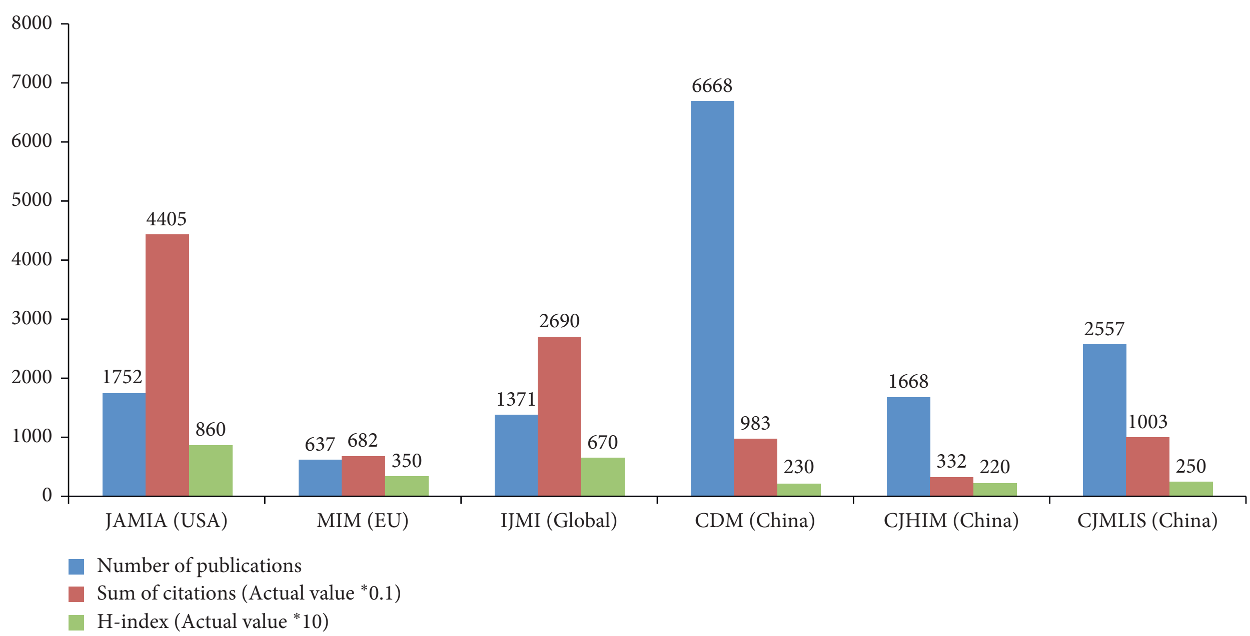

FIGURE 3: Number of publications, citations, and H-indices of IJMI, JAMIA, MIM, CDM, CJHIM, and CJMLIS in 2008–2018.

We further assessed the top five authors in each journal and analyzed their affiliations and academic and knowledge backgrounds (Supplementary Materials Table S2). We observed that the authors of JAMIA and MIM differed from those of the other journals but were similar to the authors from the proceedings of AMIA, MIE, and MedInfo because a large proportion (40%) of authors possessed MD degrees [8].

The top five authors in IJMI had academic backgrounds similar to those in the Chinese MI journals (CDM, CJHIM, CJMLIS) and Chinese MI academic journals (CMIAAS, CHINC, CHITEC, CPMI) because the majority of authors had no background in clinical medicine. Of the top five authors in IJMI, one had an MD, four had doctoral degrees, and all were from universities. Among the top five authors in CDM, one had a master's and doctoral degree, three had doctoral degrees, and two had master's degrees. Furthermore, two were from medical institutions and three were from institutes.

We also observed some differences because the top five authors from IJMI, MIM, and JAMIA all received professional academic training in MI; however, the top five authors in the Chinese MI academic journals mostly did not receive this training; usually were from the computer, public health, statistics, library science, or informatics fields; and only became involved in MI after employment.

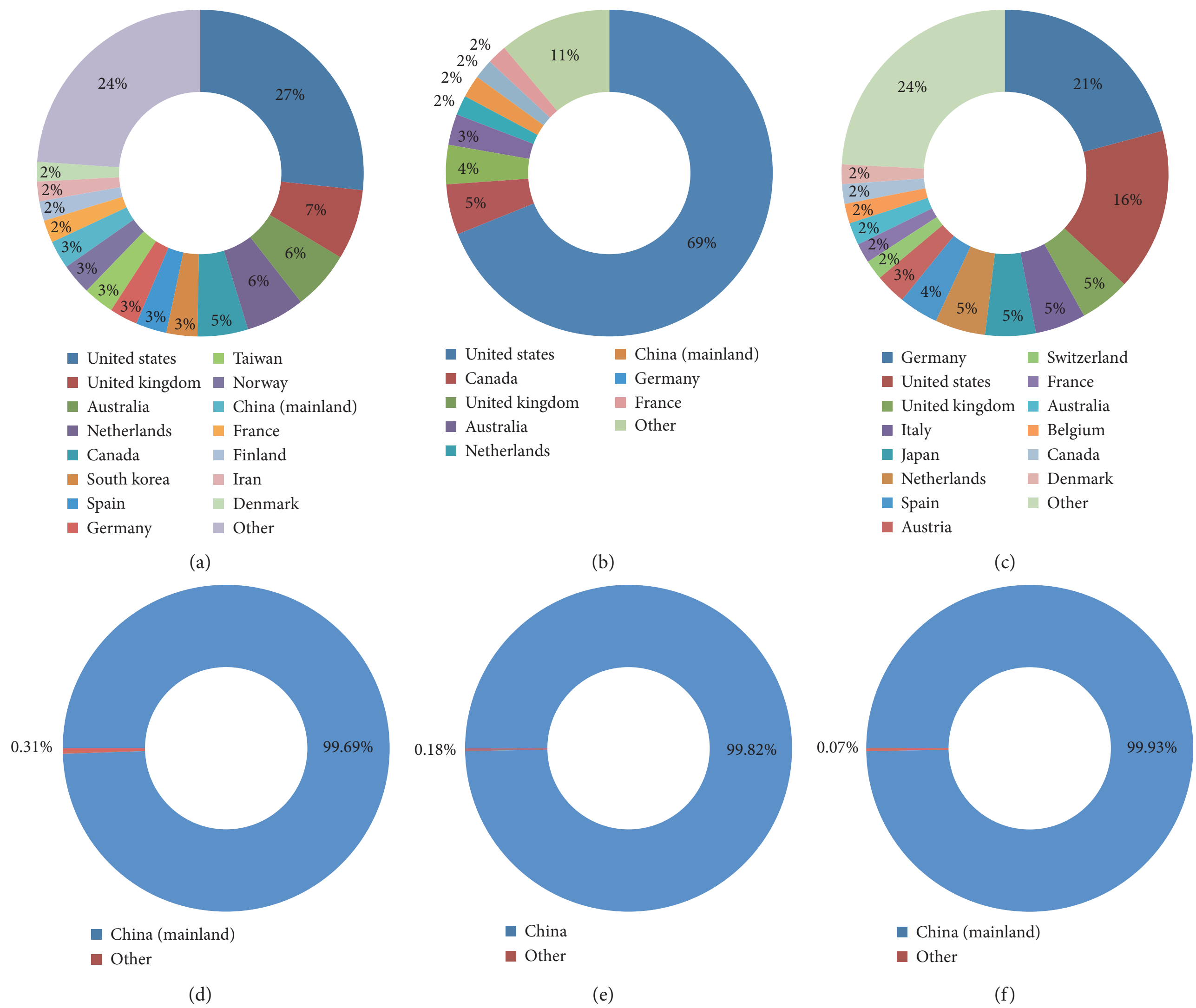

Figure 4: Analysis of author distribution among the countries in (a) IJMI (EU), (b) JAMIA (USA), (c) MIM (EU), (d) CDM (China), (e) CJHIM (China), and (f) CJMLIS (China) in 2008–2018.

3.4. Keyword Selection and Analysis of Journal Papers. The purpose of the keyword selection and analysis is to identify the focal points of research that have been confirmed as a major step in monitoring the development and trend of a discipline [26]. Here, the keywords in the papers published in the English-language journals (IJMI, MIM, JAMIA) and Chinese-language journals (CDM, CJHIM, CJMLIS) were analyzed and compared to determine the underlying rules.

3.4.1. Selection of High-Frequency Threshold of Keywords. The frequency distributions of the keywords were largely different between the Chinese- and English-language MI journals, which led to differences in the high-frequency word selection methods. To simplify the selection and analytical process and to decrease unnecessary interference from low-frequency words, we selected high-frequency words. However, no unified method is available to determine the critical levels of high-frequency words, and the available methods include the subjective empirical method, 80/20 rule [27], Price's equation [28], g-index [29], and high/low-frequency word isolation equation.

To select the appropriate frequency threshold, we first observed the frequency distributions of keywords in the six MI journals and found that the repeated rates of keywords were low in papers from Chinese MI journals compared with those in the international high-quality and mainstream MI journals (IJMI, MIM, and JAMIA). Namely, many keywords occurred once, and the rate of these words was 20% higher than those in the English-language papers, which limited the applicability of the high/low-frequency word isolation method based on Zipf's law. Specifically, the threshold value was slightly larger, and too few high-frequency words were intercepted. After multiple trials, we adopted different high-frequency word threshold computation methods according to the characteristics of English-language and Chinese-language papers and used

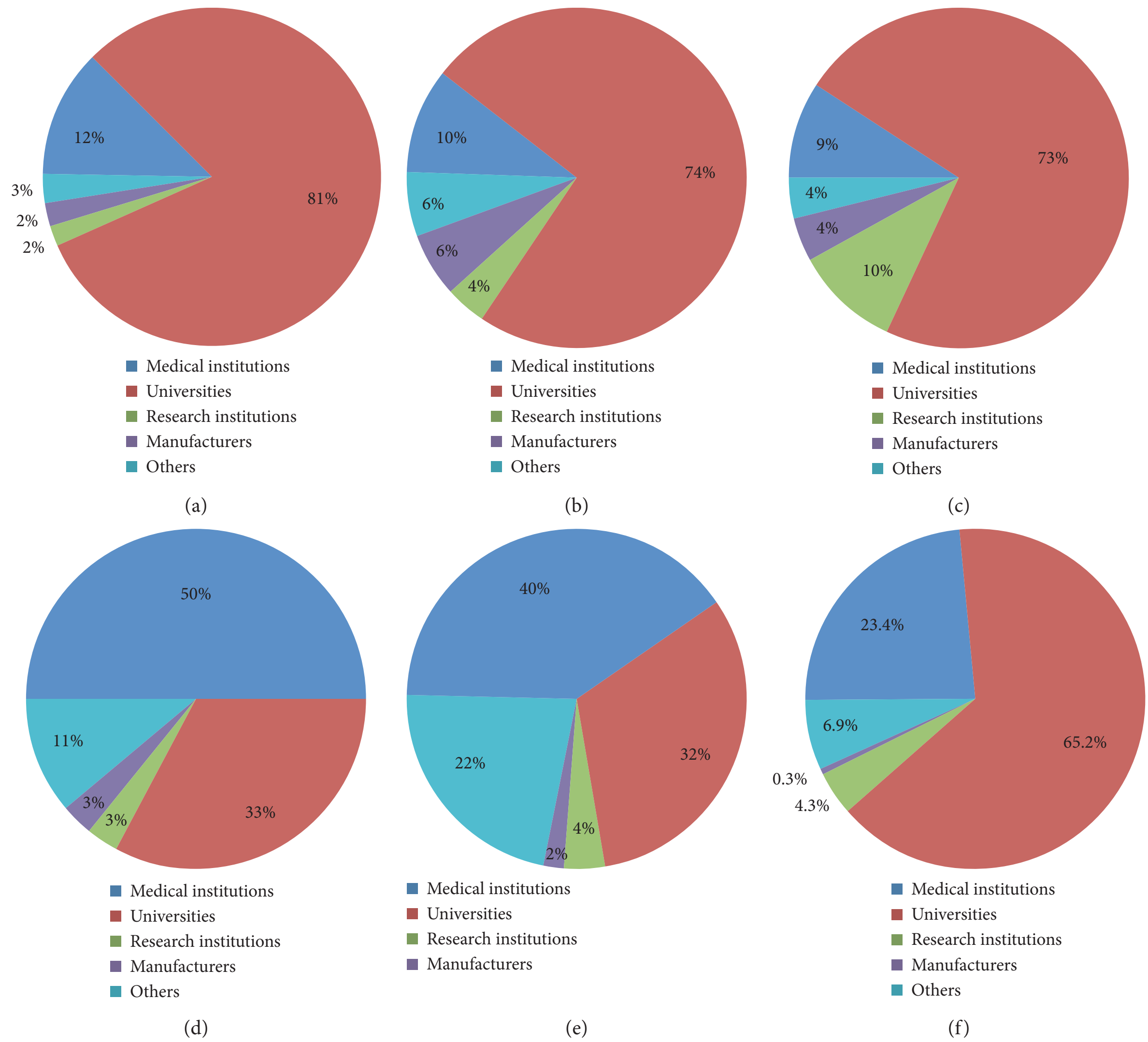

Figure 5: Author affiliations in (a) IJMI (EU), (b) JAMIA (USA), (c) MIM (EU), (d) CDM (China), (e) CJHIM (China), and (f) CJMLIS (China) in 2008–2018.

Donohue's method [30] based on Zipf's law for the English papers. The formula is as follows:

$$T = \frac{\sqrt{1 + 8 \times N_1} - 1}{2}, \tag{1}$$

where N_1 is the number of keywords with one word frequency and T is the frequency threshold of high-frequency words.

For the Chinese papers, according to the 80/20 rule [27], high-frequency words accounting for an accumulated proportion of 20% were extracted in a descending manner. The final high-frequency word frequency thresholds were 112 for the English-language journals and 26 for the Chinese-language journals.

3.4.2. High-Frequency Keyword Clustering Analysis and Research Focal Points. Analysis of keywords can indirectly reveal the hotspots and changing trends in research topics, which is critical for understanding the development of this field [31]. Next, we mined the data in the keywords in the published articles from the two groups of six MI journals. First, 28204 keywords were identified from 14653 articles. Second, these keywords were filtered by using the aforementioned high-frequency word thresholds. Next, the keywords with semantic similarity or closeness were grouped by using the "replace by" column on VOSviewer. We found 275 highly correlated high-frequency words: 153 words from the Chinese-language journals and 132 words from the English-language journals. Finally, the keywords in the two groups were clustered.

The results showed the keywords from the English-language MI journals were reorganized into four clusters, which we named (1) "Internet and Telemedicine" (yellow), (2) "Health and Clinical Information Systems" (blue), (3) "Medical Data Statistical Analysis" (green), and (4) "EHRs and Information Management" (red). Notably, our clustering results were supported by Kim et al., who mined the abstracts and texts from the articles published in 23 English-language MI journals within 12 years [10]. Only three clusters were found in the Chinese-language MI journals and were named (1) “Hospital Information Systems and EMR” (red), (2) “Library Science and Bibliometrics Analysis” (purple), and (3) “Medical Reform Policy and Health Digitization” (orange).

The results of the clustering are presented in Figures 6 and 7. Moreover, the ten keywords with the highest frequency in each cluster are listed in Table 1. Due to length limitations, a discussion of the concerns of the six journals is in Supplementary Materials Content S3.

4. Discussion

We previously analyzed the MI conference proceedings in China, the United States, Europe, and IMIA and found that MI research in China was largely different and lagged behind other developed regions in terms of academic evaluation, multisource cooperation, talent pool and quality, focal points, trends, and research investment [8]. In this study, we further comprehensively analyzed the data from MI journals to confirm our previous findings from a broader perspective and thereby propose key recommendations.

4.1. Analysis and Comparison of Academic Values between Chinese and English MI Journals. MI as an emerging interdisciplinary field has not been set within a specific category in the WOS but has a similar category—Medical Informatics—involving 25 journals. JAMIA (the 2017 impact factor: 4.27), IJMI (the 2017 impact factor: 2.95), and MIM (the 2017 impact factor: 1.53) rank as 3, 6, and 17, respectively. In particular, JAMIA has been highly approved by the Academic Committee of China Computer Society, listed by the China Computer Society as a key recommendation, is a well-known and highly reputed journal in the cross-disciplinary/comprehensive/emerging field, and encourages submissions from Chinese counterparts [32].

However, China has no authorized MI journal or any MI journal included in SCI, EI, or Medline. We believe that this may be related to the academic levels of these journals. Of the three authorized MI professional journals, the H-indices of CDM, CJHIM, and CJMLIS are 23, 22, and 25, respectively, which are less than half that of IJMI and are 70% that of MIM. However, they are slightly higher than that of MEI and the MedInfo proceedings (H-index of both: 19) and lower than that of the AMIA Annual Symposium (H-index: 32) [8]. Furthermore, the check and encouragement criteria in Chinese academia are first based on the articles included in SCI, Ei engineering village (Ei), or Medline and then on the core journals included in the Peking University Core Journals List, which are primarily graduate student dissertations [4]. However, none of CDM, CJHIM, or CJMLIS was included in the Chinese Core Journals List [33]. Thus, many researchers can only submit to nonprofessional MI Chinese core journals, which increases difficulty and limits dissemination. This phenomenon of no core journals or high-quality journals and no high-influence or high-cited journals severely constrains the development of mainstream journals and publications that support MI.

4.2. Analysis and Comparison of Regional Cooperation and Author Characteristics between Chinese and English MI Journals. IJMI, MIM, and JAMIA, as authorized academic journals in MI, have attracted submissions from academic researchers and industrial workers worldwide; however, the Chinese MI journals (CDM, CJHIM, and CJMLIS) have received submissions from only seven foreign countries. However, in the IJMI, MIM, and JAMIA journals, the proportion of Chinese authors (including mainland China, Taiwan, Hong Kong) did not exceed 6%, which implies gaps in MI development in China.

China has an insufficient talent pool for MI and has no continued support from existing educational institutions for the advancement of industrial development, which is stated as “cold in academic research, (and) incorporate(s) hot in industrial application” [4]. The author affiliations in CDM and CJHIM are mainly medical institutions, whereas the majority of those in JAMIA, IJMI, MIM, and CJMLIS are universities. A much larger proportion of authors have doctoral degrees and a medical educational background in IJMI, MIM, and JAMIA compared with the qualifications of the authors in the seven Chinese MI academic journals.

Such a difference in author characteristics between the Chinese journals and journals from other regions is because of the distinguished developmental environment for MI in China. In 2009 in China, HIT was considered one of the “ four beams and eight pillars” of the new healthcare reform [34], and MI was treated as an independent discipline. However, MI was equated as HIT to a large extent. In third-class hospitals (the highest class), the IT workers mostly undergo undergraduate courses or below; therefore, submissions are mainly summarized in the context of hospitals but ignore theories of MI, especially research on methodology and basic technology.

4.3. MI Journals from China and Western Countries: Analysis and Comparison in Keyword Clusters. In Figures 6 and 7, seven keyword clusters were identified from the six Chinese-language or English-language MI journals; of them, two clusters (EN-Cluster 2 and CN-Cluster 1) are similar, which again reflects “hot in industry application, and cold in academic research” in the MI field of China. Next, we discuss these seven clusters:

(1) EN-Cluster 1 (“Internet and Telemedicine”): this cluster results from the introduction of the Internet into the medicine field and is based on extensive research on diabetes and family care through the Internet, telemedicine, and other techniques and through questionnaires. Surprisingly, telemedicine in Europe and the United States has formed an independent system, but in China telemedicine belongs to the cluster “Hospital Information Systems and EMR” and is an important part of hospital information systems (HIS) and a supplement to out-

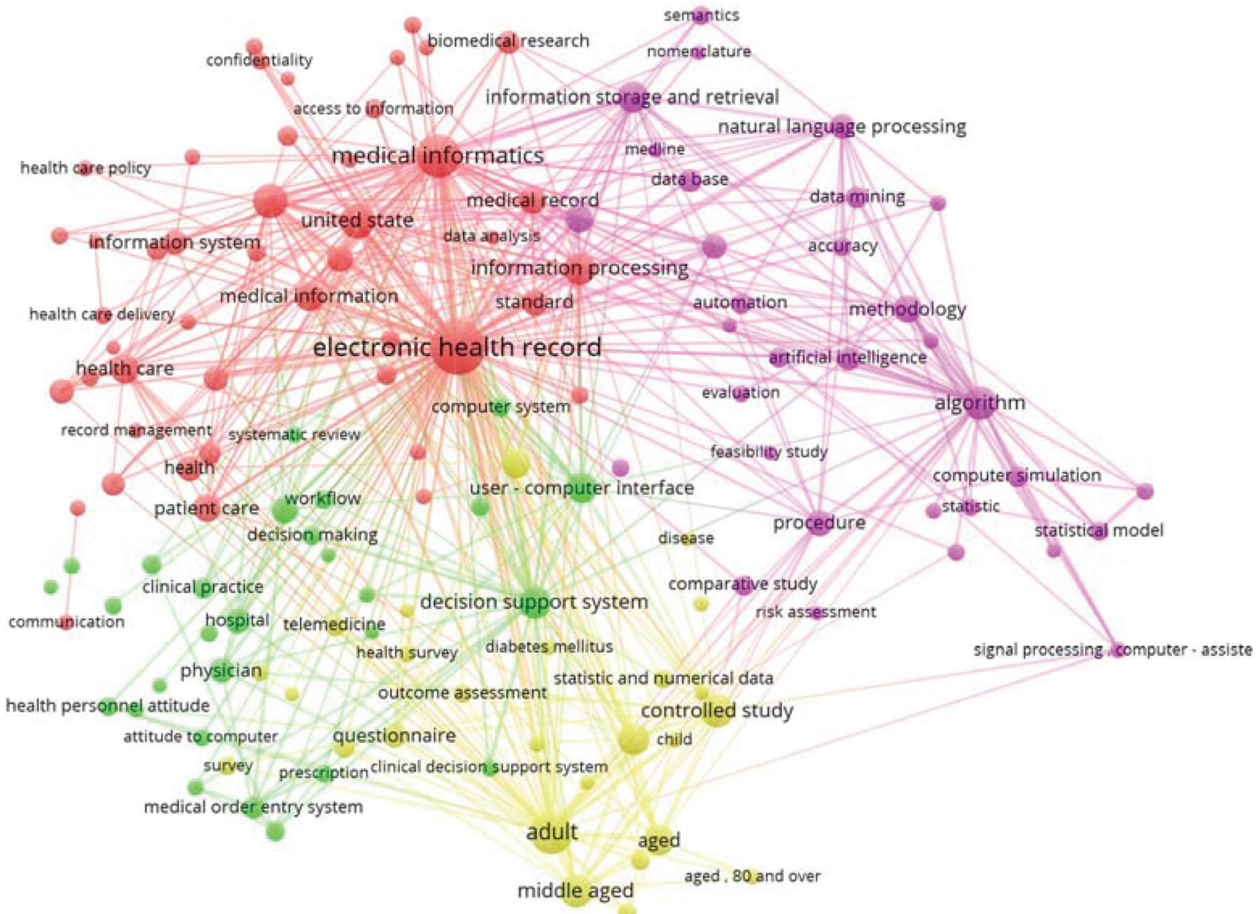

Figure 6: Cluster map of the keywords obtained by text mining 11 years (2008–2018) of articles on different topics from three English MI journals (IJMI, JAMIA and MIM). Topics are colored as red (EHRs and Information Management), blue (Health and Clinical Information Systems), yellow (Internet and Telemedicine), and green (Medical Data Statistical Analysis).

hospital continuity of medical services to patients. We posit that this situation may be related to the "digital hospital" policies in China. On the one hand, in the *EMR Function Grade Specification* issued by the National Health Commission of China in 2015, telemedicine was already included in EMR [35]; on the other hand, our preliminary research implied that the Chinese government has involved telemedicine as a major part of regional HIT construction and has achieved great success [36].

(2) EN-Cluster 2 ("Clinical and HIS") and CN-Cluster 1 ("HIS and EMR"): clinical informatics [37], especially the use of computers in hospital management, clinical diagnosis, and treatment, is the focus of global researchers and industrial workers in this field, including medical order entry systems, electronic medical records, and other HIS. We think that the reason may be that HIS have been extensively applied in hospitals [38] and that HIT has been gradually approved by the medical field [39]. Moreover, along with the deepening of medical reforms in China in recent years, the National Health Commission of China has expanded the connotations of Chinese HIS and proposed the goal of "digital hospitals" [40]. A notable requirement is that hospitals are starting to expand to digitization services, including patient engagement services (e.g., schedule appointments online; pay bills online; view, download, and print their medical information; and participate in satisfaction evaluations).

(3) EN-Cluster 3 (Medical Data Statistical Analysis): this cluster is exclusive to the English-language MI journals and involves abundant content related to theoretical models, including the topics associated with medical information methodology, artificial intelligence, natural semantic processing, and data mining software and systems.

(4) EN-Cluster 4 (EHRs and Information Management): this cluster is also exclusive to the English-language MI journals and describes an important aspect of MI. We posit that this also means that EHRs have gradually become a widely approved and accepted concept. The European and US researchers are focusing on technical issues of EHRs. Notably, EHRs are not present in the high-frequency keyword list in China; nevertheless, its in-hospital version—EMR

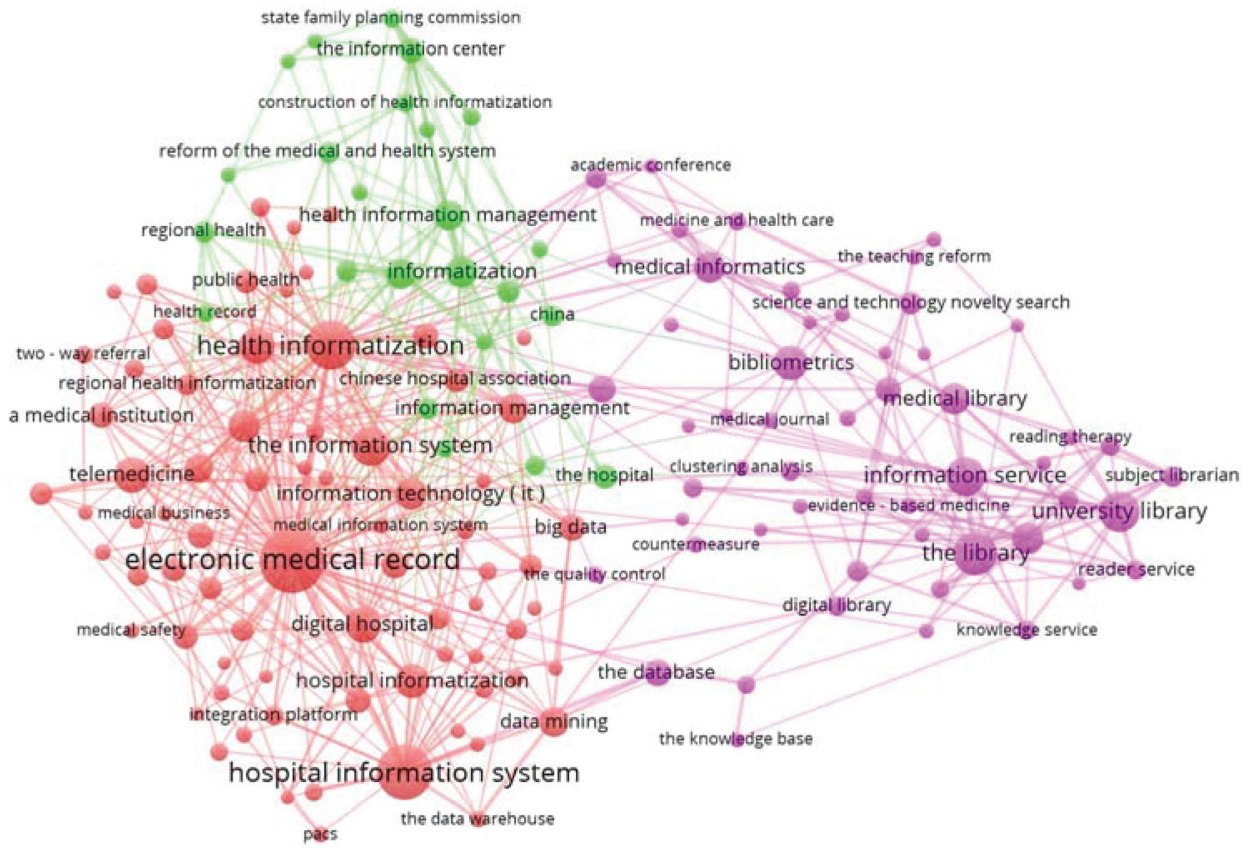

Figure 7: Cluster map of the keywords obtained by text mining 11 years (2008–2018) of articles on different topics from three Chinese MI journals (CDM, CJHIM, and CJMLIS). Topics are colored as red (Hospital Information Systems and EMR), orange (Medical Reform Policy and Health Digitization), and purple (Library Science and Bibliometrics Analysis).

[41]—is the core of "HIS and EMR" and is the keyword with the highest frequency in CN-Cluster 1. Effective use of the data of EMR/EHRs is necessary for the development of evidence-based medicine [42], but, compared with Europe and the United States with their well-developed MI, the mining, analysis, and use of data of EMR/EHRs in China remain in the early stage. Nevertheless, medical reforms in China, especially reforms of health insurance payment systems (e.g., China has released medical insurance reimbursement policies based on China Healthcare Security Diagnosis Related Groups and has gradually transited from the conventional "pay-for-service" to "pay-for-performance" system [43]), have deepened, and AI techniques [44] and the importance of medical data (China included medical big data as a national strategic resource in 2016 [45]) have been largely improved. Given these advances, we posit that the exploitation of medical data of EMR/EHRs at the level of scientific development, the improvement in medical quality, and the decrease in medical errors and medical expenses will all soon become the foci and hot spots of MI research in China. With the rapid development and wide application of wearable device technology [46, 47], more real-time health data can be included in EHRs, which further promotes this trend.

(5) CN-Cluster 2 (Library Science and Bibliometrics Analysis): this cluster is exclusive to the Chinese-language MI journals, and its research and application are concentrated in medical information research; medical information resources construction, retrieval, and services; and other health information management and evaluations. We posit that this occurs because the development of MI in China originated from library science in the mid-1980s, and this narrow sense of MI continues to account for a large proportion in China.

(6) CN-Cluster 3 (Medical Reform Policy and Health digitization): this cluster is exclusive to China and involves the propaganda, interpretation, analysis, and comments of HIT policies issued by healthcare reforms and government functional departments.

4.4. Comparative Analysis of Medical Information Education Systems. As an independent discipline, MI has been widely accepted in Europe and the United States. To date, greater than 80 US-based academic institutions offer on-site or distance MI training programs [48]. Additionally,

Table 1: Clusters of the keywords obtained by text mining 11 years (2008–2008) of English and Chinese MI journals (IJMI, JAMIA, MIM, CDM, CJHIM, and CJMLIS) with their ten most frequent keywords.

EN-cluster 1 (26)		EN-cluster 2 (38)		EN-cluster 3 (32)		EN-cluster 4 (46)		CN-cluster 1 (75)		CN-cluster 2 (54)		CN-cluster 3 (34)	
Internet and Telemedicine		Health and Clinical Information Systems		Medical Data Statistical Analysis		EHRs and Information Management		Hospital Information Systems and EMR		Library Science and Bibliometrics Analysis		Medical Reform Policy and Health Digitization	
Keyword	n	Keyword	n	Keyword	n	Keyword	n	Keyword	n	Keyword	n	Keyword	n
Adult	900	Decision support system	558	Information storage and retrieval	471	Electronic health record	1568	Electronic medical record	511	University library	233	Informatization	126
Controlled study	568	User-computer interface	475	Computer program	406		966	Hospital information system	394	Information service	216	Information platform	115
Middle aged	564	Hospital information system	346	Methodology	400	United states	646	Health informatization	309	Bibliometrics	191	Health information management	114
Major clinical study	536	Physician	328	Procedure	348	Medical information system	619	The information system	193	Hospital library	153	The hospital	75
Aged	477	Hospital	307	Software	334	Information processing	555	Digital hospital	171	Medical library	133	The information center	74
Internet	450	Medical order entry system	246	Natural language processing	328	Healthcare	453	Telemedicine	169		132	Information construction	68
Questionnaire	319	Clinical practice	233	Artificial intelligence	290	Medical information	451	Healthcare	166	Medical information	127	Application	61
Telemedicine	239	Patient safety	207	Data base	274	Medical record	423	Hospital informatization	158	The database	95	Regional health	61
Utilization	227	Health personnel attitude	206	Data mining	250	Patient care	392	Medical informatization	132	Information literacy	90	Reform of the medical and health system	58
Outcome assessment	205	Practice guideline	202	Theoretical model	235	Standard	361	Information technology (IT)	130	Science and technology novelty search	86	China	57

EN: English MI journals (IJMI, JAMIA, and MIM); CN: Chinese MI journals (CDM, CJHIM, and CJMLIS).

established universities in Western countries have all established the major of medical information, mostly in master and doctorate education, and focus on computer technology and methods, association with clinical activities, and practicality. By contrast, China established an MI-related major in 1983, which was gradually developed from the library information major in medical universities. To date, in China, education in this field mainly comprises undergraduate programs and only has 27 master's programs and five doctoral programs [4], and these numbers are less than half of those of the United States. The education focuses on information management theories and methods but rarely focuses on the technical application of computers; thus, the practical operation abilities of students are low. Consequently, the MI academy of China cannot recruit a sufficient number of qualified applied talents to the industry, and the industry does not highly evaluate the quality of these talents.

4.5. Implications of This Study. This study provides notable contributions to theory and practice.

From the theoretical perspective, first, this study further enriches and improves the knowledge of global MI literature research; in particular, for the first time, this study adds the analysis of Chinese MI journal literature. On this basis, our comparison of bibliometrics between three representative official English journals of the international MI societies and three Chinese journals of the national MI societies overcomes the limitation that some bibliometrics research in the field of MI has mainly focused on English-language literature [10, 42, 48].

Second, we explore the differences in authors between those in China and Western countries in their organizations and academic degrees. We find that on the one hand, most of the authors of Chinese papers are from medical institutions, and most of their counterparts in Western countries are from universities. The proportion of doctoral or master's degrees in the former is lower than that in the latter. By contrast, China's MI is mainly based on the traditional medical literature system, and the trainees are mainly undergraduates. Therefore, the education level and faculty's strength are far behind their counterparts in Europe and the United States. Thus, we suggest that China's MI field should establish and improve the education system of medical informatics, strengthen the training of faculty by sending teachers and researchers to study abroad, introduce advanced educational concepts of medical informatics, and employ teachers from different professional backgrounds to participate in the teaching, to improve the teaching environment and curriculum selection for students. Furthermore, for the first time, we explore the differences in the themes of the papers published in the mainstream Chinese and English MI journals during the past 11 years. On the one hand, China has fully used the latecomer advantage and application advantage in hospitals, especially the extensive implementation and application of EMR [49]; on the other hand, China's MI also has no theoretical and basic research in medical data statistics and consumer health information based on the Internet and telemedicine, which requires further improvement and development.

Third, this study has extended our previous research about the academic proceedings published by main academies of MI [4, 5, 8] and further compared the countries of origin, institutions, and academic backgrounds of major authors; the academic values; and themes of articles from the MI conferences and journal articles. We have identified some important similarities and differences. (1) As for the distributions of countries of authors in the MI proceedings (AMIA Annual conference, MIE, and MedInfo), the majority of authors are distributed similarly in terms of countries of origin. The regional MI journals, including JAMIA (AMIA, USA), MIM (EFMI, Europe), and Chinese MI journals were dominated by local authors, while the international journals such as IJMI (IMIA, global) were attended by authors from various regions. (2) From the aspect of institutions and academic backgrounds, on the one hand, like the majority of affiliations in international MI proceedings, most of the authors in English-language journals (IJMI, JAMIA, MIM) and some Chinese-language journals (CJMLIS) are from universities; on the other hand, the main academic backgrounds of authors in JAMIA and MI proceedings are different from other journals, and they majored in medicine. Moreover, in terms of academic influence, journal articles are far more influential than proceedings. On the one hand, from the aspect of integrity of article search, the MI proceedings held by Chinese academies lack any stable or unified searching database and cannot guarantee the continuity of database records. In comparison, the papers published in Chinese MI journals can be completely and timely searched from mainstream Chinese databases. We think that this suggests that Chinese MI journals, as important auxiliary disciplinary systems supporting the establishment and development of MI discipline in China, yet have been valued by the academy of MI in China and their academic values have been approved to some extent. On the other hand, in terms of bibliometrics indices of papers, the average cited times and H-index of journal papers are both highly larger than those of proceedings. In terms of research contents, the themes of proceedings and journal papers are different. On the one hand, EMR is the only shared keyword in the top 10 frequent keyword lists between the two, suggesting that clinical medical informatics is the mainstream of MI research. On the other hand, the themes of proceedings are more abundant than journal articles and include some emerging themes, such as customer health informatics and infodemiology. From the practice perspective, this study proposes a method to further promote the development of disciplines in China, based on different disciplines' positioning of MI in China and Western countries. On the one hand, MI in Western countries originated from clinical practice and hospital digitization or, namely, clinical informatics; the researchers are widely distributed in the university MI systems and hospitals and broadly cooperative; and their research contents are closely linked with medical hygiene practice. The core content of the discipline of "the computer technology applied into the medical field"

[50] gradually expanded to a series of subdisciplines, including public health informatics, clinical informatics, and nursing informatics. The current focus is how to process and mine the mass data generated and precipitated during medical practice and to finally advocate hygiene system infrastructure construction and clinical technology improvement, and the focus is the discovery of medical diagnosis and treatment rules and the provision of medical treatment decision-making, which suggests that the Western countries have treated MI as an applied basic discipline. On the other hand, because the MI in China originated from library science and the researchers mainly originated from medical schools, libraries, and medical informatics institutes, the cooperation among researchers was limited to institutes and rarely involved hospitals. Furthermore, the majority of the research was fueled by global trends and had no self-innovation; it did not shake off the current situation that theoretical research and clinical practice were isolated, and therefore this discipline did not develop significantly.

5. Limitations

Because discipline evaluation is a complicated task, we assess papers published in journals. Moreover, we use data from representative professional journals on MI in both China and Western countries but exclude all MI journals, use a limited number of searching tools to find other professional publications, and exclude achievements of patents or other forms. Furthermore, many achievements in MI may have been published in non-MI journals, but we have no perfect method or mechanism to include these papers; however, we intend to analyze these papers in subsequent studies.

6. Conclusions

We used bibliometrics to analyze Chinese- and English-language MI papers published in six representative MI journals between 2008 and 2018 in China, the United States, and Europe. The results of this study provide important insights for the development of MI in China and Western countries. First, compared with the Western counterparts, the number of papers published in the journals of professional associations in the field of MI in China is large and the application value is high, but the academic influence and academic value are relatively low; second, most of the authors of the Chinese papers are from hospitals, and most of the counterparts in the Western countries are from universities. The proportion of master's or doctoral degrees in the former is also lower than that of the latter; further, regarding paper themes, on the one hand, China MI has no theoretical and basic research on medical data statistics and consumer health based on the Internet and telemedicine; on the other hand, after nearly 10 years of hospital digital development, China has fully used the latecomer and application advances in hospitals and, through extensive international cooperation, has made significant advancements in and contributions to the development of medical information.

Abbreviations

MI:	Medical informatics
HIT:	Health information technology
CDM:	China digital medicine
CJMLIS:	Chinese Journal of Medical Library and Information Science
CSMI:	Chinese Society of Medical Information
CJHIM:	Chinese Journal of Health Informatics and Management
CMIAAS:	China Medicine Information Association Annual Symposium
CHINC:	China Hospital Information Network Conference
CHITEC:	China Health Information Technology Exchange Conference
CPMI:	China Annual Proceeding of Medical Informatics
CMIA:	China Medical Informatics Association
CSMI:	The Medical Informatics Branch, Chinese Medical Association
CHIA:	Chinese Health Information Association
CHIMA:	China Hospital Information Management Association
AMIA:	American Medical Informatics Association
JAMIA:	Journal of the American Medical Informatics Association
MedInfo:	World Congress on Medical and Health Informatics
IMIA:	International Medical Informatics Association
IJMI:	International Journal of Medical Informatics
MIE:	Medical Informatics Europe
MIM:	Methods of Information in Medicine
EFMI:	European Federation for Medical Informatics Association
CQVIP:	Science and Technology Journal Database
CNKI:	Chinese National Knowledge Infrastructure.

Data Availability

The raw data used to support the findings of this study are included in the tables and figures of the article.

Conflicts of Interest

The authors declare no conflicts of interest regarding the publication of this paper.

Acknowledgments

The authors thank Elsevier Language Editing (https://webshop.elsevier.com/languageservices/) for editing this manuscript. This study was supported by the National Natural Science Foundation of China (NSFC) (grants #81771937 and #81871455).

Supplementary Materials

Table S1: research targets, basic characteristics of IJMI (IMIA, global), JAMIA (AMIA, USA), MIM (EFMI, Europe), CDM (CHIMA, China), CJHIM (CHIA, China), and CJMLIS (CSMI, China). Table S2: top 5 authors with most publications in JAMIA, IJMI, MIM, CDM, CJHIM, and CJMLIS in 2008–2018. Content S3: comparative analysis of contents of the MI academic journals in the USA, Europe, China, and the world. (*Supplementary Materials*)

References

[1] J. A. Blaya, H. S. F. Fraser, and B. Holt, "E-health technologies show promise in developing countries," *Health Affairs*, vol. 29, no. 2, pp. 244–251, 2010.

[2] R. S. Ledley and L. B. Lusted, "Reasoning foundations of medical diagnosis; symbolic logic, probability and value theory aid our understanding of how Physicians reason," *Science*, vol. 130, no. 3366, pp. 9–21, 1959.

[3] V. Aguiar-PulidoE. Ayres et al., *Global Health Informatics: How Information Technology Can Change Our Lives in a Globalized World Discusses*, Elsevier Academic Press, Washington, DC, USA, 2017.

[4] J. Lei, Q. Meng, Y. Li, M. Liang, and K. Zheng, "The evolution of medical informatics in China: a retrospective study and lessons learned," *International Journal of Medical Informatics*, vol. 92, pp. 8–14, 2016.

[5] H. Deng, J. Wang, X. Liu, B. Liu, and J. Lei, "Evaluating the outcomes of medical informatics development as a discipline in China: a publication perspective," *Computer Methods and Programs in Biomedicine*, vol. 164, pp. 75–85, 2018.

[6] V. MaojoM. Garcia-Remesal et al., "Biomedical informatics publications: a global perspective: part I: conferences," *Methods of Information in Medicine*, vol. 51, no. 1, pp. 82–90, 2012.

[7] J. Liang, K. Wei, Q. Meng, Z. Chen, J. Zhang, and J. Lei, "The gap in medical informatics and continuing education between the United States and China: a comparison of conferences in 2016," *Journal of Medical Internet Research*, vol. 19, no. 6, p. e224, 2017.

[8] Y. Jia, W. Wang, J. Liang et al., "Trends and characteristics of global medical informatics conferences from 2007 to 2017: a bibliometric comparison of conference publications from Chinese, American, European and the Global Conferences," *Computer Methods and Programs In Biomedicine*, vol. 166, pp. 19–32, 2018.

[9] Y. Van KasterenP. A. H. Williams et al., "Identifying emerging trends in medical informatics: a synthesis approach," *Stud Health Technol Inform*, vol. 235, pp. 506–510, 2017.

[10] Y.-M. Kim and D. Delen, "Medical informatics research trend analysis: a text mining approach," *Health Informatics Journal*, vol. 24, no. 4, pp. 432–452, 2018.

[11] K. H. Gulkesen and R. Haux, "Research subjects and research trends in medical informatics," *Methods of Information in Medicine*, vol. 58, no. 01, pp. e1–e13, 2019.

[12] D. Moher, A. Liberati, J. Tetzlaff, and D. G. Altman, "Reprint-preferred reporting Items for systematic reviews and meta-analyses: the PRISMA statement," *Physical Therapy*, vol. 89, no. 9, pp. 873–880, 2009.

[13] G. Juan and S. Christian, "A bibliometric analysis of pharmacology and pharmacy journals: *Scopus versus* web of science," *Journal of Information Science*, vol. 34, no. 5, pp. 715–725, 2008.

[14] VIP China Science and Technology Journal Database http://lib.cqvip.com/.

[15] Chinese National Knowledge Infrastructure, http://www.cnki.net/.

[16] Wanfang Data, http://g.wanfangdata.com.cn/.

[17] S. Bird, "NLTK-Lite: efficient scripting for natural language processing," in *Proceedings of the 4th International Conference on Natural Language Processing (ICON)*, pp. 11–18, Kanpur, India, December 2005.

[18] ISO 7098, http://encyclopedia2.thefreedictionary.com/ISO+7098.

[19] Linge O., "Youdao-An excellent free online Chinese dictionary," https://http://www.thoughtco.com/youdao-online-chinese-dictionary-2279553.

[20] J. E. Hirsch, "An index to quantify an individual's scientific research output," *Proceedings of the National Academy of Sciences*, vol. 102, no. 46, p. 16569, 2005.

[21] T. Braun, W. Glänzel, and A. Schubert, "A Hirsch-type index for journals," *Scientometrics*, vol. 69, no. 1, pp. 169–173, 2006.

[22] C. MichelC. Jean-Pierre et al., "From translations to problematic networks: an introduction to co-word analysis," *Information (International Social Science Council)*, vol. 22, no. 2, pp. 191–235, 1983.

[23] L. Waltman and N. J. van Eck, "A smart local moving algorithm for large-scale modularity-based community detection," *The European Physical Journal B*, vol. 86, no. 11, p. 471, 2013.

[24] A. Perianes-Rodriguez, L. Waltman, and N. J. Van Eck, "Constructing bibliometric networks: a comparison between full and fractional counting," *Journal of Informetrics*, vol. 10, no. 4, pp. 1178–1195, 2016.

[25] J. LiangK. Wei et al., "Development of medical informatics in China over the past 30 years from a conference perspective and a Sino-American comparison," *PeerJ*, vol. 5, Article ID e4082, 2017.

[26] S. Donegan, P. Williamson, U. D'Alessandro, P. Garner, and C. T. Smith, "Combining individual patient data and aggregate data in mixed treatment comparison meta-analysis: individual patient data may be beneficial if only for a subset of trials," *Statistics In Medicine*, vol. 32, no. 6, pp. 914–930, 2013.

[27] R. L. Truewell, *Some Behavioral Patterns of Library User: The 80/20 Rule*, pp. 458–461, Wilson Library Bulletin, Bronx, NY, USA, 1969.

[28] D. J. d.S. Price, *Little Science Big Science*, Columbia University Press, Manhattan, NY, USA, 1963.

[29] L. Egghe, "Theory and practise of the g-index," *Scientometrics*, vol. 69, no. 1, pp. 131–152, 2006.

[30] J. C. Donohue, *Understanding Scientific Literatures: A Bibliometric Approach*, The MIT Press, Cambridge, MA, USA, 1973.

[31] T. Li, Y.-S. Ho, and C.-Y. Li, "Bibliometric analysis on global Parkinson's disease research trends during 1991-2006," *Neuroscience Letters*, vol. 441, no. 3, pp. 248–252, 2008.

[32] Committee C.C.F.A., "China Computer Federation Core Journal and Conference Lists", http://www.cnblogs.com/guolei/p/3576366.html.

[33] Peking University Library, "Explanations on problems relating to a guide to the core journals of China", http://www.lib.pku.edu.cn/portal/bggk/dtjj/qikanyaomu.

[34] J. LeiD. Wen et al., "Enabling health reform through regional health information exchange: a model study from China," *Journal of Healthcare Engineering*, vol. 20179 pages, 2017.

[35] National Health Commission of the PRC, "Chinese Electronic Medical Record System Application Level Grading Evaluation Standard (Trial)", http://www.nhc.gov.cn/yzygj/s7659/201812/3cae6834a65d48e9bfd783f3c7d54745.shtml.

[36] J. Liang, X. Zheng, Z. Chen et al., "The experience and challenges of healthcare-reform-driven medical consortia and

Regional Health Information Technologies in China: a longitudinal study," *International Journal of Medical Informatics*, vol. 131, no. 11, Article ID 103954, 2019.

[37] R. L. RichessonM. M. Horvath et al., "Clinical research informatics and electronic health record data," *Yearb Med Inform*, vol. 9, pp. 215–223, 2014.

[38] J. LiangY. Li et al., "Evaluating the applications of health information technologies in China during the past 11 Years: consecutive survey data analysis," *JMIR Med Inform*, vol. 8, no. 2, Article ID e17006, 2020.

[39] C. S. Kruse and A. Beane, "Health information technology continues to show positive effect on medical outcomes: systematic review," *Journal of Medical Internet Research*, vol. 20, no. 2, p. e41, 2018.

[40] National Health Commission of the PRC, "Chinese Hospital Smart Service Rating Evaluation Standard System (Trial)", http://wjw.fy.gov.cn/content/detail/5cd372d97f8b9a55448b457f.html.

[41] D. Garets and M. Davis, "Electronic medical records vs. electronic health records: yes, there is a difference," HIMSS Analytics, Chicago, IL, USA, AHIMSS Analytics White Paper, 2005.

[42] A. F. SimpaoL. M. Ahumada et al., "A review of analytics and clinical informatics in health care," *Journal of Medical Syst*, vol. 38, no. 4, p. 45, 2014.

[43] China National Healthcare Security Adminisitation, "Notice on Printing and Distributing China's Disease Diagnosis Related Group (DRG) on National Pilot Technical Specifications and Grouping Plans", http://www.nhsa.gov.cn/art/2019/10/24/art_37_1878.html.

[44] J. Ding, *Deciphering China's AI Dream*, Future of Humanity Institute, University of Oxford, Oxford, UK, 2018.

[45] The state council the people's republic of china, "The Outline of Healthy China 2030 Plan", http://www.gov.cn/zhengce/2016-10/25/content_5124174.htm (in Chinese).

[46] D. Wen, X. Zhang, X. Liu, and J. Lei, "Evaluating the consistency of current mainstream wearable devices in health monitoring: a comparison under free-living conditions," *Journal of Medical Internet Research*, vol. 19, no. 3, p. e68, 2017.

[47] J. Xie, D. Wen, L. Liang, Y. Jia, L. Gao, and J. Lei, "Evaluating the validity of current mainstream wearable devices in fitness tracking under various physical activities: comparative study," *JMIR mHealth and uHealth*, vol. 6, no. 4, p. e94, 2018.

[48] L. Wang, M. topaz, J. M Plasek, and L Zhou, "Content and trends in medical informatics publications over the past two decades," *Studies in Health Technology and Informatics*, vol. 245, pp. 968–972, 2017.

[49] S. Luo, K. Zhang, and B. Li, "Medical informatics in China: healthcare IT trends, academic and research developments," *Yearbook of Medical Informatics*, vol. 19, no. 01, pp. 109–115, 2010.

[50] M. A. Musen and J. H. v. Bemmel, *Handbook of Medical Informatics*, Springer, Houten, Netherlands, 2002.

Hindawi
Journal of Healthcare Engineering
Volume 2020, Article ID 8828738, 11 pages
https://doi.org/10.1155/2020/8828738

Research Article

Tianxia120: A Multimodal Medical Data Collection Bioinformatic System for Proactive Health Management in Internet of Medical Things

Zihan Jiao,[1] Yindong Xiao,[1] Yanmei Jin,[2] and Xinyu Chen[2]

[1]*School of Automation Engineering, University of Electronic Science and Technology of China, Chengdu 611731, China*
[2]*School of Information and Communication Engineering, University of Electronic Science and Technology of China, Chengdu 611731, China*

Correspondence should be addressed to Xinyu Chen; chenxinyu@uestc.edu.cn

Received 9 August 2020; Revised 8 September 2020; Accepted 14 September 2020; Published 6 October 2020

Academic Editor: Xiwei Huang

A digital medical health system named Tianxia120 that can provide patients and hospitals with "one-step service" is proposed in this paper. Evolving from the techniques of Internet of Medical Things (IoMT), medical dig data, and medical Artificial Intelligence, the system can systematically promote the change of service status between doctors and patients from "passive mode" to "proactive mode" and realize online service that is similar to offline medical treatment scenarios. The system consists of a patient terminal and a doctor terminal. They can perform online inquiry (through graphic, voice, telephone, video, etc.), electronic prescription, multiparameter self-diagnosis, cold chain logistics, medicine distribution, etc. The system can provide rich medical health information, medical tools browsing, and health care big data aggregation processing functions. Compared with the traditional medical system, this system has the characteristics of full function, rich data, and high security. It is expected to be applied to hospital applications and medical research to promote the construction and innovation of clinical medical disciplines.

1. Introduction

The world's population is rapidly aging together with people's increasing concern for healthcare [1]. It is estimated that, by 2050, people aged 60 years and older will reach 2 billion, and 80% of them will live in low- and middle-income countries [2]. In China, for example, the number of elderly people over 60 years old has exceeded 200 million and a large number of people get chronic diseases [3]. And over 90 percent of health care work needs to be carried out by primary health care institutions. However, the level of medical staff in primary health care institutions is uneven. Most patients still prefer top-level hospitals, and this phenomenon has already brought China into an imperative stage to effectively improve national health to a new level [4]. Therefore, the central government of China promulgated the "Healthy China 2030" Planning Outline [5], which is based on the whole population and the whole life cycle to promote the provision of fair and accessible, systematic and continuous health services to achieve a higher level of national health. This situation brings significant opportunities and challenges to the health platform today.

The health platform has been in development for a long time: the Clinical Documentation Architecture (CDA R1) was defined in May 2005 and became the American National Standards Institute (ANSI) approved HL7 standard, which became the specification for the Health Level 7 (HL7) Reference Information Model (RIM) [6]. Although it has been spread around the world, the application is still not extensive enough [7]. The Continuity of Care Document (CCD) is an HL7 CDA implementation of the Continuity of Care Record (CCR). And the CCR data set contains a summary of the patient's health status including problems, medications, allergies, and basic information about health insurance, care documentation, and the patient's care plan [8]. Ekonomou et al. presented a cloud-based healthcare system that provides high levels of security and privacy within a cloud environment, enabling sharing of both health records and the access rights, along the patient pathway in 2011 [9]. RF-MediSys presented an innovative electronic medical record (EMR) system, which can perform medical information sharing and retrieval effectively, and it is accessible via a "smart" medical card [10]. But Deng et al. raised concern about cloud security and privacy in home health systems [11]. Tsai et al. implemented the data leakage prevention scheme to avoid illegal duplication [12]. Pan et al. designed a novel electronic medical record system for regional clinics and health centers in China [13]. Despite all these systems, e-health platforms are still not widely used. The development of the health system platform still faces serious challenges, especially in developing countries [14].

With the development of electronic medical equipment, the formation of online medical systems has become possible [15]. Telemedicine is gradually acceptable to patients [16]. The concept of mobile health has emerged as a key beneficiary of the dual emphasis on technology and an increasing interest in health behavior and data monitoring [17]. Based on the integration of "traditional medicine +" Internet of medical things, big data, artificial intelligence, and other intelligent digital technologies, the world is experiencing a stage transition from the medical health prevention based on traditional evidence-based medicine theory and practice to precise and proactive health management mode. Considering this, a digital medical system named Tianxia120 for proactive health management is proposed in this paper as shown in Figure 1. The Tianxia120 digital medical system includes an intelligent digital hospital platform and a proactive healthcare platform.

The two platform systems interact with each other to conduct doctor-patient interaction around the one-stop service of "medical-drug-test-risk." For patients, not only can it provide online or offline integration for their individual or family members, which is similar to the online medical treatment scene for visiting the hospital for medical advice, but also it can provide a comprehensive system of disease prevention and health management for the whole family. For hospitals, it is also possible to help the medical departments and staff carry out research and applications of production, education, and research based on the "digital technology+" production and research solutions supported by the system. Taking the application of Tianxia120 as an example, this paper will share the experience of proactive health management application based on the digital technology in four main aspects, "architecture design, platform function, innovation mode, and representative application case," and explore the precision health care solutions, which can be widespread.

2. Digital Medical System Architecture

2.1. System Technology Architecture. The Tianxia120 digital medical platform system provides professional, proactive, and continuous health care services, which take patients as the center, and advocates the concept transition from "disease-centered" to "health-centered." Hospital specialist doctors can provide online consultation and communication services for patients so that the patients can consult doctors without leaving home.

As shown in Figure 2, the Tianxia120 digital medical platform system includes a client terminal for patients and a hospital terminal for doctors. In addition to the service of doctor-patient communication (graphic, voice, telephone, and video), electronic prescription, medical logistics delivery, and the remote intelligent multiparameter self-test functions based on IoMT technology, the client terminal also provides a wealth of medical health information, medical tools browsing, and health care big data aggregation processing function. It can provide solutions for the medical staff to study and research and realize the service of doctors and patients. The doctor terminal has the following functions: Expert studio, electronic prescription, medicine prescription, self-defining scale, single consultation, bed entry, and so on.

2.2. System Service Architecture. Figure 3 describes the system architecture that includes the following.

2.2.1. Patients as the Service Enjoying Center. In order to effectively solve the problem of out-of-hospital health care for patients, the Tianxia120 digital medical platform system is a patient-centered service that allows patients to enjoy one-step out-of-hospital follow-up service via smart phone when they are not in the hospital. For example, patients can consult doctors conveniently and quickly with graphic voice/telephone/video, and doctors can issue electronic consultations according to their needs. After the pharmacy pharmacist's trial, the drug is delivered by the medicine cold chain logistics, and the family health file is managed online.

2.2.2. Multiple Disciplinary Teams (MDT) as the Service Providing Center. By the guide of serving patients through MDT, and the principle of serving patients by nurse/home doctor assistant, (hospital or attending) physician and expert, it forms the "Tianxia120 MDT service model" for patients.

2.2.3. Digital Technology as the Service Guaranty Center. With the unique multiparameter monitoring technology of IoMT and the "digital medical technology +" solutions formed by other multitechnology aggregations, the Tianxia120 digital medical platform system can guarantee the complete, continuous, and professional follow-up services for patients outside the hospital.

2.2.4. Expert Studio as the Service Implementation Center. An expert studio consisting of "Nurse/Family Doctor–(Hospital or Indication) Physician–Expert" created on the Tianxia120 digital medical platform system by the experts from top-level hospital constitutes a specific service implementation unit that can provide a digital out-of-hospital follow-up service package to patients for a variety of disease prevention.

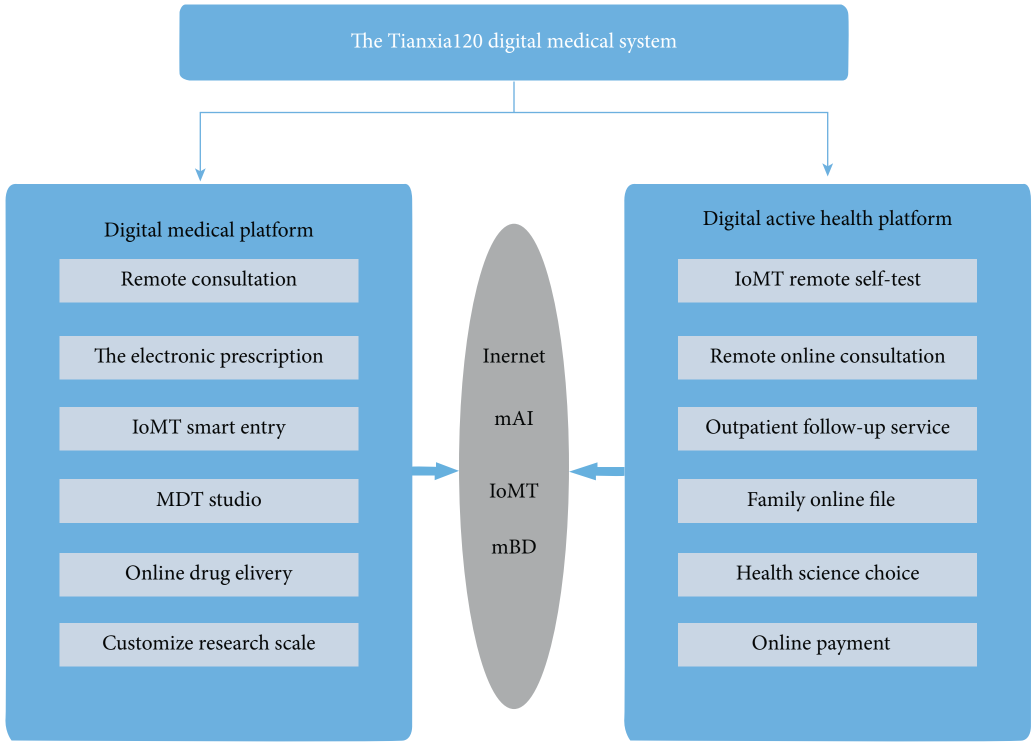

Figure 1: System technology architecture.

2.3. Proactive Health Continuous Management Architecture. As shown in Figure 4, proactive health continuous management architecture includes the following:

(1) Three active behaviors of patients

① Upload personal medical information actively
② Upload medical/physical examination data of immediate family members actively
③ Contact a nurse, doctor, or specialist for medical advice actively

(2) Three active behaviors of MDT

① Contact patients and provide counseling actively
② Remind patients to upload medical/physical data of individuals and immediate family members actively
③ Make an appointment with a physician or an expert for the patient actively

(3) Three active behaviors of the Tianxia120 platform

① Responds to the feedback promptly and actively
② Reminds both patients and expert teams actively after the patient purchases the service package automatically
③ Provides technical and operational support actively

From the feedback of actual operation, the proactive health continuous management service of the three-way linkage combination of Tianxia120 can not only provide patients with better medical experience and human emotional concern, but also help medical personnel control and manage their own fragmentation time and provide services for patients in an orderly manner.

2.4. System Operation and Information Security Assurance System. System operation and maintenance security system includes application access layer, platform service layer, business logic layer, big data support layer, and data layer, and they are combined with each other (Figure 5).

3. Digital Medical System Composition

The Tianxia120 digital medical system mainly includes a digital hospital platform and a digital proactive health platform system.

3.1. Digital Hospital Platform. At the doctor terminal, the digital hospital platform of Tianxia120APP includes the following main contents (Figure 6):

(1) The Tianxia120 digital medical system allows a limited quantity of medical resources to provide access to out-of-hospital services for more patients.

Digital hospital platform can not only support remote video, telephone, voice, and graphic communication functions, but also provide hospitals and medical staff with remote out-of-hospital follow-up for patients who are inconvenient or do not need to come to medical institutions. Meanwhile, it can also promote "top-level hospital—basic community medical institution—family" medical joint mode through the expert studio, thus truly achieving the

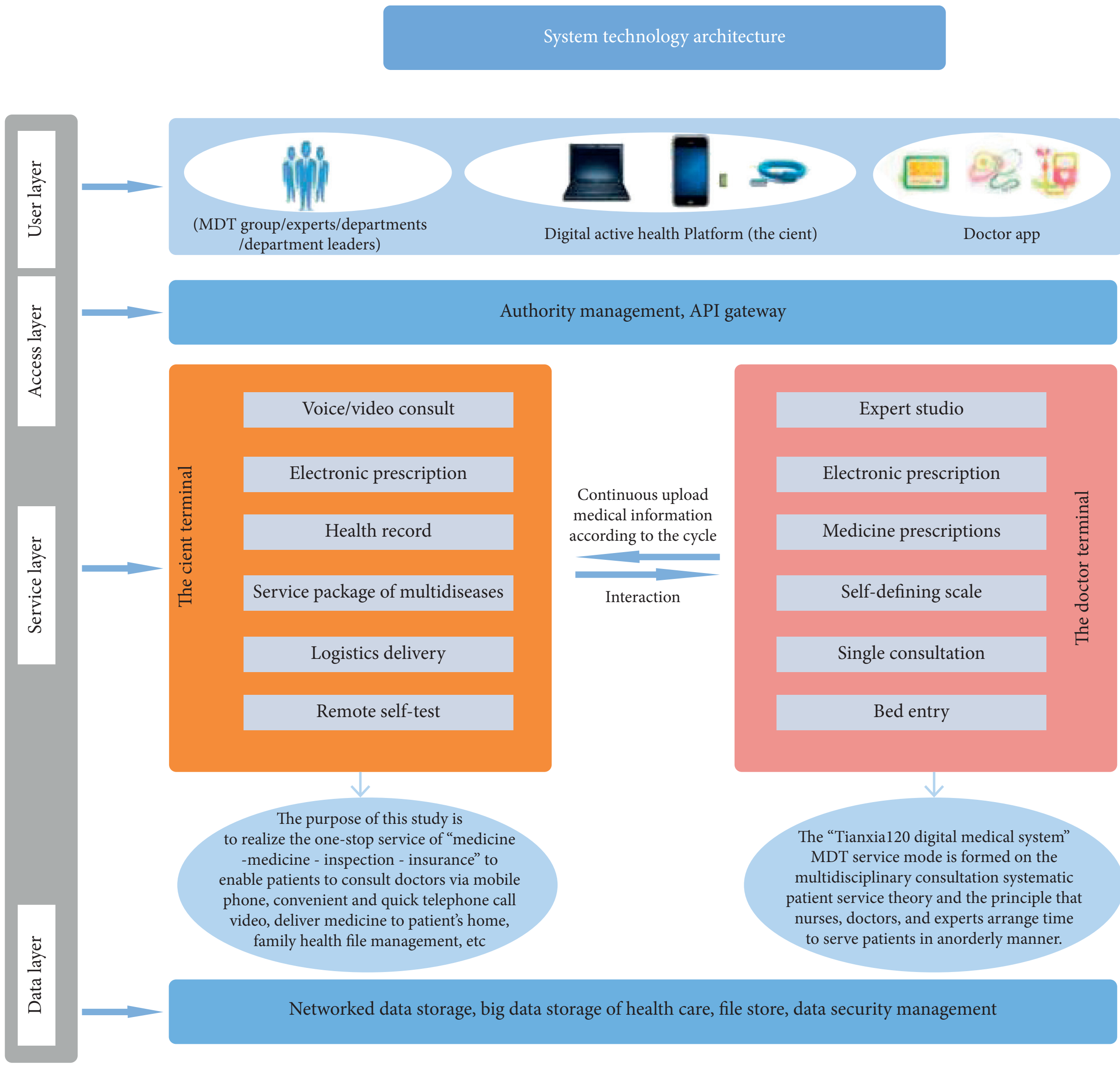

Figure 2: The Tianxia120 digital medical system.

sinking of high-quality medical resources, and allow limited quality medical resources to serve more people.

(2) The Tianxia120 digital medical system can provide research and "digital technology+" solutions for hospitals, departments, and medical staff.

The digital hospital platform can also provide assistance to the research of hospitals/departments/medical staff on production, education, and study:

① Intelligent custom scientific research data scale collection system (uploading the scientific data scale designed by the hospital/department to the Tianxia120 digital medical system APP system)

② Multiparameter detection and monitoring data collection based on IoMT technology

③ Comprehensive treatment of health care big data after desensitizing

④ Reapplication and promotion of production and research results

(3) Core function composition

① MDT expert studio: it is established by an expert of associate professor title or above, and other health care practitioners such as physicians, nurses, pharmacists, and health managers can apply to join. The number of expert studios is not limited. Each expert studio corresponds to a specific disease, and it can generate out-of-hospital follow-up service team consisting of 1 expert, 1 physician, and 1 nurse/home doctor assistant.

② Online and offline services: These mainly include online graphic speech, telephone or video consultation; making an e-prescription as needed; sending medicine by chain logistics after the drug

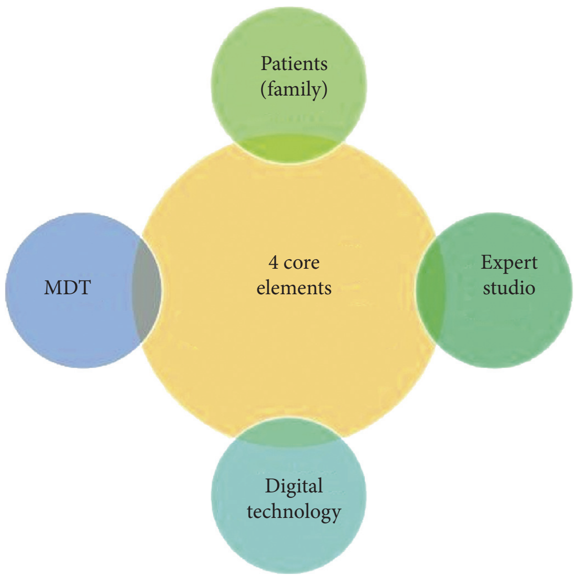

Figure 3: System service architecture.

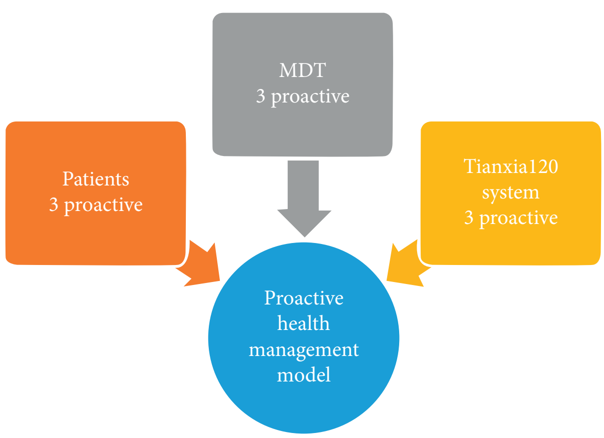

Figure 4: Proactive health continuous management architecture.

is checked by the pharmacy pharmacist; managing the family health files online.

③ Intelligent custom research scale: when carrying out scientific research projects, it is indispensable to collect data for scales. In the past, many data collection works relied on manual collection offline, and the efficiency and effect were limited. The intelligent custom scientific research scale function originally created by the Tianxia120 digital medical system greatly changed the status. The scientific research workers submit the scale document to the platform, and the Tianxia120 platform technology center uploads the scale to the platform system after the "document-technical conversion," which can easily realize the online and offline combined scale data collection. In this way, the data collected is not only large, but also widely distributed, and the acquisition time period is greatly shortened.

3.2. Digital Proactive Health Platform. Digital proactive health platform refers to the intelligent digital active health platform system. The main contents of the Tianxia120's patient terminal are as follows (Figures 2, 7, and 8). The proposed system is capable of detecting electroencephalogram (EEG), electrocardiogram (ECG), blood pressure, blood oxygen saturation, venous blood routine, urine routine, body fat, and weight with great sensitivity and stability:

(1) Online consultation: patients who are inconvenient or do not need to come to a medical institution can use the remote video, telephone, voice, graphic, and text of the smart phone to consult medical staff online.

(2) Intelligent health self-test (Figure 9): intelligent multiparameter detection and monitoring equipment based on IoMT technology enables patients to self-measure blood glucose, total cholesterol, uric acid, electrocardiogram, lung function, blood pressure, urine routine, and other human physiological indicators at any time by using IoMT-enabled biosensors, such as electrochemical sensors and immunoassay sensors. These sensors collect samples from patients' fingertips blood or body fluids through a small sample pad to induce chemical reactions and pass the generated electric current or light signals to micro-controller-unit (MCU) for further computing and storage. The measurement data is consequently uploaded to the digital active health platform via Bluetooth connection or Wi-Fi. The platform system provides real-time storage, analysis, and alarms for different values.

Doctors can quickly access the data when online and consulate and interpret the data. Because the biosensors possess great stability and sensitivity, they can completely meet the testing needs of today's medical market.

(3) Remote pharmacy service: depending on the online consultation, the physician can prescribe an electronic prescription for the returning patient, and the practicing pharmacist will review the prescription. Doctors, pharmacists, and nurses can also remind patients to take medication online, receive feedback information from patients, and pay close attention to patient medication dynamics.

(4) Creation of digital health archives: patients can upload basic information, previous medical treatment, and physical examination data and create digital health archives for the whole family through mobile phones.

(5) Online booking and offline service: if necessary, patients can also make an appointment with the medical staff to check and provide consultation services. At the same time, doctors can also check the patient's online consultation and go to the offline hospital for further examination such as blood

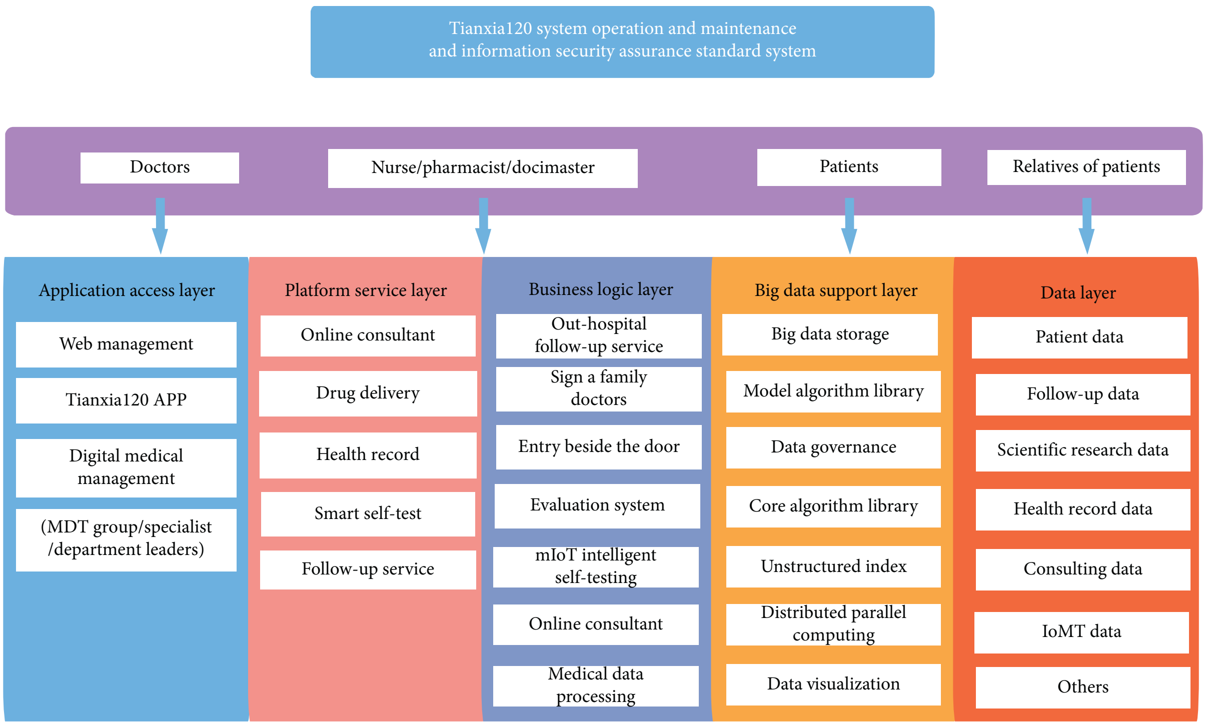

Figure 5: System operation and information security assurance system.

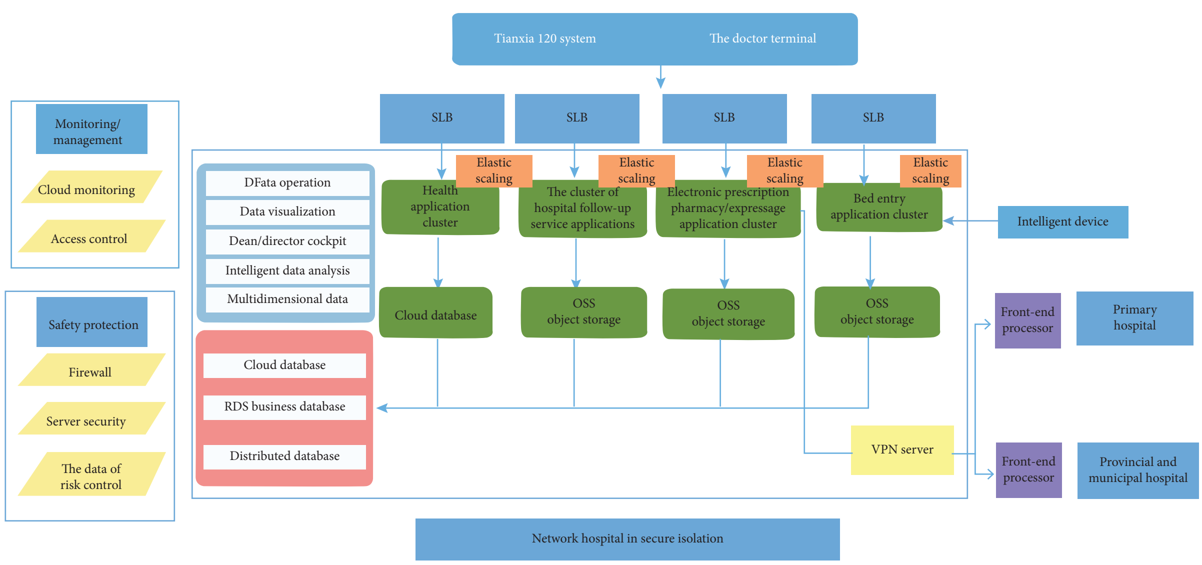

Figure 6: Technical architecture.

routine test, X-ray, CT inspection, and nuclear magnetic resonance.

(6) Architectural advantages of the digital proactive health platform:

① The intelligent micromedical equipment kit based on the IoMT provides one-stop service to quickly build stable, reliable, safe, and controllable IoMT applications

② The platform supports PB-level data volume and millions of Transaction Per Second (TPS) capabilities, providing massive data storage and access capabilities

③ The security checking service, which is to use security testing to help enterprises discover security issues in the security certification, distribution network and communication process of intelligent hardware

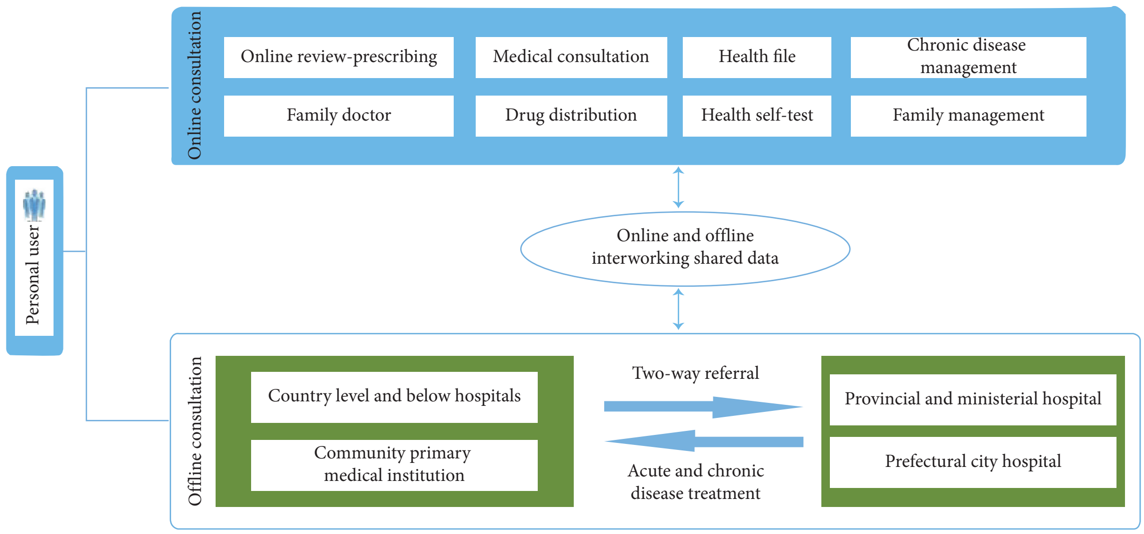

Figure 7: Business structure.

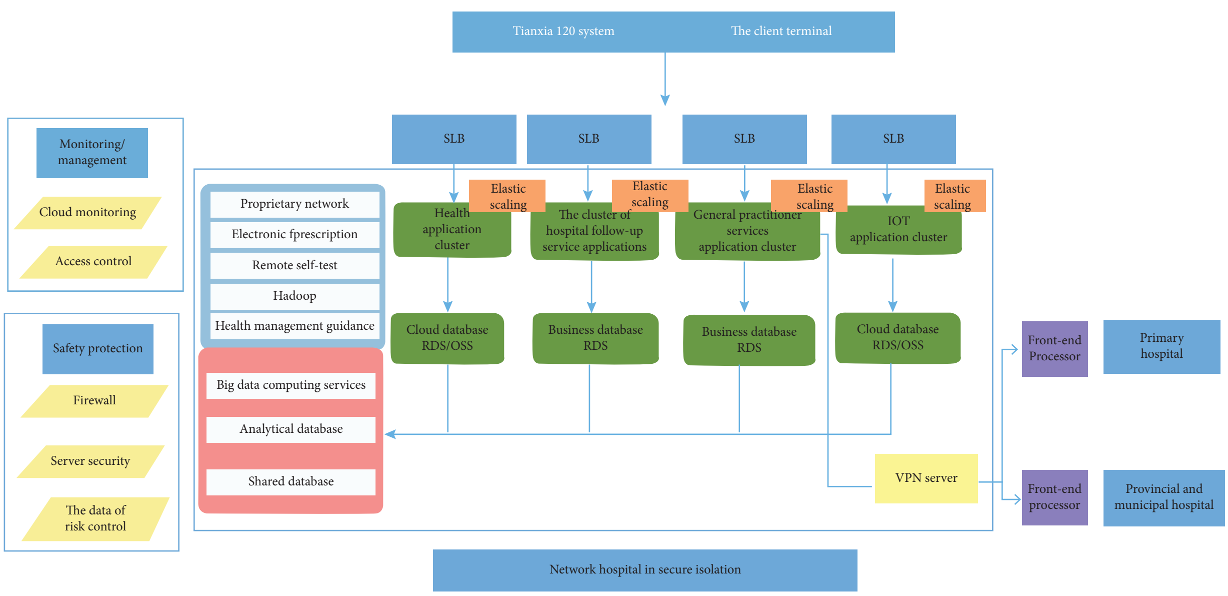

Figure 8: Technical framework.

④ Web Application Firewall (WAF) can protect against the attacks of 0 day, interface spamming, and collisions to ensure data is secure enough

⑤ Protect server security with Anker to prevent hackers. Situational awareness discovers potential intrusion and attack threats through machine learning and data modeling

⑥ The platform shares data of the National Medical Center through the dedicated VPN encryption channel

4. Application in Proactive Health Management

4.1. Application Model Innovation. The application innovation model of "Industry, University and Research" based on "Digital Technology+" is to apply the innovation of the Internet, medical Internet of things, artificial intelligence, health care big data, 4 G/5 G, biotechnology, and other technical and medical health institutions, phased and selective integration to the online and offline combined services supported by the Tianxia120 system (Figure 10). And it takes the standardized formatting of health care big data gradually formed by the dynamic service process as the core and promotes and verifies the innovation of production, education, and research of medical and health institutions in order to realize the industrial application of more innovative health and medical fields promotion. It collaborates with innovation through online and offline deep integration, develops new technologies and methods, and scientifically realizes clinical transformation to jointly address the global burden of disease and health challenges and benefit global patients.

The core of Tianxia120 "Digital Technology+" production and research application innovation model is health

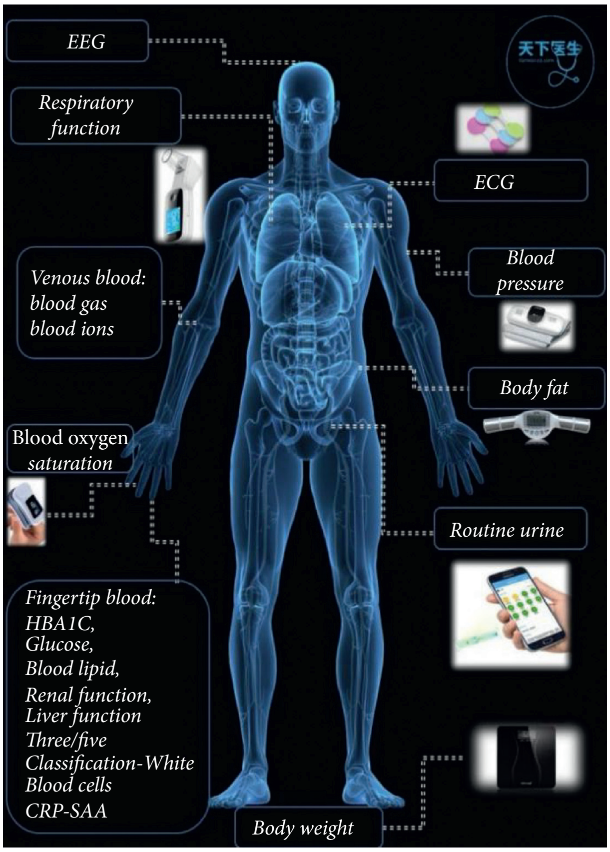

Figure 9: Intelligent multiparameter detection and monitoring device based on Internet of Medical Things (IoMT) technology application.

care big data solution, and its main contents are as shown in Figure 11:

4.1.1. Health Care Big Data Collection. It implements data collection through the Tianxia120 smart digital active health medical platform and data exchange collection and sharing management system, including Tianxia120APP patient terminal, doctor terminal, and intelligent custom scientific data acquisition system.

4.1.2. Data Collection and Operation

(1) The past medparagical health file data of patient/family

① Users can upload their own/family history medical data through the Tianxia120 client terminal actively or after being reminded by medical staff, including but not limited to CT, nuclear magnetic resonance, X-ray film, ultrasound, and other image examinations and text reports, medical reports, or test samples.
② Users can enter the "Health File" to operate easily through the Tianxia120 client terminal.
③ Medical staff can also log into the Tianxia120 APP doctor's terminal and enter the "bedside entry" to easily and conveniently collect health medical data from thousands of patients.

(2) Patients/families can monitor data remotely

Through the "Intelligent Self-Test" function of the Tianxia120 client terminal, users can detect and monitor a variety of health care data at home (requires matching intelligent medical equipment). And users manually upload the test data in the hospital including lung function, ECG, blood pressure, blood sugar, urine routine, cholesterol, uric acid, liver function, kidney function, and blood routine. The data is automatically saved after uploading. Every month, the Tianxia120 system automatically forms a health report and sends it to users.

① Intelligent self-test process: enter the "Health File" of the Tianxia120 client terminal and add the detection item, and click "Smart Self-Test"; And medical staff can log into the Tianxia120 doctor terminal, enter the "Bedside Entry" to add the detection item, click "Smart Self-test," and follow the prompts.
② Manual uploading process: enter the "Health File" of the Tianxia120 client terminal and add the detection item, and click "Manual Input"; and medical staff can log into the Tianxia120APP doctor terminal, enter the "Bedside Entry" to add the detection item, click "Manual Input," and follow the prompts.
③ Health self-test process: enter the "Health File" of the Tianxia120 client terminal and click "Health Self Test"; medical staff can log into the Tianxia120 doctor terminal to enter the "bedside entry," click "Health Self Test," and follow the prompts.

(1) Patients' network consultation data includes data generated by out-of-hospital follow-up service package consultation, data generated by online single consultation, and data generated by free consultation.
(2) The medication data of patients/family members include the prescription record data issued in the hospital uploaded by patients/family members, electronic prescription records of common diseases, and chronic diseases prescribed by the doctor of the Tianxia120 platform within the limits of regulations.

4.1.3. Health and Medical Big Data Cleaning (Figure 12). According to the needs of scientific research projects, the data should be cleaned based on Tianxia120 big data Extract-Transform-Load (ETL) cleaning and finishing technology. The process is as follows (Figure 13):

(1) Unified data standardization processing
(2) Unified description and storage management, unified modeling of various data items

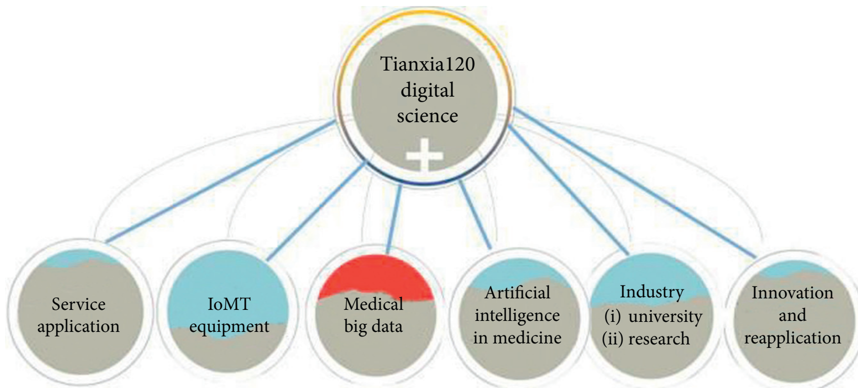

FIGURE 10: The Architecture of the application innovation model of "Industry-University-Research," which is based on "Digital Technology+."

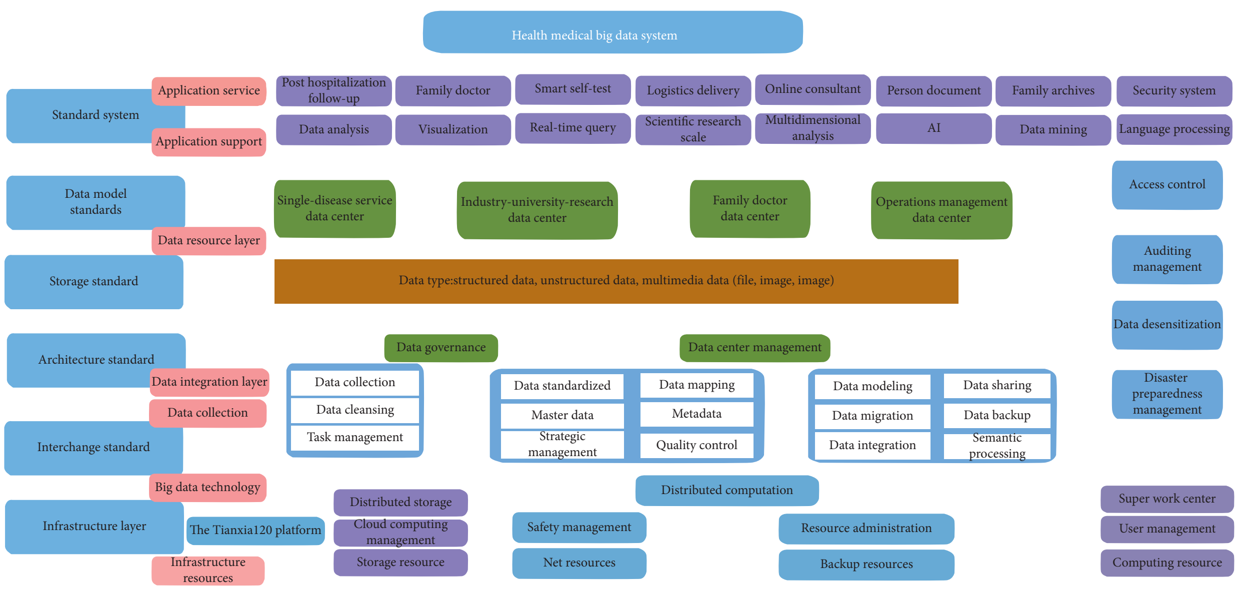

FIGURE 11: Technical framework health medical big data system.

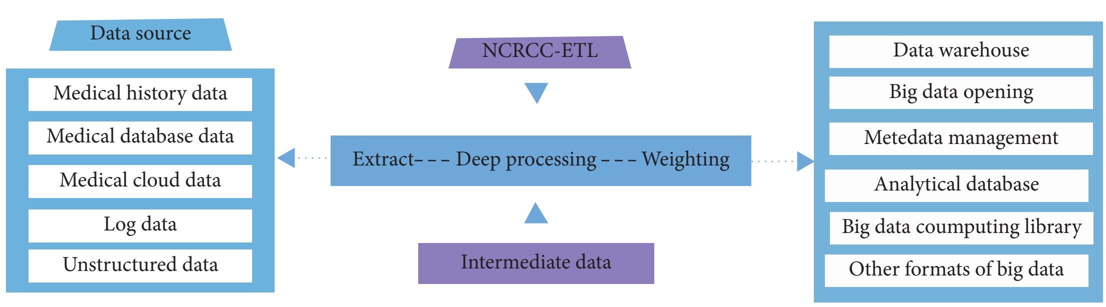

FIGURE 12: Demonstration of medical big data cleaning process.

(3) ETL operations such as cleaning, verification, and desensitization of big data warehouses

4.1.4. Analysis and Visualization Application of Health Medical Big Data. Relying on the big data analysis and visualization technology of Tianxia120 health care, the research data that has been clearly sorted should be mined, analyzed, and visualized application:

(1) Data preparation-multipath association multi-database table
(2) Data multidimensional analysis-multidimensional index database search and retrieval analysis of big data according to scientific research projects
(3) Data visualization report rendering-Computer-side browser URL view visualization report/export to excel report program report view

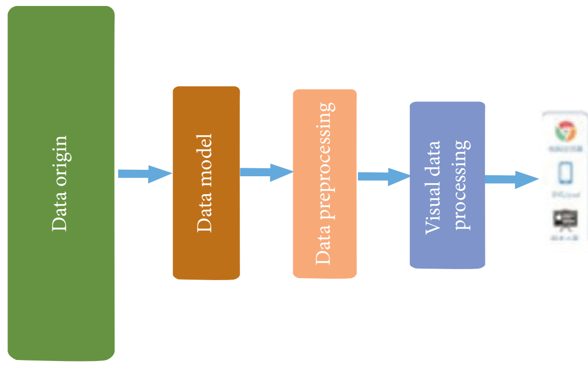

Figure 13: Process of health care big data analysis and visualization.

4.2. Results of Application Cases

(1) Multiple biochemical data collected by the Tianxia120 digital medical system can be used by the study of chronic disease management [18–22].

(2) The key research project of the Sichuan Provincial Health Planning Commission "Leshan People's Hospital: Research on the Construction Model of Digital Medical Integration and Demonstration Ward" has applied the Tianxia120 digital medical system to provide many patients for "in-hospital and out-hospital" digital medical services in Leshan downtown and surrounding areas.

(3) The key research project of Sichuan Province--"Neijiang First People's Hospital: Application Research on Regional Platform Management Mode of Family Doctor Contracting Service Using "Internet +"" is also applying Tianxia120 digital medical system to provide many patients for "in-hospital and out-hospital" digital medical services in Leshan downtown and surrounding areas.

(4) The project that won the second prize of Sichuan Science and Technology Progress Award in 2018--<West China second prize of Sichuan University: Aging and aging function promote innovative research and transformation of results> is also based on the Tianxia120 digital medical system, and provides "prehospital, in-hospital, and posthospital" intelligent medical care and new technology for elderly patients.

(5) The digital out-of-hospital follow-up service created by Tianxia120 Digital Medical System has been applied in dozens of large-scale hospitals in China, such as West China Hospital of Sichuan University, the First Affiliated Hospital of Nanchang University, the Second Affiliated Hospital of Nanchang University, the People's Hospital of Leshan City, the First People's Hospital of Neijiang City, the Third Affiliated Hospital of Guangzhou Medical University, etc.

(6) For patients, the digital outpatient follow-up proactive health service model of "Third-level hospitals-grassroots community medical institutions-families (individuals)" built by Tianxia120 digital medical system can not only provide online and offline integration for its individual or family members, which is similar to the online medical treatment scene for visiting the hospital for medical advice, but also provide a comprehensive system of disease prevention and health management for the whole family. For hospitals, it can also help hospitals/departments manage patients by disease based on system-supported "digital technology+" production and research solutions. By managing patients through mobile phones and collecting scientific research data, it can help hospitals, departments, and medical staff to carry out research data and application of production, education, and research to promote the construction and innovation of clinical medicine disciplines and the empowerment of hospitals.

Data Availability

All data used during the study are available from the corresponding author upon request.

Conflicts of Interest

The authors declare no conflicts of interest.

References

[1] U. Varshney, "Mobile health: four emerging themes of research," *Decision Support Systems*, vol. 66, pp. 20–35, 2014.

[2] World Health Organization, *Aging and Health*, World Health Organization, Geneva, Switzerland, 2018, http://www.who.int/news-room/fact-sheets/detail/ageing-and-health.

[3] E. F. Fang, M. Scheibye-Knudsen, H. J. Jahn et al., "A research agenda for aging in China in the 21st century," *Ageing Research Reviews*, vol. 24, pp. 197–205, 2015.

[4] H. Wang, Q. Wang, C. Li, C. Tan, and G. Liu, "Old-age service, health status and chronic diseases of centenarians in Zhongxiang City, Hubei Province, China," *Journal of the American Geriatrics Society*, vol. 65, no. 2, p. S333, 2017.

[5] R. H. Dolin, L. Alschuler, S. Boyer et al., "The CPC central committee, the state council, "health China 2030 strategic plan," *Chinese Journal of Ophthalmology*, vol. 54, no. 1, pp. 11–22, 2018.

[6] R. H. Dolin, L. Alschuler, S. Boyer et al., "HL7 clinical document architecture release 2," *Journal of the American Medical Informatics Association*, vol. 13, no. 1, pp. 30–39, 2006.

[7] D. Bender and K. Sartipi, "HL7 FHIR: an Agile and RESTful approach to healthcare information exchange," in *Proceedings of the CBMS 26th International Symposium*, pp. 326–331, Porto, Portugal, 2013.

[8] D. G. Vine and D. C. Kibbe, "The continuity of care record (CCR)–essential concepes for practitioners," *SAMJ South African Medical Journal*, vol. 95, no. 4, p. 224, 2005.

[9] E. Ekonomou, L. Fan, W. Buchanan, and C. Thüemmler, "An integrated cloud-based healthcare infrastructure," in *Proceedings of the Cloud Computing Technology and Science (CloudCom) 3rd International Conference*, pp. 532–536, Athens, Greece, November 2011.

[10] J. S. L. Ting, A. H. C. Tsang, A. W. H. Ip, and G. T. S. Ho, "Professional practice and innovation: RF-MediSys: a radio

frequency identification-based electronic medical record system for improving medical information accessibility and services at point of care," *Health Information Management Journal*, vol. 40, no. 1, pp. 25–32, 2011.

[11] M. Deng, M. Petkovic, M. Nalin, and I. Baroni, "A home healthcare system in the cloud-addressing security and privacy challenges," in *Proceedings of the 2011 IEEE 4th International Conference on Cloud Computing*, pp. 549–556, Washington, DC, USA, July 2011.

[12] K.-L. Tsai, F.-Y. Leu, and J.-S. Tan, "An ECC-based secure EMR transmission system with data leakage prevention scheme," *International Journal of Computer Mathematics*, vol. 93, no. 2, pp. 367–383, 2014.

[13] L. Pan, X. Fu, and F. Cai, "Design a novel electronic medical record system for regional clinics and health centers in China," in *Proceedings of the 2nd IEEE International Conference on Computer and Communications (ICCC)*, pp. 38–41, Chengdu, China, October 2016.

[14] D. Luna, A. Almerares, J. C. Mayan, F. González Bernaldo de Quirós, and C. Otero, "Health informatics in developing countries: going beyond pilot practices to sustainable implementations: a review of the current challenges," *Healthcare Informatics Research*, vol. 20, no. 1, pp. 3–10, 2014.

[15] Z. Deng, "Understanding public users' adoption of mobile health service," *International Journal of Mobile Communications*, vol. 11, no. 4, pp. 351–373, 2013.

[16] F. Mair and P. Whitten, "Systematic review of studies of patient satisfaction with telemedicine," *British Medical Journal*, vol. 320, no. 7284, pp. 1517–1520, 2000.

[17] Y. Chen, L. Yang, M. Zhang, and J. Yang, "Central or peripheral? Cognition elaboration cues' effect on users' continuance intention of mobile health applications in the developing markets," *International Journal of Medical Informatics*, vol. 116, pp. 33–45, 2018.

[18] X. Huang and J. Guo, "A photochemical dongle for point-of-care evaluation of blood lipid level," in *Proceedings of the 2017 IEEE Biomedical Circuits and Systems Conference (BioCAS)*, pp. 1–4, Turin, Italy, October 2017.

[19] J. Wang, X. Huang, S.-Y. Tang, G. M. Shi, X. Ma, and J. Guo, "Blood triglyceride monitoring with smartphone as electrochemical analyzer for cardiovascular disease prevention," *IEEE Journal of Biomedical and Health Informatics*, vol. 23, no. 1, pp. 66–71, 2019.

[20] Y. Fu and J. Guo, "Blood cholesterol monitoring with smartphone as miniaturized electrochemical analyzer for cardiovascular disease prevention," *IEEE Transactions on Biomedical Circuits and Systems*, vol. 12, no. 4, pp. 784–790, 2018.

[21] J. Guo, "Smartphone-powered electrochemical biosensing dongle for emerging medical IoTs application," *IEEE Transactions on Industrial Informatics*, vol. 14, no. 6, pp. 2592–2597, 2018.

[22] J. Xu, L. Wang, Y. Shen et al., "Family-based big medical-level data acquisition system," *IEEE Transactions on Industrial Informatics*, vol. 15, no. 4, pp. 2321–2329, 2019.

Hindawi
Journal of Healthcare Engineering
Volume 2020, Article ID 8812678, 13 pages
https://doi.org/10.1155/2020/8812678

Research Article

Neural Network-Based Study about Correlation Model between TCM Constitution and Physical Examination Indexes Based on 950 Physical Examinees

Yue Luo,[1] **Bing Lin**,[2] **Shuting Zhao**,[1] **Li He**,[1] **and Chuanbiao Wen**[1]

[1]*Chengdu University of Traditional Chinese Medicine, No. 1166 Liutai Avenue, Wenjiang District, Chengdu 611137, China*
[2]*Affiliated Hospital of Chengdu University of Traditional Chinese Medicine, No. 37 Shierqiao Avenue, Jinniu District, Chengdu 610075, China*

Correspondence should be addressed to Chuanbiao Wen; wcb@cdutcm.edu.cn

Received 4 May 2020; Revised 26 June 2020; Accepted 12 August 2020; Published 1 September 2020

Academic Editor: Xiwei Huang

Purpose. To establish the correlation model between Traditional Chinese Medicine (TCM) constitution and physical examination indexes by backpropagation neural network (BPNN) technology. A new method for the identification of TCM constitution in clinics is proposed, which is trying to solve the problem like shortage of TCM doctor, complicated process, low efficiency, and unfavorable application in the current TCM constitution identification methods. *Methods*. The corresponding effective samples were formed by sorting out and classifying the original data which were collected from physical examination indexes and TCM constitution types of 950 physical examinees, who were examined at the affiliated hospital of Chengdu University of TCM. The BPNN algorithm was implemented using the C# programming language and Google's AI library. Then, the training group and the test (validation) group of the effective samples were, respectively, input into the algorithm, to complete the construction and validation of the target model. *Results*. For all the correlation models built in this paper, the accuracy of the training group and the test group of entire physical examination indexes-constitutional-type network model, respectively, was 88% and 53%, and the error was 0.001. For the other network models, the accuracy of the learning group and the test group and error, respectively, was as follows: liver function (31%, 42%, and 11.7), renal function (41%, 38%, and 6.7), blood routine (56%, 42%, and 2.4), and urine routine (60%, 40%, and 2.6). *Conclusions*. The more the physical examination indexes are used in training, the more accurate the network model is established to predict TCM constitution. The sample data used in this paper showed that there was a relatively strong correlation between TCM constitution and physical examination indexes. Construction of the correlation model between physical examination indexes and TCM constitution is a kind of study for the integration of Chinese and Western medicine, which provides a new approach for the identification of TCM constitution, and it may be expected to avoid the existing problem of TCM constitution identification at present.

1. Introduction

In the Traditional Chinese Medicine (TCM) concepts, a person's constitution refers to such inherent qualities that are comprehensive and relatively stable in the morphological structure, physiological functions, and psychological states, which are formed during one's life on the basis of natural endowment and postnatal maintenance, which are personal features adapting to natural and social environment formed in the growth and development process of human [1, 2]. Numerous classics of TCM explain the theories of TCM constitution. It is recorded that "people here are living the same life, with the same age and the same clothes. When a strong gale or rainstorm attacks, some fall ill, some not; or everybody gets ill or nobody gets ill at all. What is the reason for this? It is because a person with fragile physique cannot survive the deficient winds in the four seasons, while a person with strong physique can easily get by" [3] in *The Inner Canon of Huangdi*, a classic work as the theoretical basis guiding TCM. This paragraph underlines the dominant role a person's constitution plays during the onset of illness. In another work by Wang, who is the founder of the TCM Constitution and master of Chinese medicine, the *Theory of TCM Constitution*, which summarizes and extends the TCM constitution, it is proposed that lots of factors can influence a human's constitution such as natural factors, age, gender, spirit, diet, living condition, and geographic environment. [1]. According to the basic theory of TCM and clinical survey, Wang also proposed the classification of nine kinds of TCM constitution, which are peaceful type, qi-deficient type (qi is the vital energy that runs through a human body), yang-deficient type (yang refers to the heat and energy that a human body possesses), yin-deficient type (yin is the opposite of yang, referring to the body fluid that cools and quiets a body), phlegm-damp type, damp and hot type, blood stasis type, qi depression type, and special type [4]. TCM theory believes that an individual's special constitution can cause him/her to be particularly sensitive to some diseases, and such particularity of an individual's constitution will directly affect the onset and progress of a disease [5]. Therefore, it is necessary for disease preventive treatment to prevent disease onset and exacerbation by distinguishing constitution.

Figure 1 shows the neural network model of physical examination indexes and TCM constitutional types. The input of backpropagation neural network (BPNN) is physical examination indexes, and the output is TCM constitution types. $X_1, X_2, \ldots, X_n$ refers to the quantified and normalized physical examination indexes; $Y_1, Y_2, \ldots, Y_m$ refers to the calculated outputs by the BPNN, corresponding to the TCM constitution types; W refers to weights from the input layer to hidden layer, and V refers to weights from the hidden layer to output layer.

Nowadays, human can live longer than before. However, stress from job and life is increasing, which causes many people to fall ill [6]. Physical examination is becoming an important approach to diagnose and prevent diseases. Physical examination indexes are the quantitative indexes used by Western medicine, which employ multiple physical and chemical parameters such as blood routine indexes, urine routine indexes, liver function indexes, and renal function indexes, to indicate physical conditions of a person. In the field of TCM, identification of constitution is the basis for formulating individualized preventive and health care measures, and it is also the prerequisite for getting rid of subhealth status and realizing "treatment without disease" [7, 8]. The current TCM constitution identification methods include TCM doctors' artificial identification, gene classifier, meridian thermal sensitivity measurement, pulse wave frequency-domain analysis, and scale method. All the methods above have been proved to have some problems: (1) the artificial identification of TCM doctors is susceptible to the doctor's theoretical level and clinical experience and faces the shortage of TCM doctors, which cannot meet the needs of constitutional identification. (2) The cost and technical requirements of genetic classification, meridian thermal sensitivity measurement, pulse wave frequency-domain analysis, and other identification methods are high. Some are still in the exploration stage. So it is not conducive to popularization and application [9, 10]. (3) The scale method, organized to form and administered by the State Administration of TCM of the People's Republic of China, is compiled by the China Association of Chinese Medicine Constitution Branch. In 2009, the document "Traditional Classification and Judging Standards for TCM Constitution," which guides and regulates the research and application of TCM constitution, was published [11]. Although the scale method has been widely used, some experts have proposed that the scale has the problems of the abolishment of observation, auscultation and olfaction, and palpation and pulse feeling in the TCM constitution identification, which are called "the diagnosis of Wang, Wen, and Qie" in Chinese medicine and the loss of the overall concept of Chinese medicine [12–15]. Therefore, parts of hospitals actually carry out the constitution identification by combining the scale method with the three clinical diagnosis methods of TCM. In this situation, the process of TCM constitution identification goes through two stages, from the independent diagnosis to the comprehensive analysis, which has the problems of complicated process and low efficiency. At the same time, the scale is susceptible to subjective factors of the tester [16]. Thus, it is quite necessary to explore a new TCM constitution identification method.

In this situation, it proposes the research based on the integrative between Chinese and Western medicine, for which it uses BP artificial intelligence neural network (BPNN) technology and the samples from clinical of hospital to establish the network model of physical examination indexes and TCM constitution. In the correlation network model, the TCM constitution is quantitatively analyzed by physical examination indexes. It provides a new approach for the identification of TCM constitution, and it may be expected to avoid the existing problem of TCM constitution identification at present.

The remainder is organized as follows. Section 2 reviews research efforts on correlation between TCM constitution and physical examination indexes and identification of TCM constitution. Section 3 describes the study method on building the correlation model. In Section 4, the proposed model for TCM constitution and physical examination is assessed in multiple clinic experiments, and various numerical results are presented and discussed. Finally, Section 5 concludes and discusses future extensions.

2. Related Work

There were some recent researches about the correlation between TCM constitution and physical examination indexes. For example, Deng and Lu made combined analysis over physical examination indexes and constitutional types through clinical study and application, aiming to provide better regulation solutions for patients [17–20]. Using physical examination indexes and constitutional types of 331 community elderly, Ren and Li from Beijing Shijingshan District TCM Hospital performed a correlation analytical study, from which some conclusions that can guide clinical practice are drawn [21]. There are some other correlation researches, such as combined analysis over TCM

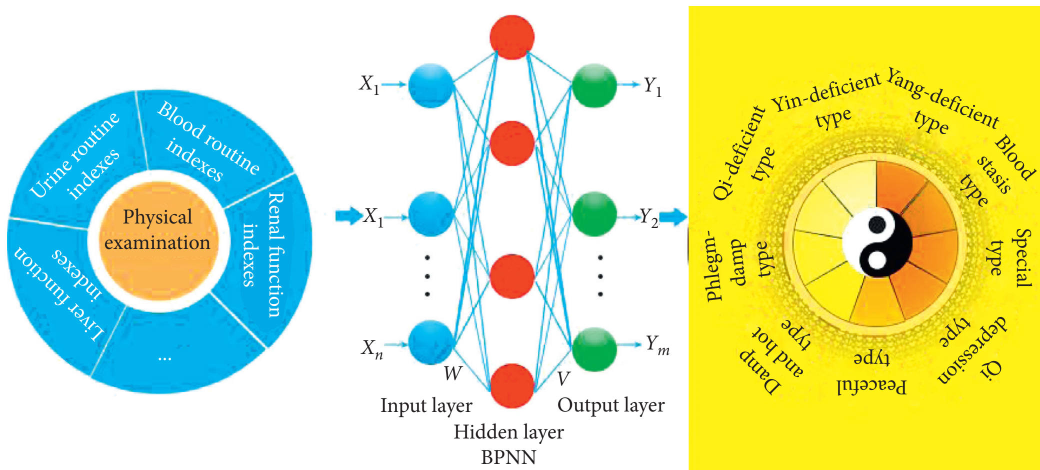

Figure 1: Neural network model of TCM constitutional types and physical examination indexes.

constitution and physical examination indexes through different diseases like obesity, cerebral apoplexy, and hypertension. With statistical or regression analysis, they made the similar conclusions that some constitution types correlated with physical examination indexes were associated with a certain disease [22–32]. All the above studies show that there is a certain correlation between physical examination indexes and TCM constitution. But they only focused on the correlation between some physical examination indexes and some physical constitution types by using traditional methods of data statistics and analysis. The above research is not only lacking in the overall situation but also has not provided a template for the correlation between physical examination indexes and TCM constitution.

In view of the problems existing in TCM constitution identification methods, there were also some studies on identification of TCM constitution in an automatic way. Zhang et al. proposed the design and implementation of an identification system for TCM constitution, which implemented the electronic questionnaire of identification for TCM constitution [33–36]. This method is based on the scale method mentioned above. In practice, one's constitution type is identification combining the result of the system and the result from TCM doctors' artificial identification, which causes the low efficiency. Liang proposed an automatic identification system of TCM constitution based on facial image features. According to the result of facial diagnosis, which is done by the system with digital image processing technology, TCM constitution can be distinguished automatically. However, the accuracy of the result is not high. Meanwhile, the study selected fewer facial features, and the selected features did not fully represent a person's constitution type [37]. Hong et al. proposed an approach for identification of TCM constitution based on the tongue manifestation [38]. Yet it depended on tongue diagnosis combining with questionnaire analysis, which is still in exploration. Bai proposed a way to distinguish TCM constitution based on BPNN [39]. For this approach, the TCM constitution was identified by combining inspection, inquiry, and palpation, which was more objective and intelligent. But the accuracy still needs to be enhanced, and its practicability remains to be verified. Xie proposed the realization of a platform for the identification of TCM constitution and data analysis, by which it could complete TCM constitution identification based on scale and tongue diagnosis and provide the function of data analysis. However, the analysis algorithm adopted in this study will lead to the platform speed being too slow. The tongue diagnosis analysis algorithm cannot accurately analyze the tongue image, and the accuracy of TCM constitution identification remains to be questioned [40].

The previous studies are short for efficiency, accuracy, and correlation template. As above, it is expected to provide a new approach for TCM constitution identification by considering the correlation between TCM constitution and physical examination indexes with overall view and constructing a correlation model. With the rapid development of artificial intelligence and machine learning technology, it is a new trend to employ machine learning and neural network in TCM for automatic and smart identification of TCM constitution. Products such as smart medical equipment, intelligent diagnosis and treatment, and intelligent image recognition, which have achieved rapid development, have been successfully applied in various fields. So, in this paper, it explored the approach with BPNN, to implement the identification of TCM constitution and to build the correlation model between TCM constitution and physical examination indexes from 950 physical examinees. The data about physical examination indexes and TCM constitutional types of the physical examinees were first collected and sorted out. The physical examination indexes were classified into four categories, namely, blood routine indexes, urine routine indexes, liver function indexes, and renal function indexes. These four categories of indexes combined with the corresponding TCM constitutional types of physical examinees were the original sample data. The effective data, obtained from proper organization of the original data, were initially divided into the training group data and test group data. Furthermore, the training group data were input into the BPNN, which was trained to establish physical examination indexes-TCM constitution-type network model. Finally, the test group data were input to verify the accuracy of the established neural network model. After the verified experiment, the accuracy of the training group and the test group was up to 88% and 53%, respectively, and the error was close to 0.001. Therefore, this research provides an automatic model to correlate physical examination indexes and TCM constitutional types, so as to use quantitative indexes of Western medicine to realize automatic and smart identification of TCM constitution and to provide a new way for TCM constitution identification.

The comparison between the previous studies and methods and the proposed method for constitution identification of TCM is shown in Figure 2.

The key contributions of this paper are summarized below:

(1) A new approach to studying the correlation between TCM constitution and physical examination indexes is firstly proposed. BPNN algorithm is applied to build the correlation model, in which physical examination indexes are the inputs, TCM constitution types are the outputs, and Sigmoid function is the activation function. Then, it comprehensively analyzes the correlation of the two mentioned before and provides an automated relevance template.

(2) A new method for identifying TCM constitution is proposed. It is successfully to construct a correlation model between physical examination indexes and TCM constitution. The model is verified by experiment with high accuracy and low error. It provides a smarter and more automatic way to realize the identification of TCM constitution types compared to the current ways including doctor and questionnaire.

3. Study Method

Neural network is a large-scale parallel distributed processor composed of simple processing units, which has characteristics in storing experiential knowledge and availability. It is similar in two ways to human's brain [41]:

(1) Neural network acquires knowledge by learning from external environment.

(2) The strength of interconnection neurons, the synaptic weight, is used to store acquired knowledge.

BPNN algorithm is a kind of artificial neural network technology that is intuitive, easily understood, and widely studied and used, with a powerful ability of nonlinear mapping and self-learning [42, 43]. It is also a kind of multilayered neural network that can be trained to learn the appropriate internal representations to allow learning any arbitrary mapping from input to output. A typical BPNN consists of three layers, i.e., input, hidden, and output layers, which are closely connected to each other [44].

The learning process of BPNN is composed of forward propagation and backpropagation. In the forward propagation process, the result is transmitted to the output layer after the data from the input layer are processed by neurons of hidden layer. The states of neurons in each layer only influence the state of neurons in the next layer. The process of backpropagation is started, while the computational output is not equal to the expected output. In the backpropagation process, error signal from an output layer is propagated up to an input layer via the hidden layer, and the link weight and offset are adjusted throughout the way. This process is finished until the accuracy reaches the requirement of algorithm. In fact, the BPNN algorithm aims at calculating a minimum error function. By repeated training of multiple samples, BPNN adjusts weight in a negative gradient of error function till the error converges to the least [45].

Based on the above theories, we adopted BPNN to establish the correlation model between TCM constitutional types and physical examination indexes in this work.

The effective data were sorted out from original data collected from the subjects, and 80% of which was input as training group data into the BPNN to establish the model. The physical examination indexes in the test group data, accounting for 20% of the effective data, were input into the network model to predict the corresponding TCM constitutional types. The reason for such percentage allocation will be discussed later. The effective data, which were randomly divided into the training group and the test group, covered the nine constitutional types of TCM as mentioned before.

3.1. TCM Constitutional Types-Physical Examination Indexes: BPNN Correlation Model Algorithm.

The BPNN model for correlation between TCM constitutional types and physical examination indexes is shown in Figure 3. The detailed description of the algorithm is as follows.

In this model, it took physical examination indexes as input and TCM constitution types as output. The weight from the input layer to hidden layer was denoted as ω_{ij} and that from the hidden layer to output layer was denoted as ω_{jk}; the offset from the input layer to hidden layer was denoted as a_j, and that from the hidden layer to output layer was denoted as b_k. The learning rate was $ç$. The excitation function was $g_{(x)}$[46]. This study chose Sigmoid function (S-function) as the excitation function to establish the correlation model and to realize conversion of variable data and weight. Because S-function is nonlinear, its parameter values need to be in [0, 1], and the physical examination index can easily satisfy this condition. The equation of S-function is shown as follows:

$$g_{(x)} = \frac{1}{1 + e^{-x}}. \quad (1)$$

The training process of the algorithm is as follows:

(1) Take random algorithm to initialize the weights ω_{ij} and ω_{jk} and the offseta_j and b_k

(2) According to formula (2), the BPNN algorithm calculates the hidden layer output H_j after inputting the quantitative physical examination indexes X_i of training group of sample

(3) Employ formula (3) to calculate the predicted output O_k, which represents the TCM constitution types

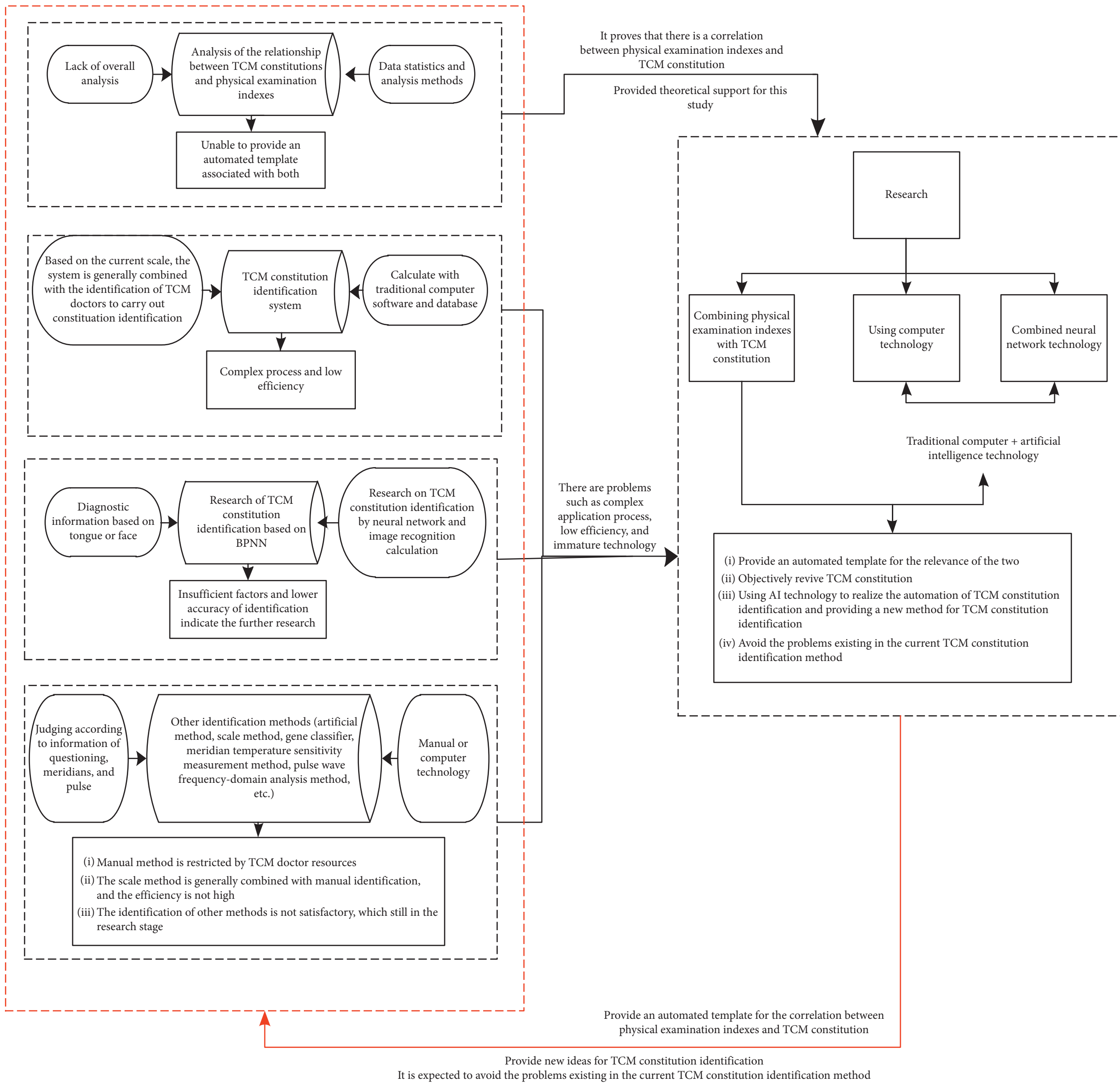

Figure 2: The comparison between the previous studies and methods and the proposed method.

(4) Compare the actual TCM constitution type quantified in the sample with the predicted value of the algorithm O_k and then employ equation (4) to calculate the error

(5) The convergence of algorithm is judged according to the iteration number, the number of training group for the same batch and the error

(6) If the convergence is achieved, stop to learn, which indicates the model is built

(7) If it does not converge, reverse the revision weights ω_{ij} and ω_{jk} and the offset a_j and b_k while continue to train about the sample

After the model is built, the test (validation) process of the algorithm is as follows:

(1) Input the physical examination indexes of test (validation) group

(2) Calculate the hidden layer H_j and the output layer O_k based on the revised weights and offsets in the training process

(3) Calculate the accuracy by comparing the output O_k of the model with the actual TCM constitution type quantified by the test group

(4) Calculate the error

(5) O_k is the predictive value of the correlation model

For the new data of the validation group, if the algorithm does not converge, the algorithm continues to reverse the revision weight and offset until the algorithm converges.

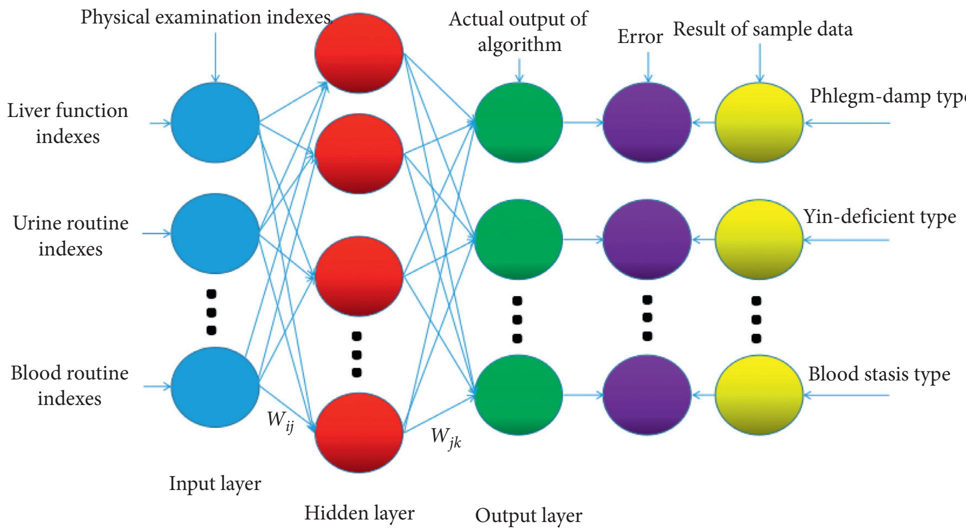

Figure 3: Neural network model of TCM constitutional types and physical examination indexes.

3.1.1. Input Layer. Physical examination indexes, namely, blood routine indexes, urine routine indexes, liver function indexes, and renal function indexes, were used as input nodes of the network model.

3.1.2. Hidden Layer. The number of hidden layer nodes, which was indicated as n in equation (2), was assigned from 1 to 10, respectively, to verify the accuracy and time efficiency of the algorithm. The hidden layer output was denoted asH_j, which was calculated as follows:

$$H_j = g\left(\sum_{i=1}^{n} w_{ij}x_i + a_j\right). \tag{2}$$

Neither too few nor too large number of hidden layer nodes can get a good convergence of the BP algorithm. Verification showed that when the number of hidden layer nodes was 5, both the convergence and time efficiency of the algorithm were satisfactory; therefore, in this paper, $n = 5$.

3.1.3. Output Layer. The nine constitutional types were used as input nodes. The output layer output was denoted as O_k, which was calculated as follows:

$$O_k = \sum_{j=1}^{n} H_j \omega_{jk} + b_k. \tag{3}$$

In equation (3), n was the number of hidden layer nodes.

3.1.4. Calculation of Error Δ. The error function was calculated as follows:

$$\Delta = \frac{1}{2}\sum_{k=1}^{m} (Y_k - O_k)^2, \tag{4}$$

where m referred to the number of output layer nodes, $m = 9.Y_k$ was the expected output (i.e., actual results of samples).

3.1.5. Initialization and Updating of Weight. Random function was employed to generate a random value to initialize the weight. The equations for updating weight were as follows.

Weight from the input layer to hidden layer was

$$w_{ij} = w_{ij} + \eta H_j\left(1 - H_j\right)x_i \sum_{k=1}^{m} \omega_{jk}(Y_k - O_k). \tag{5}$$

And weight from the hidden layer to output layer was

$$\omega_{jk} = \omega_{jk} + \eta H_j (Y_k - O_k). \tag{6}$$

3.1.6. Initialization and Updating of Offset. Random function was employed to generate a random value to initialize the offset. The equations for updating offset from the input layer to hidden layer and from the hidden layer to output layer were

$$b_k = b_k + \eta (Y_k - O_k), \tag{7}$$

$$a_j = a_j + \eta H_j\left(1 - H_j\right)\sum_{k=1}^{m} \omega_{jk}(Y_k - O_k). \tag{8}$$

3.2. BPNN Algorithm Flow. The neural network algorithm flow for correlation model of TCM constitutional types and physical examination indexes was as follows [26]:

(1) Input the physical examination indexes of samples of training group.
(2) Perform normalization of input data.
(3) Initialize weight, offset, and learning rate.
(4) Employ equation (2) to calculate hidden layer output.
(5) Employ equation (3) to calculate output layer output.

(6) Input TCM constitutional type data of samples.
(7) Employ equation (4) to calculate error.
(8) Employ equations (5)–(8) to update the weight and offset from the input layer to hidden layer and from hidden layer to output layer, respectively.
(9) Judge whether convergence is achieved, i.e., whether the error reaches designated value; if convergence is achieved, proceed to next step; otherwise, return to step 4. Convergence of the algorithm indicates that the correlation network model of TCM constitutional types and physical examination indexes has been formed.
(10) Input the physical examination indexes of the test group into the above established neural network model.
(11) Predict the TCM constitutional types of test group.
(12) Compare the prediction results of network model and the actual results of test group; calculate and output the final accuracy and error.

With the input of physical examination indexes, the type of TCM constitution can be automatically judged by the correlation model.

The above procedure flow is summarized in Figure 4.

3.3. Quantification and Normalization of Sample. According to physical examination index criteria adopted by health management center of the affiliated hospital of Chengdu University of TCM, the indexes in this paper were chosen as follows:

(1) Blood routine indexes: 20 indexes including white blood cell and neutrophil cell population, lymphocyte population, monocyte, eosinophilia granulocyte, alkaline granulocyte, and percentage of neutrophil cell.
(2) Urine routine indexes: 20 indexes including pH value, urine specific gravity, white blood cell, and red blood cell.
(3) Liver function indexes: 11 indexes including total protein, albumin, and globulin.
(4) Renal function indexes: 5 indexes including urea nitrogen, creatinine, trioxypurine, glucose, and carbon dioxide combining power.
(5) All indexes of physical examinees: 56 indexes including blood routine index, urine routine index, and liver function index and renal function index.

Prior to applying TCM constitutional type data to neural network algorithm, the TCM constitutional types should be standardized. Taking into account the characteristics of neural network algorithm and activation functions, the TCM constitutional types were digitized and standardized. Conversion standards are shown in Table 1.

The physical examination indexes were also normalized by the custom algorithm which was not depicted owing to its simplicity. As the Sigmoid activation function discussed above is valued within [0, 1], the physical examination indexes have to be normalized so that the values are within [0, 1].

4. Experiments and Results

4.1. Data Collection. The 950 physical examinees, accepted by the health management center of the affiliated hospital of Chengdu University of TCM from January 2016 to March 2017, were used as study objects. Due to the security and confidentiality of the data, it took about 7–8 months to manually collect data, to entry data, and sort out data. The collected original data were cleaned, classified, and organized to form the effective data. The effective data were randomly divided into the training group and test group. In the experiment, the accuracy and error of the network model were verified using four different data size ratios of training over testing, i.e., 95%:5%,80%:20%, 60%:40%, and 50%:50%, respectively. The results indicated that when training group data: test group data = 80%:20%, the network model has the highest accuracy and the lowest error. Therefore, this study applied this percentage allocation to establish and verify the network model.

Blood routine indexes of 383 physical examinees, urine routine indexes of 186 physical examinees, liver function indexes of 564 physical examinees, renal function indexes of 313 physical examinees, and entire physical examination indexes of 133 physical examinees, as well as those physical examinees' corresponding TCM constitutional types, were used as effective data. 80% of the effective data was regarded as training data, while 20% was regarded as the testing data. All the samples, training group, and test group data covered the nine TCM constitutional types. For example, in the data samples of blood routine indexes, the distribution of TCM constitutional types is as shown in Figure 5.

As shown in Figure 4, it has a small number of special types, which are caused by a small number of people of these types in the world.

4.2. Algorithm Implementation. Visual Studio was employed to implement the neural network algorithm for the correlation between TCM constitutional types and physical examination indexes. Google's AI library and C# programming language were utilized for algorithm implementation. The number of iterations was set to 5000000; the accuracy and error were output once for every 1000 iterations (Algorithm 1).

4.3. Accuracy and Error Results. Accuracy and error are essential to verify the prediction data of a network model. The algorithm in this paper employed the blood routine examination, urine routine examination, liver function index, renal function index, and entire physical examination index data of training group to establish the neural network model and then used the test group data for model verification. The accuracy represents the ratio of the model prediction results to the actual results of the sample, and the error is calculated by the BP neural network algorithm, as shown in equation (4). If the accuracy is higher and the error

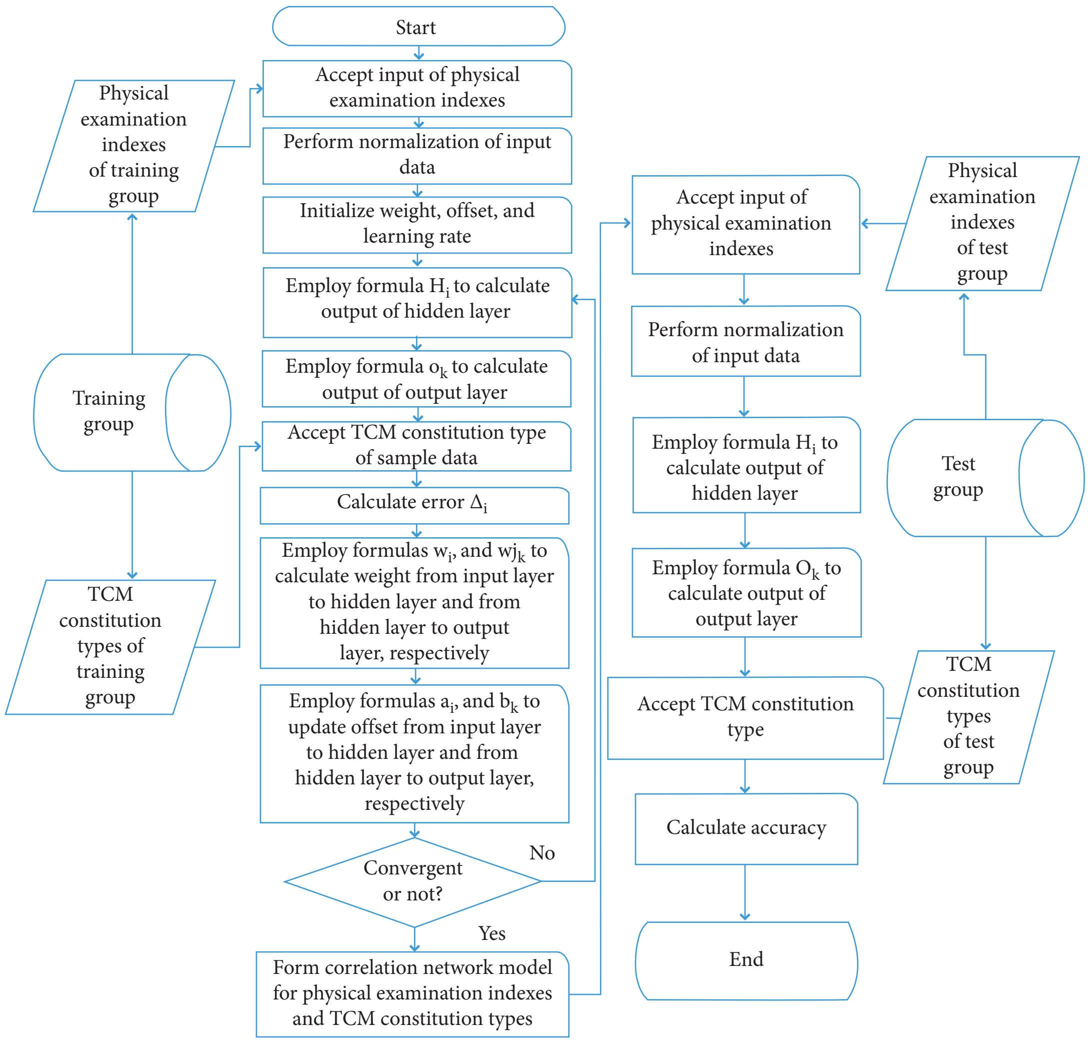

Figure 4: Neural network algorithm implementation procedures for physical examination indexes and TCM constitutional types.

Table 1: Standardization of TCM constitutional types.

SN	Constitutional type	Digitization representation
1	Peaceful type	0.1
2	*qi*-deficient type	0.2
3	*yang*-deficient type	0.3
4	*yin*-deficient type	0.4
5	Phlegm-damp type	0.5
6	Damp and hot type	0.6
7	Blood stasis type	0.7
8	*qi* depression type	0.8
9	Special type	0.9

is lower, the similarity between the predicted results of the model and the true clinical results is higher, which indicates that the model has a higher availability. Running time represents the time it takes to run the algorithm for every 1000 iterations of sample.

In order to construct and verify the correlation model between different physical examination indexes and constitution of TCM, we carried out, respectively, experiments for entire physical examination indexes, blood routine indexes, urine

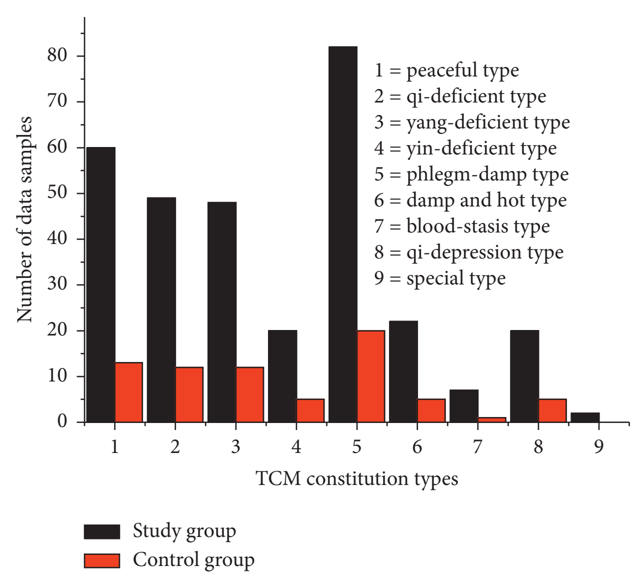

Figure 5: Blood routine indexes-effective data of the training and test groups.

```
 //Read the training group of sample
StreamReader reader = new StreamReader("trainData.txt");
   for (int i = 0; i < trainNum; ++i)
   {
      string value = reader.ReadLine();
      string[] temp = value.Split('\t');
      trainInput[i] = new double[4];
      trainOutput[i] = new double[3];
      for (int j = 0; j < 4; ++j)
      {
         trainInput[i][j] = double.Parse(temp[j]);
         if (trainInput[i][j] > max[j])
      max[j] = trainInput[i][j];
   if (trainInput[i][j] < min[j])
      min[j] = trainInput[i][j];
}
   for (int j = 0; j < 3; ++j)
      trainOutput[i][j] = 0;
   trainOutput[i][ int.Parse(temp[4]) -1 ] = 1;
}
   //Build the correlation model
   //create multilayer neural network
   ActivationNetwork network = new ActivationNetwork(new SigmoidFunction(3), 4, 5, 3);
   //create teacher
   BackPropagationLearning teacher = new BackPropagationLearning(network);
   //set learning rate and momentum
   teacher.LearningRate = 0.1;
   teacher.Momentum = 0;
   int iteration = 1;
   while(iteration < 500)
{
      teacher.RunEpoch(trainInput, trainOutput) ;
      ++iteration;
}
```

Algorithm 1: Portions of code for building the correlation model.

routine indexes, liver function indexes, renal function indexes, and corresponding constitution types of TCM and built the corresponding correlation model. The accuracy, error, and running time of every correlation model are shown in Table 2.

From Table 2, the following could be obtained:

The training group and test group of liver function indexes-TCM constitution have an accuracy of 31% and 42%, respectively, and the error is 11.7.

The training group and test group of renal function indexes-TCM constitution have an accuracy of 41% and 38%, respectively, and the error is 6.7.

The training group and test group of blood routine indexes-TCM constitution have an accuracy of 56% and 42%, respectively, and the error is 2.4.

The training group and test group of urine routine indexes-TCM constitution have an accuracy of 60% and 40%, respectively, and the error is 2.6.

The training group and test group of entire physical examination indexes-TCM constitution have an accuracy of 88% and 53%, respectively, and the error is 0.001.

It is concluded that the more the physical examination indexes are, the more accurate the correlation model is, and the lower the error is.

In Figures 6 and 7, the horizontal axis of 1–5, respectively, represents the entire physical examination indexes-TCM constitution model, blood routine indexes-TCM constitution model, urine routine indexes-TCM constitution model, liver function indexes-TCM constitution model, and renal function indexes-TCM constitution model.

Figures 6 and 7 show that the accuracy is the highest of the entire physical examination indexes-TCM constitutional model.

Figure 8 illustrates the accuracy distribution in the training group of entire physical examination indexes-constitutional-type neural network model; the accuracy reaches 88% when the number of iterations is 1834000, and it goes stable while the number of iterations reaches 3481000.

Figure 9 illustrates the accuracy distribution in the test group of entire physical examination indexes-constitutional-type neural network model; the accuracy reaches 53% when the number of iterations is 171000, and it goes stable at the same time.

Figure 10 shows the error (the computational method is shown in equation (2)) distribution of entire physical

Table 2: Accuracy results for different physical examination indexes, TCM constitution neural network models.

Name of neural network model	Accuracy of training group (%)	Accuracy of test group (%)	Error	Running time (time for every 1000 times iteration, sec)
Entire physical examination indexes-constitutional type	88 (top), 56 (stable)	53	0.001	0.1
Urine routine-constitutional type	60	40	2.6	0.051
Blood routine-constitutional type	56	42	2.4	0.063
Renal function-constitutional type	41	38	6.7	0.079
Liver function-constitutional type	31	42	11.7	0.063

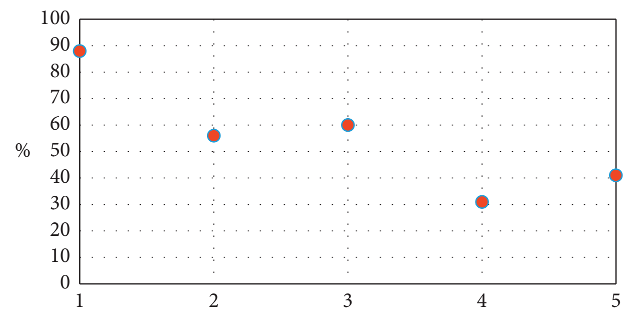

Figure 6: The accuracy chart of the learning group of different physical examination indexes-TCM constitutional model.

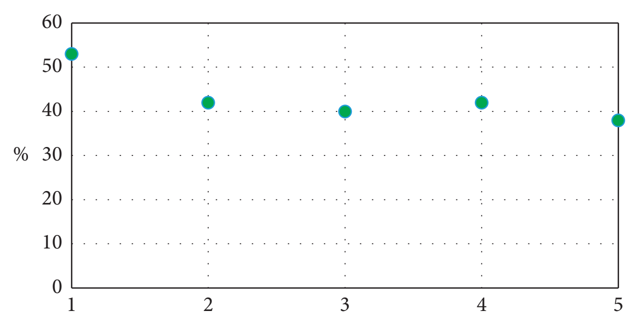

Figure 7: The correct rate chart of the test group of different physical examination indexes-TCM constitutional model.

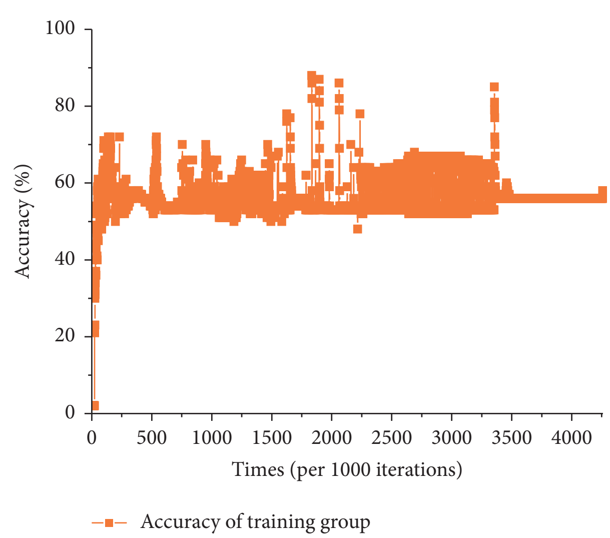

Figure 8: Accuracy of the training group of entire physical examination indexes-constitutional type network model.

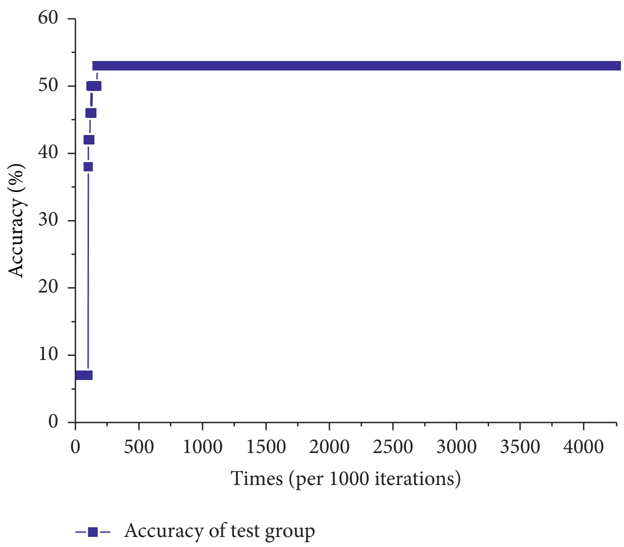

FIGURE 9: Accuracy of the test group of entire physical examination indexes-constitutional type network model.

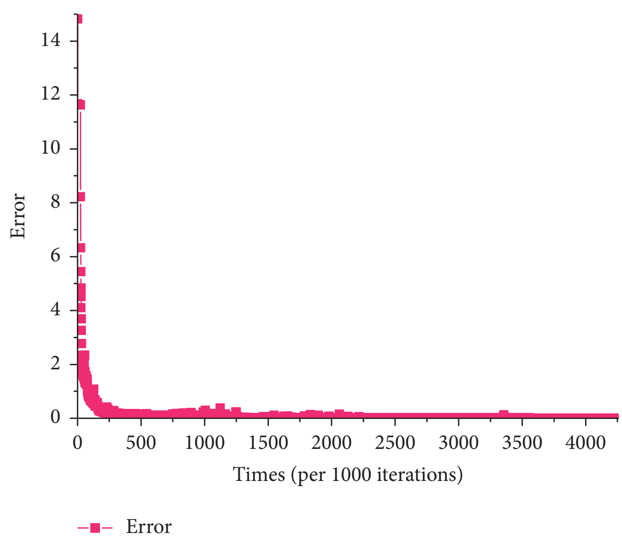

FIGURE 10: Error of entire physical examination indexes-constitutional-type network model.

examination indexes-constitutional-type neural network model. It points out that the error is less than 1 when the number of iterations reaches 81000 although it is high at the beginning.

Figure 11 illustrates the error distribution under 1. It depicts that the error decreases in a stable way, while the number of iterations reaches 3357000. It proves that the algorithm reaches convergent.

The above results prove that there is a relatively strong correlation between TCM constitution and physical examination indexes for the high accuracy and low error. It may reach the higher accuracy and lower error if the number of data increases.

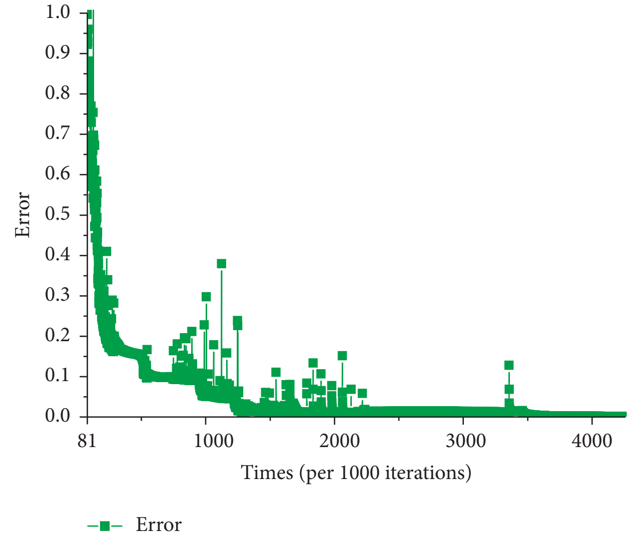

FIGURE 11: Error of entire physical examination indexes-constitutional-type network model (error<1).

5. Conclusions

In this paper, modern computer technology and AI neural network technology were employed to establish network models for physical examination indexes and TCM constitutional types. The data in the training group were used to establish the physical examination index-TCM constitution neural network model. And the data in the test group were used to verify the model. The results indicate that the more the physical examination indexes are, the more accurate the model is, and the lower the error is. For the entire physical examination indexes-TCM constitution correlation model, the training group and test group have an accuracy of 88% and 53%, respectively, and the error is 0.001. This value is higher than other experimental groups performed in this study such as urine routine examination indexes-TCM constitution model and liver function examination indexes-TCM constitution model. Verified by the text group data, this study shows that there is a relatively strong correlation between modern physical examination indexes and TCM constitutional types.

This paper fills the gaps about the researching of correlation between TCM constitution and physical examination indexes and provides the possibility for identification of TCM constitution based on the correlation model. The combined study of physical examination indexes and TCM constitution has profound meaning in exploring correlation between TCM and Western medicine, which would provide an associated automation template for both, in promoting TCM modernization and automatic and objective identification of TCM constitution in an innovative approach, which would be expected to avoid the problems existing in the current TCM constitution identification methods and in boosting preventive treatment of disease.

This paper uses clinical data and BP neural network technology which is widely used and matures in the field of artificial intelligence, to complete the construction of the physical examination indexes-TCM constitution network model, but this work still needs to be improved. For the volume of sample is not large enough, the future plans include improving algorithm and enhancing size of sample data, such as applying the remaining physical examination indexes, like the basic data of physical examination, blood lipid index, and the full set of transfusion index, and the corresponding TCM constitution, which are helpful to get a prediction model with high accuracy and low error, to do more experiments. In addition, the future endeavors will focus on identification of TCM constitution based on the correlation model. For example, the research will develop a system for identification of TCM constitution based on the correlation model. Then, the system will be applied in the identification of clinical TCM constitution to promote a new method of TCM constitution identification.

Data Availability

The 950 physical examinees, accepted by the Health Management Center of the Affiliated Hospital of Chengdu University of TCM from January 2016 to March 2017, were used as study objects.

Conflicts of Interest

The authors declare that there are no conflicts of interest.

Acknowledgments

This work was supported by the National Natural Science Foundation of China (Grant nos. 81904324 and 81804222) and National Key Research and Development Program (Grant no. 2018YFC1707606).

References

[1] Q. Wang, “Introduction and the factors forming different physical constitutions,” in *Theory of TCM Constitution*, Jiangsu Science and Technology, Jiangsu, China, 1st edition, 1982.

[2] L. L. Lin, “*The study of the tranditional chinese medicine identify constitution in the application of preventive treatment of disease*,” M.S. thesis, Nanjing University of Chinese Medicine, Nanjiang, China, 2013.

[3] H. D. Zhang and L. G. Ma, “Discuss bravery of Ling Jiu,” in *Inner Canon of Huangdi Interpretation*Sichuan Science and Technology, Beijing, China, 2009.

[4] Q. Wang, “Classification and diagnosis basis of nine basic constitutions in Chinese medicine,” *Journal of Beijing University of Traditional Chinese Medicine*, vol. 28, no. 4, 2005.

[5] W. B. Wu, B. Li, Y. X. Ge et al., “Analysis of TCM physical identification of the elderly population in Chengdu city,” *Chinese Journal of TCM*, vol. 28, no. 4, pp. 1099–1101, 2013.

[6] G. R. Li, *Research on the correlation between fatigue status and physical examination index in 2823 crowds of medical examination*, Ph.D. dissertation, Beijing University of Chinese Medicine, Beijing, China, 2013.

[7] Q. Wang, “Identification of TCM Constitution provides the opportunity to develop for preventive treatment of disease,” *Global Chinese Medicine*, vol. 3, pp. 5-6, 2008.

[8] L. J. Sun and Y. F. Bai, “The status and function of constitution identification in the disease prevention,” *Modern Traditional Chinese Medicine*, vol. 35, no. 6, pp. 58–61, 2015.

[9] Y. M. Xi, “*The exploration on meridian thermal sensitivity measurement in use of Qi deficiency constitution’s meridian constitution characteristics*,” M.S. thesis, Guangzhou University of Chinese Medicine, Guangzhou, China, 2011.

[10] Y. Zhang and Y. H. Wang, “Research on automatic identification system of traditional Chinese medicine constitution based on pulse wave,” *World Science and Technlgy/Modernization of Traditional Chinese Medicne and Materia Medical*, vol. 19, no. 10, pp. 1687–1691, 2017.

[11] China Association of Chinese Medicine, “Classification and judgment of TCM constitution,” *World Journal of Integrated Traditional and Western Medicin*, vol. 4, no. 4, pp. 303-304, 2009.

[12] S. K. Jiang and L. Li, “A number of issues were discussed for Classification and judgment of TCM constitution,” *Liaoning Journal of Traditional Chinese Medicne*, vol. 40, no. 2, pp. 262-263, 2013.

[13] H. Xin, J. K. Wu, X. Guo et al., “Discussion on the problems of nine traditional Chinese medicine constitutional types scale in clinical application,” *Chinese Journal of Traditional Chinese Medicine*, vol. 29, no. 6, pp. 1841–1843, 2014.

[14] Y. S. Li, Y. Yang, L. R. Li et al., “Interpretion on the difficult problems in application of traditional Chinese medicine constitution scale,” *Journal of Traditional Chinese Medicine*, vol. 56, no. 10, pp. 844–846, 2015.

[15] L. B. Zhu and J. Wang, “On the revision of TCM constitution questionnaire,” *Journal of Anhui University of Chinese Medicine*, vol. 35, no. 4, pp. 6–9, 2016.

[16] X. Liu and Q. Wang, “Suggestion and analysis on revise of standard of classification determination of constitution in TCM,” *Journal of Beijing University of Traditional Chinese Medicine*, vol. 36, no. 5, pp. 300–304, 2013.

[17] X. M. Deng and B. Lu, “Application and significance for physique identification of TCM in medical examination,” *Medical Tribune*, vol. 1, pp. 21–23, 2009.

[18] Q. Y. Pan, “Applicable values and expanding strategies physique identification of TCM in medical examination,” *Clinical Journal of Chinese Medicne*, vol. 4, no. 19, pp. 113-114, 2012.

[19] Z. F. Zhou, S. J. Yang, H. P. Xu et al., “Effect and significance of physique identification of TCM in medical examination,” *Guide of CN Medicne*, vol. 12, no. 28, pp. 274-275, 2014.

[20] G. T. Ni, “The discussion of application about TCM identification in health examination,” *Guide of CN Medicne*, vol. 11, no. 8, pp. 285-286, 2013.

[21] J. Ren and Z. G. Li, “Analysis on results of medical examination and characteristics of distribution for physique of Traditional Chinese Medicine for elderly community residents,” *Liaoning University of TCM*, vol. 17, no. 6, pp. 80–82, 2015.

[22] X. M. Zhang, Y. B. Zhu, N. X. Wu et al., “Correlation analysis on obesity diagnosed by different obesity indices with traditional Chinese medicine constitutions,” *TCM*, vol. 56, no. 3, pp. 212–215, 2015.

[23] W. J. Zhang, “*The study of relation between TCM physiques and stroke risk factors in 207 patients with high risk factors for stroke based on check upcrowd*,” M.S. thesis, Guangzhou University of Chinese Medicine, Guangzhou, China, 2016.

[24] D. Sun, Y. W. Tu, R. F. Hao et al., “Correlation Analysis of TCM constitution, blood lipid and body mass index in

metabolic hypertension," *Hubei University of Chinese Medicine*, vol. 39, no. 4, pp. 500–505, 2017.

[25] K. S. Deng, Z. Y. Liu, and F. M. Xiang, "Relationship between TCM constitution distribution and relevant physical examination indices in the patients of hypertension," *World Journal of Integrated Traditional and Western Medicne*, vol. 9, no. 8, pp. 840–842, 2014.

[26] K. S. Deng, F. M. Xiang, and Y. M. Deng, "TCM based constitution classification in patients with impaired glucose regulation and its relationship with physical indicators," *Nanchang Univrsity (Medical Science)*, vol. 51, no. 1, p. 24, 2011.

[27] F. M. Xiang, K. S. Deng, and Y. P. Jiang, "TCM based constitution classification in HBV infected patients and its relationship with physical indicators," *Nanchang University (Medical Science)*, vol. 51, no. 1, pp. 21–23, 2011.

[28] X. G. Deng, "Research on the correlation between TCM constitution and neuroendocrine immune network," *Shenzhen Yantian Hospital of Integrated Traditional Chinese and Western Medicine*, vol. 27, no. 11, pp. 4-5, 2017.

[29] W. Z. Zhang, "Relativity between Yin Deficiency Constitution, Yangqi Deficiency Constitution, Yinyang Harmony Constitution with cardiovascular risk factors," *Chinese Journal of Integrative Medicine on Cardiocerebro Vascular Disease*, vol. 15, no. 20, pp. 2567–2570, 2017.

[30] Q. W. Jiang and X. Xiao, "Study on the correlation between the body shape of physique and traditional Chinese medicine constitution type," *Chinese Journal of Ethnomedicine and Ethnopharmacy*, vol. 27, no. 1, pp. 13–15, 2018.

[31] Z. Y. Ye and H. Chen, "Distribution of TCM constitution types in healthy population and analysis of physical examination results," *Journal of Hubei University of Chinese Medicine*, vol. 20, no. 3, pp. 32–36, 2018.

[32] H. R. An and D. M. Zeng, "Study on the correlation between traditional Chinese medicine corporeity and physical examination parameters of college students," *Chinese Journal of Traditional Chinese Medicine*, vol. 33, no. 7, pp. 3074–3077, 2018.

[33] Y. K. Zhang, "*The research and implementation of TCM constitution identification system basde on B/S*," M.S. thesis, University of Electronic Science and Technology, Chengdu, China, 2015.

[34] B. Lin, X. Y. Zhang, Y. K. Zhang et al., "The design and implementation of identification system for TCM constitution," *Chengdu University of TCM*, vol. 39, no. 4, pp. 123–125, 2016.

[35] L. Z. Xiong and L. Peng, "Design and implementation of intelligent TCM health keeping system," *Scientific Mosaic*, vol. 3, pp. 44–46, 2016.

[36] J. P. Li, "The design and implementation of physical health identification of TCM constitution system," *Heilongjiang University of Science and Technology*, vol. 25, no. 10, 2011.

[37] Y. M. Liang, "*Research on automatic identification system of TCM constitution based on facial image feature*," M.S. thesis, Beijing University of Technology, Beijing, China, 2016.

[38] L. Hong, "Research on constitution of traditional Chinese medicine identification system based on tongue manifestation," *Chinese Medicine Modern Distance Education of China*, vol. 14, no. 2, 2016.

[39] L. N. Bai, "*Research on the identification of body physiqueal typesin Chinese medicine based on BP neural network*," M.S. thesis, Tianjin University of Technology, Tianjin, China, 2014.

[40] S. Y. Xie, "*Research on TCM constitution identification and data analysis platform and implementation*," M.S. thesis, Nanjing Univeristy of Chinese Medicine, Nanjing, China, 2018.

[41] S. Haykin, F. R. Shen, Y. Xu et al., *Neural Networks and Learning Machines*, Machine Industry, Beijing, China, 3rd edition, 2011.

[42] I. A. Basheer and M. Hajmeer, "Artificial neural networks: fundamentals, computing, design, and application," *Journal of Microbiological Methods*, vol. 43, no. 1, pp. 3–31, 2000.

[43] C. Yang, K. Huang, H. Cheng, Y. Li, and C. Su, "Haptic identification by ELM controlled uncertain manipulator," *IEEE Transactions on Systems, Man, and Cybernetics: Systems*, vol. 43, pp. 1–12, 2017.

[44] Y. Chen and M. C. Zhou, *Artificial Neural Network Simulation and Application*, China University of Geosciences, Beijing, China, 2000.

[45] H. J. Yu, C. Z. Chen, S. Zhang, and J. N. Zhou, *Intelligent Diagnosis Based on Neural Network*, Metallurgical Industry, Beijing, China, 1st edition, 2000.

[46] J. Yu, Q. L. Pan, J. F. Yang et al., "Correlations of complete blood count with alanine and aspartate transaminase in Chinese subjects and prediction based on Back Propagation artificial neural network (BP-ANN)," *Medical Sciences*, vol. 23, pp. 3001–3009, 2017.

Hindawi
Journal of Healthcare Engineering
Volume 2020, Article ID 8862256, 7 pages
https://doi.org/10.1155/2020/8862256

Review Article

Network Meta-Analysis of the Safety of Drug Therapy for Cardiogenic Shock

Xianyong Liao, Lin Qian, Song Zhang, Xiang Chen, and Jing Lei

Hospital of Chengdu University of Traditional Chinese Medicine, Chengdu, China

Correspondence should be addressed to Song Zhang; zhangyuer2000@cdutcm.edu.cn

Received 2 May 2020; Revised 2 June 2020; Accepted 1 July 2020; Published 1 August 2020

Academic Editor: Jiafeng Yao

Objectives. (1) To conduct a network meta-analysis of clinical drugs used for cardiogenic shock and (2) provide evidence for the selection of medication for the treatment of this condition. *Methods*. PubMed, EMBASE, Cochrane library, China HowNet (CNKI), Wanfang database, and Weipu database were searched using keywords Dopamine, Dobutamine, Epinephrine, Adrenaline, Norepinephrine, Noradrenaline, Milrinone, Natriuretic peptide, Recombinant human brain natriuretic peptide, Levosimendan, Cardiac shock, and Cardiogenic shock. We select literature according to prespecified inclusion and exclusion criteria and record data such as drug type, mortality, and adverse reactions. *Results*. Twenty-eight of 1387 articles met inclusion criteria, comprising 1806 patients who suffered from cardiogenic shock. Dopamine, dobutamine, epinephrine, norepinephrine, milrinone, recombinant human brain natriuretic peptide, and levosimendan were all commonly used in the treatment of cardiogenic shock. Milrinone was most effective at reducing mortality and had the lowest incidence of adverse reactions. *Conclusion*. This network meta-analysis demonstrated that milrinone was the most effective medication at reducing mortality and adverse events in patients suffering from cardiogenic shock.

1. Introduction

Cardiogenic shock is characterized by a decline in cardiac function leading to a significant decrease in cardiac output and insufficient effective circulating blood volume, resulting in severe acute peripheral circulatory failure. The mortality rate from cardiogenic shock ranges from 50% to 80% [1]. The most common cause of cardiogenic shock is acute myocardial infarction (AMI), accounting for 80% of cases [2]. Approximately 50% of patients with AMI develop cardiogenic shock within six hours, and 75% develop it within 24 hours [3]. The use of digitalis drugs in the treatment of cardiogenic shock is controversial. When AMI is complicated by cardiogenic shock, myocardium in the ischemic area does not bind well with digitalis, thus increasing its toxicity, suggesting it should be avoided [2, 4].

The drug of choice for the treatment of cardiogenic shock is controversial. Milrinone has been shown to affect long-term mortality from cardiogenic shock [5], and levosimendan and adrenaline have been shown to have adverse side effects, which increase potential risks and incidence of adverse reactions [6, 7]. Dobutamine has been shown to adversely increase the heart rate [8, 9] and yet is recommended by others with half of clinicians using it for treatment of cardiogenic shock [10, 11]. The purpose of this study was to conduct a network meta-analysis on the clinical effects of medications used for the treatment of cardiogenic shock.

2. Materials and Methods

2.1. Literature Review. PubMed, EMBASE, Cochrane library, China National Knowledge Infrastructure (CNKI), Wanfang database, and Weipu database were searched for articles in Chinese or English using keywords Dopamine, Dobutamine, Epinephrine, Adrenaline, Norepinephrine, Noradrenaline, Milrinone, Natriuretic peptide, Recombinant human brain natriuretic peptide, Levosimendan, Cardiac shock, and Cardiogenic shock from January 1, 2009, to December 31, 2019.

2.2. Inclusion and Exclusion Criteria. Articles meeting the following criteria were included: (1) randomized clinical trials related to cardiogenic shock drug therapy, (2) diagnosis of cardiogenic shock as described in the 2014 Chinese Heart Failure Guide [12], (3) cardiogenic shock as the main treatment target in the study, and (4) outcome indicators being mortality and adverse reactions. Studies were excluded if they met the following criteria: (1) nonexperimental studies such as "reviews" and "case reports," (2) contained duplicate or low quality data or insufficient information and clinical data, (3) literature on traditional Chinese medicine and proprietary Chinese medicines for cardiogenic shock, and (4) animal experiments.

2.3. Data Extraction and Literature Quality Evaluation. Extracted data included the author, publication date, average age, research method, sample number, mortality rate, and incidence of adverse reactions. We evaluated bias based on evaluation criteria from the Cochrane Handbook for Systematic Reviews of Interventions including random sequence generation, whether to hide the allocation scheme, whether to use blind method, completeness of the outcome data, whether to selectively report the research results, and other sources of bias. According to the Cochrane Handbook evaluation standards, the literature is divided into 3 levels: low deviation: all meet the Cochrane Handbook evaluation standard; medium deviation: 1 undescribed Cochrane Handbook evaluation standard; high deviation: there are 2 or more items not described or 1 item does not meet the Cochrane Handbook evaluation standard.

2.4. Statistical Processing Methods. The network meta-analysis was conducted using ADDIS 1. 16. 8. Data were first tested for consistency using a node-split model. Where there was no statistical difference between direct and indirect comparison ($P > 0.05$), the consistency model was used. Where there was a difference, an inconsistency model was used. The stability of the analysis results of the consistency model was tested using the inconsistency model. When the inconsistency factors included 0 and the inconsistency standard deviation included 1 and the consistency model results were more stable and reliable. Various analysis models were automatically iterated based on preset parameters, and the convergence of the iterative effect was judged by potential scale reduced factor (PSRF). When the PSRF value was close to or equal to 1 ($1 \leq \text{PSRRF} \leq 1.05$), the convergence is felt to be complete, and the model is believed to have good stability, rendering the analysis conclusion more reliable. Stata 14.0 was used to create the network diagram, and funnel diagrams were made to evaluate whether the included studies had publication bias.

3. Results

3.1. Literature Review. The included search terms identified 1387 articles. Using inclusion and exclusion criteria while evaluating the title, abstract, and full text of the literature, 28 articles were included, describing 1806 patients (Figure 1).

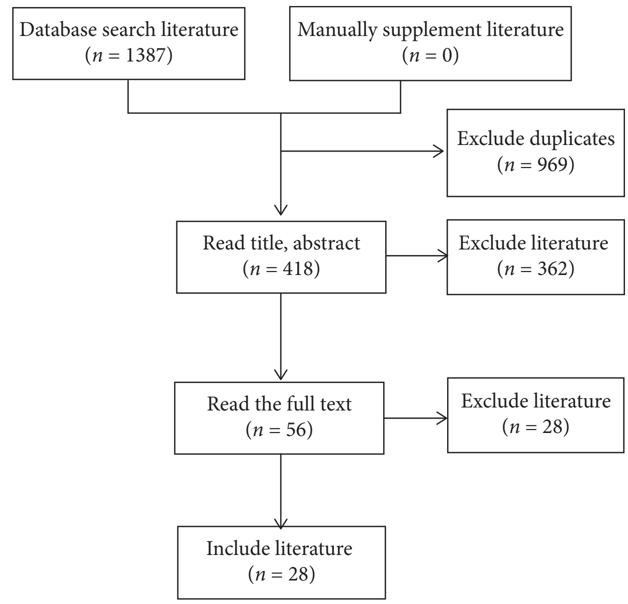

Figure 1: Literature screening process.

3.2. Basic Characteristics of the Literature. The 28 clinical studies [13–40] included were all clinical trials using medications to treat cardiogenic shock. Seven (25%) of the 28 studies were conducted before 2015, and the remaining 21 (75%) studies were concentrated after 2015. The treatment cycle and dosage of the drugs in each group were basically the same, and the difference was not statistically significant (Table 1).

3.3. Evaluation of Included Studies. Of the 28 studies [13–40], 7 (25%) clearly stated the method of randomization (random number table, admission order, etc.), 1 (3.5%) of the studies described the allocation concealment method, and none described the method of blinding; other sources of bias were unknown; the baseline patient characteristics of the studies were basically the same (Table 2).

3.4. Network Meta-Analysis Results

3.4.1. Network Diagram of Included Interventions. Each dot in the network diagram represents a drug, and a wired segment directly connected between the two points indicates a direct comparison between the two drugs. The larger the dot, the higher the frequency of study drugs being included in the reticulation analysis. The wider the line between the two dots, the higher the frequency of comparisons between drugs (Figures 2 and 3).

3.4.2. Node-Split Model Test and Convergence Judgment. Case fatality rate and incidence of adverse reactions were evaluated by node-split model method. Both P values were greater than 0.05, suggesting that there was no statistical inconsistency, supporting use of the consistency model for analysis. Both the consistency model analysis and the

Table 1: Included literature information form.

Include literature	Published time	Average age		Gender		Number of cases		Intervention measure	
		E	C	Male	Female	E	C	E	C
Levy et al. [13]	2011	66 ± 12	64 ± 10	21	9	15	15	$0.1\ \mu g/(kg\cdot min)^{e}$	$0.1\ \mu g/(kg\cdot min)^{f}$
Pan et al. [14]	2017	64.9 ± 12.6	64.1 ± 10.8	35	13	25	23	$0.005\ mg/(kg\cdot min)^{a}$	$3–12\ mg/(kg\cdot min)^{c}$
Bruno et al. [15]	2018	68 (55–79)	66 (55–77)	38	19	27	30	$0.02\ \mu g/(kg\cdot min)^{e}$	$0.02\ \mu g/(kg\cdot min)^{f}$
Zhou et al. [16]	2012	62.3 ± 1.8	60.2 ± 2.4	21	19	20	20	$60\ \mu g/kg^{g}$	b
Pang and Zhao [17]	2011	60.2 ± 9.8	60.2 ± 9.8	28	22	25	25	$75\ \mu g/kg^{g}$	NA^{d}
Li [18]	2016	68.4 ± 11.3	70.8 ± 10.7	23	17	20	20	$12\ \mu g/kg^{h}$	b
Chen [19]	2018	58.22 ± 5.03	60.05 ± 4.85	43	19	30	32	$^{f}0.05–0.19\ \mu g/(kg\cdot min)$	$5–20\ \mu g/(kg\cdot min)^{c}$
Xiong et al. [20]	2016	78.76 ± 7.17	76.77 ± 6.41	40	20	30	30	$^{f}0.05–2.0\ \mu g/(kg\cdot min)$	$5–20\ \mu g/(kg\cdot min)^{c}$
Tsagalou et al. [21]	2009	70 ± 9	69 ± 11	22	3	12	13	$6\ \mu g/(kg\cdot min)^{h}$	$10\ \mu g/(kg\cdot min)^{d}$
Yang [22]	2015	66.7 ± 6.5	65.3 ± 6.2	31	15	23	23	$6\ \mu g/kg^{h}$	$2.5\ \mu g/(kg\cdot min)^{d}$
Zhang and Xiao [23]	2010	65.9 ± 0.2	65.9 ± 0.2	48	40	44	44	$2–10\ \mu g/(kg\cdot min)^{c}$	b
Lewis et al. [24]	2019	72.5 (59–81)	75 (67–83)	51	49	50	50	$0.25\ \mu g/(kg\cdot min)^{g}$	$2.5\ \mu g/(kg\cdot min)^{d}$
Pan et al. [25]	2018	68.36 ± 10.78	68.78 ± 10.72	46	34	40	40	$12\ \mu g/kg^{h}$	b
Shen [26]	2017	46.0 ± 6.1	46.6 ± 6.3	26	22	24	24	$12\ \mu g/kg^{h}$	$^{f}0.01–0.1\ \mu g/(kg\cdot min)$
Tan [27]	2016	56.75 ± 12.17	58.37 ± 13.24	45	35	30	50	$^{f}0.05–0.19\ \mu g/(kg\cdot min)$	$10–20\ \mu g/(kg\cdot min)^{c}$
Wang et al. [28]	2011	57 ± 13	57 ± 13	31	20	25	26	$0.19\ \mu g/(kg\cdot min)^{f}$	$20\ \mu g/(kg\cdot min)^{c}$
He et al. [29]	2014	63.52 ± 1.12	63.52 ± 1.12	26	21	25	22	$^{f}0.05–0.19\ \mu g/(kg\cdot min)$	$10–20\ \mu g/(kg\cdot min)^{c}$
Li et al. [30]	2015	58.6 ± 10.1	58.6 ± 10.1	33	27	30	30	$^{f}0.05–0.5\ \mu g/(kg\cdot min)$	$1–20\ \mu g/(kg\cdot min)^{c}$
Zhou and Zhou [31]	2019	67.96 + 5.92	68.13 + 5.38	93	29	64	58	$^{f}0.05–2.00\ \mu g/(kg\cdot min)$	$10–20\ \mu g/(kg\cdot min)^{c}$
Li [32]	2019	69.4 ± 8.7	68.1 ± 8.2	55	31	43	43	$1.5\ \mu g/kg^{a}$	b
Lewis et al. [33]	2015	73	73	50	50	50	50	NA^{g}	NA^{d}
Su [34]	2019	58.5 ± 3.3	59.5 ± 3.5	38	30	34	34	$^{f}0.1–0.5\ \mu g/(kg\cdot min)$	$^{d}4.0–5.5\ \mu g/(kg\cdot min)$
Guo et al. [35]	2017	62.75 ± 2.52	62.75 ± 2.52	37	23	30	30	$12\ \mu g/(kg\cdot min)^{h}$	$2\ \mu g/(kg\cdot min)^{d}$
Peng et al. [36]	2015	59.7 ± 1.4	58.6 ± 1.2	55	53	54	54	$12\ \mu g/kg^{h}$	$2.5\ \mu g/(kg\cdot min)^{d}$
Huang et al. [37]	2018	67.2 ± 3.8	68.3 ± 4.2	37	29	33	33	$12\ \mu g/kg^{h}$	$2.5\ \mu g/(kg\cdot min)^{d}$
Huang et al. [38]	2018	67.65 ± 4.69	67.59 + 4.75	55	39	47	47	$12\ \mu g/(kg\cdot min)^{h}$	$2\ \mu g/(kg\cdot min)^{d}$
Chen et al. [39]	2019	68. 05 ± 6. 73	68. 46 ± 6. 47	25	15	20	20	$6\ \mu g/kg^{h}$	$25\ \mu g/kg^{g}$
Yang and Sun [40]	2018	61.21 ± 2.14	61.25 ± 2.44	26	24	25	25	$12\ \mu g/(kg\cdot min)^{h}$	$2\ \mu g/(kg\cdot min)^{d}$

Note. E is the treatment group; C is the control group. [a]Recombinant human brain natriuretic peptide; [b]conventional treatment. [c]dopamine; [d]dobutamine; [e]epinephrine; [f]norepinephrine; [g]milrinone; [h]levosimendan;

Table 2: Literature bias risk assessment results.

Include literature	Stochastic method	Allocation concealment	Blind method	Outcome data integrity	Selective report results	Other sources of bias
Levy et al. [13]	Randomize the code	Unclear	Unclear	Not lost to follow-up	No	Unclear
Pan et al. [14]	Unclear	Label	Unclear	Lost to follow-up, ITT analysis	No	Unclear
Bruno et al. [15]	Unclear	Unclear	Unclear	Lost to follow-up, ITT analysis	No	Unclear
Zhou et al. [16]	Admission order	Unclear	Unclear	Lost to follow-up, ITT analysis	No	Unclear
Pang and Zhao [17]	Unclear	Unclear	Unclear	Not lost to follow-up	No	Unclear
Li [18]	Unclear	Unclear	Unclear	Not lost to follow-up	No	Unclear
Chen [19]	Unclear	Unclear	Unclear	Not lost to follow-up	No	Unclear
Xiong et al. [20]	Unclear	Unclear	Unclear	Not lost to follow-up	No	Unclear
Tsagalou et al. [21]	Unclear	Unclear	Unclear	Not lost to follow-up	No	Unclear
Yang [22]	Unclear	Unclear	Unclear	Not lost to follow-up	No	Unclear
Zhang and Xiao [23]	Unclear	Unclear	Unclear	Not lost to follow-up	No	Unclear
Lewis et al. [24]	Unclear	Unclear	Unclear	Not lost to follow-up	No	Unclear
Pan et al. [25]	Unclear	Unclear	Unclear	Not lost to follow-up	No	Unclear
Shen [26]	Unclear	Unclear	Unclear	Lost to follow-up, ITT analysis	No	Unclear
Tan [27]	Unclear	Unclear	Unclear	Not lost to follow-up	No	Unclear
Wang et al. [28]	Unclear	Unclear	Unclear	Not lost to follow-up	No	Unclear
He et al. [29]	Unclear	Unclear	Unclear	Not lost to follow-up	No	Unclear
Li et al. [30]	Unclear	Unclear	Unclear	Lost to follow-up, ITT analysis	No	Unclear
Zhou and Zhou [31]	Unclear	Unclear	Unclear	Not lost to follow-up	No	Unclear
Li [32]	Random number table	Unclear	Unclear	Not lost to follow-up	No	Unclear
Lewis et al. [33]	Unclear	Unclear	Unclear	Not lost to follow-up	No	Unclear
Su [34]	Random grouping	Unclear	Unclear	Not lost to follow-up	No	Unclear
Guo et al. [35]	Random number	Unclear	Unclear	Not lost to follow-up	No	Unclear
Peng et al. [36]	Unclear	Unclear	Unclear	Not lost to follow-up	No	Unclear
Huang et al. [37]	Random number table	Unclear	Unclear	Not lost to follow-up	No	Unclear
Huang et al. [38]	Unclear	Unclear	Unclear	Not lost to follow-up	No	Unclear
Chen et al. [39]	Random number table	Unclear	Unclear	Not lost to follow-up	No	Unclear
Yang and Sun [40]	Unclear	Unclear	Unclear	Not lost to follow-up	No	Unclear

inconsistency model test of the network meta-analysis have PSRF values between 1 and 1.05, indicating that the convergence is good and the results are stable.

3.4.3. Network Meta-Analysis of Case Fatality Rate under the Consistency Model. Twenty of the 1199 studies [13–32] used case fatality rate as the outcome indicator, and these were included in a network meta-analysis. According to the ranking probability map of treatment measures (Rank 8 being the best and Rank 1 being the worst), the ability of drugs to reduce fatality was as follows: milrinone > levosimendan > norepinephrine > recombinant human brain natriuretic peptide > dobutamine > epinephrine > dopamine > conventional treatment. Milrinone appeared to be the best treatment option to reduce the case fatality rate (with a probability of 44%), with levosimendan coming in second with a probability of 26%.

3.4.4. Network Meta-Analysis of the Incidence of Adverse Reactions under the Consistency Model. Eighteen of 1317 studies [24–40] used incidence of adverse reactions as the outcome indicator, and these were included in a network meta-analysis. According to the ranking probability map of treatment measures, the side effect profile from best to worst was as follows: milrinone > recombinant human brain natriuretic peptide > norepinephrine > levosimendan > conventional treatment > epinephrine > dobutamine > dopamine. Milrinone appeared to be associated with the least amount of adverse

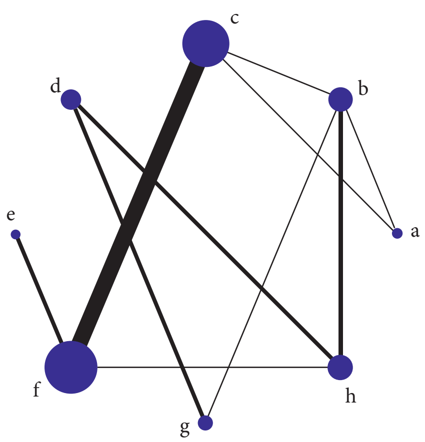

Figure 2: Network diagram of case fatality rate. Note: a, recombinant human brain natriuretic peptide; b, conventional treatment; c, dopamine; d, dobutamine; e, epinephrine; f, norepinephrine; g, milrinone; h, levosimendan.

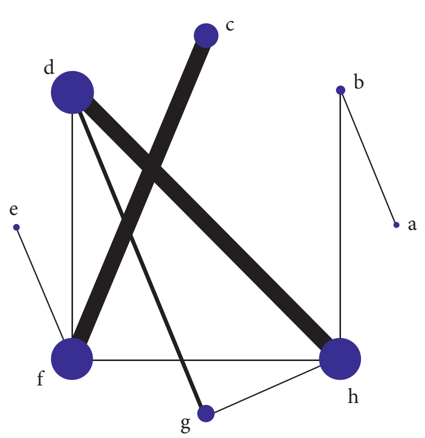

Figure 3: Network diagram of incidence of adverse reactions. Note: a, recombinant human brain natriuretic peptide; b, conventional treatment; c, dopamine; d, dobutamine; e, epinephrine; f, norepinephrine; g, milrinone; h, levosimendan.

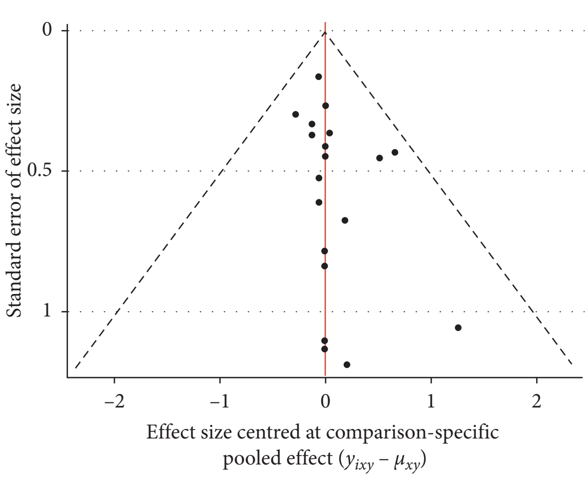

Figure 4: Funnel plot of case fatality rate for outcome indicator.

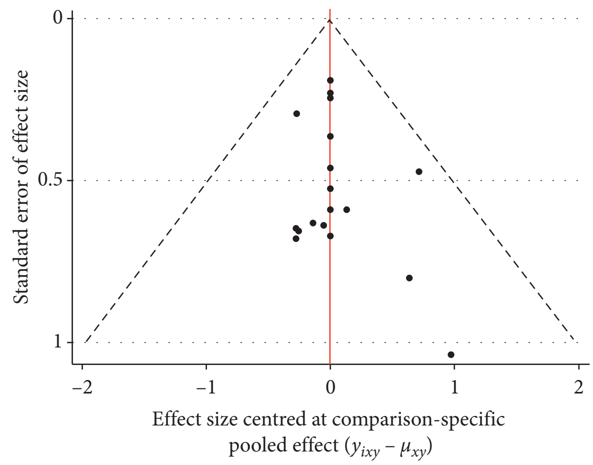

Figure 5: Funnel plot of incidence of adverse reactions for outcome indicators.

reactions (with a probability of 55%), with recombinant human brain natriuretic peptide coming in second (with a probability of 32%).

3.4.5. Inconsistency Model Testing. The consistency model of the two outcome indicators was analyzed and inconsistency models were used to test the stability of the results. Results demonstrated that the inconsistency factors all included 0 and the inconsistency standard deviations all included 1. This means that the results of the consistency model were stable and reliable.

3.5. Publication Bias. Funnel plots were created to identify small sample effects in the analysis. Funnel plots were created for the two outcome indicators for publication bias testing. Results demonstrated that the included studies were roughly symmetrically distributed on both sides of the funnel plot, and therefore the possibility of publication bias was felt to be small (Figures 4 and 5).

4. Discussion

Cardiogenic shock is a serious disease that, if not treated expeditiously and appropriately at an early stage, can have a high risk of mortality. The pathological changes of cardiogenic shock usually include two parts: one is abnormal hemodynamics and the other is insufficient perfusion of surrounding tissues. The prognosis of patients is closely related to the degree of hemodynamic abnormalities, so the rapid correction of hemodynamic abnormalities in patients with cardiogenic shock is the key to treating cardiogenic shock [41]. In clinical treatment of cardiogenic shock, blood volume is usually appropriately supplemented, and positive inotropic drugs combined with vasoactive drugs are used. For example, calcium sensitizers, levosimendan, can be combined with troponin to enhance myocardial contractility, expand coronary arteries, and improve myocardial ischemia; β-receptor agonist dobutamine mainly stimulates myocardial $\beta 1$ receptors and produces a positive inotropic effect. Phosphodiesterase inhibitors milrinone can inhibit phosphodiesterase III, increase the content of cyclic adenosine monophosphate in myocardial cells [42], exert positive inotropic effects, expand blood vessels, and improve hemodynamics. Recombinant human brain natriuretic peptide with peripheral vasodilators has similar biological activity with human-derived BNP, which can dilate blood vessels, reduce heart load, and inhibit ventricular remodeling. Although many medications have been investigated for the treatment of cardiogenic shock, a direct comparison of the effectiveness of these medications has not previously been conducted. We aimed to compare previously described medications for use in cardiogenic shock with the hope of identifying preferable medications that could be administered quickly in an emergency setting.

Our study identified milrinone as being the most effective medication for reducing fatality and having the best side effect profile. Milrinone can improve the patient's hemodynamic abnormalities and hypoperfusion status, thereby rapidly improving cardiac function and correcting heart failure, Therefore, the rapid and effective application of milrinone is of great significance to save patients' lives. Levosimendan and recombinant human brain natriuretic peptide were the second most effective drugs in reducing the case fatality rate and adverse reactions. They have a positive effect on improving the clinical symptoms and prognosis of patients, and they can be used according to the patient's condition.

5. Limitations

Limitations of this study include lesser quality of some studies included in the analysis, small sample sizes in others, and varied lengths of treatment across studies. These factors could affect the reliability of the reticulated meta-analysis. It is hoped that larger, multicenter randomized controlled trials will provide clinical data in the future to achieve a more comprehensive understanding and evaluation.

6. Conclusion

In this paper, a reticular meta-analysis system is used to evaluate the difference in the efficacy of various drugs on different outcome indicators, which provides evidence-based evidence for clinical treatment, is conducive to more effective control of clinical symptoms and disease progression, and also for further clinical trials provided a reference. The analysis results showed that milrinone had the best effect in reducing the case fatality rate and the incidence of adverse reactions in patients with cardiogenic shock. Levosimendan and recombinant human brain natriuretic peptide were the second most effective drugs in reducing the case fatality rate and adverse reactions. Milrinone can improve the patient's hemodynamic abnormalities and hypoperfusion status and has the best clinical effect to reduce the patient's case fatality rate and incidence of adverse reactions. Therefore, milrinone is recommended as the clinically preferred drug for cardiogenic shock.

Data Availability

The data used in the article come from clinical research, and the data used in the article can be obtained from PubMed, EMBASE, Cochrane library, China National Knowledge Infrastructure (CNKI), Wanfang database, and Weipu database. The data used to support the findings of this study are included within the supplementary information files.

Conflicts of Interest

The authors declare that there are no conflicts of interest regarding the publication of this paper.

Authors' Contributions

Xianyong Liao, Lin Qian, and Song Zhang contributed equally to this work.

Supplementary Materials

The [zip] data used to support the findings of this study are included within the supplementary information files. (*Supplementary Materials*)

References

[1] W. Chen, L. Zhao, L. Li et al., "Predictive value of extravascular pulmonary water index and cardiac index on the prognosis of patients with cardiogenic shock," *Chinese Journal of Circulation*, vol. 37, no. 11, pp. 895–898, 2014.

[2] S. Zhang, "Progress in diagnosis and treatment of cardiogenic shock and interpretation of guidelines," *Journal of Medical Research*, vol. 46, no. 478, pp. 7–9, 2017.

[3] K. Werdan, M. Russ, M. Buerke et al., "Evidence-based management of cardiogenic shock after acute myocardial infarction," *Interventional Cardiology Review*, vol. 8, no. 2, pp. 73–80, 2013.

[4] C. Huang, "Guidelines for cardiovascular emergency management—acute myocardial infarction complicated with cardiogenic shock," *Chinese Journal of Practical Internal Medicine*, vol. 20, no. 9, pp. 515–517, 2000.

[5] S. Jing, X. Zhang, and J. Lu, "Efficacy of milrinone in the treatment of heart failure after acute myocardial infarction," *Journal of Kunming Medical College*, vol. 31, no. 8, pp. 134–136, 2010.

[6] X. Lian, "Clinical observation of dopamine combined with norepinephrine in the treatment of cardiogenic shock," *Northern Medicine*, vol. 14, no. 4, p. 43, 2017.

[7] C. L. Erley, "Epinephrine versus norepinephrine for cardiogenic shock after acute myocardial infarction," *The Journal of Emergency Medicine*, vol. 55, no. 5, p. 736, 2018.

[8] T. Hashim, K. Sanam, M. Revilla-Martinez et al., "Clinical characteristics and outcomes of intravenous inotropic therapy in advanced heart failure," *Circulation: Heart Failure*, vol. 8, no. 5, pp. 880–886, 2015.

[9] S. Tariq and W. Aronow, "Use of inotropic agents in treatment of systolic heart failure," *International Journal of Molecular Sciences*, vol. 16, no. 12, pp. 29060–29068, 2015.

[10] S. Champion and N. Deye, "Management of cardiogenic shock: results from a survey in France and Belgium," *Annales de cardiologie et d'angeiologie*, vol. 66, no. 2, 2017.

[11] A. Mebazaa, R. Bellomo, R. Pirracchio et al., “Epinephrine and short-term survival in cardiogenic shock: an individual data meta-analysis of 2583 patients,” *Intensive Care Medicine*, vol. 44, no. 6, pp. 847–856, 2018.

[12] Chinese Medical Association Cardiovascular Disease Branch, “Chinese Journal of Cardiovascular Disease Editorial Board. Chinese heart failure diagnosis and treatment guide 2014,” *Chinese Journal of Cardiovascular Disease*, vol. 42, no. 2, pp. 98–122, 2014.

[13] B. Levy, P. Perez, J. Perny, C. Thivilier, and A. Gerard, “Comparison of norepinephrine-dobutamine to epinephrine for hemodynamics, lactate metabolism, and organ function variables in cardiogenic shock. A prospective, randomized pilot study,” *Critical Care Medicine*, vol. 39, no. 3, pp. 450–455, 2011.

[14] Y. Pan, Z. Lu, J. Hang et al., “Effects of low-dose recombinant human brain natriuretic peptide on anterior myocardial infarction complicated by cardiogenic shock,” *Brazilian Journal of Cardiovascular Surgery*, vol. 32, no. 2, pp. 96–103, 2017.

[15] L. Bruno, R. Clere-Jehl, L. Annick et al., “Epinephrine versus norepinephrine for cardiogenic shock after acute myocardial infarction,” *Journal of the American College of Cardiology*, vol. 72, no. 2, 2018.

[16] D. Zhou, L. Wang, Q. Wang et al., “Efficacy of nitroglycerin combined with milrinone in the treatment of acute myocardial infarction-induced cardiogenic shock,” *Clinical Medical Research*, vol. 29, no. 3, pp. 421-422, 2012.

[17] Z. Pang and W. Zhao, “Clinical observation of milrinone in treating cardiogenic shock induced by acute myocardial infarction,” *Journal of Practical Clinical Medicine*, vol. 15, no. 15, pp. 82-83, 2011.

[18] C. Li, *PICCO Monitoring of Levosimendan in Patients with Acute Myocardial Infarction Complicated with Cardiogenic Shock*, The Chinese People’s Liberation Army Medical College, Beijing China, 2016.

[19] X. Chen, “Dynamic blood lactate assay to evaluate the clinical efficacy of norepinephrine and dopamine in the treatment of cardiogenic shock,” *Liu Gang Technology*, no. 1, pp. 53–55, 2018.

[20] R. Xiong, Yu Zhou, J. Sun et al., “Efficacy of dopamine and norepinephrine in patients with cardiogenic shock,” *Chinese Journal of Elderly Multiple Organ Diseases*, vol. 15, no. 12, pp. 919–921, 2016.

[21] E. Tsagalou, J. Kanakakis, M. Anastasiou-Nana et al., “Hemodynamic effects of levosimendan in acute myocardial infarction complicated by cardiogenic shock and high systemic vascular resistance,” *Acute Cardiac Care*, vol. 11, no. 2, pp. 99–106, 2009.

[22] H. Yang, “Efficacy of levosimendan in the treatment of cardiogenic shock,” *Strait Pharmaceutical Journal*, vol. 26, no. 9, pp. 105–107, 2014.

[23] G. Zhang and C. Xiao, “Efficacy of dopamine combined with levocarnitine in the treatment of acute myocardial infarction with cardiogenic shock,” *Journal of Guangdong Medical College*, vol. 28, no. 4, pp. 413-414, 2010.

[24] T. C. Lewis, C. Aberle, D. Altshuler, G. L. Piper, and J. Papadopoulos, “Comparative effectiveness and safety between milrinone or dobutamine as initial inotrope therapy in cardiogenic shock,” *Journal of Cardiovascular Pharmacology and Therapeutics*, vol. 24, no. 2, pp. 130–138, 2019.

[25] X. Pan, Y. Chen, and Q. Fang, “Application of pulse indication continuous cardiac output monitoring of levosimendan in elderly patients with acute myocardial infarction and cardiogenic shock,” *Chinese Journal of Gerontology*, vol. 38, no. 3, pp. 519–521, 2018.

[26] X. Shen, “Clinical observation of levosimendan combined with norepinephrine in the treatment of cardiogenic shock,” *Health Wenhui*, no. 9, pp. 20-21, 2017.

[27] Z. Tan, “Comparison of the application of dopamine and norepinephrine in cardiogenic shock,” *Modern Diagnosis and Treatment*, vol. 27, no. 1, pp. 67-68, 2016.

[28] G. Wang, Y. Guo, J. Hou et al., “Comparison of curative effect of dopamine and norepinephrine on cardiogenic shock,” *China Practical Medical Journal*, vol. 38, no. 2, pp. 75-76, 2011.

[29] Y. He, C. Lu, Y. Jiao et al., “Comparison of clinical efficacy of dopamine and norepinephrine in the treatment of cardiogenic shock,” *Northern Pharmaceutical*, vol. 11, no. 2, p. 5151, 2014.

[30] J. Li, L. Liu, M. Guo et al., “Effects of norepinephrine and dopamine on hemodynamics and tissue perfusion oxygen metabolism in patients with cardiogenic shock,” *Medical Theory and Practice*, vol. 28, no. 23, pp. 3171–3173, 2015.

[31] Y. Zhou and B. Zhou, “Application of norepinephrine in cardiogenic shock,” *Laboratory Medicine and Clinic*, vol. 16, no. 8, pp. 1092–1096, 2019.

[32] R. Li, “Efficacy and prognosis of recombinant human brain natriuretic peptide on acute myocardial infarction and cardiogenic shock,” *Anhui Medical and Pharmaceutical Journal*, vol. 23, no. 4, pp. 696–699, 2019.

[33] T. Lewis, C. Aberle, D. Esaian, and J. Papadopoulos, “Efficacy and safety of milrinone versus dobutamine in cardiogenic shock,” *Critical Care Medicine*, vol. 43, no. 12 Suppl 1, p. 34, 2015.

[34] H. Su, “Clinical effect of norepinephrine combined with dobutamine on cardiogenic shock,” *China Contemporary Medicine*, vol. 26, no. 12, pp. 131–134, 2019.

[35] Q. Guo, W. Song, R. Cui et al., “Clinical study on the treatment of cardiogenic shock after myocardial infarction with levosimendan,” *Modern Drug and Clinical Medicine*, vol. 32, no. 6, pp. 1029–1033, 2017.

[36] L. Peng, L. Rui, Y. Zou et al., “Efficacy evaluation of levosimendan in treating 54 cases of acute myocardial infarction complicated with cardiogenic shock,” *China Pharmaceutical Industry*, vol. 24, no. 17, pp. 46-47, 2015.

[37] J. Huang, X. Hu, and J. Xie, “Clinical curative effect of levosimendan injection in treating cardiogenic shock after myocardial infarction,” *China Healthcare Nutrition*, vol. 28, no. 24, p. 222, 2018.

[38] M. Huang, W. Chen, T. Lin et al., “Evaluation of the effect of levosimendan on cardiogenic shock after myocardial infarction. Knowledge on prevention and treatment of cardiovascular diseases,” *Academic Edition*, no. 11, pp. 38–40, 2018.

[39] C. Xu, Z. Duan, and Z. Liu, “Clinical observation of levosimendan and milrinone on patients with low cardiac function during cardiac surgery,” *Modern Hospital*, vol. 19, no. 2, 2019.

[40] J. Yang and H. Sun, “Clinical analysis of levosimendan injection for cardiogenic shock after myocardial infarction,” *Health Weekly*, no. 16, pp. 18-19, 2018.

[41] C. Huang and H. Xia, “Management principles and experience of acute myocardial infarction with cardiogenic shock,” *Chinese Journal of Practical Internal Medicine*, vol. 27, no. 2, pp. 95–97, 2007.

[42] X. Ma, “Clinical observation of milrinone in the treatment of congestive heart failure,” *Journal of Practical Clinical Medicine*, vol. 15, no. 5, p. 76, 2011.

Hindawi
Journal of Healthcare Engineering
Volume 2020, Article ID 8868685, 7 pages
https://doi.org/10.1155/2020/8868685

Research Article

An Improved Real-Time R-Wave Detection Efficient Algorithm in Exercise ECG Signal Analysis

Zhou Zhang[1,2] **Zeyu Li,**[1,2] **and Zhangyong Li**[1,2]

[1]*Research Centre of Biomedical Engineering, Chongqing University of Posts and Telecommunications, Chongqing 400065, China*
[2]*Chongqing Engineering Research Center of Medical Electronics and Information Technology, Chongqing University of Posts and Telecommunications, Chongqing 400065, China*

Correspondence should be addressed to Zhangyong Li; lizy@cqupt.edu.cn

Received 2 June 2020; Revised 23 June 2020; Accepted 1 July 2020; Published 29 July 2020

Academic Editor: Jiafeng Yao

R-wave detection is a prerequisite for the extraction and recognition of ECG signal feature parameters. In the analysis and diagnosis of exercise electrocardiograms, accurate and real-time detection of QRS complexes is very important for the prevention and monitoring of heart disease. This paper proposes a lightweight R-wave real-time detection method for exercise ECG signals. After real-time denoising of the exercise ECG signal, the median line is used to correct the baseline, and the first-order difference processing is performed on the differential square signal. Max-Min Threshold (MMT) is used to realize real-time R-wave detection of the exercise ECG signal. The abovementioned method was verified by using the measured data in the MIT-BIH ECG database of the Massachusetts Institute of Technology and the exercise plate experiment. The R-wave detection rates were 99.93% and 99.98%, respectively. Experimental results show that this method has high accuracy and low computational complexity and is suitable for wearable devices and motion process monitoring.

1. Introduction

ECG (Electrocardiogram) represents the myocardial electrical activity of the heart. ECG signals play an important role in the diagnosis of cardiovascular diseases, such as arrhythmia, hypertension, or ischemic heart disease. ECG recording used to be a time-consuming process that required an on-site cardiologist to detect and diagnose various types of heart disease. Today, ECG signals can be recorded using mobile ECG sensors, such as Shimmer sensor or Alivecor sensor [1]. These sensors are not only easy to use but also economical and efficient to obtain ECG signals. However, these sensors mainly use only 1 or 2 leads (usually lead I or lead II) for recording, rather than all standard 12-lead, resulting in a poor detection performance of some QRS detection algorithms. Therefore, real-time detection and anomaly analysis of the QRS waveform is a challenging task [2].

QRS detection has become a research topic in the field of intelligent ECG detection for more than 30 years. In the meantime, researchers have developed a number of algorithms, for example, based on the digital filter [3], wavelet transform [4, 5], neural network [6–8], image segmentation [9], and so on. Tang et al. proposed a parallel incremental modulator architecture with local maximum point and local minimum point algorithms to detect QRS and PT waves [10]; Kalidas and Tamil proposed an online QRS detector algorithm using stationary wavelet transform (SWT) for real-time heartbeat detection from a single lead ECG signal [4]; Muhammad et al. proposed the use of transient phasor transformation to study the location of characteristic points (reference points) of ECG signals [11]. However, most of the studies are only applicable to the static ECG signal for a long time, and the processing ability of motion interference is not strong. Moreover, the abovementioned methods require additional process steps, such as training, setting, and predicting model parameters, when detecting R-waves, which increases the complexity of calculation load and computing cost [12].

The R-wave in the QRS waveform plays an important role in the diagnosis of arrhythmia and the recognition of heart rate variability. Due to the rise of wearable devices, the noninvasive exercise tablet experiment (stress test) and the high prediction of coronary heart disease and other diseases, wearable devices, and exercise tablet experiment have gradually become popular in the detection of the cardiovascular function. However, mobile devices are used to detect the ECG activity of patients in their daily life, rather than in the isolated hospital environment. As a result, various electrical signal noises in the environment will seriously interfere with ECG signals. Exercise ECG detection will cause the ECG signals of patients to be interfered by the electrical signals generated by human muscle movements during exercise, which will lead to a sharp increase in detection Windows, thus increasing the possibility of detecting errors and detecting omissions by the traditional R-wave detection algorithm [13].

Aiming at the characteristics of difficulty in real-time detection and abnormal analysis of single lead of motion electrocardiogram, large motion interference, and high computing cost, this paper proposes a lightweight adaptive Max-Min Threshold (MMT) algorithm for R-wave detection of a motion ECG signal, which is an optimization of the differential threshold method for R-wave detection. Compared with the traditional R-wave detection algorithm, the algorithm proposed in this paper has lower operation cost, higher anti-environment interference and anti-motion interference ability, and is suitable for the medium and long-term exercise ECG detection on the mobile ECG sensor. In order to determine the detection efficiency, the algorithm performed the exercise ECG acquisition and real-time R-wave detection on the exercise plate. Meanwhile, the ECG data from the MIT-BIH arrhythmia database were used for R-wave detection.

2. Lightweight R-Wave Detection Method

The detection of R-waves in ECG signals presents many challenges, such as EMG interference [14], power-frequency interference, and baseline drift, which can affect signal primitiveness. These noises are the difficulties in the automatic detection of ECG signals. Due to the large body swing and electrode friction caused by movement, the noise is particularly prominent in the motion ECG signals.

This paper proposes an adaptive MMT difference algorithm to detect R-wave, which includes the following steps: the whole algorithm process of preprocessing baseline correction for R-wave detection is shown in Figure 1.

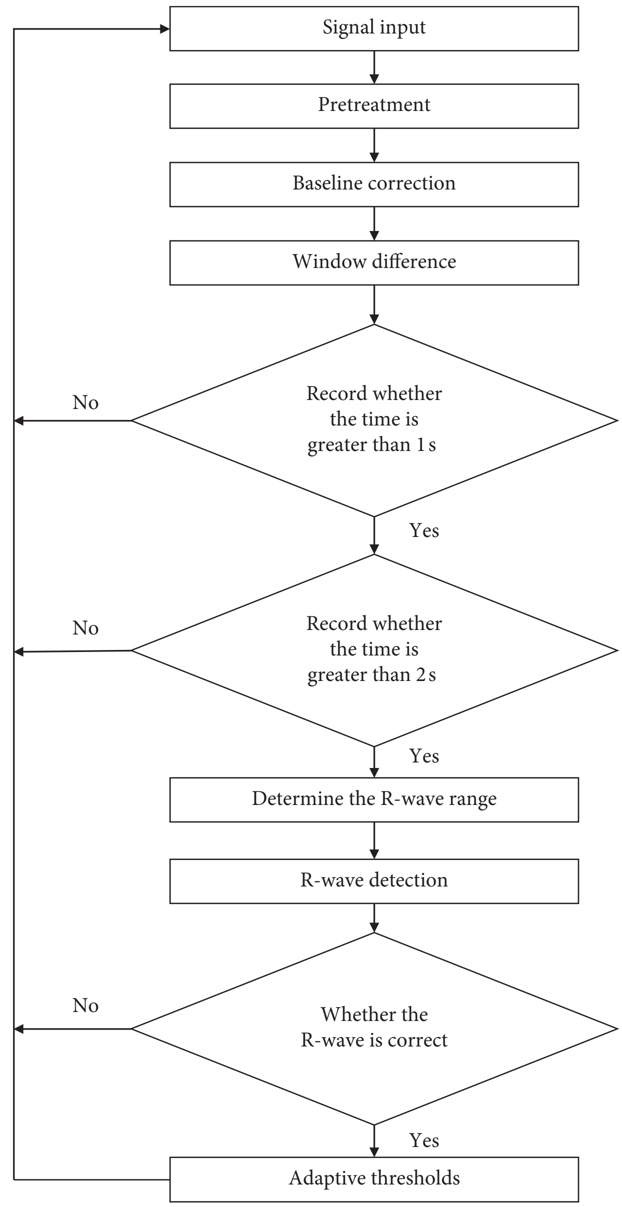

Figure 1: Algorithm flowchart.

Firstly, in order to eliminate the noise embedded in the ECG signal and enhance the ECG signal, digital filters with appropriate parameters and adaptive filters are usually used to eliminate the noise [15]. In this paper, an FIR filter and Notch filter are used to eliminate EMG interference and power-frequency interference in the ECG signal. This process has a large amount of ECG processing capacity and a lot of detail processing, but it does not affect the detection of R-wave. In addition, the calculation cost of the filtering process is lower and the space occupancy is less.

Secondly, a baseline drift can greatly interfere with overall R-wave detection, for which a sliding window is used to overcome the baseline drift. The ECG baseline was extracted from the ECG through the sliding window, and the difference between the original signal and the ECG baseline was calculated to obtain the ECG signal after the baseline was more positive.

Finally, the amplitude of the R-wave varies from person to person, and the amplitude of the R-wave varies greatly from person to person at different times. Therefore, it is very important to find the appropriate threshold. In this paper, through adaptive multithreshold to cope with different scenarios, different populations, and different collection patterns, the R-wave is accurately calculated.

2.1. Pretreatment. Based on the power-frequency interference and myoelectric interference existing in the ECG acquisition process, the R-wave detection is greatly affected, so pretreatment is needed to eliminate the corresponding interference. This section will discuss the power-frequency interference and myoelectric interference in the ECG acquisition process and how to remove the noise.

2.1.1. Power-Frequency Interference. Frequency interference at 50 Hz is usually eliminated before further analysis and processing of the signal [16]. In addition, the basic principle of an adaptive Notch filter is a center frequency of an orthogonal signal as the reference signal, using the linear combination of the orthogonal signal tracking the input signal, and through every step of the residual, continuously adjust the weights of linear combination, so as to make the input signal related to the reference signal linear part of the separation, to achieve the effect of a narrow-band filter.

In this paper, a Notch filter is used to filter the received ECG signal, so as to eliminate the capacitance and electrode lead loop distributed in the human body from 50 Hz power-frequency interference such as power-frequency electricity and magnetic field. According to the Notch filter selected, its filtering effect is shown in Figure 2.

2.1.2. EMG Interference. Because FIR and IIR filters show maximum signal-to-noise ratio improvement when used to eliminate interference, these simple filters are commonly used for ECG signal noise reduction [17].

A finite impulse response (FIR) filter is to perform weighted and average processing on N sampled data, in which the input signal is temporal and changes with the change of time. The final output of the FIR filter is the input at each moment multiplied by the corresponding weight (coefficient), then superimposed, and finally, output. The difference equation can be expressed as follows:

$$y(n) = \sum_{i=0}^{N-1} a_i x(n-i). \tag{1}$$

The low pass filter of an FIR is adopted to eliminate the noise greater than 100 Hz which does not belong to the range of the ECG signal. The filter is of order 40, with a sensitivity factor of 40, a sampling frequency (FS) of 500 Hz, a passband frequency (*F*pass) of 6, a stopband frequency (*F*stop) of 100, a passband waste (*W*pass) of 3 db, and a stopband waste (*W*stop) of 1 db. According to the optimal approximation method of FIR and other ripples selected, its filtering effect is shown in Figure 3.

2.2. Baseline Correction. Baseline drift often occurs in the motion ECG signal, especially when the subject swings too much and the lead line wobbles more, resulting in a very serious baseline drift. Because median filtering can effectively discard outliers while retaining relevant information, median filtering has been widely used as a postprocessing operator in different fields [18] and is widely used in biomedical signal processing [19].

In this paper, the ECG signal end is wrapped by a large sliding window, and the median amplitude of the ECG data in the window is calculated as the baseline drift value of the middle position of the window. The baseline correction can be completed by subtracting the ECG amplitude from the baseline drift value. The algorithm of its window size W and ECG amplitude Y after removing baseline drift is as follows:

$$\begin{aligned} W &= fs * \text{time}\,(+1), \\ Y\left(\text{index} - \frac{W}{2}\right) &= X\left(\text{index} - \frac{W}{2}\right) - X(m), \end{aligned} \tag{2}$$

where fs is the ECG signal sampling rate, time is the time length, index is the index value of the current real-time ECG record, and m meets

$$P\left(\frac{\text{count}\,(x(i) \le x(m))}{W}\right) = \frac{1}{2}, \tag{3}$$

where the value range of I is $(\text{index} - W) \le i \le \text{index}$.

Window size W is an odd-numbered window, and its window should contain at least 0.6 s of sample data, which is helpful to calculate the baseline of the ECG signal.

2.3. R-Wave Detection. The detection process of the R-wave mainly includes window difference, initial threshold calculation, MMT detection of the R-wave, error correction, and adaptive threshold.

2.3.1. Window Difference. Signal differential algorithm is the first step to detect the R-wave. In this paper, a sliding window is used to wrap the differential data of the ECG signal, which can effectively reduce the memory consumption and improve the detection efficiency of real-time ECG. The difference amplitude Y algorithm is as follows:

$$\begin{aligned} \text{Temp} &= X(n+2) - X(n), \\ Y(n) &= \begin{cases} -\text{Temp}^2, & \text{Temp} < 0, \\ \text{Temp}^2, & \text{Temp} > 0, \end{cases} \end{aligned} \tag{4}$$

where X represents the ECG signal processed by using a Notch filter (Section 2.1.1) and FIR filter (Section 2.1.2).

In this paper, a window of size 3 is set up to record the difference amplitude, which is represented by $Y(n-1)$, $Y(n)$, and $Y(n+1)$ in the follow-up, where $Y(n+1)$ represents the largest difference amplitude that can be obtained.

2.3.2. Calculation of Initial Threshold. In this paper, three thresholds are adopted to determine the position of the R-wave: the maximum threshold $T_{\max}$ of first-order difference, the minimum threshold $T_{\min}$ of first-order difference, and the threshold T_R of ECG amplitude. The initial process of the three thresholds is as follows:

$$\begin{aligned} T_R &= X_{\max} * \text{coef}_1, \\ T_{\max} &= Y_{\max} * \text{coef}_2, \\ T_{\min} &= Y_{\min} * \text{coef}_2, \end{aligned} \tag{5}$$

where $X_{\max}$ is the maximum value of ECG after processing and $Y_{\max}$ and $Y_{\min}$ are the maximum and minimum values of differential signals, respectively.

Due to the characteristics of the finite unit impulse response (FIR) filter and adaptive Notch filter (Notch), the

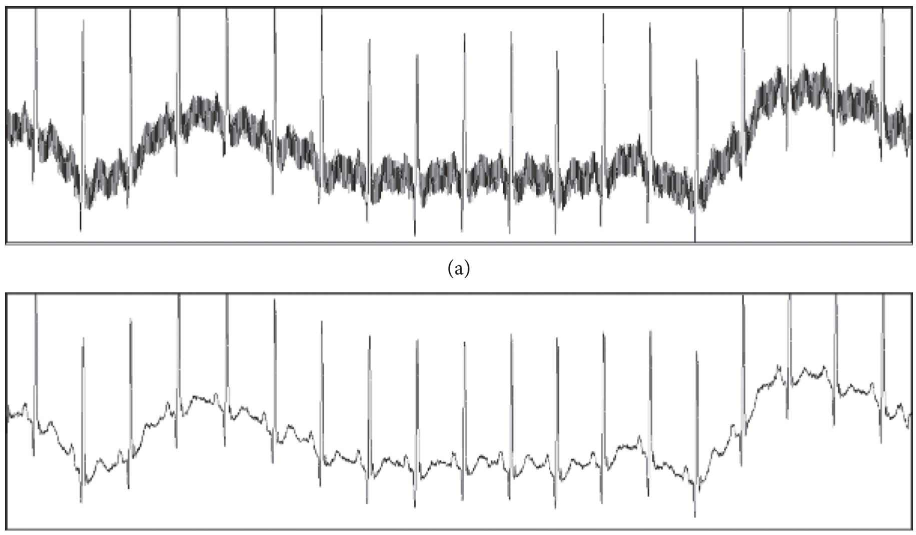

(a)

(b)

Figure 2: Notch filter effect. (a) Before the filtering. (b) After the filtering.

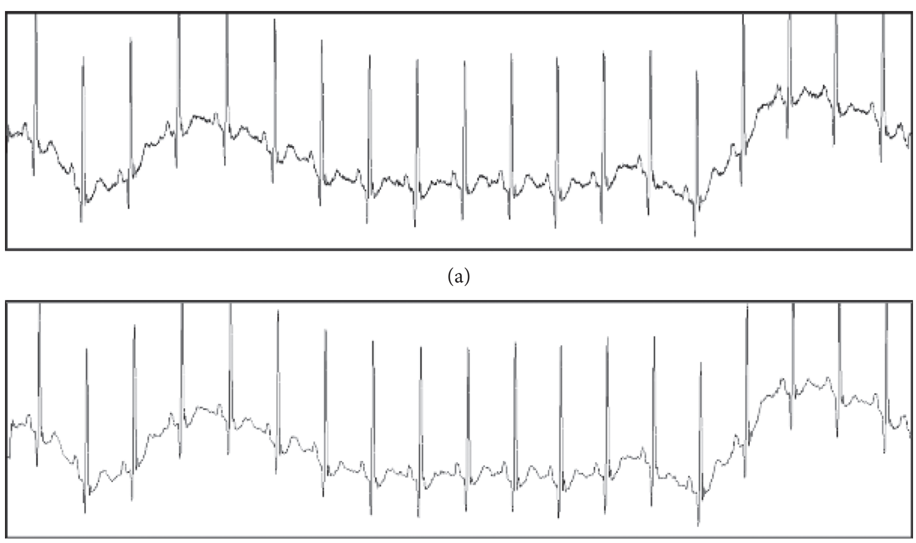

(a)

(b)

Figure 3: FIR filter effect. (a) Before the filtering. (b) After the filtering.

ECG signal 1s before recording should not be considered when calculating the threshold value.

2.3.3. MMT Detects R-Waves. According to the maximum and minimum difference thresholds $T_{\max}$ and $T_{\min}$ obtained in Section 2.3.2, the maximum point in the range of $Y(n) > T_{\max}$ amplitude of differential signals in a continuous period of time was calculated through the continuously input ECG signals, and the index S_1 of this point was recorded. The minimum point in the range of differential signal amplitude $Y(n) < T_{\min}$ in a continuous period of time is calculated, and the index S_2 of this point is recorded. When $S_1 < S_2$ and the (S_1, S_2) range is within 0.2 ms, the maximum value $X(n)_{\max}$ of ECG after processing is calculated in the index range of point S_1 and S_2. When $X(n)_{\max} > T_R$, this point is considered to be point R.

$$\begin{cases} Y(n_1 - 1) < Y(n_1) \\ Y(n_1) > Y(n_1 + 1) \\ Y(n_1) > T_{\max} \end{cases} \longrightarrow S_1 = n_1,$$
$$\begin{cases} Y(n_2 - 1) < Y(n_2) \\ Y(n_2) > Y(n_2 + 1) \\ Y(n_2) < T_{\min} \end{cases} \longrightarrow S_2 = n_2, \tag{6}$$
$$\begin{cases} X(n - 1) < X(n) \\ X(n) > X(n - 1) \\ X(n) > T_R \end{cases} \longrightarrow R_{\text{pos}} = n.$$

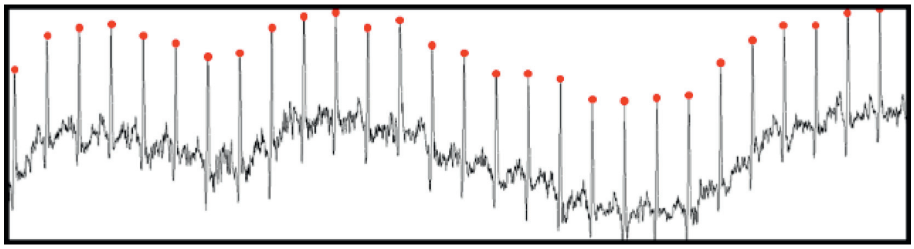

Figure 4: Exercise ECG real-time R-wave detection.

Table 1: Exercise test results.

Number of samples	Total time of exercise (s)	Maximum heart rate (bmp)	The total number of R-waves	Number of leaks or errors	Accuracy (%)
10	3922	168 ± 2	8619	2	99.98

2.3.4. Error Correction. In the detection of R-wave, some interference may lead to multiple detection and missed detection of the R-wave. In this paper, the error correction of the R-wave is carried out by the following methods. The index difference between the R-wave position and the previous R-wave position Dif is recorded, and it is compared with the previous index difference Last_Dif.

If Dif > 1.66∗Last_Dif, there may be a missed judgment between this R-wave and the previous R-wave. At this time, the threshold value of reduction amplitude is 90% of the original threshold value for redetection. If Dif < 0.6 ∗Last_Dif, the gap between the point and the previous R-wave is too small, which is considered as a misjudgment.

2.3.5. Adaptive Threshold. According to the amplitude D_{S_1} and D_{S_2} corresponding to the index S_1 and the index S_2, as well as the amplitude R_R of point R, the three thresholds T_R, $T_{\max}$, and $T_{\min}$ are updated adaptively according to the following formula:

$$\begin{aligned} T_R &= T_R * \text{Rate} + R_R * \text{coef} * (1 - \text{Rate}), \\ T_{\max} &= T_{\max} * \text{Rate} + D_{S_1} * \text{coef} * (1 - \text{Rate}), \\ T_{\min} &= T_{\min} * \text{Rate} + D_{S_2} * \text{coef} * (1 - \text{Rate}). \end{aligned} \tag{7}$$

Due to the difference in the amplitude of the R-wave in time, it is necessary to judge the amplitude of the current measured R-wave once in the abovementioned formula. If the amplitude of the R-wave is in the state of increasing (or decreasing) for two consecutive times, the adaptive updating of the threshold needs to be stopped.

3. Results and Discussion

3.1. Exercise ECG Data. A panel exercise test was performed on 10 test subjects using disposable button electrodes. The heart rate of the subject was increased through exercise, the V1 and V2 leads of the subject are recorded, and the R-wave of the ECG waveform of the subject is detected and displayed in real-time, as shown in Figure 4.

It can be seen from Table 1 that this algorithm has a good performance in 10 subjects of different genders, and it can effectively monitor and recognize the R-waves of a total of 8619 ECG waveforms of 10 subjects. When the maximum heart rate was reached (195-age) [20], the body swing amplitude of the subjects reached the maximum, and the ECG signal received the maximum interference. This algorithm also had a good performance, and the R-wave detection results were accurate. At the same time, the memory utilization is low in the detection process.

3.2. MIT-BIH Public Database. The MIT-BIH arrhythmia database contains 48 1/2 hours of excerpts from two-channel dynamic ECG recordings. The records are digitized with 360 samples per second per channel, with an 11-bit resolution in the 10 mV range [21].The ANSI/AAMI/ISO EC57 : 1998/(*R*) 2008 standard states that the QRS detection algorithm must provide statistical reports from the MIT-BIH arrhythmia database [22].

In order to evaluate the performance of the proposed algorithm, common detector performance measurements are applied and defined as follows [23].

Sensitivity (Se) represents the percentage of events detected:

$$\text{Se} = \frac{\text{TP}}{\text{TP} + \text{FN}} \times 100\%. \tag{8}$$

Positive prediction (+*P*) represents the score of the test, that is, the event:

$$+P = \frac{\text{TP}}{\text{TP} + \text{FP}} \times 100\%, \tag{9}$$

where TP is the number of true positive beats (correct detection), FN is the number of false negative beats (false detection), and FP is the number of false positive beats (missed detection) [10].

As can be seen from Table 2, this algorithm successfully detected 47,398 R-waveforms in 47,498 QRS-waveforms, indicating that this algorithm can correctly detect the vast majority of R-waveforms. In addition, Table 3 shows a

Table 2: MIT-BIH detection R-wave results.

Number of samples	The total number of R-waves	TP	FN	FP	Se (%)	+P (%)
21	47498	47398	143	31	99.70	99.93

Table 3: Comparison with other methods' test results.

Method	Se (%)	$+P$ (%)
Pandit et al. [2]	99.62	99.67
Lai et al. [24]	99.69	99.63
Method in this paper	99.70	99.93

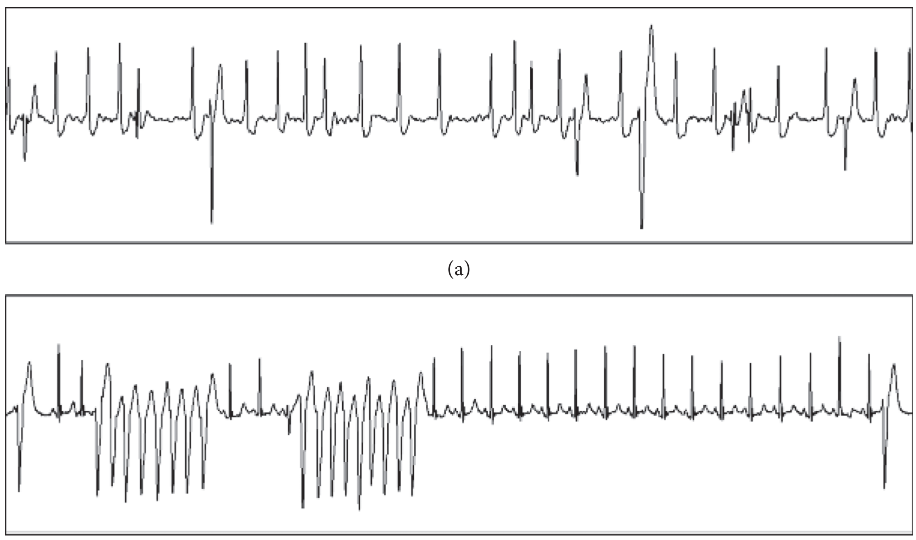

(a)

(b)

Figure 5: Two groups of ECG diagrams (203 and 205). (a) MIT-BIH ECG data no. 203. (b) MIT-BIH ECG data no. 205.

quantitative comparison of the algorithms presented in this paper with those proposed by Pandit and Lai. The values of Se and $+P$ in this paper reach 99.70% and 99.93%, while Pandit's and Lai's algorithms are 99.62% and 99.67% and 99.69% and 99.63%, respectively. The algorithms of Pandit and Lai are both R-wave recognition algorithms based on differential thresholds. In the R-wave detection results, the method of this paper has improved by 0.05% and 0.3% on average.

4. Conclusions

This paper presents a lightweight adaptive MMT ECG signal R-wave detection algorithm. After denoising the ECG signal and correcting the baseline, the algorithm performs first-order difference processing, detects the R-wave through the maximum and minimum difference threshold, and updates the threshold according to the index information of the R-wave. The algorithm of R-wave detection in an athletic flat test is in good condition, and in the MIT/BIH database of 21 ECG data detection, through comparing with Pandit algorithm and Lai algorithm, the presented method of R-wave identification not only is of high sensitivity (Se) and high positive predictive $(+P)$ but also has advantages in terms of computing requirements.

In addition, it can be seen from Figure 5 that this algorithm shows a strong anti-interference capability in the detection of moving plate experiment and can effectively reduce the ECG noise and baseline drift brought by movement, so that it can effectively detect and monitor the ECG in different motion states. At the same time, the operation speed and resource share of the algorithm can guarantee the real-time and durability of ECG monitoring.

It is important to note that the algorithm of R-wave detection is faulty in some occasions, such as MIT-BIH database in 203 and 205 of two groups of ECG data waveform, the waveform memory is intermittent R-wave inversion, the phenomenon of greater influence on the sensitivity of the proposed algorithm, leads to recognition of the R-wave in 203 and 205 groups of data, and the sensitivity of 99.00% and 98.04%, as shown in Figure 5.

In summary, R-wave detection was evaluated on the existing standard MIT-BIH database. The algorithm has a relatively high performance, with 99.70% sensitivity and 99.93% positive predictability, showing obvious advantages. In addition, its low computational requirements and good anti-interference capability make it easy to deploy and implement in portable monitoring and motion monitoring applications. We will further study the limitations of the current algorithm in order to develop a more complete and practical algorithm.

Data Availability

The ECG data used to support the findings of this study have been deposited in the MIT-BIT repository.

Conflicts of Interest

The authors declare that there are no conflicts of interest regarding the publication of this paper.

Acknowledgments

This research was funded by the National Natural Science Foundation of China under grants no. 61571070. This research was also funded by the Scientific Research and Innovation Project of Chongqing, China (project no. CYS19256).

References

[1] S. Gradl, P. Kugler, C. Lohmüller, and B. Eskofier, "Real-time ECG monitoring and arrhythmia detection using android-based mobile devices," in *Proceedings of the 2012 Annual International Conference of the IEEE Engineering in Medicine and Biology Society*, pp. 2452–2455, San Diego, CA, USA, August 2012.

[2] D. Pandit, L. Zhang, C. Liu, S. Chattopadhyay, N. Aslam, and C. P. Lim, "A lightweight QRS detector for single lead ECG signals using a max-min difference algorithm," *Computer Methods and Programs in Biomedicine*, vol. 144, pp. 61–75, 2017.

[3] M. Marouf and L. Saranovac, "Adaptive EMG noise reduction in ECG signals using noise level approximation," in *Proceedings of the 2017 International Conference on Robotics and Machine Vision*, Kitakyushu, Japan, December 2017.

[4] V. Kalidas and L. Tamil, "Real-time QRS detector using stationary wavelet transform for automated ECG analysis," in *Proceedings of the 2017 IEEE 17th International Conference on Bioinformatics and Bioengineering*, pp. 457–461, Washington, DC, USA, October 2017.

[5] S. Sabut, S. Sahoo, B. Kanungo et al., "Multiresolution wavelet transform based feature extraction and ECG classification to detect cardiac abnormalities," *Measurement*, vol. 108, pp. 55–66, 2017.

[6] M. Šarlija, F. Jurišić, and S. Popović, "A convolutional neural network based approach to QRS detection," in *Proceedings of the 10th International Symposium on Image and Signal Processing and Analysis*, pp. 121–125, Ljubljana, Slovenia, September 2017.

[7] P. Silva, E. Wanner, D. Menotti et al., "QRS detection in ECG signal with convolutional network," *Iberoamerican Congress on Pattern Recognition*, Springer, Madrid, Spain, pp. 802–809, 2018.

[8] Y. Xiang, L. Zhitao, and M. Jianyi, "Automatic QRS complex detection using two-level convolutional neural network," *Biomedical Engineering Online*, vol. 17, no. 1, pp. 1–17, 2018.

[9] M. Saadatmand-Tarzjan, N. Rashidi, and M. Iqbal, "A novel parametric deformable model based on calculus of variations for QRS detection," *Iranian Journal of Science and Technology, Transactions A: Science*, vol. 43, no. 3, pp. 1101–1107, 2019.

[10] X. Tang, Q. Hu, and W. Tang, "A real-time QRS detection system with PR/RT interval and ST segment measurements for wearable ECG sensors using parallel delta modulators," *IEEE Transactions on Biomedical Circuits and Systems*, vol. 12, no. 4, pp. 751–761, 2018.

[11] M. Kashif, S. Jonas, and T. Deserno, "Deterioration of R-wave detection in pathology and noise: a comprehensive analysis using simultaneous truth and performance level estimation," *IEEE Transactions on Biomedical Engineering*, vol. 64, no. 9, pp. 2163–2175, 2017.

[12] A. K. Dohare, V. Kumar, and R. Kumar, "An efficient new method for the detection of QRS in electrocardiogram," *Computers & Electrical Engineering*, vol. 40, no. 5, pp. 1717–1730, 2014.

[13] J. Moeyersons, E. Smets, J. Morales et al., "Artefact detection and quality assessment of ambulatory ECG signals," *Computer Methods and Programs in Biomedicine*, vol. 182, Article ID 105050, 2019.

[14] G. M. Friesen, T. C. Jannett, M. A. Jadallah, S. L. Yates, S. R. Quint, and H. T. Nagle, "A comparison of the noise sensitivity of nine QRS detection algorithms," *IEEE Transactions on Biomedical Engineering*, vol. 37, no. 1, pp. 85–98, 1990.

[15] S. Sahoo, P. Biswal, T. Das, and S. Sabut, "De-noising of ECG signal and QRS detection using hilbert transform and adaptive thresholding," *Procedia Technology*, vol. 25, pp. 68–75, 2016.

[16] Z. Peng and G. Wang, "Study on optimal selection of wavelet vanishing moments for ECG denoising," *Scientific Reports*, vol. 7, no. 1, pp. 45–64, 2017.

[17] N. Das and M. Chakraborty, "Performance analysis of FIR and IIR filters for ECG signal denoising based on SNR," in *Proceedings of the 2017 International Conference on Research in Computational Intelligence & Communication Networks*, pp. 90–97, Kolkata, India, November 2017.

[18] C. Pasquini, G. Boato, N. Alajlan et al., "A deterministic approach to detect median filtering in 1D data," *IEEE Transactions on Information Forensics and Security*, vol. 11, no. 7, pp. 1425–1437, 2017.

[19] T. Pander, "The class of M-filters in the application of ECG signal processing," *Biocybernetics & Biomedical Engineering*, vol. 26, no. 4, pp. 3–13, 2006.

[20] H. Tanaka, K. D. Monahan, and D. R. Seals, "Age-predicted maximal heart rate revisited," *Journal of the American College of Cardiology*, vol. 37, no. 1, pp. 153–156, 2001.

[21] G. B. Moody and R. G. Mark, "The impact of the MIT-BIH arrhythmia database," *IEEE Engineering in Medicine and Biology Magazine*, vol. 20, no. 3, pp. 45–50, 2001.

[22] American national standard ANSI/AAMI EC 57:2012, testing and reporting performance results of cardiac rhythm and ST-egment measurement algorithms, 2017, https://webstore.ansi.org/RecordDetail.aspx?sku=CARDIO+MEDICAL+DEVICE+PACKAGE.

[23] C. Chieh-Li and C. Chun-Te, "A QRS detection and R point recognition method for wearable single-lead ECG devices," *Sensors*, vol. 17, no. 9, p. 1969, 2017.

[24] D. Lai, F. Zhang, and C. Wang, "A real-time QRS complex detection algorithm based on differential threshold method," in *Proceedings of the 2015 IEEE International Conference on Digital Signal Processing (DSP)*, pp. 129–133, Singapore, July 2015.

Hindawi
Journal of Healthcare Engineering
Volume 2020, Article ID 8876812, 8 pages
https://doi.org/10.1155/2020/8876812

Research Article

Smoking Is a Risk Factor of Coronary Heart Disease through HDL-C in Chinese T2DM Patients: A Mediation Analysis

Ru Tang,[1] Shanshan Yang,[2,3] Weiguo Liu,[4] Bo Yang,[5] Shuang Wang,[5] Zhengguo Yang,[5] and Yao He[3,5]

[1]*The 2nd Medical Center, Chinese PLA General Hospital, Beijing 100853, China*
[2]*Department of Disease Control and Prevention, The 1st Medical Center, Chinese PLA General Hospital, Beijing 100853, China*
[3]*Institute of Geriatrics, Beijing Key Laboratory of Aging and Geriatrics, National Clinical Research Center for Geriatrics Disease, State Key Laboratory of Kidney Disease, The 2nd Medical Center, Chinese PLA General Hospital, Beijing 100853, China*
[4]*Emergency Department, Armed Police Corps Hospital in Henan Province, Zhengzhou 450000, China*
[5]*Department of Nephrology and Endocrinology, PLA 960th Hospital, Zibo 255300, China*

Correspondence should be addressed to Bo Yang; 1684624143@qq.com and Yao He; yhe301@x263.net

Received 30 April 2020; Revised 10 June 2020; Accepted 9 July 2020; Published 28 July 2020

Academic Editor: Xiwei Huang

Objective. To investigate associations between smoking and cardiovascular and cerebrovascular complications in type 2 diabetes mellitus (T2DM) patients. *Methods*. This is a cross-sectional study. Of 971 T2DM patients aged 14–93 years old in this study, 182 had ever smoked and 789 never smoked. Propensity score matching (PSM) reduced the confounding bias between groups. Logistic regression analysis was performed on matched data to evaluate coronary heart disease (CHD) and stroke risk. In addition, the mediation analysis was conducted among smoking exposure, HDL-C, and CHD. *Results*. A total of 139 pairs of patients who had never and ever smoked were matched. Logistic regression analysis showed that compared with patients who never smoked, those who smoked > 20 cigarettes per day (CPD) had a higher risk of CHD (odds ratio [OR]: 3.09, 95% confidence interval [CI]: 1.21–7.89). Additionally, after adjusting for age, sex, origin, occupation, smoking status, body mass index, waist circumference, and diabetes duration, the OR for CHD with >20 years of cumulative smoking (pack-years) was 2.21 (95% CI: 1.05–4.65). Furthermore, we observed a significant dose-response relationship between CPD and lower high-density lipoprotein cholesterol (HDL-C) ($P < 0.001$). Moreover, the mediation analysis showed that the indirect effect mediated by HDL-C accounted for 86% (effect = 0.0187, 95% CI: 0.0100–0.0316). *Conclusions*. Smoking may be a risk factor for CHD in T2DM patients. T2DM patients should stop smoking or reduce the CPD to prevent the onset of CHD. Moreover, to prevent CHD complications, monitoring HDL-C levels in T2DM patients who smoke may be necessary.

1. Introduction

More than 5% of adults worldwide have type 2 diabetes mellitus (T2DM), and the prevalence will increase to 6.3% by 2025 [1]. In China, an estimated 23.46 million people currently have diabetes, and that number is predicted to increase to 42.30 million by 2030 [2, 3]. Coronary heart disease (CHD) and stroke are the most common chronic complications of T2DM and the main cause of T2DM-related mortality [4]. Patients with T2DM have a 1.54–4.00 times higher risk of CHD [5, 6] and 1.35–1.74-times higher risk of stroke [7]. In China, the annual per patient cost of healthcare associated with T2DM patients with cardiovascular and cerebrovascular complications is estimated to be 1798 USD, compared with 484 USD for those without these complications [2]. Moreover, previous studies also showed that the morbidity of cerebrovascular disease is 2–5 times higher in patients with T2DM than in patients without T2DM [8]. Thus, identifying risk factors, especially preventable risk factors, for cardiovascular and cerebrovascular complications in T2DM is important.

Cigarette smoking is an important modifiable risk factor for cardiovascular and cerebrovascular disease in a general population [9, 10]. However, this relationship is less well-defined among individuals with diabetes [11], especially in Chinese diabetic inpatients. In previous studies, smoking exposure was usually categorized as never, current, and past only, but objective data of smoking exposure such as cigarettes per day (CPD), time of smoking, and cumulative smoking (pack-years) was not provided in these studies [12, 13]. Furthermore, the combined effect of smoking and the influence of blood pressure, glucose, and serum lipids on cardiovascular and cerebrovascular disease is also unclear. The mechanism by which smoking affects cardiovascular and cerebrovascular diseases is not clear, either. In addition, in previous studies, demographic characteristics of groups who ever and never smoked differed significantly. Thus, we designed a study to assess the association between smoking and CHD/stroke in Chinese T2DM patients using CPD, time of smoking, and cumulative smoking (pack-years) to measure smoking exposure, in addition to propensity score matching (PSM) to control for differences in characteristics between those who never and ever smoked. Further, mediation analysis was used to explore the mechanism of smoking exposure on CHD in Chinese T2DM patients.

2. Design and Methods

2.1. Study Sample. We used clinical data from the Department of Nephrology and Endocrinology, PLA 148th Hospital (renamed as PLA 960th Hospital now). Among 1,025 inpatients (between January 2010 and December 2012), we excluded 25 type 1 DM inpatients, 11 latent autoimmune diabetes in adults inpatients, and 18 inpatients with fragmentary data and recruited 971 (498 men and 473 women) as our participants (Figure 1).

We collected data regarding each participant's sex, age, occupation, region, alcohol and smoking consumption, diabetes duration, and CHD and stroke status.

2.2. Measurements. T2DM was defined according to the American Diabetes Association criteria [14]. CHD and stroke were defined using the WHO MONICA criteria [15] by physicians of the PLA 148th Hospital.

A smoker was defined as a person who had smoked daily for at least 6 months during their lives [16]. CPD, time of smoking, and cumulative smoking (pack-years) were used to measure cigarette consumption. An alcohol user was defined as a regular drinker who consumed alcohol approximately daily and had been regularly consuming alcohol for more than 6 months [3].

The information was collected by a primary nurse. Height was measured in meters (without shoes). Weight was measured in kilograms, without heavy clothing and 1 kg deducted for remaining garments. Body mass index (BMI, kg/m^2) was calculated as weight in kilograms divided by the square of height in meters. To ensure the accuracy of the information, patient answers to the questions on tobacco use were confirmed by the patients and their relatives. Central obesity was defined by a waist circumference (WC) > 90 cm in men and > 80 cm in women [17]. Venous blood was taken after fasting of eight hours. Fasting blood-glucose (FBG), hemoglobin A1c (HbA1c), cholesterol (CHO), and high-density lipoprotein cholesterol (HDL-C) were tested in the central laboratory of PLA 148th Hospital. Covariables adjusted in the study included age, sex (male and female), occupation (white collar, light physical labor and hard physical labor), region (Shandong province and other provinces), drink (yes and no), BMI, WC, and diabetes duration.

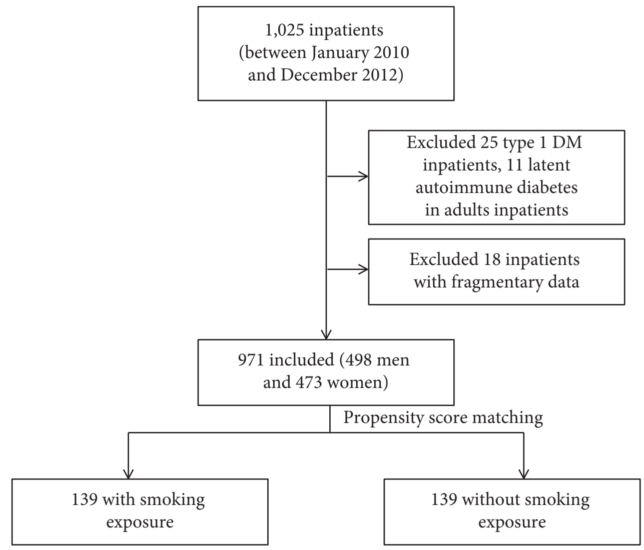

Figure 1: The flowchart of participants.

2.3. Statistical Analysis. SPSS version 19.0 was used for data analysis. The significance level for all tests was set at a two-tailed α value of 0.05. The differences in means and proportions were evaluated using Student's t-test and the chi-square test, respectively. Logistic regression models were used to identify the risk of tobacco use and linear regression models were used to identify the effect of tobacco use on FBG, HbA1c, CHO, HDL-C, and systolic pressure.

PSM [18] was used to match groups of those who did and did not consume tobacco. Sex, age, origin, occupation, drinking status, BMI, WC, and T2DM duration were included as covariates. We used nearest-neighbor matching to pair never smokers with current and former smokers at a 1 : 1 ratio with a caliper width of 0.02 [19].

Mediation analysis is a method which is used to assess the relative magnitude of different pathways and mechanisms by which an exposure may affect an outcome [20]. Mediation analysis was used to analyze the indirect effect on CPD and CHD mediated by HDL-C. Extended program of SPSS was used to do the mediation analysis (model 4 [21] was used to simulate the mediation effect, and the conceptual diagram is shown in Figure S1).

2.4. Ethical Considerations. The committee for medical ethics of the Chinese PLA General Hospital examined and approved our study. Before completing the questionnaire, each involved participant signed an informed consent form.

3. Results

A total of 971 (498 men and 473 women) inpatients were involved in our study before PSM. The average age was 56.8 ± 11.6 years (range: 14–93 years). The average ages of those who did and did not use tobacco were 53.5 ± 11.9 years and 57.6 ± 11.4 years, respectively. The general characteristics (age, sex, origin, occupation, drinking status, BMI, and central obesity) of the participants are shown in Table 1. Compared with the group of ever smokers, the group who never smoked consisted of more women, more hard physical laborers, fewer drinkers, and patients who were older and had less central obesity and longer T2DM durations (6.3 ± 6.1 years vs. 7.4 ± 6.6 years; $P = 0.05$).

After PSM, a total of 139 participant pairs were matched, and the two groups were balanced for age, sex, occupation, drinking status, BMI, central obesity, and T2DM duration (ever and never smokers: 6.8 ± 6.3 years vs. 6.6 ± 6.3 years, respectively; $P = 0.849$) (Table 1).

In logistic regression, we found that compared with never smokers, ever smokers with CPD > 20/day had a higher risk of CHD (OR: 3.09, 95% CI: 1.21–7.89) after adjusting for age, sex, origin, occupation, drinking, BMI, WC, and diabetes duration. We also observed a dose-response relationship between CPD and CHD risk (after adjustment, $P = 0.021$). Similar results were observed in cumulative smoking (pack-years) (Table 2). In addition, compared with never smokers, ever smokers with smoking years >20 years had a higher risk of CHD in a crude model (OR: 2.06, 95% CI: 1.08–3.95), and a dose-response relationship between years of tobacco use and risk of CHD was also observed in a crude model ($P = 0.027$); however, after adjustment, the effect was no longer significant (Table 2). We also examined the effect of ever smoking on stroke risk, and no significant effect was observed (Table 3).

Further, we examined the effect of CPD, smoking years, and cumulative smoking (pack-years) on FBG, HbA1c, CHO, HDL-C, and systolic pressure, and the results are shown in Table 4. CPD was negatively correlated with HDL-C in T2DM inpatients after adjustment ($\beta = -0.006$, standard $\beta = -0.312$, $P < 0.001$).

Further, the mediation analysis showed that the indirect effect on CPD and CHD mediated by HDL-C accounted for 86% (effect = 0.0187, 95% CI: 0.0100–0.0316), and the direct effect of CPD on CHD was 0.0030 (95% CI: −0.0183–0.0242).

4. Discussion

In this study, we observed a significant association between smoking exposure and CHD in T2DM patients; however, the association between smoking exposure and stroke was not significant in this population. We used PSM to comprehensively control and adjust for a wide range of potential confounders and to improve the comparability between the two groups (never and ever smokers). Further, we observed a dose-response relationship between CPD and cumulative smoking (pack-years) and the risk of CHD; this relationship was also observed between CPD and lower HDL-C in these T2DM patients.

A study of a Middle Eastern cohort [13] showed that, in men with diabetes, the HR (95% CI) of comparing current smokers and nonsmokers was 1.25 (0.74–2.12) for incident CHD, while, among nondiabetic men, current smokers showed significant risk for CHD (HR = 1.49, 1.18–1.89); however, the study did not assess the association between CPD and the risk of CHD. Another study in the US population (the National Health Interview Survey) [12] also showed that the OR of current smoking for CHD in T2DM patients was 1.61 (95% CI: 0.98–2.65) after adjustment; however, the study only used current, former, and never smoking as the measurement of exposure and did not provide information of CPD, smoking time, or cumulative smoking (pack-years). While the Nurses' Health Study in the US female population [11] showed that, in T2DM patients, compared with never smokers, the risk ratios for CHD were 1.66 (95% CI, 1.10–2.52) for current smokers of 1 to 14 CPD and 2.68 (95% CI, 2.07–3.48) for current smokers of 15 or more CPD after adjustment, our results were similar.

A study of 1,836 Chinese [22] found that participants with both diabetes and a smoking habit had an 8.94-times (95% CI: 3.77–21.19) higher risk of stroke compared with those without diabetes and a smoking habit; however, this study did not provide a comparison between T2DM patients with and without smoking exposure. Another study in a Swedish population involving 13,087 patients with T2DM [23] found that the adjusted HR of smoking for stroke was 1.3 (95% CI: 1.1–1.6); however, the study did not show the relationship between CPD and stroke in T2DM patients. We did not observe a significant association between smoking exposure and stroke in our study, possibly due to the limited sample size.

We also observed a dose-response relationship between CPD and lower HDL-C. In addition, the mediation analysis showed that the indirect effect mediated by HDL-C accounted for 86% on the association between smoking exposure and CHD in the T2DM inpatients. Previous studies showed that HDL-C can exhibit anti-inflammatory properties [24]. Moreover, HDL-C from T2DM patients with CHD stimulated the release of tumor necrosis factor-α (TNF-α) in monocytes to a greater extent than that of HDL-C from those without CHD, and HDL-C was a significant predictor of the presence of CHD in patients with T2DM [25]. This may indicate that smoking exposure increases the risk of CHD by reducing the level of HDL-C in T2DM patients.

This study had several limitations. As the information on smoking exposure was based on recall, bias could not be fully ruled out; however, the information was confirmed with patients and their relatives to ensure accuracy. Second, our

Table 1: Demographic characteristics according to tobacco use before and after propensity score matching (PSM).

Group	Number (%)	Ever smoking (before PSM)			Ever smoking (after PSM)		
	Total $N = 971$	Yes ($n = 182$)	None ($n = 789$)	P	Yes ($n = 139$)	None ($n = 139$)	P
Age (years)				0.001			0.728
≤60	81 (8.3)	24 (13.2)	57 (7.2)		15 (10.8)	19 (13.7)	
60–69	529 (54.5)	109 (59.9)	420 (53.2)		85 (61.2)	80 (57.6)	
≥70	361 (37.2)	49 (26.9)	312 (39.5)		39 (28.1)	40 (28.8)	
Sex				<0.001			1.000
Male	498 (51.3)	177 (97.3)	321 (40.7)		136 (97.8)	136 (97.8)	
Female	473 (48.7)	5 (2.7)	468 (59.3)		3 (2.2)	3 (2.2)	
Occupation				0.014			0.464
White collar	103 (10.6)	27 (14.8)	76 (9.6)		21 (15.1)	15 (10.8)	
Light physical labor	117 (12.0)	29 (15.9)	88 (11.2)		21 (15.1)	26 (18.7)	
Hard physical labor	751 (77.3)	126 (69.2)	625 (79.2)		97 (69.8)	98 (70.5)	
Region				0.397			0.562
Shandong province	940 (96.8)	178 (97.8)	862 (96.6)		138 (99.3)	137 (98.6)	
Other provinces	31 (3.2)	4 (2.2)	27 (3.4)		1 (0.7)	2 (1.4)	
Drink				<0.001			1.000
Yes	182 (18.7)	90 (49.5)	48 (6.1)		47 (33.8)	47 (33.8)	
No	789 (81.3)	92 (50.5)	741 (93.9)		92 (66.2)	92 (66.2)	
BMI				0.002			0.167
<24.00	368 (37.9)	39 (21.4)	317 (40.2)		43 (30.9)	46 (33.1)	
24.00–27.99	388 (40.0)	92 (50.5)	296 (37.5)		70 (50.4)	56 (40.3)	
≥28.00	215 (22.1)	51 (28.0)	176 (22.3)		26 (18.7)	37 (26.6)	
Central obesity				<0.001			0.472
Yes	625 (64.4)	90 (49.5)	535 (67.8)		71 (51.1)	65 (46.8)	
No	346 (35.6)	92 (50.5)	254 (32.2)		68 (48.9)	74 (53.2)	
Mean ± SD							
Age	56.8 ± 11.6	53.5 ± 11.9	57.6 ± 11.4	<0.001	54.2 ± 11.7	53.4 ± 13.1	0.583
Duration of diabetes	7.3 ± 6.5	6.3 ± 6.1	7.4 ± 6.6	0.05	6.8 ± 6.3	6.6 ± 6.3	0.849
BMI	25.3 ± 4.1	25.6 ± 3.6	25.3 ± 4.2	0.333	25.4 ± 3.6	25.6 ± 4.0	0.552
WC	88.6 ± 8.8	90.7 ± 8.3	88.2 ± 8.9	0.001	90.7 ± 7.9	90.6 ± 8.6	0.904

Table 2: Odds ratio (95% confidence interval, CI) of CHD for smoking in participants.

		N (%)	Model A OR (95% CI)	Model B OR (95% CI)	Model C OR (95% CI)
Smoking	None (reference)	29 (20.9)	1	1	1
	Yes	35 (25.2)	1.28 (0.73–2.24)	1.29 (0.69–2.40)	1.36 (0.72–2.58)
	P		0.393	0.429	0.347
CPD	None (reference)	29 (20.9)	1	1	1
	≤20 (day)	23 (21.7)	1.05 (0.57–1.95)	0.95 (0.48–1.90)	1.00 (0.49–2.04)
	>20 (day)	12 (36.4)	2.17 (0.96–4.92)	**3.00 (1.19–7.55)**	**3.09 (1.21–7.89)**
	P for trend		0.127	0.076	0.05
Time of smoking	None (reference)	29 (20.9)	1	1	1
	≤20 years	11 (15.7)	0.70 (0.33–1.50)	0.95 (0.41–2.21)	0.97 (0.41–2.29)
	>20 years	23 (35.4)	**2.06 (1.08–3.95)**	1.51 (0.74–3.08)	1.59 (0.77–3.30)
	P for trend		0.058	0.294	0.243
Cumulative smoking	None (reference)	29 (20.9)	1	1	1
	≤20 pack-years	11 (14.7)	0.65 (0.31–1.39)	0.70 (0.30–1.61)	0.74 (0.31–1.73)
	>20 pack-years	24 (37.5)	**2.28 (1.19–4.36)**	**2.08 (1.01–4.28)**	**2.21 (1.05–4.65)**
	P for trend		0.032	0.060	0.026

Table 2: Continued.

		N (%)	Model A OR (95% CI)	Model B OR (95% CI)	Model C OR (95% CI)
Variables are included as continuous variables	None (reference)		1	1	1
	CPD		**1.02 (1.00–1.04)**	**1.03 (1.00–1.05)**	**1.03 (1.00–1.05)**
	P		0.055	0.024	0.021
	None (reference)		1	1	1
	Smoking time (years)		**1.02 (1.00–1.04)**	1.00 (0.99–1.03)	1.01 (0.99–1.03)
	P		0.027	0.36	0.251
	None (reference)		1	1	1
	Cumulative smoking (pack-years)		**1.02 (1.01–1.03)**	**1.02 (1.00–1.03)**	**1.02 (1.00–1.03)**
	P		0.008	0.037	0.032

Model A: crude model; Model B: adjusted for age, sex, origin, and occupation; Model C: adjusted for age, sex, origin, occupation, drinking, BMI, WC, and diabetes duration; and CPD: cigarettes per day.

Table 3: Odds ratio (95% confidence interval, CI) of stroke for smoking in participants.

		N (%)	Model A OR (95% CI)	Model B OR (95% CI)	Model C OR (95% CI)
Smoking	None (reference)	18 (12.9)	1	1	1
	Yes	21 (15.1)	1.20 (0.61–2.36)	1.15 (0.55–2.53)	1.25 (0.57–2.74)
	P		0.605	0.673	0.573
CPD	None (reference)	18 (12.9)	1	1	1
	≤20 (day)	14 (13.2)	1.02 (0.48–2.16)	0.90 (0.38–2.09)	0.94 (0.40–2.25)
	>20 (day)	7 (21.2)	1.81 (0.69–4.78)	2.68 (0.87–8.28)	2.76 (0.89–8.53)
	P for trend		0.333	0.228	0.186
Time of smoking	None (reference)	18 (12.9)	1	1	1
	≤20 years	10 (14.3)	1.16 (0.50–2.66)	1.88 (0.71–4.98)	1.91 (0.70–5.21)
	>20 years	11 (16.9)	1.42 (0.63–3.20)	0.92 (0.37–2.30)	1.01 (0.39–2.56)
	P for trend		0.406	0.999	0.856
Cumulative smoking	None (reference)	18 (12.9)	1	1	1
	≤20 pack-years	7 (9.3)	0.69 (0.28–1.74)	0.75 (0.27–2.07)	0.77 (0.27–2.21)
	>20 pack-years	14 (21.9)	1.88 (0.87–4.07)	1.66 (0.69–3.98)	1.79 (0.73–4.39)
	P for trend		0.167	0.314	0.255
Variables are included as continuous variables	None (reference)		1	1	1
	CPD		1.02 (0.99–1.04)	1.02 (1.00–1.05)	1.02 (1.00–1.05)
	P		0.18	0.09	0.051
	None (reference)		1	1	1
	Smoking time (years)		1.01 (0.99–1.03)	1.00 (0.97–1.02)	1.00 (0.97–1.02)
	P		0.421	0.678	0.885
	None (reference)		1	1	1
	Cumulative smoking (pack-years)		1.01 (1.00–1.03)	1.01 (0.99–1.03)	1.01 (0.99–1.03)
	P		0.083	0.385	0.336

Model A: crude model; Model B: adjusted for age, gender, origin, and occupation; Model C: adjusted for age, gender, origin, occupation, drinking, BMI, WC, and diabetes duration; and CPD: cigarettes per day.

sample may not be completely representative of T2DM patients in China because our hospital is one of the best hospitals in Zibo, and the inpatients here have higher proportions of diabetic complications; however, the representativeness of our sample should not substantially affect the internal validity of this study. Finally, we could not examine the hazard ratio (HR) of smoking exposure with respect to CHD because of the lack of detailed information regarding the onset time of CHD.

In summary, our study found a dose-response relationship between smoking exposure and CHD among T2DM inpatients. We used the PSM method to increase the comparability of the never and ever smokers groups. We also observed a dose-response relationship between CPD and

Table 4: Effect of smoking exposure on fasting blood-glucose (FBG), hemoglobin A1c (HbA1c), cholesterol (CHO), high-density lipoprotein cholesterol (HDL-C), and systolic pressure.

	Model A					Model B					Model C				
		95% CI					95% CI					95% CI			
CPD	β	Lower	Upper	Standard β	P	β	Lower	Upper	Standard β	P	β	Lower	Upper	Standard β	P
FBG	−0.026	−0.069	0.016	−0.074	0.220	−0.027	−0.067	0.014	−0.075	0.199	−0.026	−0.067	0.015	−0.073	0.209
HbA1c	0.000	−0.023	0.022	−0.002	0.976	0.000	−0.022	0.023	0.001	0.983	−0.001	−0.022	0.021	−0.004	0.951
CHO	−0.013	−0.028	0.002	−0.109	0.093	−0.013	−0.027	0.002	−0.108	0.092	−0.013	−0.028	0.001	−0.113	0.073
HDL-C	−0.006	−0.009	−0.004	−0.323	<0.001	−0.006	−0.008	−0.004	−0.316	<0.001	−0.006	−0.008	−0.004	−0.312	<0.001
Systolic pressure	0.044	−0.265	0.176	0.025	0.693	0.041	−0.255	0.174	0.023	0.711	0.031	−0.241	0.180	0.018	0.775
Time of smoking															
FBG	−0.029	−0.069	0.011	−0.086	0.151	−0.013	−0.053	0.027	−0.039	0.516	−0.016	−0.056	0.024	−0.046	0.440
HbA1c	0.001	−0.019	0.022	0.009	0.889	0.006	−0.015	0.027	0.037	0.585	0.000	−0.021	0.020	−0.002	0.970
CHO	−0.011	−0.025	0.003	−0.103	0.112	−0.006	−0.020	0.008	−0.052	0.427	−0.008	−0.022	0.006	−0.070	0.282
HDL-C	−0.005	−0.007	−0.002	−0.245	<0.001	−0.004	−0.006	−0.002	−0.223	<0.001	−0.004	−0.007	−0.002	−0.231	<0.001
Systolic pressure	−0.006	−0.223	0.211	−0.003	0.958	−0.077	−0.293	0.138	−0.045	0.480	−0.052	−0.264	0.160	−0.030	0.631
Cumulative smoking															
FBG	−0.020	−0.049	0.010	−0.078	0.194	−0.011	−0.040	0.018	−0.046	0.439	−0.011	−0.040	0.018	−0.043	0.467
HbA1c	−0.004	−0.019	0.012	−0.029	0.652	−0.002	−0.017	0.014	−0.013	0.843	−0.002	−0.017	0.013	−0.016	0.796
CHO	−0.009	−0.019	0.002	−0.105	0.105	−0.006	−0.016	0.004	−0.072	0.265	−0.006	−0.016	0.004	−0.077	0.230
HDL-C	−0.002	−0.005	0.000	−0.141	0.058	−0.002	−0.005	0.000	−0.134	0.059	−0.002	−0.005	0.000	−0.128	0.051
Systolic pressure	0.010	−0.144	0.163	0.008	0.901	0.019	−0.170	0.132	0.015	0.807	0.021	−0.169	0.126	0.018	0.776

Model A: crude model; Model B: adjusted for age, sex, occupation, and region; Model C: adjusted for age, sex, occupation, region, drinking, BMI, WC, and duration of diabetes; and CPD: cigarettes per day.

lower HDL-C, which may indicate that smoking exposure increased the risk of CHD by influencing the level of HDL-C in T2DM patients. However, further cohort studies should be conducted to verify the causal relationship. Our findings demonstrated that T2DM patients should be advised to stop smoking, or at least to reduce the amount of CPD, to prevent the onset of CHD. Moreover, to prevent the onset of CHD complications in T2DM patients, monitoring of HDL-C levels in T2DM patients with a smoking habit may be necessary.

Data Availability

The datasets used to support this study are not freely available in view of participants' privacy protection.

Conflicts of Interest

The authors declare that there are no conflicts of interest regarding the publication this article.

Authors' Contributions

Ru Tang, Shanshan Yang, and Weiguo Liu contributed equally to this work.

Acknowledgments

The authors would like to thank Lei Xu, Qian Li, Wei Jia, Xinli Cai, Lihui Liu, Ying Zhang, Jinjuan Zhao, and Xinai Yan from the 960th PLA Hospital for their research assistance with the study. This study was supported by the National Natural Science Foundation of China (81773502 and 81703308) and the Army Special Care Foundation (17BJZ51).

Supplementary Materials

Figure S1: the conceptual diagram of model 4. (*Supplementary Materials*)

References

[1] C. Bommer and E. Heesemann, V. Sagalova et al., "The global economic burden of diabetes in adults aged 20–79 years: a cost-of-illness study," *The Lancet Diabetes & Endocrinology*, vol. 5, no. 6, pp. 423–430, 2017.

[2] W. Wang, W. P. Mcgreevey, C. Fu et al., "Type 2 diabetes mellitus in China: a preventable economic burden," *The American Journal of Managed Care*, vol. 15, no. 9, pp. 593–601, 2009.

[3] S. Yang, S. Wang, B. Yang, J. Zheng, Y. Cai, and Z. Yang, "Alcohol consumption is a risk factor for lower extremity arterial disease in Chinese patients with T2DM," *Journal of Diabetes Research*, vol. 2017, Article ID 8756978, 6 pages, 2017.

[4] M. Zhu, J. Li, Z. Li, W. Luo, D. Dai, and S. R. Weaver, "Mortality rates and the causes of death related to diabetes mellitus in Shanghai Songjiang district: an 11-year retrospective analysis of death certificates," *BMC Endocrine Disorders*, vol. 15, p. 45, 2015.

[5] A. D. Shah, C. Langenberg, E. Rapsomaniki et al., "Type 2 diabetes and incidence of cardiovascular diseases: a cohort study in 1.9 million people," *The Lancet Diabetes & Endocrinology*, vol. 3, no. 2, pp. 105–113, 2015.

[6] X. Yang, Y. Luo, X. Guo et al., "Exposure to type 2 diabetes and risk of coronary heart disease in Chinese men and women: findings from a cross-sectional national survey," *The Lancet Diabetes & Endocrinology*, vol. 4, p. S3, 2016.

[7] M. Boulanger, R. Al-Shahi Salman, J. Kerssens, and S. H. Wild, "Association between diabetes mellitus and incidence of intracerebral haemorrhage and case fatality rates: a retrospective population-based cohort study," *Diabetes, Obesity and Metabolism*, vol. 19, no. 8, pp. 1193–1197, 2017.

[8] J.-T. Kim, S. H. Lee, N. Hur, and S.-K. Jeong, "Blood flow velocities of cerebral arteries in lacunar infarction and other ischemic strokes," *Journal of the Neurological Sciences*, vol. 308, no. 1-2, pp. 57–61, 2011.

[9] M.-F. Yao, J. He, X. Sun et al., "Gender differences in risks of coronary heart disease and stroke in patients with type 2 diabetes mellitus and their association with metabolic syndrome in China," *International Journal of Endocrinology*, vol. 2016, Article ID 8483405, 7 pages, 2016.

[10] T. Ohkuma, M. Iwase, H. Fujii, S. Kaizu, H. Ide, and T. Jodai, "Dose-and time-dependent association of smoking and its cessation with glycemic control and insulin resistance in male patients with type 2 diabetes mellitus: the fukuoka diabetes registry," *PLoS One*, vol. 10, Article ID e0122023, 2015.

[11] W. K. Al-Delaimy, J. E. Manson, C. G. Solomon et al., "Smoking and risk of coronary heart disease among women with type 2 diabetes mellitus," *Archives of Internal Medicine*, vol. 162, no. 3, pp. 273–279, 2002.

[12] L. Li, S. Gong, C. Xu, J. Y. Zhou, and K.-S. Wang, "Sleep duration and smoking are associated with coronary heart disease among US adults with type 2 diabetes: gender differences," *Diabetes Research and Clinical Practice*, vol. 124, pp. 93–101, 2017.

[13] H. Farzad, D. Arash, M. Amirhossein, H. Mitra, K. Davood, and A. Fereidoun, "Twelve-year cardiovascular and mortality risk in relation to smoking habits in type 2 diabetic and non-diabetic men: tehran lipid and glucose study," *PLoS One*, vol. 11, no. 3, Article ID e0149780, 2016.

[14] D. Power, "Standards of medical care in diabetes," *Diabetes Care*, vol. 29, pp. S4–S36, 2006.

[15] WHO MONICA Project Principal Invest, "The World Health Organization MONICA Project (monitoring trends and determinants in cardiovascular disease): a major international collaboration. WHO MONICA Project Principal Investigators," *Journal of Clinical Epidemiology*, vol. 41, no. 2, pp. 105–114, 1988.

[16] World Health Organization, *Guidelines for the Conduct of Tobacco-Smoking Surveys Among Health Professionals: Report of a WHO Meeting Held in Winnipeg, Canada, 7–9 July 1983 in Collaboration with UICC and ACS*, World Health Organization, Geneva, Switzerland, 1984.

[17] J. Xiao, X. Xing, J. Lu, J. Weng, W. Jia, and L. Ji, "Prevalence and associated factors of microalbuminuria in Chinese individuals without diabetes: cross-sectional study," *BMJ Open*, vol. 3, Article ID e003325, 2013.

[18] F. Thoemmes, *Propensity Score Matching in SPSS*, Cornell University Press, Ithaca, NY, USA, 2012.

[19] P. C. Austin, "Optimal caliper widths for propensity-score matching when estimating differences in means and differences in proportions in observational studies," *Pharmaceutical Statistics*, vol. 10, no. 2, pp. 150–161, 2011.

[20] T. J. Vanderweele, "Mediation analysis: a practitioner's guide," *Annual Review of Public Health*, vol. 37, no. 1, pp. 17–32, 2015.

[21] A. F. Hayes, "Model templates for process v2.16 for SPSS and SAS," *Model Templates for PROCESS for SPSS and SAS*, vol. 42, pp. 185–227, 2013.

[22] H. Q. Lou, Z. M. Dong, X. P. Shao, P. Zhang, Y. Shi, and P. P. Chen, "[Joint effect of smoking and diabetes on stroke]," *Zhonghua Liu Xing Bing Xue Za Zhi = Zhonghua Liuxingbingxue Zazhi*, vol. 38, pp. 1274–1277, 2017.

[23] P. M. Nilsson, J. Cederholm, K. Eeg-Olofsson et al., "Smoking as an independent risk factor for myocardial infarction or stroke in type 2 diabetes: a report from the Swedish National Diabetes Register," *European Journal of Cardiovascular Prevention & Rehabilitation*, vol. 16, no. 4, pp. 506–512, 2009.

[24] A. Schwendeman, D. O. Sviridov, W. Yuan et al., "The effect of phospholipid composition of reconstituted HDL on its cholesterol efflux and anti-inflammatory properties," *Journal of Lipid Research*, vol. 56, no. 9, pp. 1727–1737, 2015.

[25] J. T. Sun, Y. Liu, L. Lu et al., "Diabetes-invoked high-density lipoprotein and its association with coronary artery disease in patients with type 2 diabetes mellitus," *The American Journal of Cardiology*, vol. 118, no. 11, pp. 1674–1679, 2016.